SAPIENZA
UNIVERSITÀ DI ROMA

DOTTORATO DI RICERCA IN BIOCHIMICA
CICLO XXV (A.A. 2009-2012)

Enzymes or signals?
Functional characterization of *Pseudomonas aeruginosa* HD-GYP phosphodiesterases involved in the homeostasis of the second messenger c-di-GMP

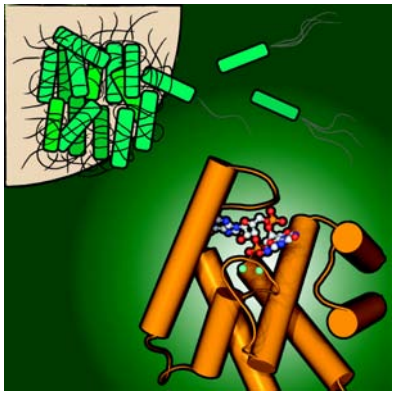

Docente guida
Prof. Francesca Cutruzzolà

Coordinatore
Prof. Paolo Sarti

Dottoranda
Valentina Stelitano

Dicembre 2012

TABLE OF CONTENTS

INTRODUCTION

Bacteria are able to communicate and behave like a multicellular organism forming biofilms, highly organized structures consisting of cells embedded within a matrix of extracellular polymeric substance (EPS) and attached to a surface. As a matter of fact, bacteria exist in nature in a planktonic single-cell state or in a sessile multicellular state, the biofilm (Bhinu, 2005); biofilms are abundant in many industrial, environmental and clinical settings, such as, for example, food processing environments, potable water and medical devices (Bryers, 2008; Kokare, *et al.*, 2009). In particular, bacterial biofilms found on the surface of medical devices are a major cause of hospital-associated infections (Lindsay and von Holy, 2006; Wenzel, 2007). Moreover, biofilms formed by pathogens play an important role in the infection of living tissues and are responsible for the resistance to antibiotics and to the host immune system (Bryers, 2008; Moreau-Marquis, *et al.*, 2008). Bacteria growing as a microbial community are less sensitive to treatments with antimicrobial agents compared to planktonic cells (Bhinu, 2005; Moreau-Marquis, *et al.*, 2008) and produce many virulence factors (Wagner, *et al.*, 2004). According to the Centers for Disease Control and Prevention, 65% of all infections in developed countries are caused by biofilms.

Pseudomonas aeruginosa

A good model organism to study biofilm is the opportunistic human pathogen *Pseudomonas aeruginosa*, leading cause of both community- and hospital-acquired infections (13% of all nosocomial infections) (Moreau-Marquis, *et al.*, 2008). *P. aeruginosa* is the major cause of death in patients of cystic fibrosis (CF), a genetic disease affecting 1/2500 newborns in Europe (Driscoll, *et al.*, 2007). In the CF lung the environment is poor of oxygen and rich of nitrate; under these conditions, *P.aeruginosa* is able to survive thanks to its anaerobic metabolism (Barraud, *et al.*, 2006; Hassett, *et al.*, 2002; Moreau-Marquis, *et al.*, 2008) causing chronic infections (Hassett, *et al.*, 2002). The stagnant mucus overlaying the CF lung epithelium constitutes a nitrate-rich microaerobic/anaerobic environment (fig. 1.1); nitrate in CF mucus is generated in part by the host inflammatory response to infection via NO. In this environment, *P. aeruginosa* produces energy from nitrate also using the

metabolic pathway of denitrification (Alvarez-Ortega and Harwood, 2007; Hassett, *et al.*, 2002) (fig. 1.1). Four reductases are involved in this process (Zumft, 1997), namely, nitrate reductase (Nar), NiR, Nor, and nitrous oxide reductase (N_2OR), whose expression is tightly regulated, being the intermediate NO a cytotoxic compound. Genetic mutants lacking *nar* and *nir* genes show swarming defects and reduced virulence (Van Alst, *et al.*, 2007). The molecular mechanisms controlling enhanced biofilm formation during anaerobic growth are not clearly defined.

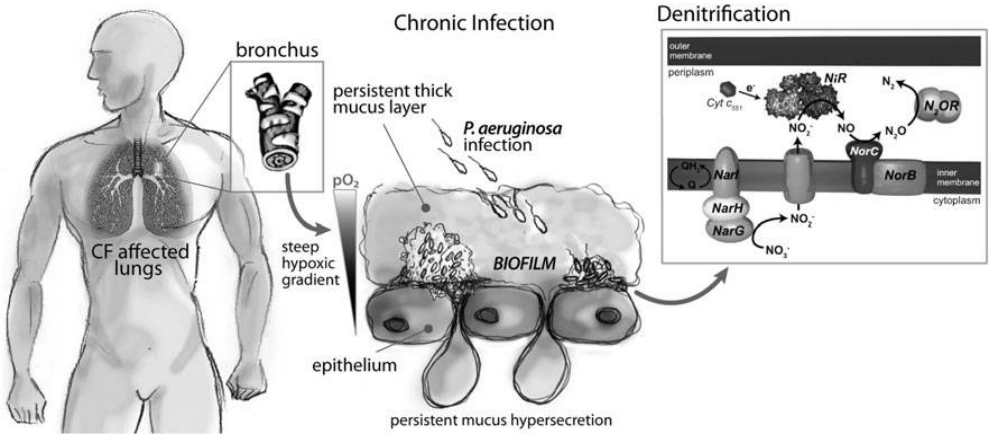

Figure 1.1 Denitrification, pathogenesis, and biofilm formation in *Pseudomonas aeruginosa*.

Low concentrations of NO have been shown to promote biofilm dispersion (Barraud, *et al.*, 2006); on the other hand, Yoon and coworkers (Yoon, *et al.*, 2011) have shown that *P. aeruginosa* PAO1 grown anaerobically is more elongated than that grown aerobically and is defective in cell division. Elongated cells easily form highly cohesive clumps, thus yielding a robust biofilm. Cell elongation is dependent on the presence of NiR and is repressed in *P. aeruginosa* PAO1 in the presence of an NO antagonist (2-(4-carboxyphenyl)-4,4,5,5-tetramethylimidazoline-1-oxyl-3-oxide [carboxy-PTIO]); these evidence suggests a link between cell elongation, NO, and anaerobic respiration (Yoon, *et al.*, 2011). Importantly, the nonelongated NiR-deficient mutant failed to form biofilm, while the wildtype PAO1 is highly elongated and formed robust biofilm. In addition to its role in anaerobic growth of *P. aeruginosa*, the NiR activity controls other important aspects of pathogenesis even under conditions where O_2 is apparently not limiting, including motility, initiation of

biofilm formation, and virulence. As an example, a recent study has demonstrated that the NO produced by *P. aeruginosa* NiR regulates the activity of type III secretion system (Van Alst, *et al.*, 2009), an apparatus whereby cytotoxic effector proteins are directly secreted into the host cell cytoplasm after contact of the bacterium with a target cell. Therefore, in *P. aeruginosa*, pathogenesis, biofilm formation, and denitrification, expecially nitrite reduction, are closely related. The enzyme responsible for nitrite reduction to NO is *P. aeruginosa* cytochrome cd_1 nitrite reductase (PA-cd_1NiR), a homodimer containing one c-heme and one d_1-heme group in each subunit.

The d_1-heme (3,8-dioxo-17-acrylate-porphyrindione) is a partially saturated macrocycle which is synthesized by a specialized pathway present only in denitrifiers (strongly induced in *P. aeruginosa* upon nitrite treatment). The d_1-heme cofactor confers peculiar and physiologically relevant feature of all cd_1NiRs, such as the rapid dissociation of NO (Rinaldo, *et al.*, 2011), and the high affinity for nitrite (and other anions such as cyanide) (Jafferji, *et al.*, 2000; Sun, *et al.*, 2002). These behaviours are remarkably different from that observed in the b-type heme-containing proteins.

Therefore, the ability of *P. aeruginosa* to survive in the low O_2 environment of the airway mucus of CF patients by using anaerobic metabolism and forming robust biofilms represent an important medical problem. *P. aeruginosa* is intrinsically resistant to a wide array of antibiotics; moreover, it is prone to acquire new resistance genes through horizontal gene transfer and it produces an impressive array of virulence factors. The low efficacy of existing therapies in eradicating *P. aeruginosa* infection calls for the development of new therapeutic options (Castiglione, *et al.*, 2011).

Within the frame of a previous project in our lab, during the very first part of my PhD a detailed analysis of the reactivity of NIR with NO has been carried out in order to improve the comprehension of the catalytic mechanism of these enzyme. In such context my main contribution during my PhD course has been to start a novel research line whose primary aim was to improve the knowledge on the molecular mechanism of c-di-GMP-dependent biofilm formation in *P. aeruginosa*.

Communication in biofilm formation: the nucleotides signalling

The biofilm formation is a multistage process that occurs step by step and which comprises formation of conditioning layer, bacterial adhesion, bacterial growth and the dispersion of some cells that often go to colonize other surfaces (biofilm expantion) (Kokare, *et al.*, 2009)

Biofilm formation takes place *via* two major signalling systems, the quorum sensing (QS) system and nucleotides signalling system. The QS system is a form of population-dependent bacterial cell-to-cell communication based on secretion and detection of small molecules induced by environmental stimuli. On the other hand, the cyclic nucleotide second messengers control an array of cellular processes linking environmental sensing with intracellular responses, representing a cornerstone signal transduction mechanism in all domains of life. Both prokaryotes and eukaryotes utilize linear and cyclic nucleotides to regulate diverse cellular processes in response to extracellular cues. In bacteria, a plethora of cyclic nucleotides as well as some linear nucleotides have emerged as important second messengers involved in the regulation of processes that regulate virulence factor production or biofilm formation. Quorum sensing regulates these same processes (Sintim, *et al.*, 2010), and accumulating evidence now points to an interaction between signalling by nucleotides and QS, the small molecules that bacteria use to make "decisions" (Rutherford and Bassler, 2012; Sifri, 2008).

Over the last few years, the universe of bacterial cyclic nucleotide messengers has been rapidly expanding (fig. 1.2). In 1957, Earl Sutherland, who would later receive the Nobel Prize in 1971, discovered that cAMP mediated the hyperglycaemic effects of epinephrine and glucagon (Berthet, *et al.*, 1957).

A few years later, in 1963, cGMP was isolated from rat urine (Ashman, *et al.*, 1963) and it took a decade before it was demonstrated in 1974 that cGMP was not unique to eukaryotes but also existed in prokaryotes. (Bernlohr, *et al.*, 1974). In 1970, Cashel and co-workers first reported the existence of ppGpp and pppGpp in *E. coli* (Cashel and Kalbacher, 1970) and it was later shown that the concentrations of ppGpp and pppGpp increased during stress. (Magnusson, *et al.*, 2005). It would take another decade before the next nucleotide second messenger would be discovered in bacteria.

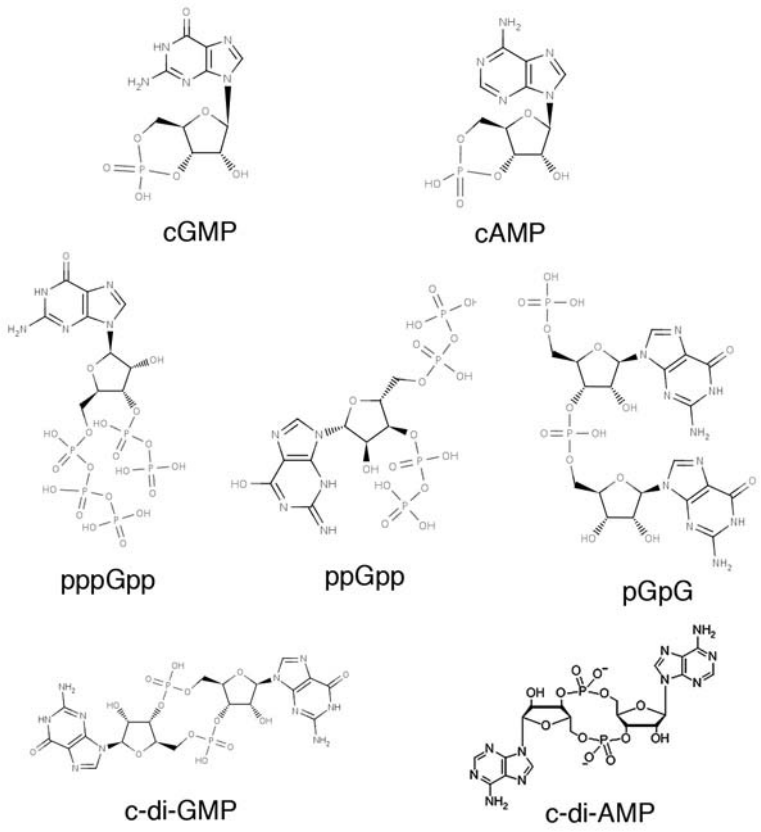

Figure 1.2. Structure of nucleotide second messengers found in bacteria.

In 1987 Benziman discovered that c-di-GMP (fig. 1.2) acted as an allosteric modulator of cellulose synthase in *Gluconacetobacter xylinus* (formerly called *Acetobacter xylinum*) (Ross, *et al.*, 1987), but only 15 years later the c-di-GMP rose from obscurity to the limelight of a ubiquitous second messenger (Ryjenkov, *et al.*, 2005). c-di-GMP is now known to control the transition from a single-cell motile state to a surface-attached multicellular state (Jenal, 2004) as well as virulence factor production in a number of clinically important bacteria and hence there is immense interest in c-di-GMP signalling. In the multicellular state, c-di-GMP plays a central role in formation and dissolution of biofilms by regulating – via diverse mechanisms – production of extracellular polysaccharides, adhesive proteins, pili and flagella (Wolfe and Visick, 2009).

Almost two decades after Benziman's seminal discovery of cyclic dinucleotide signalling in bacteria, Hopfner reported that bacteria also use c-di-AMP for signalling (fig. 1.2) (Witte, *et al.*, 2008).

c-di-GMP signalling - C-di-GMP is an ubiquitous intracellular second messenger crucial in physiology and pathogenesis of a variety of bacteria, including those of clinical relevance. In fact, this signal molecule controls complex prokaryotic processes such as virulence, motility and biofilm formation (fig. 1.3A) (Romling, *et al.*, 2005; Schirmer and Jenal, 2009) hence there is immense interest in c-di-GMP signalling (Jenal, 2004).

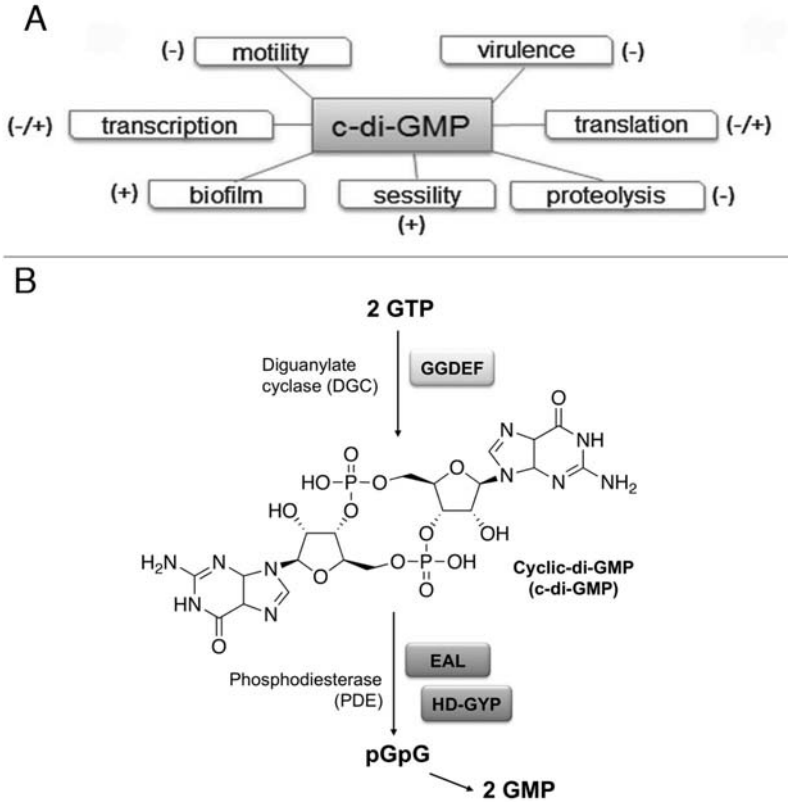

Figure 1.3. A) Cyclic-di-GMP controls many cellular processes like motility, virulence, biofilm formation and differentiation. B) Cyclic-di-GMP turnover: Cyclic-di-GMP synthesis and degradation are, respectively, controlled by two classes of enzymes, diguanylate cyclases (DGC), characterized by a GGDEF domain, and phosphodiesterases (PDE), characterized by an EAL or a HD-GYP domain.

During biofilm formation, the pattern of gene expression is changed with respect to planktonic cells and new intracellular signalling pathways are

activated. When c-di-GMP reaches a threshold concentration in response to environmental signals, it induces a response regulating gene expression that stimulates the switching between the motile planktonic and the sessile lifestyle (Jenal, 2004), as well as the formation of extracellular polymeric substance. Therefore, biofilm formation can be viewed as a developmental process (Kokare*, et al.*, 2009), regulated by the key signal molecule c-di-GMP.

C-di-GMP biosynthesis, degradation and signalling

The intracellular levels of c-di-GMP are modulated by the opposite activity of diguanilate cyclase (DGC), and phosphodiesterase (PDE) enzymes (fig. 1.3B). DGC enzymes synthesize c-di-GMP starting from two GTP molecules, while PDEs hydrolysed it producing linear 5'phosohoguanylyl-(3'-5')-guanosine (pGpG) or GMP. DGCs are often called GGDEF proteins due to the conserved aminoacids found in their active site; similarly, PDEs are grouped into the EAL and the HD-GYP families (Camilli and Bassler, 2006; Cotter and Stibitz, 2007; Hengge, 2009). GGDEF and EAL domains are also found in tandem within the same protein; these hybrid proteins frequently show only one enzymatic activity with the catalytically inactive domain, potentially serving a regulatory function (Jenal and Malone, 2006) Structural and functional studies of LapD, an internal membrane protein that regulates surface attachment in *Pseudomonas fluorescens*, and of FimX from *P.aeruginosa* (Navarro*, et al.*, 2009) indicate that both hybrid proteins function as c-di-GMP-sensors, able to communicate the levels of c-di-GMP from the cytoplasm to the periplasm (Newell*, et al.*, 2009); nucleotide binding studies in solution confirmed that EAL domain works as the sole c-di-GMP binding module of FimX (Navarro*, et al.*, 2009).

Most DGCs and PDEs are also associated with known or hypothetical signal input domains (globin-like, CheY-like, PAS/PACM, GAF, HAMP, CHASE4 or membrane sensory domains MHYT or MASE1) (Galperin*, et al.*, 2001), putatively involved in sensing a range of environmental signals (oxygen, blue light, nutrient starvation, antibiotics, etc). Little is known on the intracellular receptors of c-di-GMP, which convert the increase/decrease of c-di-GMP into a biological response. Possible c-di-GMP-sensing domains include the PilZ, BcsA or PelD domains (Camilli and Bassler, 2006; Lee*, et al.*, 2007; Ryjenkov*, et al.*, 2006), the GGDEF/EAL containing hybrid proteins (Newell*, et al.*, 2009)

and even riboswitches (Sudarsan, *et al.*, 2008). However, the high number of genes coding for GGDEF, EAL, HD-GYP or GGDEF-EAL fused proteins in the genome of many bacterial species (Hengge, 2009) indicate that bacteria regulate the c-di-GMP turnover and biofilm formation in an extremely sophisticated manner. The large number of GGDEF and EAL domain proteins in a single species is somewhat puzzling (Hengge, 2009). In general, Gram-positive bacteria have less of DGC/PDE proteins than Gram-negative bacteria; by contrast, proteins containing the HD-GYP domain are less common or even absent in some species such as *E.coli*, whereas in other species, such as *Thermotoga maritima*, they account for all PDE activity in the cell (Galperin, 2005; Galperin, *et al.*, 2001). The number of these proteins encoded in bacterial genomes is highly variable (for example over 60 in *Vibrio cholerae*, 41 in *P. aeruginosa*, none in *Helicobacter pylori*): this may reflect the ability to survive in different environmental niches. However, how the DGCs and PDEs function together to produce a coherent output signal is still unclear; different c-di-GMP circuits could be separate in time and in space, through compartmentalization (Jenal and Malone, 2006; Malone, *et al.*, 2012; Massie, *et al.*, 2012).

Given the heterogeneity and the large number of factors involved, the c-di-GMP signalling pathway appears to be very elaborate and difficult to understand. To date, few biochemical data on the proteins involved in c-di-GMP turnover are available. A brief summary of the major structural and functional data on the DGCs and the PDEs is given below.

Diguanylate cyclases

The structure of the GGDEF domain resembles that of the adenylate cyclase catalytic domain, as evident in the structure of the PleD response regulator from *Caulobacter crescentus* (Chan, *et al.*, 2004; Christen, *et al.*, 2006), that is considered as a prototype DGC. PleD has REC1-REC2-GGDEF domains; the two CheY-like phosphoryl receiver (REC) domains modulate the activity of the protein. Activation is achieved by phosphorylation of an aspartate residue that induces dimerization: two GTP molecules, bound to the active sites of the GGDEF domains, come together to form c-di-GMP. PleD is regulated by non-competitive product inhibition: c-di-GMP can bind to a high affinity inhibition

site (I-site) causing a conformational change that separates the two GGDEF domains, thus hampering catalysis (Paul, *et al.*, 2007).
In *P. aeruginosa*, the only known DGC structure is that of WspR (De, *et al.*, 2009) (fig. 1.4). This DGC has a similar domain organization as PleD, but lacks the second CheY-like domain. As observed with PleD, WspR appears to be regulated by phosphorylation of the N-terminal CheY-like domain (Hickman, *et al.*, 2005).

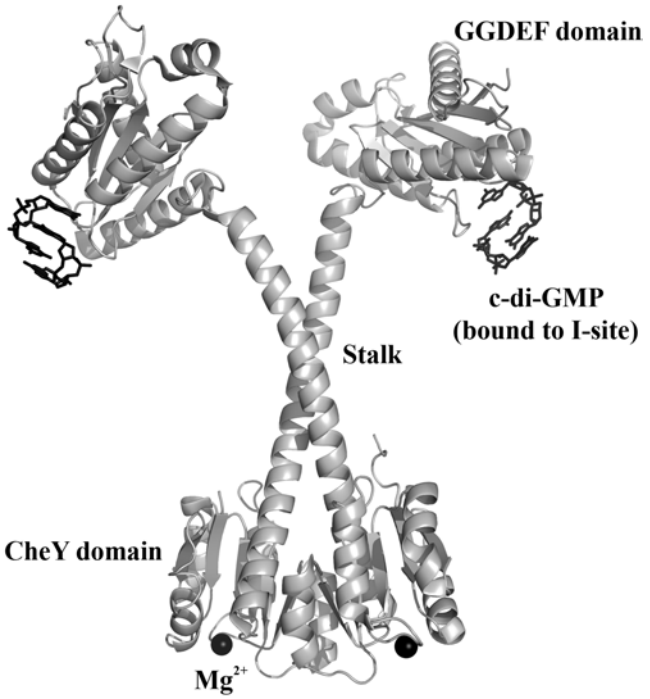

Figure 1.4. Crystal structure of WspR from *P. aeruginosa*: The N-terminal CheY-like phospho-receiver domain is connected via a helical stalk to the GGDEF domain with diguanylate cyclase activity. Cyclic-di-GMP molecules bound to the inhibitory site (I-site) are located distal to the active site and are shown as black sticks. Mg^{2+} ions are shown as black spheres (Tesmer, *et al.*, 1997) (Protein Data Bank id. 3BRE).

In the structure of the protein (fig. 1.4) this domain contains the Mg^{2+} ion (necessary for catalysis) and it is connected via a helical stalk to the GGDEF domain; the latter is oriented such that the two active sites face each other, similarly to the active conformation of adenylate cyclases (Tesmer, *et al.*, 1997). In addition, binding of a c-di-GMP dimer to the conserved inhibitory site (I-site) is observed (Christen, *et al.*, 2006) (fig. 1.4). In summary, the protein is

activated by phosphorylation and inhibited by product binding to the I-site; however, the feedback inhibition mechanism of WspR is even more complex than in PleD (De, *et al.*, 2008).

Surprisingly, recent data indicate that the c-di-GMP has also a role in signalling of eukaryotic cells (Chen and Schaap, 2012). In fact, species representing all major groups of Dictyostelia contain one or more conserved diguanylate cyclase that were previously only found in eubacteria.

D. discoideum is a eukaryote that transitions from a collection of unicellular amoebae into a multicellular slug and then into a fruiting body within its lifetime. Chen Z. and Schaap P. demonstrated that the *Dictyostelium discoideum* diguanylate cyclase (DgcA) synthesizes c-di-GMP and is essential for the transition from slug migration to fructification (Chen and Schaap, 2012).

Thus in Dictyostelia as in bacteria, c-di-GMP also triggers the transition from motile slugs into sessile fruiting bodies, and the question arises of whether this represents either convergent evolution or deep ancestral connections between Dictyostelid fructification and bacterial sessility.

Furthermore, numerous studies have demonstrated that cyclic dinucleotides are potent immunostimulatory compounds (Chen, *et al.*, 2010; Karaolis, *et al.*, 2007); recently, it was identified as mammalian innate immune sensor of c-di-GMP the a transmembrane protein called STING (STimulator of INterferon Genes) (Burdette, *et al.*, 2011), that is known for its role as signalling adaptor linking cytosolic detection of pathogen-derived DNA to the IFN induction (Ishikawa and Barber, 2008; Ishikawa, *et al.*, 2009; Jin, *et al.*, 2008; Sun, *et al.*, 2009; Zhong, *et al.*, 2008). Recognition of microbial ligands leads to the production of cytokines, such as type I interferons (IFN) that are essential for successful pathogen elimination.

Burdette D.L. and co-workers demonstrated that STING can bind directly c-di-GMP and that the cyclic dinucleotide sensing and DNA sensing can be uncoupled, suggesting that these two pathways are discrete but share STING as a common signalling molecule (Burdette, *et al.*, 2011). Thus, the finding that STING is a direct detector of cyclic dinucleotides provides insight into the fundamental mechanisms by which the innate immune system can detect bacterial infection and allow to valuate the cyclic dinucleotides as novel vaccine adjuvants and immunotherapeutics (Chen, *et al.*, 2010; Karaolis, *et al.*, 2007).

EAL and HD-GYP Phosphodiesterases

Both classes of PDE require Mg^{2+} or Mn^{2+} ions for the phosphodiester hydrolysis. (Christen, *et al.*, 2005). To date, a detailed mechanism for the cleavage of c-di-GMP by PDEs has not been worked out but analyses of crystal structures of PDEs, with or without bound c-di-GMP, have provided some clues about c-di-GMP hydrolysis.

The crystal structures of few proteins with EAL domains have been determined: TdEAL from *Thiobacillus denitrificans*, YkuI from *Bacillus subtilis* (Minasov, *et al.*, 2009), BlrP1 from *Klebsiella pneumonite* (Barends, *et al.*, 2009). The general fold of the EAL domain consists of a beta-barrel harbouring the catalytic residues at the top of the barrel.

In the case of *P. aeruginosa*, the catalytic mechanism of the RocR protein has been discussed and its structural model has been settled (Rao, *et al.*, 2008); Despite extensive screening of crystallization conditions, the wild-type RocR could not be crystallized. Very recently, the crystal structure of a mutant protein (R286W) was been obtained (Chen, *et al.*, 2012) revealing that RocR adopts a highly unusual quaternary structure in solution with its four subunits adopting two distinct conformations (fig. 1.5).

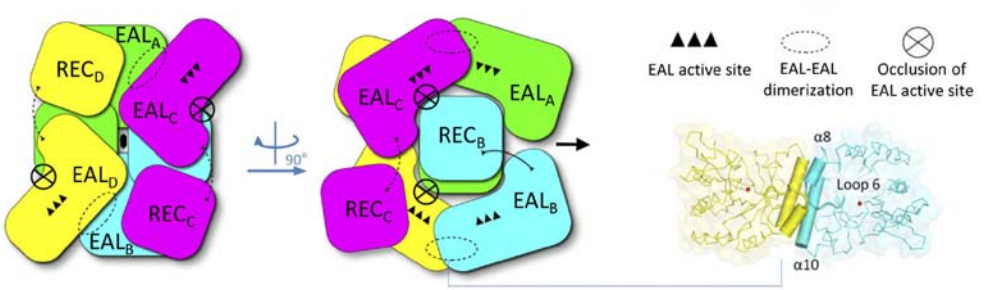

Figure 1.5. Schematic depiction of the RocR tetramer highlighting the open conformation of its C and D subunits, which form a saddle-like structure into which the REC domains of the closed subunits A and B are inserted, forming the core of the tetramer. The EAL active sites are represented as three black triangles. EAL active sites of subunits C and D are concealed (crossed circle) in trans by the REC domains located at the center of the structure. The interdomain linker is depicted as a line (dashed line if it is partially disordered in the crystal structure) (Chen, *et al.*, 2012).

Two of the four substrate-binding pockets of RocR (C and D) are not accessible to c-di-GMP and thus likely to be constitutively enzymatically

inhibited. Inhibition of the enzymatic activity of the subunits C and D is achieved in trans by using the REC domains from the other two subunits to physically block the access of the c-di-GMP substrate. The EAL domains from the subunits A and B are likely to contain the functional active sites with open c-di-GMP binding pockets.

The EAL domain of RocR adopt a $(\beta/\alpha)_8$ barrel-like fold (Chen, *et al.*, 2012), confirming previous data; the catalytic residues are located at the C-terminal end of the barrel, including residues that form the metal ion binding site and the evolutionarily conserved residues of loop 6: $D^{296}FGAGYSS^{303}$. This motif seems to play an important role in signal transduction; sequence analysis of the 5,862 EAL domains in the bacterial genomes revealed that about half of the EAL domains harbour a degenerated loop 6, suggesting that the mutation of this loop may indicate a divergence of function for EAL domains during evolution (Rao, *et al.*, 2009).

Moreover, as predicted by the structural model of RocR (Rao, *et al.*, 2008), hydrolysis of one O-3'-P ester bond to yield the linear dinucleotide 5'-pGpG is achieved by an activated water molecule and involves one or two Mg^{2+} or Mn^{2+} ions and seven catalytic residues, including the Glu residue of the EAL signature motif.

In contrast to EAL-domain PDEs, only one structure is available to date for HD-GYP containing proteins, which have so far resisted high-resolution crystallography. This domain is widespread in bacteria (over 1000 genes have been found); it is classified as a metal-dependent phosphohydrolase and a divalent cation (most likely Mg^{2+} or Mn^{2+}) is required for catalysis, but the molecular mechanism of action is still unknown. Lovering and co-workers recently solved the first structure of Bd1817, an unconventional HD-GYP protein from predatory bacterium *Bdellovibrio bacteriovorus* (Lovering, *et al.*, 2011). Bd1817 present an uncharacterized N-terminal domain (NTD), and the C-terminal HD-GYP phosphodiesterase domain that lacks the active-site tyrosine present in most HD-GYP family members. Nevertheless it yet remains an excellent structural model, sharing 48% sequence similarity with the family archetype RpfG (from *Xanthomonas campestris*) (Lovering, *et al.*, 2011). The crystal structure of Bd1817 reveals the presence of a binuclear iron center into the active site (fig. 1.6) Sequence alignment of Bd1817 with other HD-GYP-containing proteins reveals that the majority of conserved residues cluster

around the binuclear metal centre, which is observed complexed to a molecule of phosphate. The fold and active site of the HD-GYP domain are different from those of EAL proteins, and restricted access to the active-site cleft is indicative of a different mode of activity regulation.

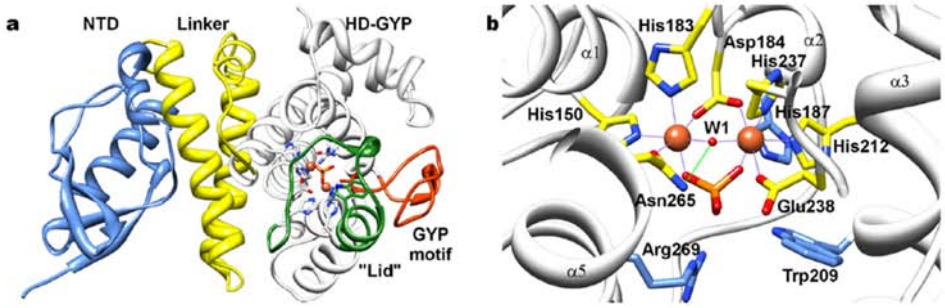

Figure 1.6. Modular nature of the Bd1817 HD-GYP protein and active-site coordination of metal ions. Selected side chains and bound phosphate are shown in stick form, and metal ions and bound hydroxide (red, W1) are shown in sphere form. A) Ribbon diagram of Bd1817 with individual domains colored separately as follows: NTD, blue; linker helices, yellow; HD-GYP domain, white; lid region subdomain, green; GYP motif subdomain, orange. B) Detail of binuclear metal active site (HD-GYP domain). Fe-protein interactions, purple dashed lines; hydroxide-protein interaction, green dashed line (Lovering, *et al.*, 2011).

The region encompassing the GYP motif has a novel conformation and is surface exposed and available for complexation with binding partners, including GGDEF proteins (Lovering, *et al.*, 2011), as seen for the RpfG (Ryan and Dow, 2010). RpfG and the sensor kinase RpfC compose a two-component system implied in sensing and responding to the diffusible signalling factor (DSF), which is essential for cell-cell signalling (Barber, *et al.*, 1997; Dow, *et al.*, 2003; Ryan, *et al.*, 2006; Slater, *et al.*, 2000). Mutation in *rpfG* gene leads to a reduction in the synthesis of virulence factor (including extracellular enzymes), alteration in biofilm formation, reduced pilus dependent motility and reduction in virulence (Ryan, *et al.*, 2010). However, the availability of more structures would allow a greater understanding of HD-GYP catalytic mechanism for c-di-GMP hydrolysis.

In *P. aeruginosa* 3 genes harbour HD-GYP domain proteins: PA4108, PA4781 and PA2572. The first two proteins control the swarming motility and the production of virulence factors and show to have a PDE activity *in vivo*, indeed their mutation leads to increased levels of c-di-GMP (Ryan, *et al.*, 2009). On

the other hand, the role of the third protein PA2572 (which has a different YN-GYP signature) is uncertain (Ryan, *et al.*, 2009): this protein is inactive in c-di-GMP hydrolysis and it has a cryptic negative influence on swarming. Nevertheless, all three proteins regulate virulence of *P. aeruginosa* since their mutation led to a reduction of the bacterial virulence in the larvae of *Galleria mellonella* (Ryan, *et al.*, 2009). Due to their importance in virulence and since the biochemical and structural information about HD-GYP are still poor, a deep characterization of this class of proteins is highly desirable.

	C-di-GMP levels	Swarming/ twitching	Pyoverdin	Pyocyanin	Ramnolypid	ExoS	Biofilm structure	virulence
ΔPa4108	↑	↓	=	↓	=	↓	Flatter biofilm, smaller mushroom structure	↓
ΔPa4781	↑	↓	↑	=	=	=	Biofilm that covered large surface %, few mushroom-like structure	↓
ΔPa2572	=	=	↓	=	↑	=	Simil wild-type	↓

Table 1.1. Effects of HD-GYP genes deletion in *P. aeruginosa* strains compared to wild-type strain PAO1.

The metabolic network involving c-di-GMP is highly complex and the exact molecular mechanism of c-di-GMP action remain to be fully elucidated. A detailed understanding of such complex regulatory mechanism will not only help to explain the specificity of c-di-GMP signalling systems, but may also favour a biotechnological research aimed to develop new strategies to fight biofilm in medical/industrial/environmental settings (Castiglione, *et al.*, 2011; Wood, *et al.*, 2011). Moreover, a great deal of research is still needed to use the c-di-GMP as a potential vaccine adjuvant in human clinical trials. Understanding how microbes control c-di-GMP metabolism to activate specific pathways is complicated by the apparent multifold redundancy of enzymes involved in the synthesis, degradation and/or binding of this crucial second messenger. Moreover, the mechanisms by which c-di-GMP exerts its regulatory effect are incompletely understood, probably due also to the evidence that c-

di-GMP present a rich polymorphism in association with effectors (Yang, *et al.*, 2011) and in solution (Zhang, *et al.*, 2004; Zhang, *et al.*, 2006).

Heterogeneity of c-di-GMP binding to proteins

The mechanisms by which c-di-GMP exerts its regulatory effect are not completely understood. As mentioned above, also when bound to proteins, several distinct c-di-GMP conformations have been found, including the monomeric (Minasov, *et al.*, 2009; Navarro, *et al.*, 2009; Wang, *et al.*, 2011) and the self-intercalated dimeric form (Benach, *et al.*, 2007; Duvel, *et al.*, 2012; Ko, *et al.*, 2010). A wide variety of different protein-based or RNA-based recognition motifs for c-di-GMP have been discovered, including the transcription factor Clp (Chin, *et al.*, 2010), RNA-processing polynucleotide phosphorylase (PNPase; (Tuckerman, *et al.*, 2011)), inhibitory site of DGC protein (Schirmer and Jenal, 2009), degenerate GGDEF- or EAL-domain proteins (Navarro, *et al.*, 2011), PilZ-domain proteins (Benach, *et al.*, 2007; Li, *et al.*, 2009) and riboswitches (Smith, *et al.*, 2011) The binding of c-di-GMP self-intercalated dimer to the PleD and WspR allosteric I sites, comprising an RxxD motif and other less conserved secondary inhibition residues, has been shown to allow the DGC activity inhibition (Schirmer and Jenal, 2009). However, it is important to note that a recent computational analysis of 867 prokaryotic genomes revealed that approximately half of over 10 000 GGDEF sequences lack the canonical allosteric inhibition sites (Seshasayee, *et al.*, 2010). Whether these significant numbers of GGDEF-domain proteins are also subject to product inhibition and how this is achieved remain largely unknown. Very recently, Yang and co-workers report the structure of the GGDEF domain of an *X. campestris* diguanylate cyclase (XCC4471) in complex with c-di-GMP (Yang, *et al.*, 2011). Unexpectly, the structure of the complex indicates that two molecules of c-di-GMP reside in the GGDEF active site. Each c-di-GMP molecule is also found to adopt an unusual partially intercalated conformation, different to that adopted by c-di-GMP binding the allosteric inhibitory sites (Yang, *et al.*, 2011), which adopts a self-intercalated stack comprising four guanine bases. Such a novel GGDEF–c-di-GMP complex structure implies the existence of an unusual product bound mode for DGCs.

c-di-GMP polymorphism in solution and detection strategy

It is known that c-di-GMP displays a rich polymorphism in solution, and that the equilibrium among the monomeric, dimeric, tetrameric and octameric species is affected by the presence of metal ions (Gentner, *et al.*, 2012; Zhang, *et al.*, 2004; Zhang, *et al.*, 2006). However, only the monomeric and dimeric forms (fig. 1.7) have been found under physiological conditions, while higher oligomer formation occurs only at mM concentration or in presence of additional aromatic intercalators (Nakayama, *et al.*, 2011; Nakayama, *et al.*, 2011). The monomer-dimer equilibrium is also likely to play a physiological role, allowing bacteria to sense and control different local c-di-GMP concentrations. Indeed PilZ receptors binding to c-di-GMP as a monomer or as an intercalated dimer have been reported (Benach, *et al.*, 2007; Duvel, *et al.*, 2012; Ko, *et al.*, 2010). The dimeric form is also observed in complex with DGCs, bound to a non competitive inhibitory site (De, *et al.*, 2008; Yang, *et al.*, 2011), while PDEs bind c-di-GMP as a monomer at the active site (Minasov, *et al.*, 2009; Navarro, *et al.*, 2009; Wang, *et al.*, 2011).

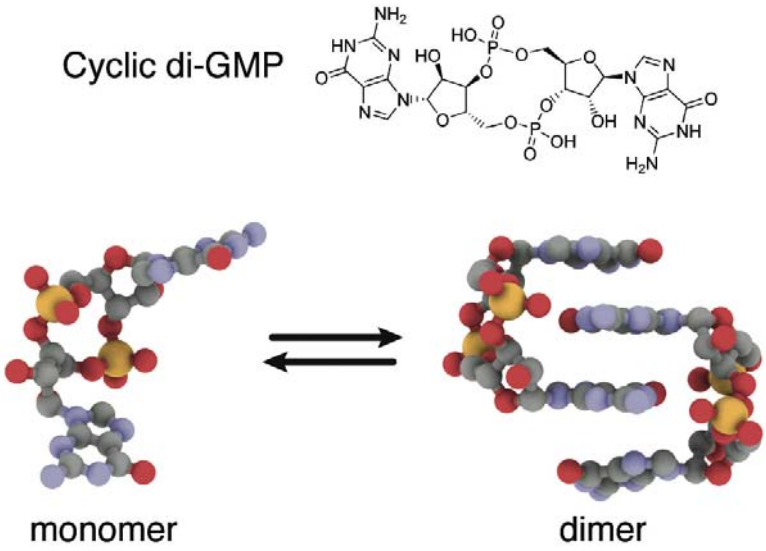

Figure 1.7. Chemical structure of c-di-GMP and 3D structure of monomeric and dimeric c-di-GMP as observed in the active and inhibitory site of PleD, respectively (PDB id: 1w25) (Chan, *et al.*, 2004). The equilibrium in solution of the two species is affected by the presence of monovalent or divalent cations (Gentner, *et al.*, 2012; Zhang, *et al.*, 2004; Zhang, *et al.*, 2006)

However, the dearth of detailed information regarding c-di-GMP signalling is probably also dueto the lack of a rapid and unexpensive experimental strategy to readily detect c-di-GMP. Indeed, despite the great effort in understanding the molecular basis of the c-di-GMP signalling pathways and the growing number of groups working in this field, a method for *in vitro* detection and quantification of c-di-GMP is still not available for reliable real-time measurements. Current direct c-di-GMP detection methods rely on the use of analytical techniques, like reverse phase HPLC and mass spectrometry (Antoniani, *et al.*, 2009; Simm, *et al.*, 2009; Spangler, *et al.*, 2010), which require a complex and time consuming sample preparation, since small molecules need to be separated from macromolecules before analysis. Furthermore, mass spectrometry is not always readily available in many biochemistry and molecular biology labs. Thin layer chromatography, although being a semi-quantitative technique, could be a fast alternative method, but it carries the disadvantage of requiring radiolabeled nucleotides as substrates, given the low concentration of c-di-GMP that are usually detected in enzymatic studies (low µM range). The use of the EnzChek® Pyrophosphate Assay Kit has also been reported (De, *et al.*, 2008). This is an indirect method based on several enzymatic reactions to quantify the inorganic pyrophosphate (PPi) produced as side product in the synthesis of c-di-GMP by diguanylate cyclases. Recently, new spectroscopic methods have been reported: one method is based on the ability of c-di-GMP to form tetramers with a G-quadruplex-like structure in the presence of specific dyes (Nakayama, *et al.*, 2011). This method is limited by the dyes solubility and by the extremely slow kinetics (>10 hours at 4°C) of complex formation between c-di-GMP quadruplex and the dye. Moreover, in our hands, it showed a non linear dependence with the c-di-GMP concentration in the low µM range (data not shown), possibly given that the multiple equilibrium between monomeric, dimeric and tetrameric c-di-GMP is strongly affected by the initial monomer concentration (Gentner, *et al.*, 2012). Fluorescence-based detection of c-di-GMP has been recently proposed using either an RNA-based aptamer (Nakayama, *et al.*, 2012) or a fluorescent derivative of c-di-GMP (Sharma, *et al.*, 2012); although fluorescence guarantees high sensitivity to these approaches, limitations related to long pre-incubation times or side-effects such as inhibition of the enzymes suggest that they are more suitable for binding studies than for kinetic real-time measurements of

both DGCs and PDEs. An indirect method has also been proposed based on the ability of the c-di-GMP G-quadruplex to enhance hemin peroxidation in the presence of proflavine (Nakayama, *et al.*, 2012). This strategy, however, is unlikely to be useful for real-time quantification of c-di-GMP since it involves redox reactions, which may damage or interfere with the stability of the enzymes producing or consuming c-di-GMP.

The availability of a direct experimental strategy to detect and quantify c-di-GMP could provide significant advances and important clues to direct future experimental work on enzymes able to synthesize and degrade c-di-GMP.

AIM OF THE WORK

Bacteria are not only simple single-cell organisms inhabiting our world but they are able to communicate and behave like a multicellular organism forming biofilms.

The impact of biofilms on human health is huge: more than 60% of all infections in developed countries are caused by bacterial biofilms. These bacterial communities are difficult to eradicate since they are highly resistant to antimicrobials and to the host immune system. The scientific challenge is therefore to find new therapeutic options, which specifically target bacteria growing in biofilms.

Biofilm formation is a complex event: it implies the transition from the planktonic to the sessile way of life. One of the most important signal involved in controlling biofilm formation is the intracellular second messenger 3',5'-cyclic diguanylic acid (c-di-GMP); moreover c-di-GMP is involved in the mechanism by which immune system can detect bacterial infection. Therefore, targeting c-di-GMP metabolism could represent an attractive strategy for the development of novel therapeutic approaches against bacterial biofilm.

The aim of this PhD project is to gain mechanistic insights on the enzymes involved in the c-di-GMP signalling system, in order to contribute to the search for novel anti-biofilm compounds.

Our model organism is the human pathogen *Pseudomonas aeruginosa*, leading agent of nosocomial infections and the main cause of death in patients affected by cystic fibrosis (CF), a genetic disease affecting 1/3000 newborns in Europe. Several evidences suggest that the c-di-GMP signalling pathway is important for *P. aeruginosa* biofilm establishment and persistence, but the molecular mechanisms controlling this bacterial process leading to biofilm formation during cystic fibrosis infections are still largely unknown.

This project has been divided into two major tasks:

(1) Biochemistry of selected HD-GYP proteins involved in c-di-GMP hydrolysis - In the framework of broader research project ongoing in my group and focused on the metabolism of c-di-GMP in *P. aeruginosa*, the present study aims at analyzing the catalytic mechanism of selected HD-GYP

phosphodiesterases, whose involvement in biofilm formation and virulence has been already demonstrated (Ryan*, et al.*, 2009). More in detail, we have analyzed the HD-GYP proteins encoded by the PA4781 and PA4108 genes.
Beyond the catalytic HD-GYP domain, these enzymes contain a CheY-like or an uncharacterized domain, respectively, at the N-terminus. These domains are presumably involved in the regulation of the catalysis; this aspect has been analyzed in particular for PA4781.

(2) Development of medium throughput assay for c-di-GMP quantification - The kinetic characterization, needed to pursue the goal described above, requires a reliable enzymatic assay able to quantify the nucleotide content along the reaction time-course.
It should be mentioned that, despite the relevance of the c-di-GMP signalling, to date, the continuous and prompt measurement of c-di-GMP (enzymatically produced/consumed) is demanding and difficult to be carried out with the quantification methods available. This constrain could represent also a limiting step for future screening of a large number of putative inhibitors of diguanylate cyclases or phosphodiesterases.
For this reason we have set up a novel Circular Dicroism (CD) assay for rapid spectroscopic quantification of c-di-GMP levels, based on the capability of the manganese ion to promote c-di-GMP dimerization; this species displays a peculiar circular dichroism signal which is linearly dependent on c-di-GMP concentration.

The knowledge gained in the present study allowed us to obtain novel data on these *P.aeruginosa* HD-GYP proteins; moreover, the experiments carried out for the HD-GYP project and for the set up of the novel kinetic assay will be crucial for the characterization of other PDEs and DGCs relevant to pathogenesis in other microrganisms.
The data presented here will be extended in the future in order to find a strategy capable to target selectively c-di-GMP metabolism, to be used also in combination with traditional antimicrobial therapies, given that there is no compound on the market able to specifically interfere with biofilm formation. Since biofilm-mediated infections are wide-diffused, the potential therapeutic impact deriving from the inhibition of biofilm *via* c-di-GMP in several human diseases is huge.

METHODS

3.1 HD-GYP characterization

Cloning and site-direct mutagenesis

Synthetic PA4781 and PA4108 genes were purchased from Geneart subcloned into the Pet28b and Pet24 vector in frame with a N-terminal and C-terminal His-tag, respectively (GENEART). A truncated version of PA4781 (hereinafter PA4781G) was produced by PCR, starting from PA4781 as template, in order to remove the first 111 residues, corresponding to the REC domain. The corresponding fragment was then cloned into the NdeI and XhoI restriction sites of pet28.

Mutation of Phe290 into Tyr was performed with the QuikChange mutagenesis kit (Stratagene), according to the manufacturer's instructions, on both pet28-PA4781 or pet28-PA4781G templates (the residues number refer to the full length sequence).

Proteins expression and purification

For each vector, protein expression was obtained after transformation of *E. coli* BL21 (DE3) strain. Overnight cultures were used to inoculate (1:100) 400 ml of liquid Luria-Bertani broth with Kanamycin (30mg/ml) and 0,1 mM IPTG (isopropyl B-d-thiogalactoside). Cultures were grown under constant shaking at 37°C (full-length proteins) or 25°C (PA4781Gstart mutant) until the cells reached late-exponential phase (OD_{600}= 0,8-1,0). Cells were harvested by centrifugation and resuspended in lysis buffer (50mM TRIS pH 8, 50mM NaCl, 1mM PMSF). In order to increase the expression and the solubility of PA4108 protein, the expression was also carried out in BL21plysS (DE3) *E. coli* strain under constant shaking at 37°C; protein expression was induced with 1 mM IPTG when OD_{600} was 0,7. Cells were harvested by centrifugation after 2h and the protein was purified as described below.

Cell lysis has been carried out by ultrasonic treatment on ice and the cleared soluble extract was obtained by centrifugation. Proteins were purified as His-tagged fusion using a 5ml HisTrap column (GE Healtcare) equilibrated with

buffer A (20 mM TRIS pH 7.6, 150 mM NaCl). Eluition has been carried out with a stepwise increase in imidazole concentration, with all proteins eluting at 200mM imidazole. The buffer exchange of pooled fractions was performed with PD-10 Desalting column (GE Healtcare). The aggregation state of the proteins was analyzed with a Superdex-75 10/30 column equilibrated with buffer A, using a HPLC apparatus.

Phosphodiesterase activity assay on purified proteins

c-di-GMP and pGpG hydrolysis - The ability of the aforementioned proteins to hydrolyze c-di-GMP, was assayed incubating the proteins (110 µg of purified PA4781 full-length and of PA4781G; 10 µg of PA4108) four hours at 30°C in the reaction buffer (50 mM Tris–HCl pH 8, 150 mM NaCl) in the presence of 2,5 mM $MnCl_2$, and/or 10 mM $MgCl_2$ and 30 µM c-di-GMP or pGpG (BIOLOG) as substrate. The reaction was stopped boiling the sample for 10 min; the precipitated protein was removed with 0,2 µm filters (Bilk GHP Acrodisc 13mm). At least two independent assays for each sample were performed; protein storage buffer was used as negative control.
The nucleotide content of the samples was measured by HPLC analysis using a 150 x 4.6 mm reverse phase column (Prevail C8, Grace Davison Discovery Science) at room temperature on a LabFlow 4000 apparatus (LabService Analytica). Detection wavelength was 252 nm and mobile phase was 100 mM phosphate buffer pH 5.8 / methanol (98/2, v/v). Synthetic c-di-GMP, pGpG (Biolog) and GMP (GE Healtcare) were used as standard.
Determination of kinetic parameters of PA4108- The initial velocity at given substrate concentration was obtained by analyzing aliquots of the reaction mixture at different times. The initial velocity was measured at 4 substrate concentrations (10, 60, 150, 300 µM c-di-GMP). The K_m value was obtained by fitting the initial velocities obtained at various substrate concentrations with the Michaelis-Menten equation, using the software Igor Pro.
Activation of PA4781 by BeF_3^- modification - PA4781 was incubated at room temperature in reaction buffer with beryllium fluoride (BeF_3^-) for at least 30 min before substrate addition, according to Paul et al. 2007. The assay was performed at several $BeCl_2$ concentrations (0, 0.1, 0.15, 0.2, 0.3, 0.5, 1, 1.5,

2.5, 5 mM) in the presence of 10 mM NaF, and subsequently at several NaF concentrations (0, 0.3, 0.5, 0.8, 1, 1.5, 2, 2.5, 5, 10 mM) in the presence of 0.15 mM $BeCl_2$.

Isothermal Titration Calorimetry (ITC)

ITC experiment was carried out using an iTC200 microcalorimeter (MicroCal). A PA4781 solution was prepared in 100 mM Tris (pH 8.5), 50 mM NaCl, 10 mM $MgCl_2$ and 2.5 mM $MnCl_2$. c-di-GMP solution was prepared by dilution of a 1mM stock solution (in water) with PA4781 buffer. 2-µl aliquots of c-di-GMP solution (80 µM) were injected into a 3 µM protein solution at 25°C. Data were fitted using the "one-binding-site model" of the MicroCal version of ORIGIN. The heat of binding (ΔH), the stoichiometry (n), and the dissociation constant (K_D) calculated from the plot of the heat evolved per mole of ligand injected *versus* the molar ratio of ligand to protein presents high errors of fit, being very low the affinity of binding.

Determination of intracellular c-di-GMP content

The *E.coli* strain (AB1548: AB472ΔyhjH) lacking the endogenous PDE yhjH (a kind gift of Dr A. Boehm), was used to perform the PA4108, PA4781 and PA4781G complementation assays. This strain, which presents high level of c-di-GMP, was also transformed with the pet28b control vector, as negative control. Cultures were grown at 37°C in LB medium, 0,1 mM IPTG was added when OD was 0.8 and cells were harvested by centrifugation after 2 hours of further growth. Soluble cell extract was prepared as previously described (Antoniani*, et al.*, 2009) and the nucleotide content was analyzed by C8 reverse-phase column (Prevail 150x4.6mm, 5µm). Wild-type strain (MG1655) was used as reference of normal c-di-GMP levels.

Phosphodiesterase activity assay on soluble cell extracts

E.coli wild-type strain (BL21 (DE3)) overexpressing PA4781 or PA4781Gstart or PA4108 was used to analyze the PDE activity of these proteins in soluble cell extract. Cultures were grown in 25 ml of growth medium under constant shaking at 37°C until the cells reached late-exponential phase (OD_{600}= 0,8-

1,0). *E.coli* strain containing pET28 vector was grown under the same conditions, as control. Cells were harvested by centrifugation and resuspended in 4 ml of PDE buffer (50 mM Tris-HCl pH 8.0, 10 mM $MgCl_2$, 250 mM NaCl, 5 mM 2-mercaptoethanol, 1 mM PMSF, Complete EDTA-free protease inhibitor (Roche Diagnostics, Indianapolis)) and frozen overnight at -80°C, according to (Kulasakara*, et al.*, 2006). Cultures were than thawed on ice and sonicated. Synthetic c-di-GMP (final concentration 10 µM) was added to each lysate, and the reaction was allowed to proceed for 3.5 h at 30°C. The reaction was stopped by the addition of 2 ml of 1 M $HClO_4$ and, after neutralization with 2 M K_2CO_3 each sample was centrifugated (Kulasakara*, et al.*, 2006). The supernatant was evaporated to dryness using a Speed Vac, resuspended in 500 µl of HPLC-running buffer (100mM NaPhO pH 5.8), filtered with 2µm filters and analyzed by HPLC, as described above. We performed at least two independent assays for each sample and c-di-GMP peak in each sample was compared with that detected in the extract from the control strain, after incubation whit c-di-GMP, as described above.

3.2 New strategy for c-di-GMP detection and quantification.

General methods

CD experiments were carried out using quartz cuvettes (Hellma) with a path length of 1 cm on a JASCO J-710 spectropolarimeter. Spectra were baseline corrected by subtracting the buffer from the raw data and the signal was adjusted to zero at 340 nm as no optical activity is expected at this wavelength. HPLC analysis was performed as described above.

Influence of metal ions on c-di-GMP

To verify the influence of metal ions on the c-di-GMP dimer formation, samples containing 15 µM c-di-GMP (Biolog) in 20 mM Tris pH 8 and 100 mM NaCl were analyzed in the presence of 2.5-10 mM of $MnCl_2$, and/or $MgCl_2$. CD spectra were measured at 10°C. To obtain the calibration curves, increasing concentrations of c-di-GMP (1, 5, 10, 15, 20, 25 and 30 µM) in 20

mM Tris pH 8, 100 mM NaCl, 10 mM $MgCl_2$, 1 mM $BeCl_2$, 10 mM NaF and 2.5 mM $MnCl_2$ (reaction buffer of PleD) were analyzed. The same profile is obtained in the absence of BeF_3^- (data not shown). CD analysis was performed in duplicates at 10°C, 25°C and 37°C.

Analysis of manganese affinity for c-di-GMP

Increasing concentrations of $MnCl_2$ (0.2 to 15 mM) were added to a sample containing 15 µM c-di-GMP (Biolog) in 50 mM Tris pH 7.5, 150 mM NaCl and 10 mM $MgCl_2$. CD spectra were recorded at 10°C after allowing the samples to equilibrate for 10 minutes. A K_D of 262 ± 36 µM for the c-di-GMP-Mn_{2+} complex was calculated by fitting the observed CD_{282} signal as a function of $MnCl_2$ concentration.

CD spectra of other nucleotides

The CD spectra of 15 µM pGpG (Biolog), c-di-GMP, GMP (Sigma Aldrich) and GTP (Amersham Bioscience) and c-di-AMP (Biolog) were recorded in 50 mM Tris pH 8, 150 mM NaCl, 10 mM $MgCl_2$ and 2.5 mM $MnCl_2$. The spectra vary slightly with buffer conditions. The concentration of stock solutions of GTP and GMP was determined by measuring the absorption at 253 nm using 13,700 M^{-1} cm^{-1} and 13,300 M^{-1} cm^{-1} as molar extinction coefficients.

Kinetic studies

To study the diguanylate cyclase activity of purified *Caulobacter crescentus* PleD, a 0.5 µM enzyme solution was incubated for 10 minutes at room temperature in 20 mM Tris pH 8, 100 mM NaCl, 10 mM $MgCl_2$. The enzyme was then activated by adding 1 mM $BeCl_2$ and 10 mM NaF and kept at room temperature for 30 minutes. The diguanylate cyclase reaction was performed at 20°C in the presence of 2.5 mM $MnCl_2$ and was started by adding 100 µM GTP; the time course of the reaction was followed by directly measuring the CD signal at 282 nm. In parallel, the reaction was followed under the same experimental conditions but aliquots were taken at different times (1, 3, 5, 10,

30 and 60 min), samples were boiled for 10 min to stop the enzymatic reaction, spun down and filtered to remove the precipitated protein. The samples were then analyzed both by CD spectroscopy at 20°C and by reverse phase HPLC as described above. The experiment was performed in duplicate. PleD was purified as previously described by Wassmann and coll. (Wassmann, *et al.*, 2007). The enzymatic activity of Beryllium-activated PleD was found to be 20 nmol/min/mg, in good agreement with the value previously published (Paul, *et al.*, 2004) (Paul, *et al.*, 2007).

To study the phosphodiesterase activity of *Pseudomonas aeruginosa* RocR, a 0.5 µM enzyme solution was incubated for 10 minutes at room temperature in 20 mM Tris pH 8, 100 mM NaCl, 5 mM $MgCl_2$, 2.5 mM $MnCl_2$. The reaction was performed at 20°C and was started by adding 30 µM c-di-GMP. The enzymatic reaction was followed in real-time at 282nm. In parallel, aliquots were taken at different times (3, 5, 15, 30 and 45 min), and 100mM CaCl2 or 25mM EDTA pH 6.0 were added to stop the enzymatic reaction; samples were boiled for 10 min, spun down and filtered to remove the precipitated protein. Samples were then analyzed by CD spectroscopy at 20°C and by RP-HPLC. The experiment was performed in duplicate. RocR was expressed in BL21(DE3) strain transformed with pProExHTb-RocR (a kind gift of Prof. H. Sondermann, CH) and purified as previously described by De and coworkers (De, *et al.*, 2008). The turnover number of RocR was found to be 0.1 s^{-1}, somewhat slower than the value previously published (0.67 s^{-1}), in which the activity was measured by following the production of pGpG at 23°C in the presence of 25 mM $MgCl_2$ (Rao, *et al.*, 2008); this difference is not surprising given the different experimental conditions employed in the present work (lower temperature and $MgCl_2$ concentration).

To analyze by CD spectroscopy the phosphodiesterase activity of PA4781 the sample was prepared as previously described for HPLC analysis; the enzymatic reaction was followed at 30°C in real-time at 282nm.

Titration of PleD with c-di-GMP.

To study the binding of c-di-GMP to PleD, increasing concentrations of c-di-GMP were added to a sample containing 10 µM of PleD in 20 mM Tris pH 8, 100 mM NaCl, 10 mM $MgCl_2$, 1 mM $BeCl_2$, 10 mM NaF. CD spectra were taken at 25°C after equilibration of the system. The spectra of the samples

containing 25, 30, 35 and 40 μM c-di-GMP were measured again after the addition of MnCl2 to a final concentration of 2.5 mM. The order of addition of the three components in the mixture (i.e. PleD+c-di-GMP+Mn^{2+} or c-di-GMP+PleD+Mn^{2+} or c-di-GMP+PleD+Mn^{2+}) did not change the final spectrum (data not shown). The experiment was performed in triplicate. The experiment was performed in triplicate.

RESULTS and DISCUSSION

4.1 HD-GYP characterization

Previous *in vivo* studies (Ryan, *et al.*, 2009) have shown that two HD-GYP proteins from *P.aeruginosa*, PA4781 and PA4108 (see tab 1.1), are involved in the control of swarming motility and production of virulence factors, leading to increased levels of c-di-GMP in mutant strains (Ryan, *et al.*, 2009). In order to get a deeper insight into these HD-GYP-mediated responses and their reaction mechanism, we decided to characterize *in vitro* the PDE activity of both PA4781 and PA4108, produced as recombinant proteins expressed in *E.coli*.
The characterization of phosphodiesterase activity requires the analysis of nucleotide content in the reaction mixture, which can be carried out by different methods (discussed in more detail later). One of the widely used approach for studying both DGCs and PDEs is based on the reverse phase chromatography. Basically, an aliquot of the reaction is analysed through this technique at different times, following the removal of the protein content (by boiling and filtration). The c-di-GMP detection method was set up and implemented in the group during the first part of my PhD.

Optimization of reverse phase chromatography method

In order to optimize the nucleotide separation by HPLC on a c8 reverse phase column, several elution buffers were tested. The retenction time of GMP (GE healtcare), pGpG (biolog) and c-di-GMP (biolog) was assayed using as mobile phase different concentrations of sodium phosphate buffer (NaPhO) mixed with several concentrations of methanol or acetonitrile. The optimum separation was obtained by mixing 98% of 100 mM NaPhO pH 5.8 (buffer A) and 2% Methanol absolute (buffer B) (fig. 4.1A).

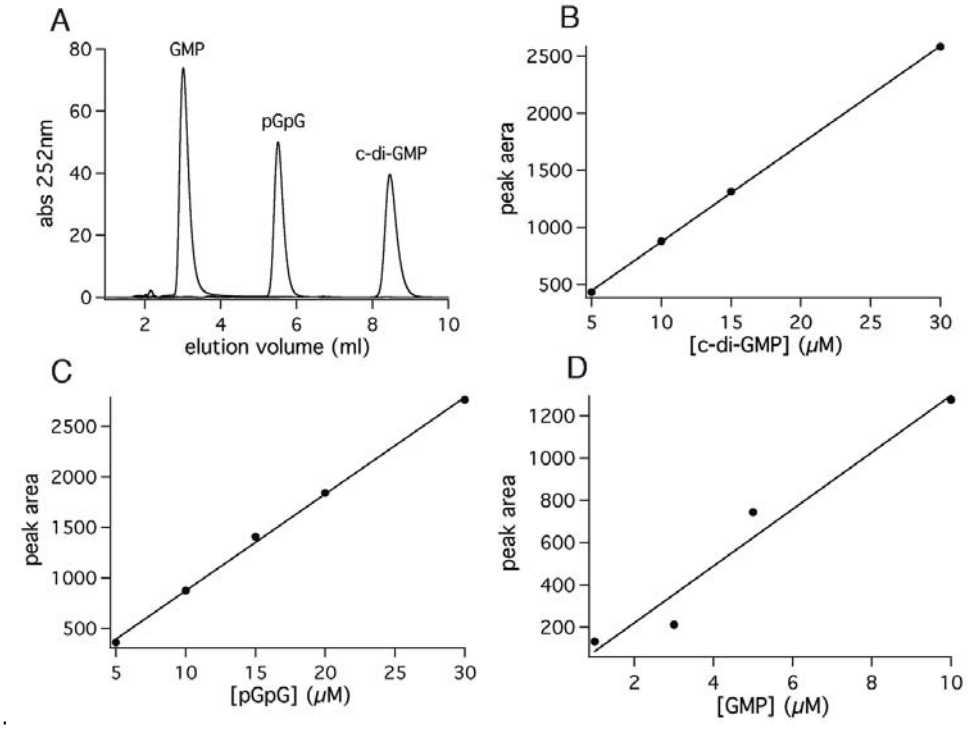

Figure 4.1. A) HPLC profile of GMP, pGpG and GMP; B,C and D) nucleotides calibration curves.

Different concentrations of these nucleotides were than analyzed under these elution conditions (fig. 4.1, B,C and D panels), in order to obtain a linear correlation between peak area and the nucleotide concentration. These calibration curves were used to quantify the content of these nucleotides during the characterization of the enzymatic c-di-GMP hydrolysis.

PA4108

Purification and preliminary characterization - PA4108 is composed by a HD-GYP catalytic domain and by an uncharacterized domain (NTD) located at the N-terminus of the protein (fig. 4.2).

Figure 4.2. PA4108 domain organization: N-terminal uncharacterized domain (NTD) and C-terminal HD-GYP catalytic domain.

Synthetic PA4108 gene was purchased from Geneart subcloned into the Pet24b vector in frame with 6xHistidine tail at the C- terminal of the protein (pET-PA4781-HIS). Initially, the BL21(DE3) *E. coli* strain was transformed with the pET-PA4781-HIS plasmid and the protein was expressed in the presence of 0,1 mM IPTG; bacterial growth was stopped in the mid-log phase, since the prolonged over-expression of this protein strongly slowed down the exponential phase of cellular growth. This behaviour may suggest that this protein could be involved in the regulation of bacterial cell cycle. Under these growth conditions, we obtained very low yield of purified protein (0,006 mg/l), which presents a very low solubility.

In order to obtain higher levels of soluble protein, the expression was also carried out in BL21plysS (DE3) *E. coli* strain; this expression condition was choose to purify PA4108, even though also in this background, low yield of purified protein (2 mg/l) was obtained.

The analysis of the aggregation state of purified PA4108, obtained by gel filtration chromatography in 20 mM TRIS pH 7.6, 150 mM NaCl (fig. 4.3A), revealed that PA4108 is mainly a monomer in solution and that higher aggregation states are not significantly populated.

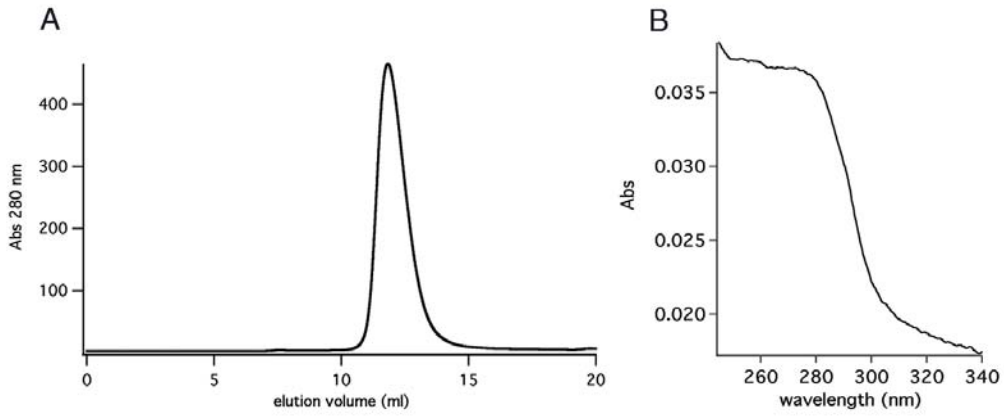

Figure 4.3. A) PA4108 gel filtration profile (superdex 75): the elution volume was 11,84 ml corresponding to a molecular weight of 45kDa, indicating that PA4108 is mainly a monomer in solution. B) UV-spectrum (250-340nm): the high absorption contribution below 270 nm is typical of nucleotide species.

The spectroscopic analysis of purified PA4108 has shown an UV-Vis spectrum (250-340 nm) with a broadened peak ranging between 260-280 nm (fig. 4.3B), with high absorption contribution below 270 nm, typical of nucleotide species. It is, indeed, reported in the literature that proteins involved in c-di-GMP turnover are purified in association with this nucleotide (De, *et al.*, 2009; Paul, *et al.*, 2007); it is not excluded that, also in the case of PA4108, a fraction of c-di-GMP co-purified with the protein. In order to verify this hypothesis, the protein content was removed by boiling the sample and the nucleotide content was analyzed by reverse phase HPLC. A small but significative amount of c-di-GMP and pGpG was observed, thus demonstrating that a small fraction of the protein (~4%) was purified in complex with these nucleotides.

Pde activity assays - As mentioned in the introduction, PDEs require metal ions for the phosphodiester hydrolysis (Christen, *et al.*, 2005). For this reason, we first tested the c-di-GMP hydrolytic activity incubating the purified PA4108 for 4 hours with excess of substrate in the presence of Mg^{2+} and/or Mn^{2+}, since a large number of enzyme involved in c-di-GMP synthesis and degradation need these metal ions to be catalytically active. The analysis of nucleotide content, performed by reverse phase HPLC, revealed that PA4108 need both Mg^{2+} and Mn^{2+} to hydrolyze c-di-GMP (tab. 4.1). Moreover several pH (7.5-9) and temperature (25-37°C) were tested, identifying the optimum at pH 8 at 30°C.

Metal ion	**c-di-GMP hydrolyzed (μM)**
2,5 mM Mn^{2+}	1,46
10mM Mg^{2+}	1,58
2,5mM Mn^{2+}+ 10mM Mg^{2+}	2,3

Talbe 4.1: c-di-GMP hydrolysis in the presence of different metal ions. PA4108 (0,73μM) was incubated for four hours at 30°C with 30μM substrate.

The c-di-GMP hydrolysis obtained under these experimental conditions demonstrates for the first time the activity of the purified PA4108 protein as c-di-GMP PDE (fig. 4.4).

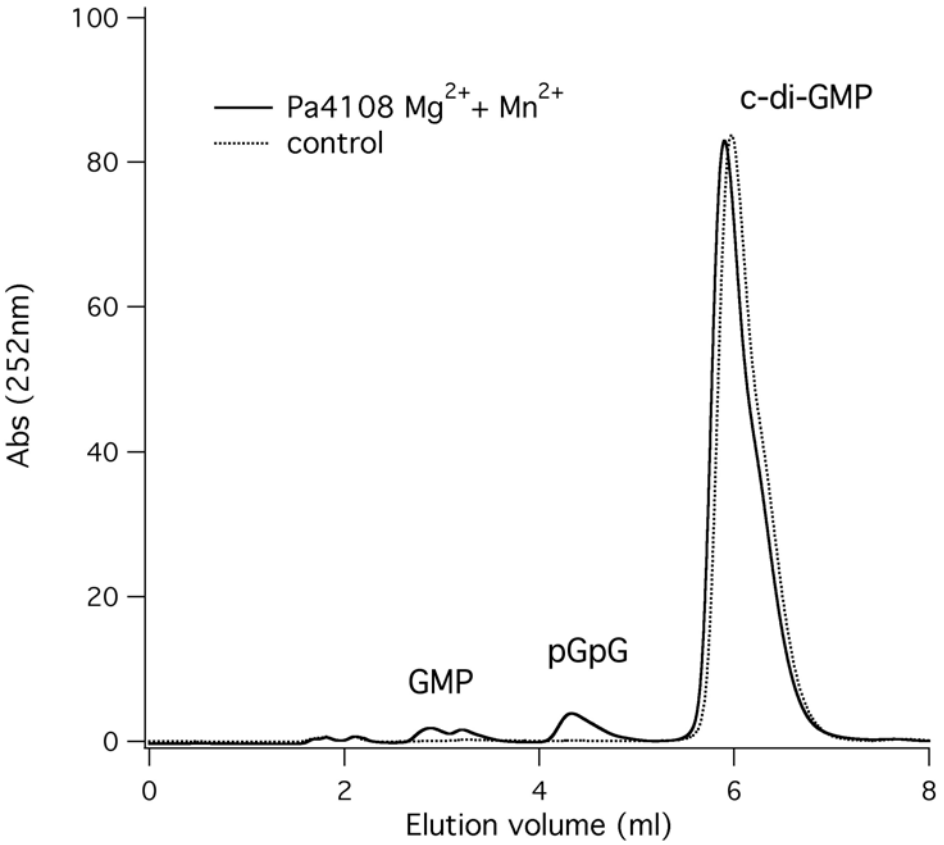

Figure 4.4. PA4108 c-di-GMP hydrolysis: 0.73 µM PA4108 incubated for 4 hours at 30°C with of 10 mM $MgCl_2$ and 2,5 mM $MnCl_2$.(bold line). As control the sample without the protein (dotted line) was also analysed.

However, a low fraction of substrate was hydrolyzed after four hours of incubation suggesting that under these experimental conditions PA4108 displayed a very low phosphodiesterase activity. In order to improve the hydrolysis of c-di-GMP, the K_M parameter was determined by analyzing the time course of c-di-GMP hydrolysis at different substrate concentrations (10, 60, 150, 300 µM c-di-GMP) (fig. 4.5). These experiments revealed that the K_M for c-di-GMP is ~160 µM, a value significantly higher than that typical of other catalytically active enzymes (for example RocR K_M=3,3 µM (Rao, *et al.*, 2008)).

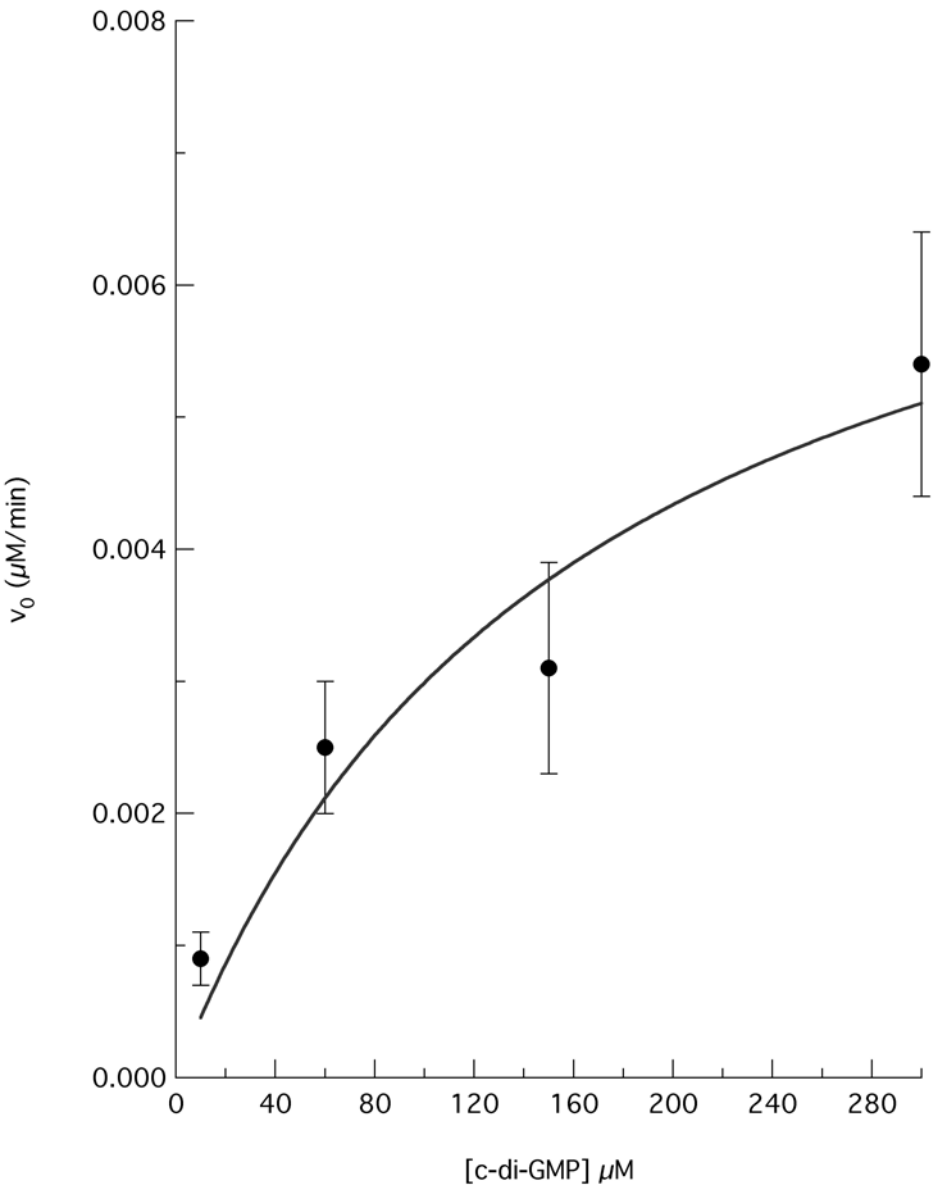

Figure 4.5. Plot of the initial rate of c-di-GMP hydrolysis measured at different c-di-GMP concentration (black circles). Date were then fitted with the Michaelis Menten equation (continous line) in other to extrapolate the Km and Vmax ($8 \cdot 10^{-3}$ μM/min) parameters

As mentioned in the introduction, the final product of c-di-GMP hydrolysis catalyzed by PDE-EAL subclass is pGpG (Hengge, 2009); this nucleotide undergoes further degradation by non-specific hydrolases in the cell. On the other hand, it has been attributed to the PDE-HD-GYP subclass capability to

further hydrolyse pGpG to GMP (Ryan, *et al.*, 2006) as confirmed also by our data (fig. 4.4); for this reason, it is not excluded that the HD-GYP proteins are able to hydrolyze exogenous pGpG used as a substrate. The hydrolytic activity of PA4108 toward pGpG was assayed using pGpG (30 μM) in the absence of c-di-GMP; the result indicates that a small fraction of pGpG was indeed converted in GMP, thus demonstrating that, although low, PA4108 does display a pGpG hydrolase activity (data not shown).

PA4781

PA4781 is composed by a HD-GYP catalytic domain and by a CheY-like regulatory domain (REC-domain) located at the N-terminus of the protein (fig. 4.6). Synthetic PA4781 gene was purchased from Geneart subcloned into the Pet28b plasmid in frame with 6xHistidine tail at the N- terminal of the protein.

Figure 4.6. PA4781 domain organization: N-terminal CheYlike regulatory domain (REC domain) and C-terminal HD-GYP catalytic domain

Purification and preliminary characterization - The BL21(DE3) *E. coli* strain was transformed with pET-PA4781-HIS plasmid and the protein was expressed in the presence of 0,1 mM IPTG. Contrary to PA4108, the presence of the IPTG inducer from the beginning of the bacterial growth does not alter the growth profile, as compared to the control strain lacking the PA4781 gene. This setup allows us to purify to the homogeneity PA4781 in good yields (10 mg/l).

It was found by gel filtration chromatography that the protein is mainly in the monomeric state (fig 4.7A).

The UV-Vis spectra (250-400 nm) of purified PA4781display a single peak at 280 nm without any other peaks in the 250-260 nm range; this feature suggests that the purified protein does not contain a significant fraction of nucleotide species, contrary to PA4108 (fig. 4.7B).

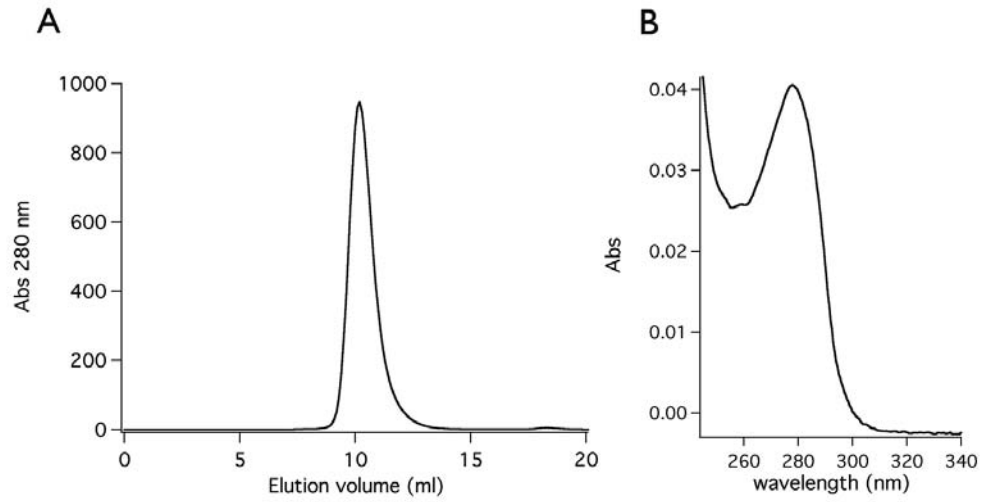

Figure 4.7. A) PA4781 gel filtration profile (superdex 75): PA4781Mw=43kDa, the elution volume of 10,2 ml, corresponding to a molecular weight of ~60kDa, indicates that PA4781 is mainly a monomer in solution. B) UV-spectrum (250-340nm): no absorption peaks below 270 nm.

PDE activity assay - As described for PA4108, the enzymatic assays were carried out in the presence of Mg^{2+} and/or Mn^{2+} by incubating the protein for four hours with synthetic c-di-GMP and analysing the nucleotide content in the reaction mixture by reverse phase HPLC (see methods). The absence of peaks corresponding to the products in the resulting chromatograms indicated that no hydrolysis has occurred (not shown); this evidence suggests that, under these experimental conditions, PA4781 is not active. No hydrolytic activity was observed also using pGpG as substrate.

A sequence alignment (fig 4.8) of several HD-GYP proteins revealed that PA4781 contains a suboptimal signature in the catalytic domain, being the canonical tyrosine in the GYP signature substituted with a phenylalanine residue in PA4781. It is not excluded that the presence of a suboptimal sequence in the GYP signature may account for the lack of catalytic activity observed with PA4781. For this reason, the phenylalanine residue (F290 in the sequence) in the GYP signature has been substituted with a tyrosine, by site-directed mutagenesis and the enzymatic activity was assayed; despite the mutation, no c-di-GMP hydrolysis was observed, suggesting that the GYP

signature is not necessary or sufficient for catalysis (Lovering, *et al.*, 2011; Ryan, *et al.*, 2010).

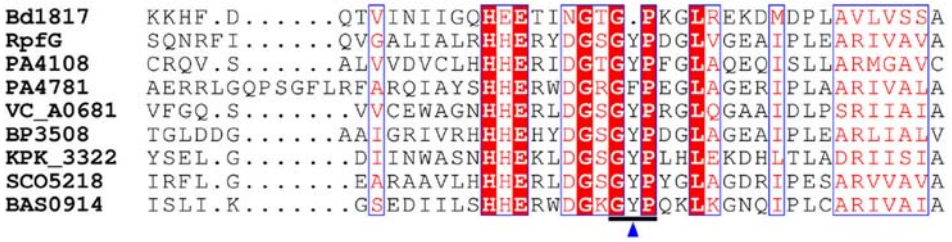

Figure 4.8. PA4781 sequence is indicated by black arrow. The GYP signature is indicated by blue triangles. Conserved residues are boxed in white font on a red background, and partially conserved residues are boxed in red font on a white background (Lovering, *et al.*, 2011).

As mentioned above, PA4781 presents a regulatory REC domain upstream the catalytic one that belongs to a class of domains which requires the transfer of a phosphoryl group onto a conserved Aspartic acid acceptor residue (Paul, *et al.*, 2007). In many two-component regulators, the unphosphorylated receiver domain restricts the effector domain in an unfavourable conformation which reverts to a favourable one upon phosphorylation of the REC domain (Gao and Stock, 2010). This evidence suggests that the presence of this domain and the need of activation by phosphorylation, could be the cause of the observed PA4781 inactivity. In order to trigger REC domain activation, PA4781 has been incubated with berillium floride (BeF_3^-), a compound known to mimic the phosphoryl group (Paul, *et al.*, 2007). PA4781 enzymatic activity was then assayed in the presence of different concentrations of BeF_3^- (0,1-5 mM $BeCl_2$ and 0,3 -10 mM NaF); this setting does not activate the protein, thus suggesting that the mechanism of activation of the REC domain of PA4781 is more complex then that of other proteins (Paul, *et al.*, 2007). The inactivity of PA4781 could be due to an inability to the recombinant form to bind the substrate c-di-GMP. The protein is indeed purified without any nucleotide bound, contrary to PA4108. The affinity for c-di-GMP was than probed by means of Isothermal Titration Calorimetry (ITC) approach (fig. 4.9), a technique which allows the determination of the thermodynamic profile of molecular interactions

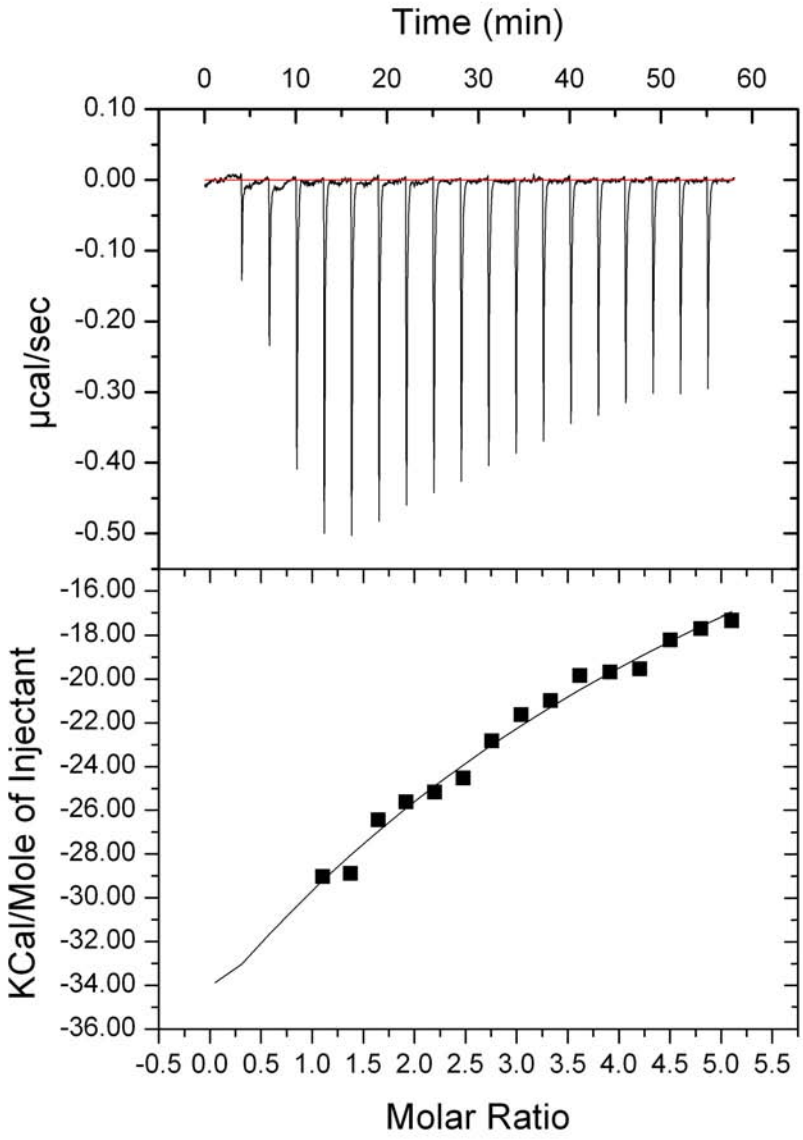

Figure 4.9. Microcalorimetric titration of 3 µM PA4781 with 80 µM c-di-GMP. Upper panel: Raw ITC data. As previously published (Paul, *et al.*, 2007), the calorimetric data obtained at very low c-di-GMP concentrations (first three injections) show a deviation from the simple binding model used to fit the data. This may be related to the varying degree of dimerization of c-di-GMP in solution (Paul, *et al.*, 2007). As reported for PleD, since the peculiar effect due to c-di-GMP dilution is limited to the first few injections and does not interfere with the sigmoidal part of the binding curve, these points have been eliminated from the fit. Lower panel: Integrated peak areas (black circles) and fit with the one-binding-site model of ORIGIN provided by MicroCal (continuous line).

As described in figure 4.9, PA4781 binds c-di-GMP with very low affinity (K_D > 100 μM) and no catalysis has followed upon nucleotide addition (confirming HPLC data). In such a contest, the low affinity does not allow us to saturate the protein in the ITC experiment and, consequently, to extrapolate the exact parameters. However, this result may suggest that the conformation of the HD-GYP domain, where c-di-GMP hydrolysis should occur, is not optimal for substrate binding. It is not excluded that phosphorylation of the REC domain triggers a conformational change also in the catalytic one; this event may constitute an high-affinity binding site for c-di-GMP which allow PA4781 to enter a catalytic cycle.

Characterization and enzymatic activity of PA4781G - In order to by-pass the limitation due to the REC domain activation, a truncated version of the protein lacking the entire REC domain has been produced by removing the first 111 residues (PA4781G) (fig. 4.10).

Figure 4.10. PA4781G Domain organization: mutant lacking the regulatory REC domain.

High yields of purified soluble PA4781G (9 mg/l) was obtained by growing the expression strain at 25 °C, in the presence of 0.1 mM IPTG. As previously observed for PA4108, the over-expression of this protein slowed down the exponential phase of cellular growth (8 hours compared to the 4 of the full-length protein).
It has been shown by gel filtration chromatography (fig. 4.11A) that the purified protein is mainly in the dimeric state.

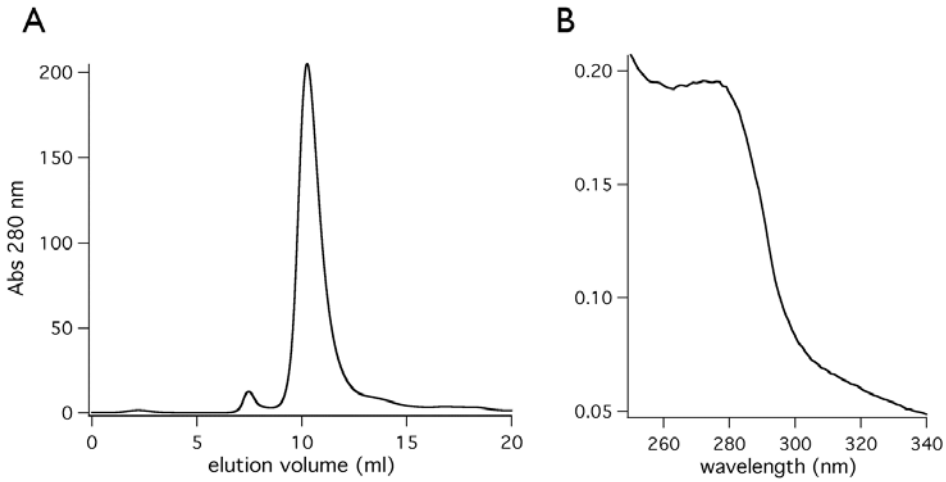

Figure 4.11. A) PA4781G gel filtration profile (superdex 75): PA4781G Mw=31kDa, the elution volume of 10,26 ml correspondent to a molecular weight of ~60kDa, indicate that PA4781G is mainly a dimer in solution. B) UV-spectrum (250-340nm): high absorption contribution below 270 nm typical of nucleotide species.

Interestingly UV-Vis spectra (250-400 nm) of purified PA4781G display a broadened peak ranging between 260-280 nm (fig. 4.11B); in agreement with previous hypothesis (see PA4108 characterization) the shape of this spectrum strongly suggests that the protein has been purified with nucleotides bound. The analysis of nucleotide content unveiled, indeed, that a small amount of pGpG and GMP was present, suggesting that a small fraction of the protein (~4%) binds both pGpG and GMP, contrary to PA4781 full length protein.
The catalytic activity of PA4781G was assayed as reported above; little but significative hydrolysis of both c-di-GMP and pGpG was observed (fig. 4.12) suggesting that the absence of the REC domain promotes the PDE activity. This evidence confirms that the activation of the regulatory domain is necessary for the hydrolytic activity.

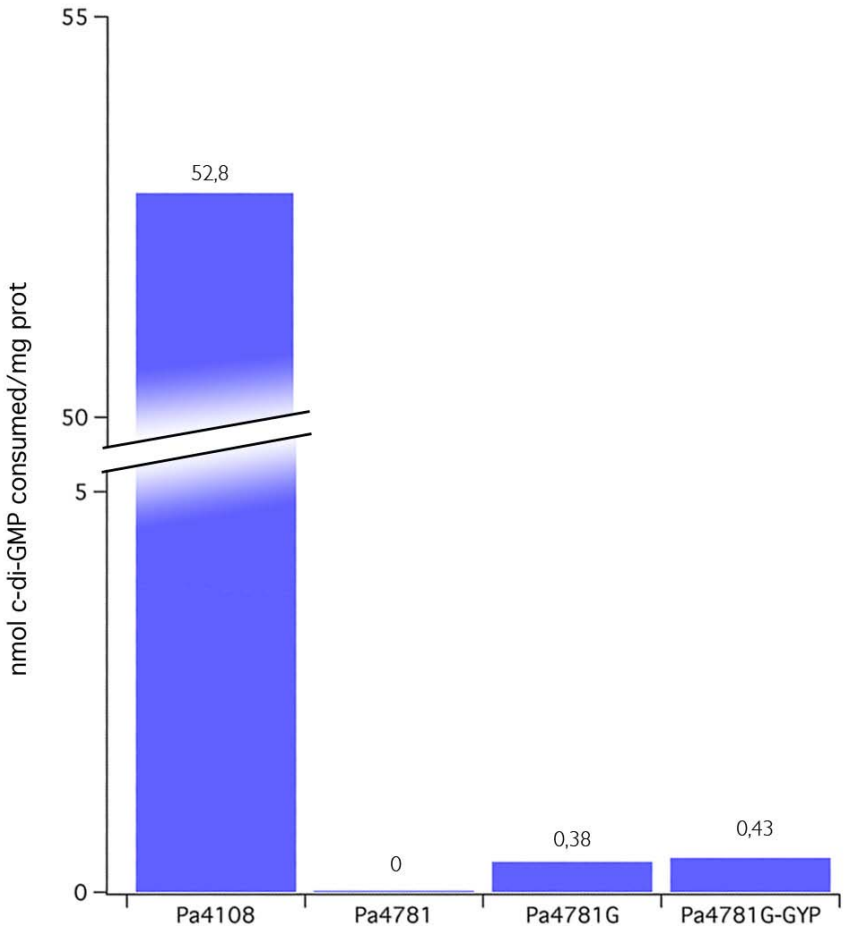

Figure 4.12. : Comparison of c-di-GMP hydrolytic activity of purified proteins.

The substitution of phenylalanine into tyrosine in the GYP signature was carried out also in this construct, even though, no significant increase in hydrolytic activities was observed (fig.4.12).

PDE activity in *E.coli* background

Our data on purified PA4781 full-length and PA4781G are not in agreement with that previously reported by Ryan and co-workers (Ryan, *et al.*, 2009), who demonstrated that *P.aeruginosa* mutant strains lacking PA4781 or PA4108 genes presents lowered c-di-GMP intracellular levels. Moreover these authors demonstrated that PA4781 complements mutation into a *X.campestris* mutant

strain lacking the endogenous HD-GYP *rpfG* gene (strain characterized by high c-di-GMP levels). In order to understand the difference observed between the present study on purified proteins and previous *in vivo* results, we decided to analyze the effect of PA4108, PA4781 full-length and PA4781G overexpression on *E.coli* intracellular c-di-GMP levels. Overexpression of these proteins was verified by Western analysis with antisera against the His6 tag tail (not shown).

The overexpression of these proteins was assayed using an *E.coli* strain mutant (AB1548), lacking the endogenous phosphodiesterase *yhjH*, which is characterized by higher levels of c-di-GMP. Intracellular content of c-di-GMP were determined by HPLC analysis and compared with those observed with the wild-type strain (MG1655) and with the AB1548 cells transformed with pet28b vector (as negative control).

The overexperssion of PA4108 results in a significant reduction of c-di-GMP intracellular levels (fig. 4.13), thus restoring the levels observed in the wild-type strain (MG1655); this evidence indicates that cellular environment strongly enhanced the activity of this protein compared to the low hydrolytic activity measured *in vitro* on purified protein.

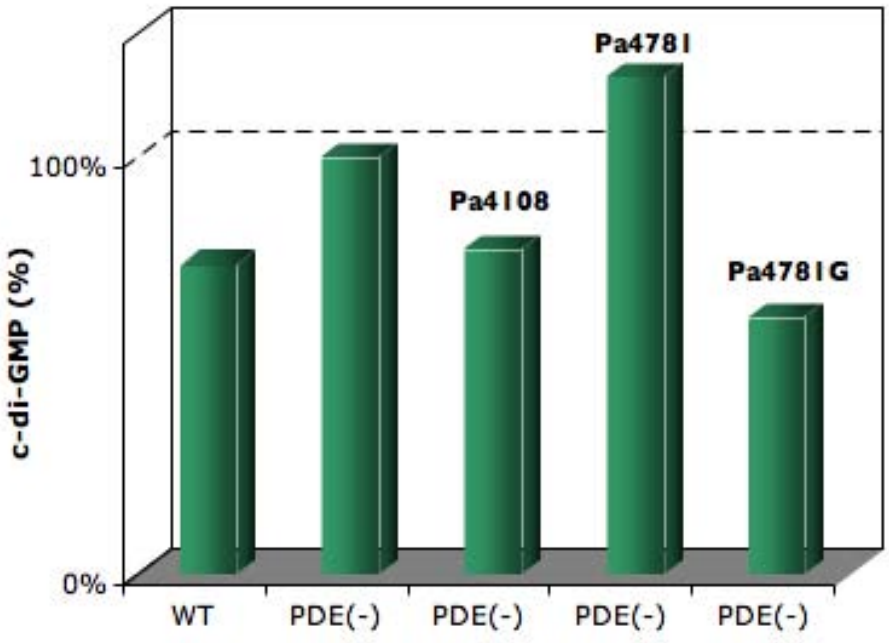

Figure 4.13. Effect of overexpression of PA4108, PA4781 or PA4781G on intracellular c-di-GMP levels of a *E.coli* mutant strain, lacking the endogenous DGC YhjH. As control, the *E.coli* wild-type strain was also analysed.

On the other hand, the overexpression of PA4781 protein did not alter c-di-GMP content compared to the same strain transformed with the control vector (fig. 4.13). This result, in agreement with data on purified protein, indicated that the REC domain of PA4781 full length cannot be allosterically activated in the *E. coli* background. It is not excluded that a specific kinase targeting PA4781 REC domain is required and absent in *E.coli*.
Surprisingly, a dramatic lowered c-di-GMP content was observed also in the strain transformed with PA4781G construct (fig. 4.13), which displays a nucleotides profile comparable to that found in the wild-type strain and in that expressing PA4108. This evidence indicates that, contrary to the full-length protein, the isolated catalytic domain of PA4781 is active in *E. coli* background. Moreover, also in the case of PA4781G, cellular environment strongly enhanced the PDE activity of the protein compared with that observed in the *in vitro* assay on purified protein.
In order to gain mechanistic insights on PDE catalysis, the enzymatic activity of the aforementioned proteins was assayed also on soluble cell extract of wild-type *E.coli* overexpressing strains. This experiment has been carried out also in a strain containing the sole pet28 vector as negative control. The assay was carried out through the addition of synthetic c-di-GMP to each cell extract and the consumption of this nucleotide was measured by reverse-phase chromatography, as previously described. According to the *in vivo* data described above, c-di-GMP hydrolysis was detected in the cell extract of the strain expressing PA4108 or PA4781G (fig. 4.14); these samples displayed c-di-GMP levels comparable to the negative control, thus confirming the capability of *E.coli milieu* to strongly improve the catalytic activity of these proteins. On the other hand, lack of c-di-GMP consumption in the PA4781 full-length sample confirms the inability of the *E. coli* background to trigger the enzymatic activity of the full-length protein (fig. 4.14).

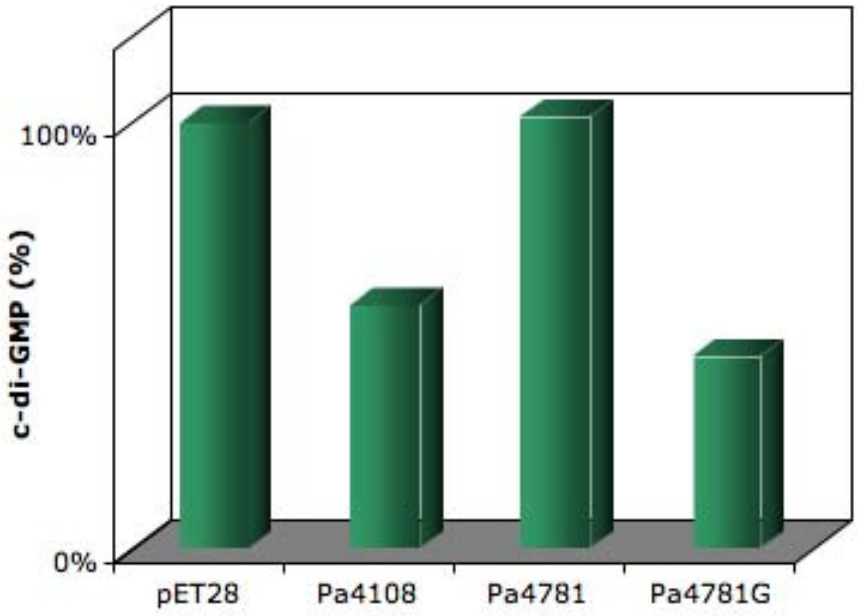

Figure 4.14. PDE activity on soluble cell extract of *E.coli* wild type strain transformed with PA4108, PA4781, or PA4781G. As contol, the wild-type strain containing the sole p28 vector was also analysed.

The discrepancy between data in *E.coli* cells and those obtained with PA4108 and PA4781G purified proteins may indicate that other species (possibly a partner or a cofactor lost during purification) assist these proteins during phosphodiesterase activity. This hypothesis is supported by literature data (Ryan, *et al.*, 2010) on a HD-GYP protein (RpfG) from the plant pathogen *Xanthomonas campestris* pv. *campestris* (Xcc) that demonstrated the interaction between RpfG and a subset of GGDEF domain-containing protein. It has been shown that the physical interaction between RpfG and these GGDEF proteins influence some of the biological effects controlled by RpfG such as the regulation of motility (Ryan, *et al.*, 2010).

Interestingly, the control of motility by RpfG-GGDEF-protein complex does not depend to the PDE and/or DGC activity of both proteins; the role of this interaction seems to be to recruit a specific PilZ domain protein implicated in controlling motility in *Xcc* (Ryan, *et al.*, 2012). It has been shown that protein-protein interaction among proteins controlling the c-di-GMP levels, could play a key role in regulating different cellular functions in several bacteria (Abel, *et*

al., 2011; Duerig, *et al.*, 2009; Newell, *et al.*, 2011; Tschowri, *et al.*, 2009). Our results suggest that also the HD-GYP proteins analysed in present study may need to interact with other cellular components to be active as PDE and to regulate different bacterial functions.

4.2 New stategy for c-di-GMP detection and quantification

As previously mentioned, the metabolic network involving c-di-GMP is highly complex and, despite the great effort in understanding the molecular basis of the c-di-GMP signalling pathways and the growing number of groups working on it, the exact molecular mechanism of c-di-GMP action remain to be fully elucidated. However, the dearth of detailed information regarding c-di-GMP signalling is probably due, also, to the lack of a rapid and unexpensive experimental strategy to readily detect c-di-GMP. In fact, despite several methods are available for c-di-GMP detection of, to date a strategy for *in vitro* detection and quantification of c-di-GMP is still not available for reliable real-time measurements (tab 4.2).

For this reason during my PhD, we developed a strategy that could provide significant advances and important clues to direct future experimental work on enzymes able to synthesize or degrade c-di-GMP (tab 4.2).

METHOD	REAL-TIME	ADVANTAGE	DISADVANTAGE	ENZYME ANALYSED		REF.
				DGC	PDE[a]	
Circular Dichroism*	YES	Pre-steady and steady-state kinetics	Micromolar detection limit	PleD	RocR PA4108	1
Thin Layer Chromatography (alfa^{32}P-GTP or ^{33}P-C-DI-GMP)	NO	Good Sensitivity (<µM)	Radiolabeled precursors required Enzyme inactivation step required prior analysis	PleD DosC [b] All2874[b]	 CC3396 PdeB (HD-GYP)	2-8
ENZ.CHECK Pyrophosphate Detection Kit® Coupled colorimetric assay (monitors PPi production)	YES	Steady state kinetics	Only valid for DGCs Upper limit for PPi detection (5 µM/min) Susceptible of Pi contamination	WspR XCC4471 PleD		9-11
MALACHITE GREEN Coupled colorimetric assay (monitors Pi production)	NO		Enzyme inactivation step required prior analysis Susceptible of Pi contamination	PleD[b]		12
Reverse Phase-HPLC Detection of nucleotides	NO	Nucleotides can be analysed by MS	Enzyme inactivation step required prior analysis	WspR[b] PleD PleD[b] HemDGC thermoDGC[b]	 RavR[b] RocR BlrP1 PA2567 PdeR RpfG (HD-GYP)	2, 9, 13-19
DYE(S) BINDING to c-di-GMP quadruplex	NO		Only valid for DGCs Limited Dye solubility Enzyme inactivation step required prior analysis Slow kinetics of complex formation	WspR		20, 21
Fluorescence (MANT-c-di-GMP)	YES (PDEs)	Steady state kinetics	Only valid for PDEs		MSDGC-1	22

Tabel 4.2. Analytical methods used to measure enzymatic c-di-GMP synthesis and degradation
Abbreviations: Pi: inorganic phosphate. PPi: inorganic pirophosphate.

(a) All c-di-GMP phosphodiesterases listed in the Table belong to the EAL-type PDEs, unless specifically indicated in brackets.; (b) qualitative analysis: catalytic parameters were not determined in the corresponding publication.; (c) due to lack of space the references are quoted as numbers in the table; the list of references is as below: **1)** (Stelitano, *et al.*); **2)** (Paul, *et al.*, 2004); **3)** (Christen, *et al.*, 2006); **4)** (Paul, *et al.*, 2007); **5)** (Tuckerman, *et al.*, 2009); **6)** (Neunuebel and Golden, 2008); **7)** (Christen, *et al.*, 2005); **8)** (Sultan, *et al.*, 2011); **9)** (De, *et al.*, 2008); **10)** (Yang, *et al.*, 2011); **11)** (Wassmann, *et al.*, 2007); **12)** (Chan, *et al.*, 2004); **13)** (Lai, *et al.*, 2009); **14)** (Sawai, *et al.*, 2010); **15)** (Rao, *et al.*, 2009); **16)** (He, *et al.*, 2009) **17)** (Rao, *et al.*, 2008); **18)** (Yang, *et al.*, 2012); **19)** (Ryan, *et al.*, 2006); **20)** (Nakayama, *et al.*, 2011)a; **21)** (Nakayama, *et al.*, 2011)b; **22)** (Sharma, *et al.*, 2012);

Formation of the complex between c-di-GMP and manganese

The method presented here is based on the specific CD signal displayed by the intercalated dimer of c-di-GMP and on the ability of manganese ions to promote dimerization of this cyclic dinucleotide. The CD profile of c-di-GMP shows two peaks in the absence of metal ions, one positive at 255 nm and one negative at 282 nm, similarly to that of left-handed Z DNA and inverted relative to right handed DNA and RNA (fig 4.15) (Zhang, *et al.*, 2006).

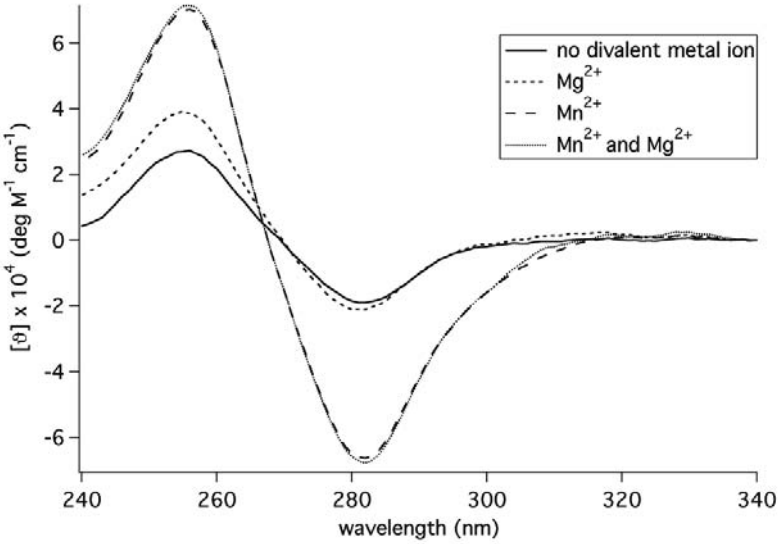

Figure 4.15. Influence of divalent metal ions on c-di-GMP dimer formation analyzed in 50 mM Tris-HCl pH 7.5, 150 mM NaCl, at 10°C. $MnCl_2$ and $MgCl_2$ were added to a final concentration of 2.5 mM and 10 mM, respectively.

A sigmoidal CD profile is obtained when two or more identical chromophores are in close proximity (Kelly and Price, 2000); in the case of c-di-GMP, which can form a stable dimer in solution, a strong hyperchromic effect is observed, as previously reported (Zhang, *et al.*, 2006), due to the stacking of the four guanine rings. Since divalent metal ions are known to shift the equilibrium towards the dimer (Zhang, *et al.*, 2004; Zhang, *et al.*, 2006), we have analyzed the c-di-GMP CD profile in the presence of Mn^{2+} and/or Mg^{2+}, which are normally added to the reaction buffer of DGCs and PDEs enzymatic assays. Surprisingly, while the influence of Mg^{2+} on the spectroscopic signal was not

significative, we found that the intensity of both 255 nm and 282 nm peaks increases in the presence of Mn^{2+} (fig 4.15). This is due to the formation of a stable complex between the intercalated dimer of c-di-GMP and the manganese hydrated cation. Titration of c-di-GMP with Mn^{2+} shows that the CD signal at 282 nm reaches a *plateau* for Mn^{2+} concentrations above 2,5 mM (figure 4.16, inset) suggesting that the complex is more than 95% populated above this threshold.

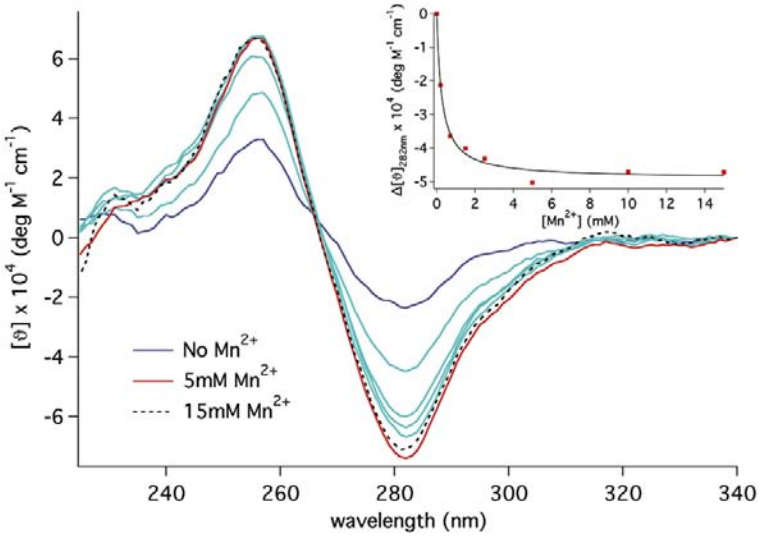

Figure 4.15. CD spectra of c-di-GMP showing the increase in the intensity of the dimer-specific peaks in the presence of increasing manganese concentrations, analyzed in 50 mM Tris-HCl pH 7.5, 150 mM NaCl, at 10°C. (Inset) Plot of the CD signal at 282 nm as function of Mn^{2+} concentration. 95% of signal saturation is observed at 2.5 mM $MnCl_2$ (i.e. K_D for c-di-GMP-Mn^{2+} complex formation of 262 ± 36 μM). The experimental data was fitted with a hyperbolic curve (continuous line). The signal is corrected for the Mn^{2+} free signal.

The different dichroic features of c-di-GMP in the presence of Mn^{2+} and Mg^{2+} were unexpected due to the similarity of many properties between the two cations. Only two structures of a c-di-GMP intercalated dimer were solved, in complex with Mg^{2+} or Co^{2+} respectively, both in the early 90s (Egli, *et al.*, 1990; Liaw, *et al.*, 1990). Our group in collaboration with Prof.ssa Filomena Sica (Università di Napoli Federico II), has solved the crystal structure of c-di-GMP in complex with Mn^{2+} in order to establish whether this cation, compared to Mg^{2+} (Egli, *et al.*, 1990), may induce any conformational changes in the

structural organization of the complex that could account for the different ability of the two divalent cations to populate the complex in solution. The crystal structure of the complex $[Mn(H_2O)_4(c\text{-di-GMP})_2]^{2+}$, determined at 0.9 Å resolution, is shown in figure 4.16.

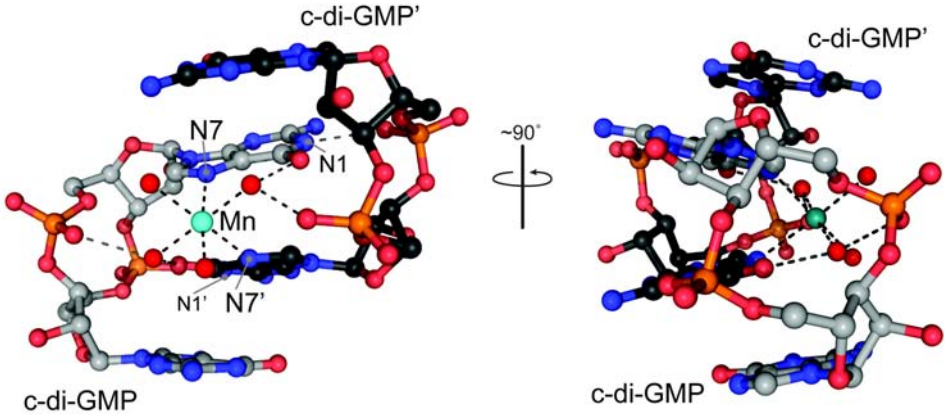

Figure 4.16. Ball and stick representation of $[Mn(H_2O)_4(c\text{-di-GMP})_2]^{2+}$. Two c-di-GMP molecules are kept together by a manganese ion (cyan), which is six-coordinated by four water molecules (red) and the N7 and N7' nitrogen atoms of guanines belonging to two different molecules. Each of the two axial water molecules is H-bonding to the carbonyl of one central guanine and to the oxygen of the cognate phosphate. The central base N1 of each molecule is hydrogen-bonded to the sugar phosphate backbone of the other. G-G base-pairing interactions stabilize both the dinucleotides and the overall assembly. Finally, The guanine rings coordinated to Mn^{2+} are forced out of the ideal coplanarity and appear partially unstacked similarly to the central bases of the complex with Mg^{2+} (Egli, *et al.*, 1990).

The structure shows non-significant differences with respect to that of the Mg^{2+}-c-di-GMP complex (Egli, *et al.*, 1990), indicating that the substitution of manganese with magnesium does not interfere with the assembly of the intercalated dimeric structure or with the binding mode of the metal ion. On the basis of these data it seems reasonable to assign the different effect of Mn^{2+} and Mg^{2+} on the dichroic spectra of c-di-GMP to the presence of d-electrons in Mn^{2+}, which contribute to the electrostatic interactions between the cation and guanine bases (Zhang and Huang, 2007) This is in agreement with the order of nucleotide-binding ability of divalent cations (Mg^{2+}< Co^{2+}< Ni^{2+}< Mn^{2+}< Zn^{2+}< Cd^{2+}< Cu^{2+}) deduced by empirical studies in the late 60's (Eichhorn and Shin, 1968), and with quantum chemical calculations, which suggest that the different action of Mg^{2+} and Mn^{2+} toward nucleobases derives

from the greater polarization and charge-transfer effects in the Mn^{2+} complexes (Solt, *et al.*, 2007; Sponer, *et al.*, 2004) Finally, comparative studies of the guanine ligand binding properties of Mn^{2+}, Zn^{2+}, Ni^{2+} and Mg^{2+} have demonstrated that the transition metals shows an higher affinity for the nucleobase N7 . This could determine the stabilization of the complex in the presence of Mn^{2+} (Zhang and Huang, 2007). Accordingly, an enhancement of the CD signal similar to that of Mn^{2+} was observed also in the presence of zinc and nichel divalent cations (data not shown).

The formation of the c-di-GMP-Mn^{2+} complex occurs rapidly, within five minutes at 10°C and within the mixing time at 25°C (data not shown). In the presence of 2.5 mM Mn^{2+}, the CD signal shows a linear dependence on c-di-GMP concentration; this linearity is maintained at the different temperatures analyzed (10, 25 and 37°C) (fig. 4.17).

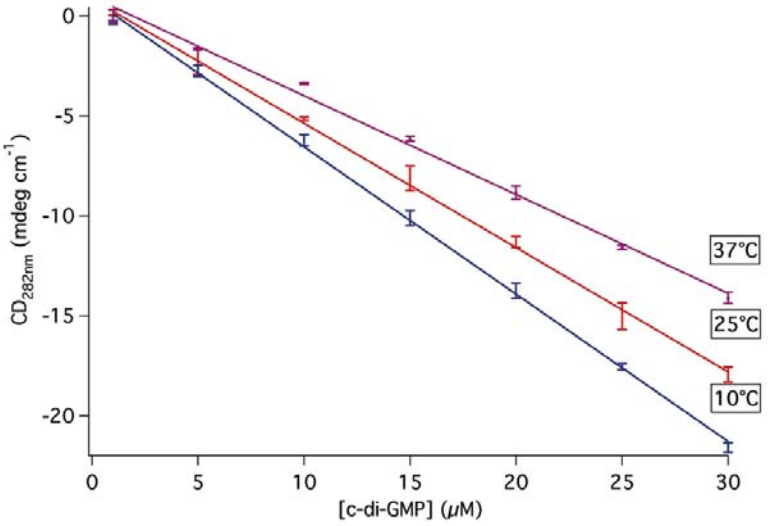

Figure 4.17. Linear dependence of the CD signal on c-di-GMP concentration. Analysis was performed at three different temperatures, i.e. 10, 25 and 37°C, in the following buffer: 20 mM Tris-HCl pH 8, 100 mM NaCl, 10 mM $MgCl_2$, 1 mM $BeCl_2$, 10 mM NaF and 2.5 mM $MnCl_2$. The CD signals at 282 and 255 nm show the same profile. The assays were performed in duplicate.

The CD signal of the samples is stable for at least 4 h in the temperature range needed for enzymatic reactions (10°C-37°C) and is also reproducible after a 12 h storage at 4°C (not shown), making this method adaptable to very

different protocols; from real time detection to multiple analysis of many stored samples. The very intense CD signature of the intercalated dimer is specific, thus c-di-GMP can be detected and quantified (even in the low μM range) in the presence of all the other nucleotides involved in c-di-GMP turnover. GTP and GMP are spectroscopically silent in the near-UV region, while pGpG displays a CD spectrum with a single band at 255 nm that possibly originates from the coupling of the two guanines, which are in close proximity (fig. 4.18). However, since it does not significantly contribute at 282 nm, the presence of pGpG does not hamper the quantification of c-di-GMP at 282 nm (fig. 4.18).

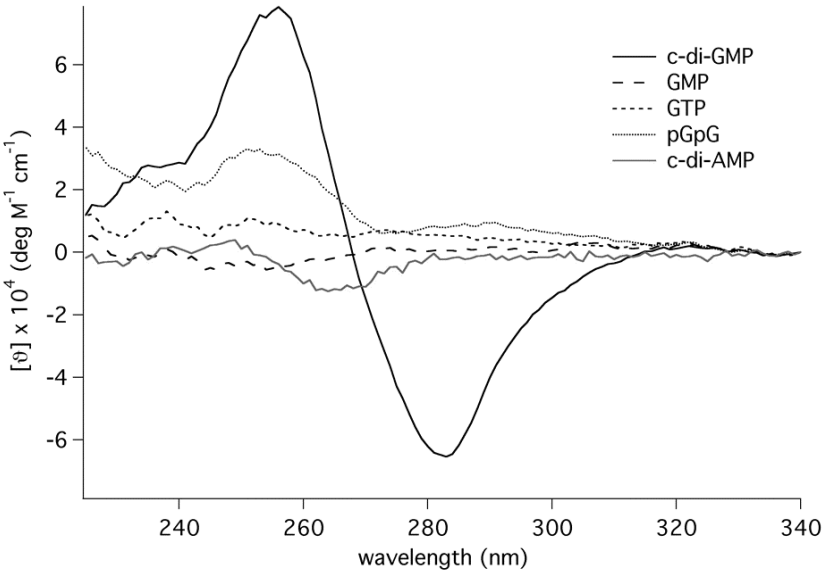

Figure 4.18. CD spectra of the nucleotides involved in c-di-GMP turnover. The nucleotides were analyzed at the concentration of 15 μM at 10°C in 50 mM Tris-HCl pH 7.5, 150 mM NaCl, 10 mM $MgCl_2$ and 2.5 mM $MnCl_2$. The spectrum of cyclic-di-AMP is also shown to compare the behaviour of the two cyclic dinucleotides (c-di-GMP and c-di-AMP).

To assign the spectroscopic signature seen by CD to the stacking of the guanine bases, we have also measured the spectrum of another dinucleotide, i.e. 3'-5' cyclic diadenilic acid (c-di-AMP): as shown in figure 4.18 this dinucleotide shows a much lower intensity and a different profile in the presence of Mn ions with respect to c-di-GMP. The observation that c-di-AMP

does not show the same spectroscopic signature of c-di-GMP strongly suggests that the sigmoidal CD signal arises from the stacking of the guanine bases. A comparison of the chemical structure of c-di-GMP and c-di-AMP highlights that the difference in the substituents in position N1 and the absence of the carbonyl group in the purine ring of c-di-AMP may disfavour the formation of a stacked dimer by c-di-AMP (fig. 4.19).

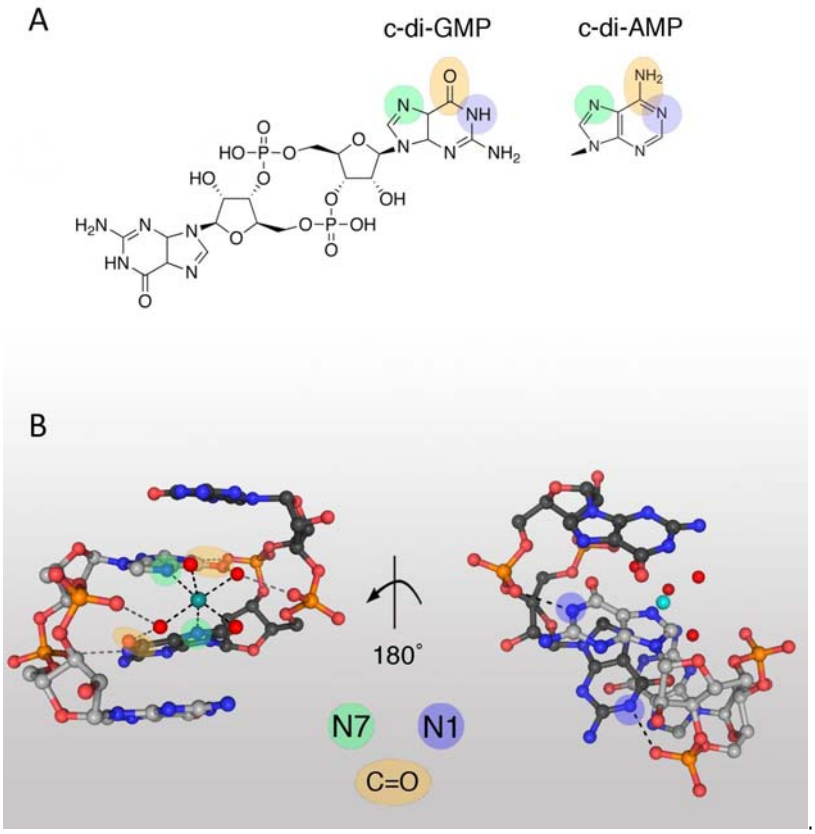

Figure 4.19. A) Position of N1, N7 and carbonyl in the purine ring of guanine compared to adenine. These atoms are involved both in dimer formation and in metal ion coordination, as illustrated in B), where they are highlighted in cyan, green and yellow respectively. N1 is involved in the formation of the c-di-GMP dimer serving as a donor in the H-bond between N1 and O2 of the cognate molecule. This H-bond cannot be formed by an hypothetical c-di-AMP dimer since in adenine N1 is a hydrogen acceptor. N7 and the carbonyl are recruited for metal ion coordination, with N7 of the two central purines occupying two equatorial positions, while the carbonyl together with an oxygen of the cognate phosphate are H-bonding to the two water molecules in the axial position. In the purine ring of adenine, given that an amino group substitutes the carbonyl, this interaction cannot be established.

Probing the enzymatic activity of DGCs and PDEs in real-time

The formation of the c-di-GMP/Mn^{2+} complex allows measuring c-di-GMP concentration in the working range typical of DGCs and PDEs enzymes. We have used the CD analysis to measure the enzymatic activity of two reference enzymes, i.e. PleD, a well characterized DGC from *Caulobacter crescentus* and RocR from *Pseudomonas aeruginosa*, an EAL-type PDE (Paul*, et al.*, 2004; Rao*, et al.*, 2008).

The time course of the reactions catalysed by these two enzymes was measured in real-time at 282 nm as shown in Figure 6 (panels A and B, respectively). The reaction rates were found to be in good agreement with the published values (Paul*, et al.*, 2007; Paul*, et al.*, 2004; Rao*, et al.*, 2008) (see Methods). As a control, the time course was also measured by extracting the nucleotides from aliquots of the reaction mixture taken at given times; these aliquots were then analyzed in parallel both by CD spectroscopy and by reverse phase HPLC chromatography, the most common method to quantify c-di-GMP (Antoniani*, et al.*, 2009). The results obtained by CD analysis (point measurements) are fully consistent with data obtained by reverse phase HPLC. The comparison of the kinetics as followed by real-time measurements with that obtained by point measurements (see Figure 6) clearly shows (more evidently in the case of RocR) that the real-time approach is an absolute requirement for an accurate determination of the time course of the reaction. The time-course of the reaction of RocR was also measured in the absence of Mn^{2+} (with Mg^{2+} ions alone), and no difference was observed in the kinetic parameters (data not shown), suggesting that the real-time measurement can be carried out, if needed, also in the presence of Mg^{2+} ions alone (using a consistent calibration curve).

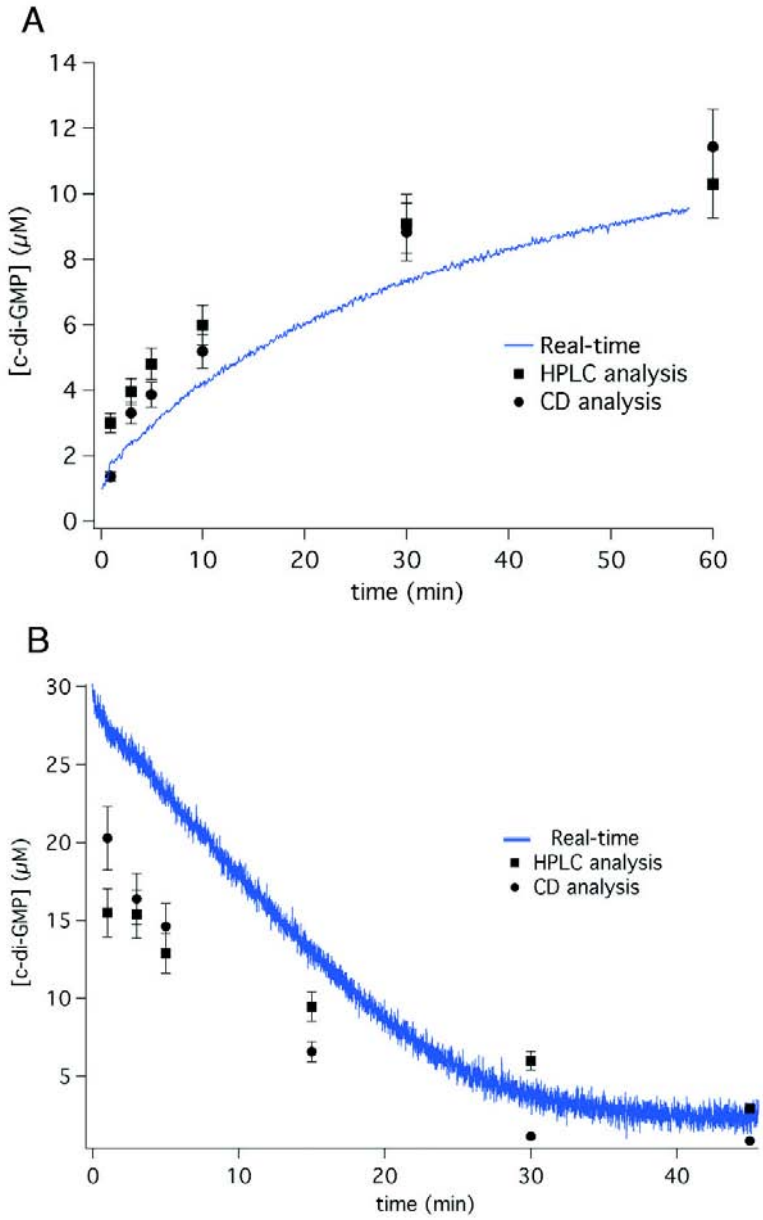

Figure 4.20. Time course of the reaction catalyzed by the diguanylate cyclase PleD (Panel A) and by the phosphodiesterase RocR (Panel B) as monitored in real-time by following the CD signal at 282 nm at 20°C (continuous line). As a control, the concentration of c-di-GMP in individual samples taken at given times during the reaction was determined separately by CD spectroscopy (black circles) and reverse-phase HPLC (black squares). All assays were performed in duplicate. The diguanylate cyclase activity of PleD (0.5 μM) was monitored using 100 μM GTP (Panel A). The phosphodiesterase activity of RocR (0.5 μM) was monitored using 30 μM c-di-GMP (Panel B).

The time course of the reactions catalysed by the HD-GYP protein PA4108 was, also measured in real-time at 282 nm as shown in figure 4.21. Although, the CD signal at 282 nm is small due to the low activity of the protein, data obtained using the CD spectroscopy-based strategy, also in this case, are fully consistent with data obtained by reverse phase HPLC (point measurements) (fig. 4.21)

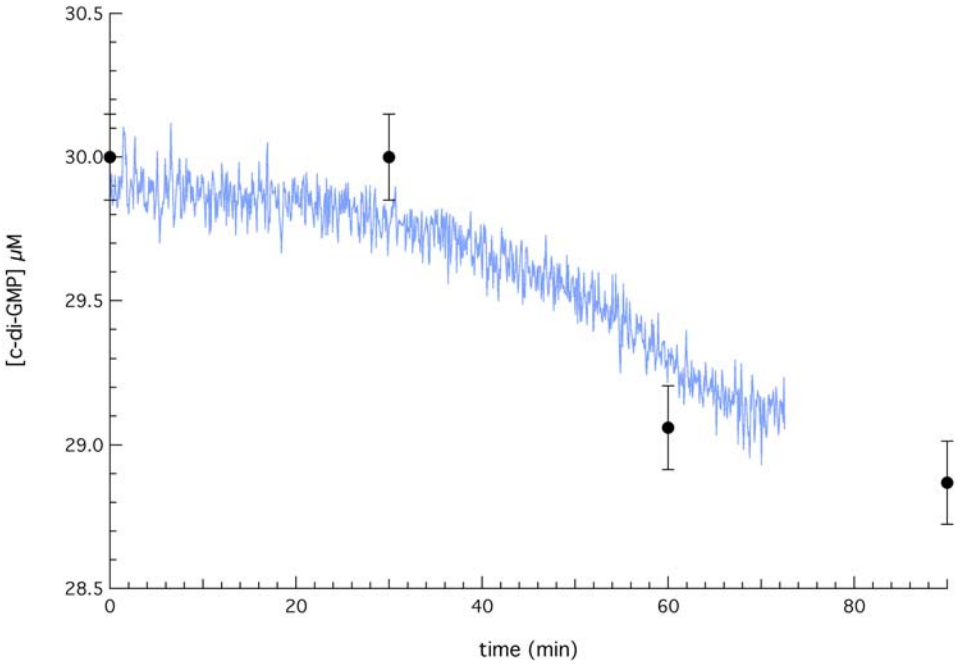

Figure 4.21. Time course of the reaction catalyzed by the the phosphodiesterase HD-GYP PA4108 as monitored in real-time by following the CD signal at 282 nm at 30°C (continuous line). As a control, the concentration of c-di-GMP in individual samples taken at given times during the reaction was determined by reverse-phase HPLC (black circles). All assays were performed in duplicate. The phosphodiesterase activity of PA4108 (1,4 μM) was monitored using 30 μM c-di-GMP.

Interestingly, we have also observed that, in the presence of the diguanylate cyclase PleD, the CD signal of c-di-GMP increases even in absence of manganese in the buffer (fig. 4.22, black circles). This is due to c-di-GMP binding to the enzyme inhibitory site as an intercalated dimer (Chan, *et al.*, 2004) with a similar structure of the c-di-GMP-Mn^{2+} complex (fig. 4.16).

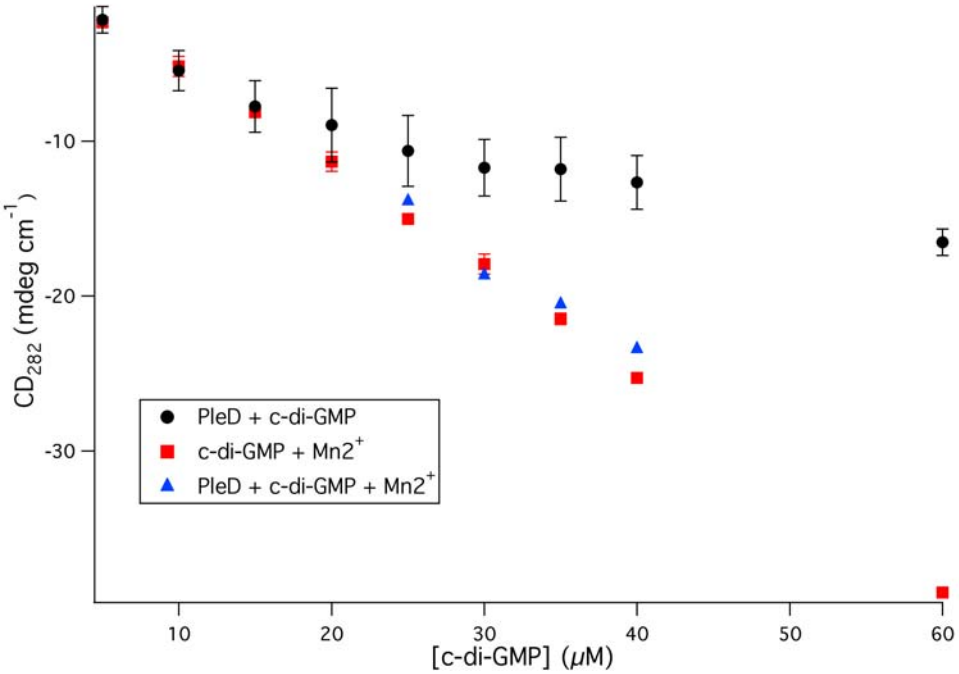

Figure 4.22. Plot of the CD signal at 282 nm of samples containing increasing amounts of c-di-GMP in presence of 10 μM PleD (monomer) (black circles) or 2.5 mM $MnCl_2$ (red squares). Addition of 2.5 mM $MnCl_2$ to the samples containing 25, 30, 35 and 40 μM c-di-GMP and 10 μM PleD yields the same CD signal (blue triangles) of the manganese-alone samples. Experimental conditions: 20 mM Tris-HCl pH 8, 100 mM NaCl, 10 mM $MgCl_2$, 1 mM $BeCl_2$, 10 mM NaF. The assays were performed in triplicate.

Accordingly, titrating PleD with c-di-GMP the CD signal increases linearly with c-di-GMP concentration until all the inhibitory sites of PleD are saturated (i.e. a PleD:c-di-GMP binding stoichiometry of 1:2) (fig. 4.22). Further addition of c-di-GMP does not correspond to a significant increase of the signal given that, in the absence of free binding sites, c-di-GMP is prevalently monomeric. Addition of manganese to the titration solution results in a further increase in the intensity of the signal, which indicates a shift of the equilibrium of free c-di-GMP towards the dimeric form (fig. 4.22 blue triangles). This result confirms that a sigmoidal CD spectra peaking at 255 and 282 nm can be regarded as the spectroscopic fingerprint of the intercalated dimer.

CONCLUSIONS

The involvement of the bacterial second messenger c-di-GMP in controlling biofilm formation and stimulation of the host immune system represents an hot topic among the scientific community due to the bioclinical relevance of biofilm-mediated infections. Despite the growing number of groups currently working on this attractive issue, few biochemical data are available on the enzymes involved in c-di-GMP homeostasis. This is particularly true for the HD-GYP subclass of phosphodiesterases, whose functional characterization is preliminary (Ryan, *et al.*, 2010; Ryan, *et al.*, 2012) and only one crystallographic structure (Lovering, *et al.*, 2011) is available to date.

The main aim of my PhD was thus to characterize this class of enzymes. This study has been carried out by analysing HD-GYP proteins from *Pseudomonas aeruginosa*, a model organism for studying biofilm. Particularly, two HD-GYP proteins, whose involvement in controlling biofilm has been demonstrated *in vivo* (Ryan, *et al.*, 2009), have been analysed, namely PA4108 and PA4781.

Surprisingly, in contrast to the results obtained by analysis of the role in *P.aeruginosa* biofilm formation (Ryan, *et al.*, 2009), the functional characterization reported in this thesis indicates that purified PA4108 presents a very low c-di-GMP hydrolytic activity, while purified PA4781 results completely inactive. The latter enzyme contains a regulatory REC domain upstream of the catalytic one, which probably negatively regulates the enzyme when unphosphorylated. This regulatory mechanism has been indeed previously proposed for many other two-component regulators (Gao and Stock, 2010). The role of the REC domain in PA4781 was confirmed by the results on the isolated catalytic domain (PA4781G), which partially gains the c-di-GMP hydrolytic activity, although with lower efficiency than PA4108.

In order to better understand, on a structural basis, whether the observed lack of activity of PA4781 is due to the inability of the enzyme to bind c-di-GMP efficiently, the docking of c-di-GMP into the active sites of PA4108 and PA4781 was carried out in collaboration with Dr. A. Paiardini (Sapienza, Università di Roma). Briefly, once we obtained the homology models and the docking analysis of PA4108 and PA4781 (fig. 5.1A and 5.1B, respectively), using Bd1817 (pdb code: 3TM8) as a structural template, we identified the residues involved in the interaction of PA4108 with the substrate (fig 5.1C).

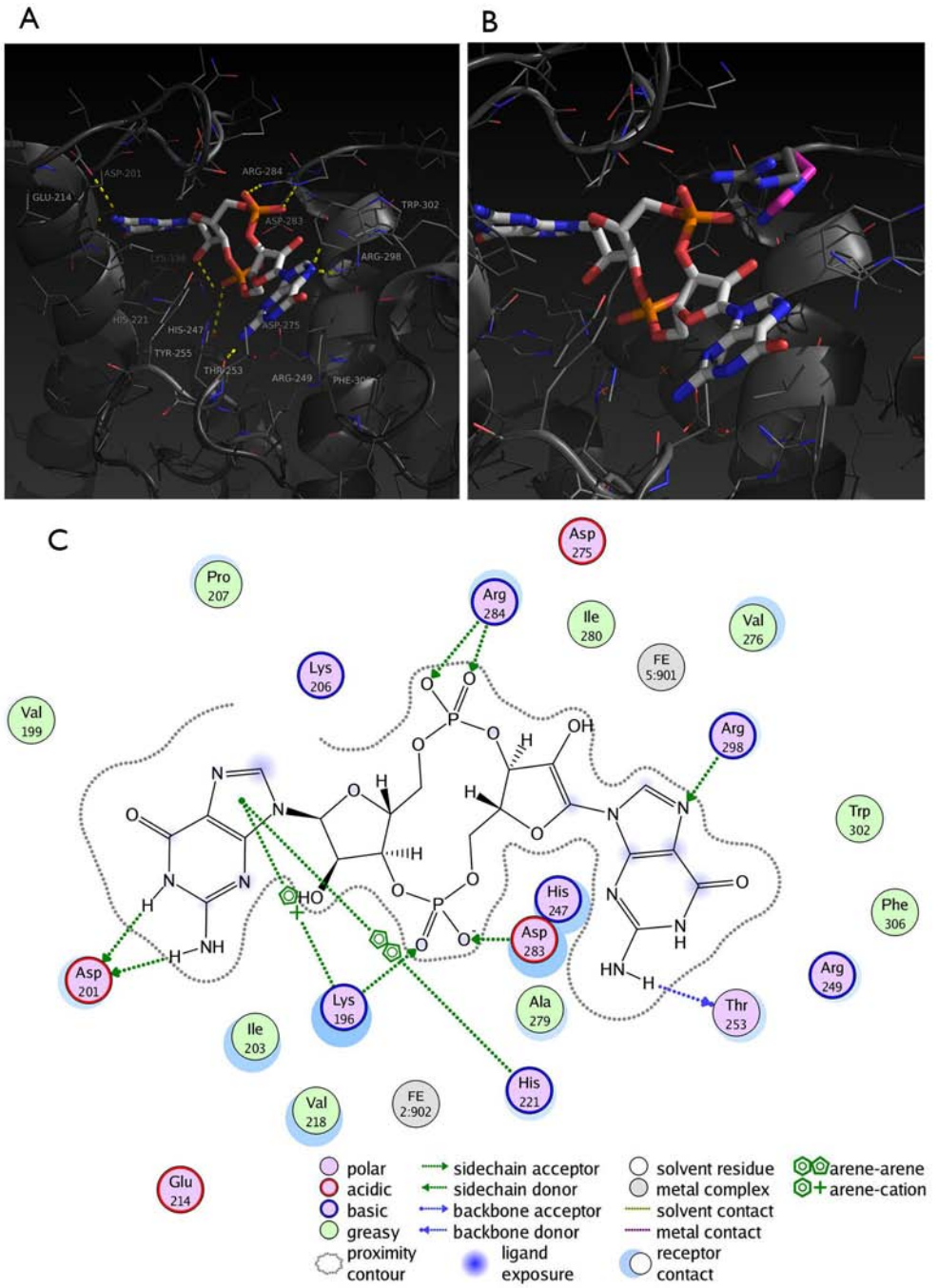

Figure 5.1. Molecular docking of c-di-GMP on PA4108 (A) and PA4781 (B) homology models obtained using as a structural template Bd1817; in panel C the interaction of PA4108 with the substrate is represented.

PA4108 is predicted to interact and accommodate c-di-GMP into a shallow binding groove, where a number of favourable interactions take place: the guanidine rings of c-di-GMP are stabilized by hydrogen-bonding interactions with Thr253, Arg298 and Asp201, and by arene-arene and arene-cation interactions with His221 and Lys196. The latter residue is also involved in an ion-pair interaction with a phosphate moiety of c-di-GMP. The other phosphate moiety is mainly stabilized by ion-pair interactions with Arg284. Interestingly, the latter residue is substituted by a His residue in PA4781 (fig. 5.1B). This substitution could be responsible, at least in part, of the observed low affinity of PA4781 for c-di-GMP. This feature, together with the negative effect of the REC domain discussed above, may explain the observed inability of PA4781 to hydrolyze c-di-GMP *in vitro*.

It should be underlined that also PA4108 displays a very low catalytic activity and high K_M for c-di-GMP (compared to the known EAL PDE (Rao*, et al.*, 2009; Rao*, et al.*, 2008)). The unexpected evidence of the very low activity of the aforementioned HD-GYP proteins *in vitro* and the literature data available on the family archetype RpfG (Ryan*, et al.*, 2010; Ryan*, et al.*, 2012) suggest that the HD-GYP proteins might act as enzymes or signals, depending on the cellular context. This hypothesis is in agreement with recent data showing that proteins involved in c-di-GMP signalling can be multifunctional, with other activities assisting or replacing the predicted enzymatic function (as an example see (Ryan*, et al.*, 2012)).

Contrary to the data on purified proteins, the assays performed in the *E.coli* background presented in this thesis demonstrate that the expression of PA4108 and PA4781G (containing only the catalytic domain of PA4781) influence significantly the intracellular levels of c-di-GMP. For this reason, we propose that, in the cell, other partners or cofactors are required to trigger the PDE activity of PA4108 and PA4781G. We expect to extend this analysis by solving the structure of PA4781G, whose crystals have been obtained very recently.

Anyhow, the *E.coli milieu* does not revert the negative regulatory effect of the REC domain on the full-length PA4781, suggesting that this protein needs a specific kinase (absent in *E.coli*) for its phosphorylation.

Experiments aimed at identifying the putative partners of PA4108 and PA4781 are currently ongoing by means of a pull-down approach on both *E.coli* and,

more interestingly, *P.aeruginosa* cell extracts. Moreover, we plan to identify a third actor of this metabolic pathway, i.e. the specific kinase able to phosphorylate in *P.aeruginosa* the PA4781 REC domain, by merging bioinformatics, microbiology and biochemistry.

The present and future studies on the biochemistry of c-di-GMP synthesis and consumption are strongly limited by the detection methods currently available to detect c-di-GMP. For this reason, during my PhD I have developed a new strategy for the detection and identification of c-di-GMP. This method is based on the specific CD signal displayed by the intercalated dimer of c-di-GMP and on the ability of manganese ions to promote dimerization of this cyclic dinucleotide. This approach can be employed to measure the enzymatic rate of c-di-GMP production and degradation, as shown by the real-time measurements presented above. The CD signal of c-di-GMP at 282 nm is very specific of the dimeric form of the molecule; other nucleotides such as GTP, pGpG or GMP, which are present during the reaction of diguanylate cyclases or phosphodiesterases, do not show the same signal. Moreover, the observation that the adenine dinucleotide c-di-AMP does not have the same spectroscopic signature suggests that the sigmoidal CD signal can be assigned to the stacking of the guanine bases.

Comparison of the distinctive features of present strategy with those of the other strategies available to measure enzymatic activities (as summarized in tab. 4.I) underlines that this method is effective to measure steady-state kinetics of both DGCs and PDEs in real-time. As shown in table 4.I, the kinetic properties of few enzymes have been studied to date with the methods already available; on the other hand, it is clear that a deep understanding of the mechanism controlling the turnover of c-di-GMP requires the biochemistry of its synthesis and degradation to be fully elucidated. A clear advantage of the approach presented here is that it allows to detect and quantify c-di-GMP directly, without the need of additional chromophores, biosensors or dyes, and does not require time-consuming sample preparation. In common with most methods, the sensitivity of the CD analysis lies in the micromolar range of c-di-GMP concentrations (tab. 4.I).

In our opinion the present experimental approach also opens novel scenarios and attractive possibilities in the field of c-di-GMP enzymes. The method will allow to conceive pre-steady kinetic experiments, to date unexplored for these

enzymes, but of crucial value to determine the reaction mechanism of both DGCs and PDEs. A detailed knowledge of the mechanistic details of these reactions is a necessary pre-requisite to design and to validate effective inhibitors that could be used as antimicrobial agents able to modulate c-di-GMP levels and to interfere with the formation of biofilms or with development of specific (antibiotic-resistant) phenotypes such as those found in persister cells (Malone, *et al.*, 2012). Moreover, the experimental approach presented here might be employed to explore the interplay of DGCs and PDEs in controlling c-di-GMP levels by allowing to measure the activity of these enzymes not only individually, but also in combination in the same reaction mixture; this may provide quantitative evaluation of the interaction of proteins putatively involved in the same signalling pathway. As suggested by the recent evaluation of the different phenotypic output of the activity of the DCGs in *Vibrio cholerae*, the mechanism and rate whereby each individual DCG produces c-di-GMP and/or is regulated determine the stringent biological specificity of c-di-GMP signalling in the cell (Massie, *et al.*, 2012).

REFERENCES

Abel, S., Chien, P., Wassmann, P., Schirmer, T., Kaever, V., Laub, M.T., Baker, T.A. and Jenal, U. (2011) Regulatory cohesion of cell cycle and cell differentiation through interlinked phosphorylation and second messenger networks. *Mol Cell*, **43**, 550-560.

Alvarez-Ortega, C. and Harwood, C.S. (2007) Responses of *Pseudomonas aeruginosa* to low oxygen indicate that growth in the cystic fibrosis lung is by aerobic respiration. *Mol Microbiol*, **65**, 153-165.

Antoniani, D., Bocci, P., Maciag, A., Raffaelli, N. and Landini, P. (2009) Monitoring of diguanylate cyclase activity and of cyclic-di-GMP biosynthesis by whole-cell assays suitable for high-throughput screening of biofilm inhibitors. *Appl Microbiol Biotechnol*, **85**, 1095-1104.

Ashman, D.F., Lipton, R., Melicow, M.M. and Price, T.D. (1963) Isolation of adenosine 3', 5'-monophosphate and guanosine 3', 5'-monophosphate from rat urine. *Biochem Biophys Res Commun*, **11**, 330-334.

Barber, C.E., Tang, J.L., Feng, J.X., Pan, M.Q., Wilson, T.J., Slater, H., Dow, J.M., Williams, P. and Daniels, M.J. (1997) A novel regulatory system required for pathogenicity of *Xanthomonas campestris* is mediated by a small diffusible signal molecule. *Mol Microbiol*, **24**, 555-566.

Barends, T.R., Hartmann, E., Griese, J.J., Beitlich, T., Kirienko, N.V., Ryjenkov, D.A., Reinstein, J., Shoeman, R.L., Gomelsky, M. and Schlichting, I. (2009) Structure and mechanism of a bacterial light-regulated cyclic nucleotide phosphodiesterase. *Nature*, **459**, 1015-1018.

Barraud, N., Hassett, D.J., Hwang, S.H., Rice, S.A., Kjelleberg, S. and Webb, J.S. (2006) Involvement of nitric oxide in biofilm dispersal of *Pseudomonas aeruginosa*. *J Bacteriol*, **188**, 7344-7353.

Benach, J., Swaminathan, S.S., Tamayo, R., Handelman, S.K., Folta-Stogniew, E., Ramos, J.E., Forouhar, F., Neely, H., Seetharaman, J., Camilli, A. and Hunt, J.F. (2007) The structural basis of cyclic diguanylate signal transduction by PilZ domains. *EMBO J*, **26**, 5153-5166.

Bernlohr, R.W., Haddox, M.K. and Goldberg, N.D. (1974) Cyclic guanosine 3':5'-monophosphate in *Escherichia coli* and *Bacillus lichenformis*. *J Biol Chem*, **249**, 4329-4331.

Berthet, J., Rall, T.W. and Sutherland, E.W. (1957) The relationship of epinephrine and glucagon to liver phosphorylase. IV. Effect of epinephrine and glucagon on the reactivation of phosphorylase in liver homogenates. *J Biol Chem*, **224**, 463-475.

Bhinu, V.S. (2005) Insight into biofilm-associated microbial life. *J Mol Microbiol Biotechnol*, **10**, 15-21.

Bryers, J.D. (2008) Medical biofilms. *Biotechnol Bioeng*, **100**, 1-18.

Burdette, D.L., Monroe, K.M., Sotelo-Troha, K., Iwig, J.S., Eckert, B., Hyodo, M., Hayakawa, Y. and Vance, R.E. (2011) STING is a direct innate immune sensor of cyclic di-GMP. *Nature*, **478**, 515-518.

Camilli, A. and Bassler, B.L. (2006) Bacterial small-molecule signaling pathways. *Science*, **311**, 1113-1116.

Cashel, M. and Kalbacher, B. (1970) The control of ribonucleic acid synthesis in *Escherichia coli*. V. Characterization of a nucleotide associated with the stringent response. *J Biol Chem*, **245**, 2309-2318.

Castiglione, N., Stelitano, V., Rinaldo, S., Giardina, G., Caruso, M. and Cutruzzola, F. (2011) Metabolism of cyclic-di-GMP in bacterial biofilms: From a general overview to biotechnological applications. *Indian Journal of Biotechnology* **10**, 423-431.

Chan, C., Paul, R., Samoray, D., Amiot, N.C., Giese, B., Jenal, U. and Schirmer, T. (2004) Structural basis of activity and allosteric control of diguanylate cyclase. *Proc Natl Acad Sci U S A*, **101**, 17084-17089.

Chen, M.W., Kotaka, M., Vonrhein, C., Bricogne, G., Rao, F., Chuah, M.L., Svergun, D., Schneider, G., Liang, Z.X. and Lescar, J. (2012) Structural insights into the regulatory mechanism of the response regulator RocR from *Pseudomonas aeruginosa* in cyclic Di-GMP signaling. *J Bacteriol*, **194**, 4837-4846.

Chen, W., Kuolee, R. and Yan, H. (2010) The potential of 3',5'-cyclic diguanylic acid (c-di-GMP) as an effective vaccine adjuvant. *Vaccine*, **28**, 3080-3085.

Chen, Z.H. and Schaap, P. (2012) The prokaryote messenger c-di-GMP triggers stalk cell differentiation in Dictyostelium. *Nature*, **488**, 680-683.

Chin, K.H., Lee, Y.C., Tu, Z.L., Chen, C.H., Tseng, Y.H., Yang, J.M., Ryan, R.P., McCarthy, Y., Dow, J.M., Wang, A.H. and Chou, S.H. (2010) The cAMP receptor-like protein CLP is a novel c-di-GMP receptor linking cell-cell signaling to virulence gene expression in *Xanthomonas campestris*. *J Mol Biol*, **396**, 646-662.

Christen, B., Christen, M., Paul, R., Schmid, F., Folcher, M., Jenoe, P., Meuwly, M. and Jenal, U. (2006) Allosteric control of cyclic di-GMP signaling. *J Biol Chem*, **281**, 32015-32024.

Christen, M., Christen, B., Folcher, M., Schauerte, A. and Jenal, U. (2005) Identification and characterization of a cyclic di-GMP-specific phosphodiesterase and its allosteric control by GTP. *J Biol Chem*, **280**, 30829-30837.

Cotter, P.A. and Stibitz, S. (2007) c-di-GMP-mediated regulation of virulence and biofilm formation. *Curr Opin Microbiol*, **10**, 17-23.

De, N., Navarro, M.V., Raghavan, R.V. and Sondermann, H. (2009) Determinants for the activation and autoinhibition of the diguanylate cyclase response regulator WspR. *J Mol Biol*, **393**, 619-633.

De, N., Pirruccello, M., Krasteva, P.V., Bae, N., Raghavan, R.V. and Sondermann, H. (2008) Phosphorylation-independent regulation of the diguanylate cyclase WspR. *PLoS Biol*, **6**, e67.

Dow, J.M., Crossman, L., Findlay, K., He, Y.Q., Feng, J.X. and Tang, J.L. (2003) Biofilm dispersal in *Xanthomonas campestris* is controlled by cell-cell signaling and is required for full virulence to plants. *Proc Natl Acad Sci U S A*, **100**, 10995-11000.

Driscoll, J.A., Brody, S.L. and Kollef, M.H. (2007) The epidemiology, pathogenesis and treatment of *Pseudomonas aeruginosa* infections. *Drugs*, **67**, 351-368.

Duerig, A., Abel, S., Folcher, M., Nicollier, M., Schwede, T., Amiot, N., Giese, B. and Jenal, U. (2009) Second messenger-mediated spatiotemporal control of

protein degradation regulates bacterial cell cycle progression. *Genes Dev*, **23**, 93-104.

Duvel, J., Bertinetti, D., Moller, S., Schwede, F., Morr, M., Wissing, J., Radamm, L., Zimmermann, B., Genieser, H.G., Jansch, L., Herberg, F.W. and Haussler, S. (2012) A chemical proteomics approach to identify c-di-GMP binding proteins in *Pseudomonas aeruginosa*. *J Microbiol Methods*, **88**, 229-236.

Egli, M., Gessner, R.V., Williams, L.D., Quigley, G.J., van der Marel, G.A., van Boom, J.H., Rich, A. and Frederick, C.A. (1990) Atomic-resolution structure of the cellulose synthase regulator cyclic diguanylic acid. *Proc Natl Acad Sci U S A*, **87**, 3235-3239.

Eichhorn, G.L. and Shin, Y.A. (1968) Interaction of metal ions with polynucleotides and related compounds. XII. The relative effect of various metal ions on DNA helicity. *J Am Chem Soc*, **90**, 7323-7328.

Galperin, M.Y. (2005) A census of membrane-bound and intracellular signal transduction proteins in bacteria: bacterial IQ, extroverts and introverts. *BMC Microbiol*, **5**, 35.

Galperin, M.Y., Nikolskaya, A.N. and Koonin, E.V. (2001) Novel domains of the prokaryotic two-component signal transduction systems. *FEMS Microbiol Lett*, **203**, 11-21.

Gao, R. and Stock, A.M. (2010) Molecular strategies for phosphorylation-mediated regulation of response regulator activity. *Curr Opin Microbiol*, **13**, 160-167.

Gentner, M., Allan, M.G., Zaehringer, F., Schirmer, T. and Grzesiek, S. (2012) Oligomer Formation of the Bacterial Second Messenger c-di-GMP: Reaction Rates and Equilibrium Constants Indicate a Monomeric State at Physiological Concentrations. *J Am Chem Soc*, **134**, 1019-1029.

Hassett, D.J., Cuppoletti, J., Trapnell, B., Lymar, S.V., Rowe, J.J., Yoon, S.S., Hilliard, G.M., Parvatiyar, K., Kamani, M.C., Wozniak, D.J., Hwang, S.H., McDermott, T.R. and Ochsner, U.A. (2002) Anaerobic metabolism and quorum sensing by *Pseudomonas aeruginosa* biofilms in chronically infected cystic fibrosis airways: rethinking antibiotic treatment strategies and drug targets. *Adv Drug Deliv Rev*, **54**, 1425-1443.

He, Y.W., Boon, C., Zhou, L. and Zhang, L.H. (2009) Co-regulation of *Xanthomonas campestris* virulence by quorum sensing and a novel two-component regulatory system RavS/RavR. *Mol Microbiol.*, **71**, 1464-1476.

Hengge, R. (2009) Principles of c-di-GMP signalling in bacteria. *Nat Rev Microbiol*, **7**, 263-273.

Hickman, J.W., Tifrea, D.F. and Harwood, C.S. (2005) A chemosensory system that regulates biofilm formation through modulation of cyclic diguanylate levels. *Proc Natl Acad Sci U S A*, **102**, 14422-14427.

Ishikawa, H. and Barber, G.N. (2008) STING is an endoplasmic reticulum adaptor that facilitates innate immune signalling. *Nature*, **455**, 674-678.

Ishikawa, H., Ma, Z. and Barber, G.N. (2009) STING regulates intracellular DNA-mediated, type I interferon-dependent innate immunity. *Nature*, **461**, 788-792.

Jafferji, A., Allen, J.W., Ferguson, S.J. and Fulop, V. (2000) X-ray crystallographic study of cyanide binding provides insights into the structure-function relationship for cytochrome cd1 nitrite reductase from *Paracoccus pantotrophus*. *J Biol Chem*, **275**, 25089-25094.

Jenal, U. (2004) Cyclic di-guanosine-monophosphate comes of age: a novel secondary messenger involved in modulating cell surface structures in bacteria? *Curr Opin Microbiol*, **7**, 185-191.

Jenal, U. and Malone, J. (2006) Mechanisms of cyclic-di-GMP signaling in bacteria. *Annu Rev Genet*, **40**, 385-407.

Jin, L., Waterman, P.M., Jonscher, K.R., Short, C.M., Reisdorph, N.A. and Cambier, J.C. (2008) MPYS, a novel membrane tetraspanner, is associated with major histocompatibility complex class II and mediates transduction of apoptotic signals. *Mol Cell Biol*, **28**, 5014-5026.

Karaolis, D.K., Means, T.K., Yang, D., Takahashi, M., Yoshimura, T., Muraille, E., Philpott, D., Schroeder, J.T., Hyodo, M., Hayakawa, Y., Talbot, B.G., Brouillette, E. and Malouin, F. (2007) Bacterial c-di-GMP is an immunostimulatory molecule. *J Immunol*, **178**, 2171-2181.

Kelly, S.M. and Price, N.C. (2000) The use of circular dichroism in the investigation of protein structure and function. *Curr Protein Pept Sci*, **1**, 349-384.

Ko, J., Ryu, K.S., Kim, H., Shin, J.S., Lee, J.O., Cheong, C. and Choi, B.S. (2010) Structure of PP4397 reveals the molecular basis for different c-di-GMP binding modes by Pilz domain proteins. *J Mol Biol*, **398**, 97-110.

Kokare, C.R., Chakraborty, S., Khopade, A.N. and Mahadik, K.R. (2009) Biofilm: Importance and applications. *Indian journal of biotechnology*, **8**, 159-168.

Kulasakara, H., Lee, V., Brencic, A., Liberati, N., Urbach, J., Miyata, S., Lee, D.G., Neely, A.N., Hyodo, M., Hayakawa, Y., Ausubel, F.M. and Lory, S. (2006) Analysis of *Pseudomonas aeruginosa* diguanylate cyclases and phosphodiesterases reveals a role for bis-(3'-5')-cyclic-GMP in virulence. *Proc Natl Acad Sci U S A*, **103**, 2839-2844.

Lai, T.H., Kumagai, Y., Hyodo, M., Hayakawa, Y. and Rikihisa, Y. (2009) The *Anaplasma phagocytophilum* PleC histidine kinase and PleD diguanylate cyclase two-component system and role of cyclic Di-GMP in host cell infection. *J Bacteriol.*, **191**, 693-700.

Lee, V.T., Matewish, J.M., Kessler, J.L., Hyodo, M., Hayakawa, Y. and Lory, S. (2007) A cyclic-di-GMP receptor required for bacterial exopolysaccharide production. *Mol Microbiol*, **65**, 1474-1484.

Li, T.N., Chin, K.H., Liu, J.H., Wang, A.H. and Chou, S.H. (2009) XC1028 from *Xanthomonas campestris* adopts a PilZ domain-like structure without a c-di-GMP switch. *Proteins*, **75**, 282-288.

Liaw, Y.C., Gao, Y.G., Robinson, H., Sheldrick, G.M., Sliedregt, L.A., van der Marel, G.A., van Boom, J.H. and Wang, A.H. (1990) Cyclic diguanylic acid behaves as a host molecule for planar intercalators. *FEBS Lett*, **264**, 223-227.

Lindsay, D. and von Holy, A. (2006) Bacterial biofilms within the clinical setting: what healthcare professionals should know. *J Hosp Infect*, **64**, 313-325.

Lovering, A.L., Capeness, M.J., Lambert, C., Hobley, L. and Sockett, R.E. (2011) The structure of an unconventional HD-GYP protein from Bdellovibrio reveals the roles of conserved residues in this class of cyclic-di-GMP phosphodiesterases. *MBio*, **2**, e00163-00111.

Magnusson, L.U., Farewell, A. and Nystrom, T. (2005) ppGpp: a global regulator in *Escherichia coli*. *Trends Microbiol*, **13**, 236-242.

Malone, J.G., Jaeger, T., Manfredi, P., Dotsch, A., Blanka, A., Bos, R., Cornelis, G.R., Haussler, S. and Jenal, U. (2012) The YfiBNR signal transduction mechanism reveals novel targets for the evolution of persistent *Pseudomonas aeruginosa* in cystic fibrosis airways. *PLoS Pathog*, **8**, e1002760.

Massie, J.P., Reynolds, E.L., Koestler, B.J., Cong, J.P., Agostoni, M. and Waters, C.M. (2012) Quantification of high-specificity cyclic diguanylate signaling. *Proc Natl Acad Sci U S A*, **109**, 12746-12751.

Minasov, G., Padavattan, S., Shuvalova, L., Brunzelle, J.S., Miller, D.J., Basle, A., Massa, C., Collart, F.R., Schirmer, T. and Anderson, W.F. (2009) Crystal structures of YkuI and its complex with second messenger cyclic Di-GMP suggest catalytic mechanism of phosphodiester bond cleavage by EAL domains. *J Biol Chem*, **284**, 13174-13184.

Moreau-Marquis, S., Stanton, B.A. and O'Toole, G.A. (2008) *Pseudomonas aeruginosa* biofilm formation in the cystic fibrosis airway. *Pulm Pharmacol Ther*, **21**, 595-599.

Nakayama, S., Kelsey, I., Wang, J., Roelofs, K., Stefane, B., Luo, Y., Lee, V.T. and Sintim, H.O. (2011) Thiazole orange-induced c-di-GMP quadruplex formation facilitates a simple fluorescent detection of this ubiquitous biofilm regulating molecule. *J Am Chem Soc*, **133**, 4856-4864.

Nakayama, S., Kelsey, I., Wang, J. and Sintim, H.O. (2011) c-di-GMP can form remarkably stable G-quadruplexes at physiological conditions in the presence of some planar intercalators. *Chem Commun (Camb)*, **47**, 4766-4768.

Nakayama, S., Luo, Y., Zhou, J., Dayie, T.K. and Sintim, H.O. (2012) Nanomolar fluorescent detection of c-di-GMP using a modular aptamer strategy. *Chem Commun (Camb)*, **48**, 9059-9061.

Nakayama, S., Roelofs, K., Lee, V.T. and Sintim, H.O. (2012) A c-di-GMP-proflavine-hemin supramolecular complex has peroxidase activity-implication for a simple colorimetric detection. *Mol Biosyst*, **8**, 726-729.

Navarro, M.V., De, N., Bae, N., Wang, Q. and Sondermann, H. (2009) Structural analysis of the GGDEF-EAL domain-containing c-di-GMP receptor FimX. *Structure*, **17**, 1104-1116.

Navarro, M.V., Newell, P.D., Krasteva, P.V., Chatterjee, D., Madden, D.R., O'Toole, G.A. and Sondermann, H. (2011) Structural basis for c-di-GMP-mediated inside-out signaling controlling periplasmic proteolysis. *PLoS Biol*, **9**, e1000588.

Neunuebel, M.R. and Golden, J.W. (2008) The *Anabaena sp.* strain PCC 7120 gene all2874 encodes a diguanylate cyclase and is required for normal heterocyst development under high-light growth conditions. *J Bacteriol.* , **190**, 6829-6836.

Newell, P.D., Boyd, C.D., Sondermann, H. and O'Toole, G.A. (2011) A c-di-GMP effector system controls cell adhesion by inside-out signaling and surface protein cleavage. *PLoS Biol*, **9**, e1000587.

Newell, P.D., Monds, R.D. and O'Toole, G.A. (2009) LapD is a bis-(3',5')-cyclic dimeric GMP-binding protein that regulates surface attachment by *Pseudomonas fluorescens* Pf0-1. *Proc Natl Acad Sci U S A*, **106**, 3461-3466.

Paul, R., Abel, S., Wassmann, P., Beck, A., Heerklotz, H. and Jenal, U. (2007) Activation of the diguanylate cyclase PleD by phosphorylation-mediated dimerization. *J Biol Chem*, **282**, 29170-29177.

Paul, R., Weiser, S., Amiot, N.C., Chan, C., Schirmer, T., Giese, B. and Jenal, U. (2004) Cell cycle-dependent dynamic localization of a bacterial response regulator with a novel di-guanylate cyclase output domain. *Genes Dev*, **18**, 715-727.

Rao, F., Qi, Y., Chong, H.S., Kotaka, M., Li, B., Li, J., Lescar, J., Tang, K. and Liang, Z.X. (2009) The functional role of a conserved loop in EAL domain-based cyclic di-GMP-specific phosphodiesterase. *J Bacteriol*, **191**, 4722-4731.

Rao, F., Yang, Y., Qi, Y. and Liang, Z.X. (2008) Catalytic mechanism of cyclic di-GMP-specific phosphodiesterase: a study of the EAL domain-containing RocR from *Pseudomonas aeruginosa*. *J Bacteriol*, **190**, 3622-3631.

Rinaldo, S., Sam, K.A., Castiglione, N., Stelitano, V., Arcovito, A., Brunori, M., Allen, J.W., Ferguson, S.J. and Cutruzzola, F. (2011) Observation of fast release of NO from ferrous d haem allows formulation of a unified reaction mechanism for cytochrome cd nitrite reductases. *Biochem J*, **435**, 217-225.

Romling, U., Gomelsky, M. and Galperin, M.Y. (2005) C-di-GMP: the dawning of a novel bacterial signalling system. *Mol Microbiol*, **57**, 629-639.

Ross, P., Weinhouse, H., Aloni, Y., Michaeli, D., Weinberger-Ohana, P., Mayer, R., Braun, S., de Vroom, E., van der Marel, G.A., van Boom, J.H. and Benziman, M. (1987) Regulation of cellulose synthesis in *Acetobacter xylinum* by cyclic diguanylic acid. *Nature*, **325**, 279-281.

Rutherford, S.T. and Bassler, B.L. (2012) Bacterial quorum sensing: its role in virulence and possibilities for its control. *Cold Spring Harb Perspect Med*, **2**.

Ryan, R.P. and Dow, J.M. (2010) Intermolecular interactions between HD-GYP and GGDEF domain proteins mediate virulence-related signal transduction in *Xanthomonas campestris*. *Virulence*, **1**, 404-408.

Ryan, R.P., Fouhy, Y., Lucey, J.F., Crossman, L.C., Spiro, S., He, Y.W., Zhang, L.H., Heeb, S., Camara, M., Williams, P. and Dow, J.M. (2006) Cell-cell signaling in *Xanthomonas campestris* involves an HD-GYP domain protein that functions in cyclic di-GMP turnover. *Proc Natl Acad Sci U S A*, **103**, 6712-6717.

Ryan, R.P., Lucey, J., O'Donovan, K., McCarthy, Y., Yang, L., Tolker-Nielsen, T. and Dow, J.M. (2009) HD-GYP domain proteins regulate biofilm formation and virulence in *Pseudomonas aeruginosa*. *Environ Microbiol*, **11**, 1126-1136.

Ryan, R.P., McCarthy, Y., Andrade, M., Farah, C.S., Armitage, J.P. and Dow, J.M. (2010) Cell-cell signal-dependent dynamic interactions between HD-GYP and GGDEF domain proteins mediate virulence in *Xanthomonas campestris*. *Proc Natl Acad Sci U S A*, **107**, 5989-5994.

Ryan, R.P., McCarthy, Y., Kiely, P.A., O'Connor, R., Farah, C.S., Armitage, J.P. and Dow, J.M. (2012) Dynamic complex formation between HD-GYP, GGDEF and PilZ domain proteins regulates motility in *Xanthomonas campestris*. *Mol Microbiol*, **86**, 557-567.

Ryjenkov, D.A., Simm, R., Romling, U. and Gomelsky, M. (2006) The PilZ domain is a receptor for the second messenger c-di-GMP: the PilZ domain protein YcgR controls motility in enterobacteria. *J Biol Chem*, **281**, 30310-30314.

Ryjenkov, D.A., Tarutina, M., Moskvin, O.V. and Gomelsky, M. (2005) Cyclic diguanylate is a ubiquitous signaling molecule in bacteria: insights into biochemistry of the GGDEF protein domain. *J Bacteriol*, **187**, 1792-1798.

Sawai, H., Yoshioka, S., Uchida, T., Hyodo, M., Hayakawa, Y., Ishimori, K. and Aono, S. (2010) Molecular oxygen regulates the enzymatic activity of a heme-containing diguanylate cyclase (HemDGC) for the synthesis of cyclic di-GMP. *Biochim Biophys Acta*, **1804**, 166-172.

Schirmer, T. and Jenal, U. (2009) Structural and mechanistic determinants of c-di-GMP signalling. *Nat Rev Microbiol*, **7**, 724-735.

Seshasayee, A.S., Fraser, G.M. and Luscombe, N.M. (2010) Comparative genomics of cyclic-di-GMP signalling in bacteria: post-translational regulation and catalytic activity. *Nucleic Acids Res.*, **38**, 5970-5981.

Sharma, I.M., Dhanaraman, T., Mathew, R. and Chatterji, D. (2012) Synthesis and Characterization of a Fluorescent Analogue of Cyclic di-GMP. *Biochemistry*, **51**, 5443-5453.

Sifri, C.D. (2008) Healthcare epidemiology: quorum sensing: bacteria talk sense. *Clin Infect Dis*, **47**, 1070-1076.

Simm, R., Morr, M., Remminghorst, U., Andersson, M. and Romling, U. (2009) Quantitative determination of cyclic diguanosine monophosphate concentrations in nucleotide extracts of bacteria by matrix-assisted laser desorption/ionization-time-of-flight mass spectrometry. *Anal Biochem*, **386**, 53-58.

Sintim, H.O., Smith, J.A., Wang, J., Nakayama, S. and Yan, L. (2010) Paradigm shift in discovering next-generation anti-infective agents: targeting quorum sensing, c-di-GMP signaling and biofilm formation in bacteria with small molecules. *Future Med Chem*, **2**, 1005-1035.

Slater, H., Alvarez-Morales, A., Barber, C.E., Daniels, M.J. and Dow, J.M. (2000) A two-component system involving an HD-GYP domain protein links cell-cell signalling to pathogenicity gene expression in *Xanthomonas campestris*. *Mol Microbiol*, **38**, 986-1003.

Smith, K.D., Shanahan, C.A., Moore, E.L., Simon, A.C. and Strobel, S.A. (2011) Structural basis of differential ligand recognition by two classes of bis-(3'-5')-cyclic dimeric guanosine monophosphate-binding riboswitches. *Proc Natl Acad Sci U S A*, **108**, 7757-7762.

Solt, I., Simon, I., Csaszar, A.G. and Fuxreiter, M. (2007) Electrostatic versus nonelectrostatic effects in DNA sequence discrimination by divalent ions Mg2+ and Mn2+. *J Phys Chem B*, **111**, 6272-6279.

Spangler, C., Bohm, A., Jenal, U., Seifert, R. and Kaever, V. (2010) A liquid chromatography-coupled tandem mass spectrometry method for quantitation of cyclic di-guanosine monophosphate. *J Microbiol Methods*, **81**, 226-231.

Sponer, J.E., Sychrovsky, V., Hobza, P. and Sponer, J. (2004) Interactions of hydrated divalent metal cations with nucleic acid bases. How to relate the gas phase data to solution situation and binding selectivity in nucleic acids. *Physical Chemistry Chemical Physics*, **6**, 2772-2780.

Stelitano, V., Brandt, A., Fernicola, S., Franceschini, S., Giardina, G., Pica, A., Rinaldo S., Sica, F. and Cutruzzolà, F. Probing the activity of diguanylate cyclases and c-di-GMP phosphodiesterases in real-time *Submitted*.

Sudarsan, N., Lee, E.R., Weinberg, Z., Moy, R.H., Kim, J.N., Link, K.H. and Breaker, R.R. (2008) Riboswitches in eubacteria sense the second messenger cyclic di-GMP. *Science*, **321**, 411-413.

Sultan, S.Z., Pitzer, J.E., Boquoi, T., Hobbs, G., Miller, M.R. and Motaleb, M.A. (2011) Analysis of the HD-GYP domain cyclic dimeric GMP phosphodiesterase reveals a role in motility and the enzootic life cycle of *Borrelia burgdorferi*. *Infect Immun.* , **79**, 3273-3283.

Sun, W., Arese, M., Brunori, M., Nurizzo, D., Brown, K., Cambillau, C., Tegoni, M. and Cutruzzolà, F. (2002) Cyanide binding to cd(1) nitrite reductase from *Pseudomonas aeruginosa*: role of the active-site His369 in ligand stabilization. *Biochem Biophys Res Commun.*, **291**, 1-7.

Sun, W., Li, Y., Chen, L., Chen, H., You, F., Zhou, X., Zhou, Y., Zhai, Z., Chen, D. and Jiang, Z. (2009) ERIS, an endoplasmic reticulum IFN stimulator, activates innate immune signaling through dimerization. *Proc Natl Acad Sci U S A*, **106**, 8653-8658.

Tesmer, J.J., Sunahara, R.K., Gilman, A.G. and Sprang, S.R. (1997) Crystal structure of the catalytic domains of adenylyl cyclase in a complex with Gsalpha.GTPgammaS. *Science*, **278**, 1907-1916.

Tschowri, N., Busse, S. and Hengge, R. (2009) The BLUF-EAL protein YcgF acts as a direct anti-repressor in a blue-light response of *Escherichia coli*. *Genes Dev*, **23**, 522-534.

Tuckerman, J.R., Gonzalez, G. and Gilles-Gonzalez, M.A. (2011) Cyclic di-GMP activation of polynucleotide phosphorylase signal-dependent RNA processing. *J Mol Biol*, **407**, 633-639.

Tuckerman, J.R., Gonzalez, G., Sousa, E.H., Wan, X., Saito, J.A., Alam, M. and Gilles-Gonzalez, M.A. (2009) An oxygen-sensing diguanylate cyclase and phosphodiesterase couple for c-di-GMP control. *Biochemistry*, **48**, 9764-9774.

Van Alst, N.E., Picardo, K.F., Iglewski, B.H. and Haidaris, C.G. (2007) Nitrate sensing and metabolism modulate motility, biofilm formation, and virulence in *Pseudomonas aeruginosa*. *Infect Immun*, **75**, 3780-3790.

Van Alst, N.E., Wellington, M., Clark, V.L., Haidaris, C.G. and Iglewski, B.H. (2009) Nitrite reductase NirS is required for type III secretion system expression and virulence in the human monocyte cell line THP-1 by *Pseudomonas aeruginosa*. *Infect Immun*, **77**, 4446-4454.

Wagner, V.E., Gillis, R.J. and Iglewski, B.H. (2004) Transcriptome analysis of quorum-sensing regulation and virulence factor expression in *Pseudomonas aeruginosa*. *Vaccine*, **22 Suppl 1**, S15-20.

Wang, J., Zhou, J., Donaldson, G.P., Nakayama, S., Yan, L., Lam, Y.F., Lee, V.T. and Sintim, H.O. (2011) Conservative change to the phosphate moiety of cyclic diguanylic monophosphate remarkably affects its polymorphism and ability to bind DGC, PDE, and PilZ proteins. *J Am Chem Soc*, **133**, 9320-9330.

Wassmann, P., Chan, C., Paul, R., Beck, A., Heerklotz, H., Jenal, U. and Schirmer, T. (2007) Structure of BeF3- -modified response regulator PleD: implications for diguanylate cyclase activation, catalysis, and feedback inhibition. *Structure*, **15**, 915-927.

Wenzel, R.P. (2007) Health care-associated infections: major issues in the early years of the 21st century. *Clin Infect Dis*, **45 Suppl 1**, S85-88.

Witte, G., Hartung, S., Buttner, K. and Hopfner, K.P. (2008) Structural biochemistry of a bacterial checkpoint protein reveals diadenylate cyclase activity regulated by DNA recombination intermediates. *Mol Cell*, **30**, 167-178.

Wolfe, A. and Visick, K., (eds). (2009) *The Second Messenger Cyclic Di-GMP*. ASM Press., Washington, DC.

Wood, T.K., Hong, S.H. and Ma, Q. (2011) Engineering biofilm formation and dispersal. *Trends Biotechnol*, **29**, 87-94.

Yang, C.Y., Chin, K.H., Chuah, M.L., Liang, Z.X., Wang, A.H. and Chou, S.H. (2011) The structure and inhibition of a GGDEF diguanylate cyclase complexed with (c-di-GMP)(2) at the active site. *Acta Crystallogr D Biol Crystallogr*, **67**, 997-1008.

Yang, F., Tian, F., Sun, L., Chen, H., Wu, M., Yang, C.H. and He, C. (2012) A novel two-component system PdeK/PdeR regulates c-di-GMP turnover and virulence of *Xanthomonas oryzae* pv. oryzae. *Mol Plant Microbe Interact.*, **25**, 1361-1369.

Yoon, M.Y., Lee, K.M., Park, Y. and Yoon, S.S. (2011) Contribution of cell elongation to the biofilm formation of *Pseudomonas aeruginosa* during anaerobic respiration. *PLoS One*, **6**, e16105.

Zhang, Y. and Huang, K. (2007) On the interactions of hydrated metal cations (Mg2+, Mn2+, Ni2+, Zn2+) with guanine–cytosine Watson–Crick and guanine–guanine reverse-Hoogsteen DNA base pairs. *Journal of Molecular Structure: THEOCHEM*, **812**, 51–62.

Zhang, Z., Gaffney, B.L. and Jones, R.A. (2004) c-di-GMP displays a monovalent metal ion-dependent polymorphism. *J Am Chem Soc*, **126**, 16700-16701.

Zhang, Z., Kim, S., Gaffney, B.L. and Jones, R.A. (2006) Polymorphism of the signaling molecule c-di-GMP. *J Am Chem Soc*, **128**, 7015-7024.

Zhong, B., Yang, Y., Li, S., Wang, Y.Y., Li, Y., Diao, F., Lei, C., He, X., Zhang, L., Tien, P. and Shu, H.B. (2008) The adaptor protein MITA links virus-sensing receptors to IRF3 transcription factor activation. *Immunity*, **29**, 538-550.

Zumft, W.G. (1997) Cell biology and molecular basis of denitrification. *Microbiol. Mol. Biol. Rev.*, **61**, 533-616.

ATTACHMENTS

Rinaldo S., Giardina G., Castiglione N., Stelitano V., Cutruzzola F. (2011) The catalytic mechanism of *Pseudomonas aeruginosa* cd_1 nitrite reductase. *Biochemical Society Transactions* **39**,195-200

Rinaldo S., Sam.K.A., Castiglione N., Stelitano V., Arcovito A., Allen J., Brunori M., Ferguson S.J., Cutruzzola' F. (2011) Observation of fast release of NO from ferrous *d1* haem allows formulation of a unified reaction mechanism for cytochrome *cd1* nitrite reductases *Biochem J.* **435**, 217-25

Castiglione N., Stelitano V., Rinaldo S., Giardina G., Caruso M. and Cutruzzola F. (2011) Metabolism of cyclic-di-GMP in bacterial biofilms: From a general overview to biotechnological applications. *Indian Journal of Biotechnology* **10**, 423-431.

Castiglione N.*, Rinaldo S.**, Giardina G., Stelitano V. and Cutruzzolà F. (2012) Nitrite and Nitrite Reductases: From Molecular Mechanisms to Significance in Human Health and Disease. Antioxid Redox Signal **17**,684-716

Biochemical Society Transactions www.biochemsoctrans.org

The catalytic mechanism of *Pseudomonas aeruginosa* cd_1 nitrite reductase

Serena Rinaldo, Giorgio Giardina, Nicoletta Castiglione, Valentina Stelitano and Francesca Cutruzzolà[1]
Dipartimento di Scienze Biochimiche 'A. Rossi Fanelli', Sapienza–Università di Roma, Rome, Italy

Abstract

The cd_1 NiRs (nitrite reductases) are enzymes catalysing the reduction of nitrite to NO (nitric oxide) in the bacterial energy conversion denitrification process. These enzymes contain two distinct redox centres: one covalently bound *c*-haem, which is reduced by external electron donors, and another peculiar porphyrin, the d_1-haem (3,8-dioxo-17-acrylate-porphyrindione), where nitrite is reduced to NO. In the present paper, we summarize the most recent results on the mechanism of nitrite reduction by the cd_1 NiR from *Pseudomonas aeruginosa*. We discuss the essential catalytic features of this enzyme, with special attention to the allosteric regulation of the enzyme's activity and to the mechanism employed to avoid product inhibition, i.e. trapping of the active-site reduced haem by the product NO. These results shed light on the reactivity of cd_1 NiRs and assign a central role to the unique d_1-haem, present only in this class of enzymes.

Introduction

Pseudomonas aeruginosa is a Gram-negative bacterium commonly found in soil and water, well known for its metabolic versatility; under anaerobic conditions it can use nitrate and nitrite to produce energy via the denitrification pathway. In natural environment, denitrification is the part of the biological nitrogen cycle in which nitrate is transformed into nitrogen gas; reduction of nitrate occurs in four stages each catalysed by a specific metalloenzyme [i.e. the nitrate, nitrite, NO (nitric oxide) and N_2O reductases] [1], according to the following scheme: $NO_3^- \rightarrow NO_2^- \rightarrow NO \rightarrow N_2O \rightarrow N_2$.

The denitrification pathway is expressed under low oxygen tension in the presence of nitrogen oxides such as nitrate and nitrite [1].

It is well known that facultative aerobic bacteria are capable of adapting their respiratory capability and reorganizing their metabolism to cope with O_2 availability. A striking example is given by denitrifiers, including human pathogens such as *Ps. aeruginosa* and *Neisseria meningitidis*, which were shown to adapt to the variable supply of O_2 and nitrate/nitrite by regulating the expression and activity of the various reductases involved in respiratory metabolism.

In the denitrification pathway, NO is produced from nitrite by the enzyme NiR (nitrite reductase); two distinct classes of NiRs are found in bacteria both yielding NO as the main product. The two types of NiR contain either copper (CuNiR) or haem (cd_1NiR) as cofactor, with the haem-containing enzymes occurring more frequently; in *Ps. aeruginosa*, nitrite reduction is carried out by cd_1NiR. The membrane-bound enzyme NOR (nitric oxide reductase) is responsible for NO conversion into N_2O.

Ps. aeruginosa is also a human pathogen, responsible for severe nosocomial infections, in particular in chronic respiratory diseases such as cystic fibrosis. In the airways of the patients, *Ps. aeruginosa* is capable of anaerobic growth by respiration using nitrate or nitrite as terminal electron acceptors [1]; thus pathogenesis, NO metabolism and anaerobic denitrification are strictly related [2,3]. Denitrification is important to detoxify NO under anaerobic conditions: the host's defence systems are neutralized by the activity of NOR [4]. On the other hand, the denitrification machinery is a key signal for the expression of virulence factors; in a recent paper, van Alst et al. [5] demonstrated that production of NO by cd_1NiR is required under aerobic conditions for *Ps. aeruginosa* virulence in a *Caenorhabditis elegans* model. Given that excess free NO may cause metabolic suicide of the pathogen [2], during anaerobic growth, *Ps. aeruginosa* controls the levels of NO by regulating its synthesis and degradation [6]. The key role of nitrite reduction is also highlighted by experiments showing that exposure to 15 m*M* NO_2^- at pH 6.5 kills a mucoid variant of *Ps. aeruginosa*, abundant in the airways of cystic fibrosis patients, in part because of the low NiR activity present in this mutant strain [7,8].

In the present paper, we describe the mechanism of nitrite reduction by cd_1NiR from *Ps. aeruginosa* (Pa-cd_1NiR) [9,10]. We discuss the essential catalytic features of this enzyme, with special attention to the recent experiments on the allosteric regulation of the activity and to the mechanism employed to avoid product inhibition, i.e. trapping of the active-site reduced haem by the product NO.

Pa-cd_1NiR is a homodimer containing one *c*-haem and one d_1-haem (3,8-dioxo-17-acrylate-porphyrindione) group in each subunit. Electrons are transferred from cytochrome c_{551} to the *c*-haem moiety of the enzyme [11], and thereby

Key words: allosteric transition, cd_1 nitrite reductase (NiR), d_1-haem, nitric oxide, *Pseudomonas aeruginosa*.

Abbreviations used: d_1-haem, 3,8-dioxo-17-acrylate-porphyrindione; NiR, nitrite reductase; NOR, nitric oxide reductase.

[1]To whom correspondence should be addressed (email francesca.cutruzzola@uniroma1.it).

Biochem. Soc. Trans. (2011) 39, 195–200; doi:10.1042/BST0390195

Figure 1 | Chemical structure of the d_1-haem and other partially saturated porphyrins:
(**A**) d_1-haem (cd_1NiR); (**B**) *b*-haem (myoglobin); (**C**) *d*-haem (*bd* oxidase) and (**D**) sirohaem (sulfite and nitrite reductase).

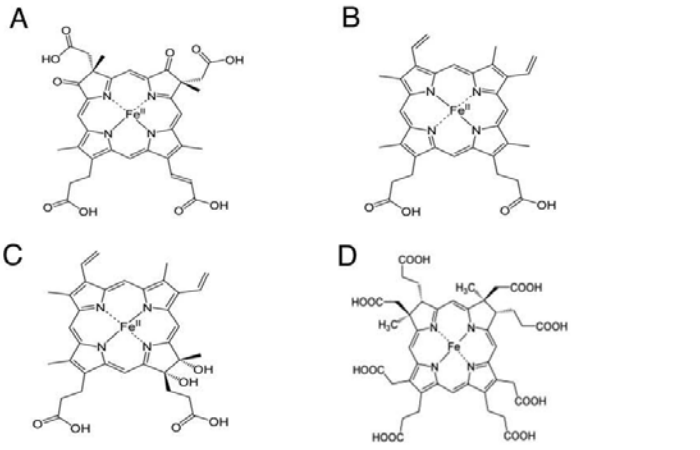

internally to the active-site Fe(III) d_1-haem, to which the substrate NO_2^- binds and is reduced to NO [1]. The d_1-haem (Figure 1A) is a partially saturated macrocycle with a set of oxo, methyl and acrylate substituents; other haems in biology in which the porphyrin ring is partially saturated are the *d*-haem in *Escherichia coli* and sirohaem of bacterial and plant sulfite and NiRs (Figures 1C and 1D) [12,13]. The d_1-haem is unique to the cd_1NiRs [1,14] and is synthesized by a specialized pathway present only in denitrifiers (strongly induced in *Ps. aeruginosa* upon nitrite treatment).

Nitrite reduction by cd_1NIR

Nitrite reduction to NO is the physiologically relevant activity of cd_1NiR [15,16]; indeed the expression of cd_1NiR is induced by low O_2 tensions and presence of nitrogen oxides [1]. NO is produced efficiently by Pa-cd_1NiR (catalytic-centre activity = 6 s^{-1} at pH 7.0) [17] and the activity is pH dependent with an optimum between pH 5.8 and pH 6.5 [15,17]. The current knowledge on the individual steps in the catalytic cycle is summarized below.

Substrate binding

In cd_1NiR, nitrite binds to the reduced d_1-haem with high affinity (K_m = 6 μM) [18]; binding of nitrite to the Fe(II)-iron is expected in the reaction mechanism since this state of the iron has to supply the electron needed for the reduction process. The nitrite molecule is thought to bind via the nitrogen atom in Pa-cd_1NiR forming the so-called nitro complex; this is an important point to clarify since the chemical reactivity of the nitrite molecule may differ considerably depending on the mode of binding. The crystal structure of the reduced nitrite-bound derivative of Pa-cd_1NiR is not available, but in the *Paracoccus pantotrophus* cd_1NiR the nitrite molecule binds via the nitrogen atom [19]. This observation agrees with results on other haem proteins [20,21] and on synthetic iron porphyrin nitrite complexes in which, regardless of the iron oxidation state, the N-binding mode is observed [22–24]. The nitrite N-binding mode also agrees with the current mechanism of the reduction of nitrite by cd_1NiRs which is thought to occur via a double protonation of a terminal O atom of the nitrite molecule. Theoretical calculations have suggested that the O-binding mode is also possible for nitrite binding and reduction of cd_1NiR [25] and also for other haem proteins such as haemoglobin [26]. Although nitrite can bind through the O-binding mode (the so-called nitrito mode) to the haem of myoglobin and haemoglobin [27–29], in the case of the d_1-haem there is no experimental evidence that such O-binding mode may occur.

The high affinity for nitrite of the ferrous d_1-haem (see above) is a peculiar and physiologically relevant feature of all cd_1NiRs; indeed these proteins display unusually high affinity for several anionic molecules in the ferrous state, including the inhibitor cyanide [30,31]. This behaviour is remarkably different from that observed in the *b*-type haem-containing proteins in which the negatively charged molecules (nitrite and cyanide) usually bind much better to the Fe(III) iron. The

Figure 2 | Conformational changes seen after the reduction of Pa-cd_1NiR

Superimposition of the three-dimensional structure of the oxidized (in black) and the reduced form (in grey). Three relevant residues in the d_1-haem pocket are shown, i.e. His^{369} and His^{327} coming from monomer A (HIS327A and HIS369A in the Figure), whereas Tyr^{10} comes from the adjacent monomer B (TYR10B in the Figure). The reorganization of the 56–62 loop and the new hydrogen bond (broken line) formed between Thr^{59} and Gln^{11} in the reduced structure are clearly seen (THR59A and GLN11B in the Figure respectively).

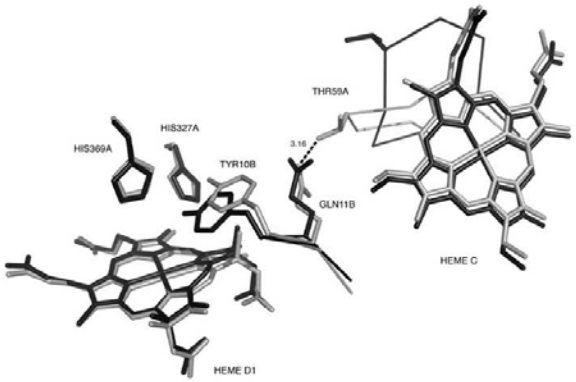

much higher affinity for nitrite of the d_1-haem can be partially explained with the presence of two electron withdrawing carbonyl groups on the d_1-haem ring (Figure 1A). The two conserved histidine residues (His^{327} and His^{369}) in the active-site pocket [32] (see Figure 2) also contribute to the stabilization of the nitrite anion: upon mutagenesis of the latter histidine residues into alanine, the affinity for nitrite falls and the turnover rate is reduced 100-fold [18]. The high affinity for nitrite of reduced Pa-cd_1NiR is important for the catalytic mechanism as discussed below.

Electron transfer from the *c*-haem to the d_1-haem

As mentioned above, in the catalytic cycle the substrate (i.e. nitrite) binds to the ferrous enzyme and is then reduced to yield NO and oxidized d_1-haem. Reduction of the d_1-haem occurs (by intramolecular electron transfer) from the *c*-haem, which in turn is reduced by external electron donors (see above). Early kinetic studies of cd_1NiRs isolated from *Ps. aeruginosa* [33], *P. pantotrophus* [34] and *Pseudomonas stutzeri* [35] yielded considerably different rate constants for this step: 3, 1400 and 23 s^{-1} respectively. Interestingly, the internal electron transfer rate in Pa-cd_1NiR is very similar to that of the overall turnover of the enzyme at pH 7.0 (6 s^{-1}) [17], suggesting that this step may kinetically control the rate of reaction.

Recently, the reduction process of Pa-cd_1NiR was investigated using the pulse radiolysis method by employing 1-MNA$^{\bullet}$ (1-methylnicotinamide) and $CO_2^{\bullet-}$ radicals as reductants [36]; the results provide clear kinetic evidence for negative co-operativity between the two d_1-haem sites in the dimer and suggest that, in Pa-cd_1NiR, the internal electron transfer rate from the *c*-haem to the d_1-haem is tightly regulated by an allosteric mechanism. In more detail, the *c*-haem to d_1-haem electron transfer rate constant was found to decrease (by more than one order of magnitude) as the number of electrons introduced in the enzyme is increased [36]. This decrease in rate may, in principle, arise from a decrease in the electronic coupling between donor and acceptor sites due to conformational changes between reduced and oxidized Pa-cd_1NiR [37]. These conformational changes include the relocation of the side chain of Tyr^{10} located nearby the d_1-haem, the coupled dissociation of the OH^- ligand of the Fe(III) iron and the disruption of the hydrogen bonds at the interface between the two haem domains (Figure 2). In agreement with this structural interpretation, the intramolecular electron transfer is faster (approx. 10-fold) when the conserved His^{369} is replaced by alanine [36]. The positive charge density on the distal side of the d_1-haem is decreased in this mutant and thus the hydroxide ligand is destabilized, lowering the energy barrier for electron transfer and thus increasing the rate.

In summary, we propose that, in Pa-cd_1NiR, allosteric communication between identical monomers may depend on a perturbation of the domain–domain interface within each monomer and a coupled large relocation of the

c-haem domain [38] on reduction of the enzyme. These conformational changes disrupt the above-mentioned hydrogen bonds, decreasing the electronic coupling between the c-haem and the d_1-haem. Thus the control of the electron transfer rates in Pa-cd_1NiR involves contributions from local changes, affecting the driving force of the intramolecular electron transfer, and more global changes, which may affect the electronic coupling between sites (within and between monomers), further rising the energy barrier for electron transfer as the enzyme undergoes reduction.

The complex allosteric behaviour observed for the homodimeric Pa-cd_1NiR indirectly confirms in our opinion the relevance of this step in the control of the reactivity of the enzyme.

Catalysis and product release

In the catalytic cycle, the formation of a complex between NO and the reduced d_1-haem might slow down product release; indeed, the reduced d_1-haem–NO complex may be considered an inhibited species [39] given that NO binds tightly to ferrous haem proteins [40,41]. However, we have clearly shown that the rate constant of NO dissociation from reduced Pa-cd_1NiR is high (up to 70 s^{-1}) [17], several orders of magnitude greater than that of haem *b*-containing proteins. Consequently, the affinity of Pa-cd_1NiR for NO is lowered and the ferrous enzyme is not firmly inhibited by NO [17,42]. It is noteworthy that nitrite reduction can still be monitored after pre-incubation of reduced Pa-cd_1NiR with NO [17].

These conclusions on Pa-cd_1NiR are also supported by the experiments carried out on the enzyme from *P. pantotrophus* suggesting that intramolecular c-haem to d_1-haem electron transfer triggers product release [43]; indeed it has been shown that *P. pantotrophus* d_1Fe(III)–NO complex is a very long-lived species in the absence of excess reductant [44,45]. Therefore also *P. pantotrophus* cd_1NiR works efficiently only in the presence of substrate and electron donor proteins [16,44,46], i.e. it cannot release NO in the absence of reducing equivalents.

We have also shown that nitrite can displace the NO bound to the ferrous enzyme [42], allowing the enzyme to enter a new catalytic cycle; therefore the high affinity of the active-site ferrous d_1-haem for nitrite (see above) actively contributes to NO dissociation during the catalytic cycle. In agreement with this observation, if the affinity of Pa-cd_1NiR for nitrite is decreased (as in the H369A mutant) the fully reduced NO-bound derivative accumulates [18,42]. The observation that NO and nitrite can compete for binding may suggest that the formation of N_2O_3 could in principle occur, for example, in a reaction similar to that proposed for Hb [47]. This event is, however, highly unlikely, mainly because during catalysis the d_1-haem is maintained in the reduced state by internal electron transfer from the c-haem. Moreover, ferric d_1-haem has low affinity for nitrite [48], a feature that probably limits further reaction with free NO to produce N_2O_3.

In summary, the high affinity for nitrite, the allosteric control of the internal electron transfer rate and the exceptionally high NO dissociation rate ascertain that, when nitrite is available, the NiR is active and can actively produce and release NO.

Concluding remarks

In facultative aerobic bacteria, such as *Ps. aeruginosa*, nitrite is used as an electron acceptor and converted into NO by the specialized class of haem-containing enzymes called cd_1NiRs [1]. The mechanism employed by cd_1NiRs is now becoming clear, highlighting the essential role of the peculiar d_1-haem, whose presence in these enzymes was largely unexplained. As mentioned above, the high affinity of reduced d_1-haem for nitrite [18] and the exceptionally fast NO dissociation [17] are trademarks of the d_1-haem, and are tuned by two conserved histidine residues present in the active site of Pa-cd_1NiR.

We previously proposed [49] that ancient haems, such as the d_1-haem of cd_1NiR or the sirohaem of bacterial and plant nitrite and sulfite reductases, have been evolutionaily conserved because their role is strategic to the organism where they are found today. The peculiar low affinity for NO of the reduced d_1-haem of *Ps. aeruginosa* cd_1NiR is a component of this strategy, which could not be achieved by the more common *b*-type haem. It would be very interesting to measure and compare the NO releasing properties of the various porphyrins shown in Figure 1; such experiments, together with a computational study of the electronic structure of the same porphyrins may allow us to correlate the functional properties of these partially saturated macrocycles with NO with their structure.

Finally, the recent evidence that nitrite can also be reduced to NO under hypoxic conditions in eukaryotes, suggests that anaerobic/microaerobic nitrite reduction in higher organisms is a vestigial function originating from the denitrifying metabolism and operative long before the advent of aerobic respiration [50].

Funding

This work was funded by the Ministero della Università of Italy [projects 20074T3ZB and RBRN07BMCT] and from the University of Rome La Sapienza.

References

1 Zumft, W.G. (1997) Cell biology and molecular basis of denitrification. Microbiol. Mol. Biol. Rev. **61**, 533–616
2 Yoon, S.S., Hennigan, R.F., Hilliard, G.M., Ochsner, U.A., Parvatiyar, K., Kamani, M.C., Allen, H.L., DeKievit, T.R., Gardner, P.R., Schwab, U. et al. (2002) *Pseudomonas aeruginosa* anaerobic respiration in biofilms: relationships to cystic fibrosis pathogenesis. Dev. Cell **3**, 593–603
3 Hassett, D.J., Korfhagen, T.R., Irvin, R.T., Schurr, M.J., Sauer, K., Lau, G.W., Sutton, M.D., Yu, H. and Hoiby, N. (2010) *Pseudomonas aeruginosa* biofilm infections in cystic fibrosis: insights into pathogenic processes and treatment strategies. Expert Opin. Ther. Targets **14**, 117–130
4 Kakishima, K., Shiratsuchi, A., Taoka, A., Nakanishi, Y. and Fukumori, Y. (2007) Participation of nitric oxide reductase in survival of *Pseudomonas aeruginosa* in LPS-activated macrophages. Biochem. Biophys. Res. Commun. **355**, 587–591

5 van Alst, N.E., Wellington, M., Clark, V.L., Haidaris, C.G. and Iglewski, B.H. (2009) Nitrite reductase NirS is required for type III secretion system expression an virulence in the human monocyte cell line THP-1 by *Pseudomonas aeruginosa*. Infect. Immun. **77**, 4446–4454
6 Hassett, D.J., Cuppoletti, J., Trapnell, B., Lymar, S.V., Rowe, J.J., Yoon, S.S., Hilliard, G.M., Parvatiyar, K., Kamani, M.C., Wozniak, D.J. et al. (2002) Anaerobic metabolism and quorum sensing by *Pseudomonas aeruginosa* biofilms in chronically infected cystic fibrosis airways: rethinking antibiotic treatment strategies and drug targets. Adv. Drug Delivery Rev. **54**, 1425–1443
7 Yoon, S.S., Coakley, R., Lau, G.W., Lymar, S.V., Gaston, B., Karabulut, A.C., Hennigan, R.F., Hwang, S.H., Buettner, G., Schurr, M.J. et al. (2006) Anaerobic killing of mucoid *Pseudomonas aeruginosa* by acidified nitrite derivatives under cystic fibrosis airway conditions. Clin. Invest. **116**, 436–446
8 Major, T.A., Panmanee, W., Mortensen, J.E., Gray, L.D., Hoglen, N. and Hassett, D.J. (2010) Sodium nitrite-mediated killing of the major cystic fibrosis pathogens *Pseudomonas aeruginosa*, *Staphylococcus aureus* and *Burkholderia cepacia* under anaerobic planktonic and biofilm conditions. Antimicrob. Agents Chemother. **54**, 4671–4677
9 Rinaldo, S. and Cutruzzolà, F. (2007) Nitrite reductases in denitrification. Biology of the Nitrogen Cycle (Bothe, H., Ferguson, S. and Newton, W.E., eds), pp. 37–55, Elsevier, Amsterdam
10 Rinaldo, S., Arcovito, A., Giardina, G., Castiglione, N., Brunori, M. and Cutruzzolà, F. (2008) New insights into the activity of *Pseudomonas aeruginosa* cd_1 nitrite reductase. Biochem. Soc. Trans. **36**, 1155–1159
11 Vijgenboom, E., Busch, J.E. and Canters, G.W. (1997) *In vivo* studies disprove an obligatory role of azurin in denitrification in *Pseudomonas aeruginosa* and show that azu expression is under control of rpoS and ANR. Microbiology **143**, 2853–2863
12 Frankenberg, N., Moser, J. and Jahn, D. (2003) Bacterial heme biosynthesis and its biotechnological application. Appl. Microbiol. Biotechnol. **63**, 115–127
13 Tanaka, R. and Tanaka, A. (2007) Tetrapyrrole biosynthesis in higher plants. Annu. Rev. Plant Biol. **58**, 321–346
14 Allen, J.W., Barker, P.D., Daltrop, O., Stevens, J.M., Tomlinson, E.J., Sinha, N., Sambongi, Y. and Ferguson, S.J. (2005) Why isn't 'standard' heme good enough for *c*-type and d_1-type cytochromes? Dalton Trans. **7**, 3410–3418
15 Yamanaka, T., Ota, A. and Okunuki, K. (1961) A nitrite reducing system reconstructed with purified cytochrome components of *Pseudomonas aeruginosa*. Biochim. Biophys. Acta **53**, 294–308
16 Richter, C.D., Allen, J.W., Higham, C.W., Koppenhofer, A., Zajicek, R.S., Watmough, N.J. and Ferguson, S.J. (2002) Cytochrome cd_1, reductive activation and kinetic analysis of a multifunctional respiratory enzyme. J. Biol. Chem. **277**, 3093–3100
17 Rinaldo, S., Arcovito, A., Brunori, M. and Cutruzzolà, F. (2007) Fast dissociation of nitric oxide from ferrous *Pseudomonas aeruginosa* cd_1 nitrite reductase: a novel outlook on the catalytic mechanism. J. Biol. Chem. **282**, 14761–14767
18 Cutruzzolà, F., Brown, K., Wilson, E.K., Bellelli, A., Arese, M., Tegoni, M., Cambillau, C. and Brunori, M. (2001) The nitrite reductase from *Pseudomonas aeruginosa*: essential role of two active-site histidines in the catalytic and structural properties. Proc. Natl. Acad. Sci. U.S.A. **98**, 2232–2237
19 Williams, P.A., Fülöp, V., Garman, E.F., Saunders, N.F., Ferguson, S.J. and Hajdu, J. (1997) Haem-ligand switching during catalysis in crystals of a nitrogen-cycle enzyme. Nature **389**, 406–412
20 Crane, B.R., Siegel, L.M. and Getzoff, E.D. (1997) Probing the catalytic mechanism of sulfite reductase by X-ray crystallography: structures of the *Escherichia coli* hemoprotein in complex with substrates, inhibitors, intermediates, and products. Biochemistry **36**, 12120–12137
21 Einsle, O., Messerschmidt, A., Huber, R., Kroneck, P.M.J. and Neese, F. (2002) Mechanism of the six-electron reduction of nitrite to ammonia by cytochrome *c* nitrite reductase. J. Am. Chem. Soc. **124**, 11737–11745
22 Wyllie, G.R. and Scheidt, W.R. (2002) Solid-state structures of metalloporphyrin NO_x compounds. Chem. Rev. **102**, 1067–1090
23 Nasri, H., Ellison, M.K., Shang, M., Schultz, C.E. and Scheidt, W.R. (2004) Variable π-bonding in iron(II) porphyrinates with nitrite, CO, and tert-butyl isocyanide: characterization of [Fe(TpivPP)(NO_2)(CO)]. Inorg. Chem. **43**, 2932–2942
24 Cheng, L., Khan, M.A., Richter-Addo, G.B. and Powell, D.R. (2000) The first unambiguous determination of a nitrosyl-to-nitrite conversion in an iron nitrosyl porphyrin. Chem. Commun. 2301–2302
25 Silaghi-Dumitrescu, R. (2004) Linkage isomerism in nitrite reduction by cytochrome cd_1 nitnte reductase. Inorg. Chem. **43**, 3715–3718
26 Perissinotti, L.L., Marti, M.A., Doctorovich, F., Luque, F.J. and Estrin, D.A. (2008) A microscopic study of the deoxyhemoglobin-catalyzed generation of nitric oxide from nitrite anion. Biochemistry **47**, 9793–9802
27 Copeland, D.M., Soares, A.S., West, A.H. and Richter-Addo, G.B. (2006) Crystal structures of the nitrite and nitric oxide complexes of horse heart myoglobin. J. Inorg. Biochem. **100**, 1413–1425
28 Yi, J., Safo, M.F. and Richter-Addo, G.B. (2008) The nitrite anion binds to human hemoglobin via the uncommon O-nitrito mode. Biochemistry **47**, 8247–8249
29 Yi, J., Orville, A.M., Skinner, J.M., Skinner, M.J. and Richter-Addo, G.B. (2010) Synchrotron X-ray-induced photoreduction of ferric myoglobin nitrite crystals gives the ferrous derivative with retention of the O-bonded nitrite ligand. Biochemistry **49**, 5969–5971
30 Jafferji, A., Allen, J.W., Ferguson, S.J. and Fulop, V. (2000) X-ray crystallographic study of cyanide binding provides insights into the structure–function relationship for cytochrome cd_1 nitrite reductase from *Paracoccus pantotrophus*. J. Biol. Chem. **275**, 25089–25094
31 Sun, W., Arese, M., Brunori, M., Nurizzo, D., Brown, K., Cambillau, C., Tegoni, M. and Cutruzzolà, F. (2002) Cyanide binding to cd_1 nitrite reductase from *Pseudomonas aeruginosa*: role of the active-site His^{369} in ligand stabilization. Biochem. Biophys. Res. Commun. **291**, 1–7
32 Nurizzo, D., Silvestrini, M.C., Mathieu, M., Cutruzzolà, F., Bourgeois, D., Fülöp, V., Hajdu, J., Brunori, M., Tegoni, M. and Cambillau, C. (1997) N-terminal arm exchange is observed in the 2.15 Å crystal structure of oxidized nitrite reductase from *Pseudomonas aeruginosa*. Structure **5**, 1157–1171
33 Kobayashi, K., Koppenhoefer, A., Ferguson, S.J., Watmough, N.J. and Tagawa, S. (2001) Intramolecular electron transfer from *c* heme to d_1 heme in bacterial cytochrome cd_1 nitrite reductase occurs over the same distances at very different rates depending on the source of the enzyme. Biochemistry **40**, 8542–8547
34 Kobayashi, K., Koppenhöer, A., Ferguson, S.J. and Tagawa, S. (1997) Pulse radiolysis studies on cytochrome cd_1 nitrite reductase from *Thiosphaera pantotropha*: evidence for a fast intramolecular electron transfer from *c*-heme to d_1-heme. Biochemistry **36**, 13611–13616
35 Farver, O., Kroneck, P.M.H., Zumft, W.G. and Pecht, I. (2002) Intramolecular electron transfer in cytochrome cd_1 nitrite reductase from *Pseudomonas stutzeri*: kinetics and thermodynamics. Biophys. Chem. **98**, 27–34
36 Farver, O., Brunori, M., Cutruzzolà, F., Rinaldo, S., Wherland, S. and Pecht, I. (2009) Intramolecular electron-transfer in *Pseudomonas aeruginosa* cd_1 nitrite reductase: thermodynamics and kinetics. Biophys. J. **96**, 2849–2856
37 Nurizzo, D., Cutruzzolà, F., Arese, M., Bourgeois, D., Brunori, M., Cambillau, C. and Tegoni, M. (1998) Conformational changes occurring upon reduction and NO binding in nitrite reductase from *Pseudomonas aeruginosa*. Biochemistry **37**, 13987–13996
38 Brown, K., Roig-Zamboni, V., Cutruzzolà, F., Arese, M., Sun, W., Brunori, M., Cambillau, C. and Tegoni, M. (2001) Domain swing upon His to Ala mutation in nitrite reductase of *Pseudomonas aeruginosa*. J. Mol. Biol. **312**, 541–554
39 Averill, B.A. (1996) Dissimilatory nitrite and nitric oxide reductases. Chem. Rev. **96**, 2951–2964
40 Moore, E.G. and Gibson, Q.H. (1976) Cooperativity in the dissociation of nitric oxide from hemoglobin. J. Biol. Chem. **251**, 2788–2794
41 Kharitonov, V.G., Sharma, V.S., Magde, D. and Koesling, D. (1997) Kinetics of nitric oxide dissociation from five- and six-coordinate nitrosyl hemes and heme proteins, including soluble guanylate cyclase. Biochemistry **36**, 6814–6818
42 Rinaldo, S., Brunori, M. and Cutruzzolà, F. (2007) Nitrite controls the release of nitric oxide in *Pseudomonas aeruginosa* cd_1 nitrite reductase. Biochem. Biophys. Res. Commun. **363**, 662–666
43 Sam, K.A., Strampraad, M.J., de Vries, S. and Ferguson, S.J. (2008) Very early reaction intermediates detected by microsecond time scale kinetics of cytochrome cd_1-catalyzed reduction of nitrite. J. Biol. Chem. **283**, 27403–27409
44 George, S.J., Allen, J.W., Ferguson, S.J. and Thorneley, R.N. (2000) Time-resolved infrared spectroscopy reveals a stable ferric heme-NO intermediate in the reaction of *Paracoccus pantotrophus* cytochrome cd_1 nitrite reductase with nitrite. J. Biol. Chem. **275**, 33231–33237
45 Sam, K.A., Tolland, J.D., Fairhurst, S.A., Higham, C.W., Lowe, D.J., Thorneley, R.N., Allen, J.W. and Ferguson, S.J. (2008) Unexpected dependence on pH of NO release from *Paracoccus pantotrophus* cytochrome cd_1. Biochem. Biophys. Res. Commun. **371**, 719–723

46 Sam, K.A., Fairhurst, S.A., Thorneley, R.N., Allen, J.W. and Ferguson, S.J. (2008) Pseudoazurin dramatically enhances the reaction profile of nitrite reduction by *Paracoccus pantotrophus* cytochrome cd_1 and facilitates release of product nitric oxide. J. Biol. Chem. **283**, 12555–12563
47 Basu, S., Grubina, R., Huang, J., Conradie, J., Huang, Z., Jeffers, A., Jiang, A., He, X., Azarov, I., Seibert, R. et al. (2007) Catalytic generation of N_2O_3 by the concerted nitrite reductase and anhydrase activity of hemoglobin. Nat. Chem. Biol. **3**, 785–794
48 Timkovich, R. and Cork, M.S. (1982) Nitrogen-15 nuclear magnetic resonance investigation of nitrite reductase-substrate interaction. Biochemistry **21**, 3794-3797
49 Rinaldo, S., Brunori, M. and Cutruzzolà, F. (2008) Ancient hemes for ancient catalysts. Plant Signal. Behav. **3**, 135–136
50 Cutruzzolà, F., Rinaldo, S., Castiglione, N., Giardina, G., Pecht, I. and Brunori, M. (2009) Nitrite reduction: an ubiquitous function from a pre-aerobic past. BioEssays **31**, 885–891

Received 29 August 2010
doi:10.1042/BST0390195

BJ www.biochemj.org

Biochem. J. (2011) 435, 217–225 (Printed in Great Britain) doi:10.1042/BJ20101615

Observation of fast release of NO from ferrous d_1 haem allows formulation of a unified reaction mechanism for cytochrome cd_1 nitrite reductases

Serena RINALDO*[1], Katharine A. SAM†[1], Nicoletta CASTIGLIONE*, Valentina STELITANO*, Alessandro ARCOVITO‡, Maurizio BRUNORI*, James W. A. ALLEN†, Stuart J. FERGUSON†[2] and Francesca CUTRUZZOLÀ*[2]

*Dipartimento di Scienze Biochimiche 'A. Rossi Fanelli', Sapienza - Università di Roma, P. A. Moro, 5 00185 Rome, Italy, †Department of Biochemistry, University of Oxford, South Parks Road, Oxford OX1 3QU, U.K., and ‡Istituto di Biochimica e Biochimica Clinica, Università Cattolica del Sacro Cuore, L.go F. Vito, 1-00168, Rome, Italy

Cytochrome cd_1 nitrite reductase is a haem-containing enzyme responsible for the reduction of nitrite into NO, a key step in the anaerobic respiratory process of denitrification. The active site of cytochrome cd_1 contains the unique d_1 haem cofactor, from which NO must be released. In general, reduced haems bind NO tightly relative to oxidized haems. In the present paper, we present experimental evidence that the reduced d_1 haem of cytochrome cd_1 from *Paracoccus pantotrophus* releases NO rapidly ($k = 65$–$200\ s^{-1}$); this result suggests that NO release is the rate-limiting step of the catalytic cycle (turnover number $= 72\ s^{-1}$). We also demonstrate, using a complex of the d_1 haem and apomyoglobin, that the rapid dissociation of NO is largely controlled by the d_1 haem cofactor itself. We present a reaction mechanism proposed to be applicable to all cytochromes cd_1 and conclude that the d_1 haem has evolved to have low affinity for NO, as compared with other ferrous haems.

Key words: haemoprotein, nitric oxide, nitrite, nitrite reductase, *Pseudomonas aeruginosa*, *Paracoccus pantotrophus*.

INTRODUCTION

Denitrification is an anaerobic respiratory process, found widely in both autotrophic and heterotrophic micro-organisms [1], in which oxidized nitrogen compounds, such as nitrate and nitrite, are used as electron acceptors for energy production. Denitrification has been implicated in the virulence of several bacterial species, including *Brucella* [2], *Pseudomonas* [3] and *Neisseria* [4]. In *Pseudomonas aeruginosa*, denitrification is also a source of NO, a crucial signalling molecule during infection and growth of bacteria in anaerobic biofilms [5]. The biological role of NO under physiological and pathological situations is well-known [6]; a critical aspect of the biology of NO is the interaction of this molecule with the haem group. The general rule is that NO binds much more strongly to the ferrous than to the ferric haem, a consideration that imposes mechanistic constraints on many proteins that synthesize or bind NO [7–9].

In a wide range of denitrifying bacteria the reduction of nitrite (NO_2^-) to NO is carried out by periplasmic cytochrome cd_1 nitrite reductase (cytochrome cd_1) [1], a homodimeric, haem-containing protein with one *c* haem and one d_1 haem per monomer [10] (Supplementary Figure S1 at http://www.BiochemJ.org/bj/435/bj4350217add.htm). The d_1 haem (3,8-dioxo-17-acrylate-porphyrindione) is an unusual macrocycle with partial saturation and a set of oxo, methyl and acrylate substituents, which makes it unique among tetrapyrroles (Supplementary Figure S2 at http://www.BiochemJ.org/bj/435/bj4350217add.htm). The best-studied examples of cytochrome cd_1 nitrite reductases are those from *Paracoccus pantotrophus* and *P. aeruginosa* [10]. The *c* haem moiety of cytochrome cd_1 accepts electrons from soluble electron carriers, such as *c*-type cytochromes (cyt c_{550}, cyt c_{551} and cyt c_{554}) or copper proteins, such as azurin or pseudoazurin [10]. The electrons are transferred from the *c* haem of cytochrome cd_1 to the d_1 haem (of the same monomer), where the substrate binds and is converted into NO.

Nitrite co-ordination to *P. pantotrophus* cytochrome cd_1 is via the N-atom as shown by crystallography [11]. The reduction of nitrite by cytochrome cd_1 involves binding of the substrate to the reduced d_1 haem iron (d_1^{2+}), followed by one-electron reduction to yield NO, which is then released [1]. The last step in the catalytic cycle of cytochrome cd_1, i.e. NO dissociation, has been the subject of much debate [12–14]. Previously it was shown that NO is released rapidly from the ferrous d_1 haem ($k_{off} = 71\ s^{-1}$) of *P. aeruginosa* cytochrome cd_1 [15,16]. This surprising result suggested that the affinity for NO of the ferrous d_1 haem in the enzyme from *P. aeruginosa* was 3–4 orders of magnitude smaller ($K_a \sim 10^7\ M^{-1}$) than for many other haemoproteins such as myoglobin and haemoglobin ($K_a \sim 10^{11}$–$10^{12}\ M^{-1}$) [7], and cytochrome aa_3 oxidase ($K_a \sim 10^{10}\ M^{-1}$) [17].

In order to clarify whether the capability to release NO rapidly from ferrous d_1 haem iron is a general property of cytochrome cd_1 nitrite reductases, we have investigated the reactivity of ferrous *P. pantotrophus* cytochrome cd_1 with NO. There are a number of significant differences between the enzymes from *P. pantotrophus* and *P. aeruginosa*. In steady-state turnover of nitrite, *P. pantotrophus* cytochrome cd_1 displays a considerably higher k_{cat} ($72\ s^{-1}$ at pH 7.0 and 25°C) [18] than the value for *P. aeruginosa* cytochrome cd_1 ($6\ s^{-1}$ at pH 7.0 and 20°C) [15]. Also, the internal electron transfer between the *c* haem and the d_1 haem occurs several orders of magnitude faster in *P. pantotrophus* cytochrome cd_1 ($\sim 1000\ s^{-1}$) [14,19] than in *P. aeruginosa* cytochrome cd_1 ($3\ s^{-1}$) [20]. These differences raised the question as to whether NO release from ferrous d_1 haem of the *P. pantotrophus* enzyme would be sufficiently rapid to be catalytically competent.

In the present paper we report that NO is released rapidly from *P. pantotrophus* cytochrome cd_1; the value of the NO dissociation rate suggests that this process represents the rate-limiting step of the catalytic cycle. The finding that the reaction mechanism for cytochrome cd_1 involves fast NO dissociation from ferrous d_1 haem supports the idea that the chemical properties of this unique

Abbreviations used: a.m., after mixing; Mbd_1, haem d_1–apomyoglobin; RZ, Reinheitzahl.

[1] These authors contributed equally to this work.

[2] Correspondence may be addressed to either of these authors (email francesca.cutruzzola@uniroma1.it or stuart.ferguson@bioch.ox.ac.uk).

cofactor are crucial for activity. To corroborate this hypothesis we have also investigated the kinetics of NO dissociation from ferrous d_1 haem complexed with sperm whale apomyoglobin, in order to probe NO reactivity in a protein environment different from cytochrome cd_1. We found that ferrous d_1 haem bound to apomyoglobin releases NO rapidly, confirming the leading role of this cofactor in controlling reactivity of cytochrome cd_1 with NO.

EXPERIMENTAL

Preparation of *P. pantotrophus* cytochrome cd_1

P. pantotrophus was grown in anaerobic conditions at 37°C. Cytochrome cd_1 was purified from the periplasm of the cells according to the method of Moir et al. [21] as modified by Koppenhöfer et al. [22]. The purity of the enzyme was determined by the RZ (Reinheitzahl) value ($A_{406(Ox)}/A_{280}$) and all the cytochrome cd_1 used in the present study had an RZ>1.25. The concentration of the enzyme was determined at 406 nm for the oxidized enzyme and 418 nm for the reduced enzyme, using the respective molar absorption coefficients of 142.5 $mM^{-1} \cdot cm^{-1}$ and 161.5 $mM^{-1} \cdot cm^{-1}$ [19,22]. These molar absorption coefficients refer to the concentration of the enzyme monomer; throughout the present study, the enzyme concentration will be given as monomer concentration and thus catalytic constants will refer to turnover per monomer. Fully reduced cytochrome cd_1 was prepared by reduction with sodium dithionite in an anaerobic glove box; the excess reductant was removed by passing the enzyme down a desalting column packed with P6-DG resin (Bio-Rad) and equilibrated with 50 mM potassium phosphate buffer (pH 7.0), in the presence of 5 mM sodium ascorbate and 13 μg/ml ascorbate oxidase (Sigma). The reduced NO-bound and cyanide-bound derivatives were obtained after the addition of either a stoichiometric amount of NO or excess KCN to the reduced protein. Stock solutions of NO were prepared by equilibrating NO with buffer (50 mM potassium phosphate pH 7.0) at 25°C, assuming the aqueous concentration of NO at 1 atm (101.325 kPa) to be 1.9 mM. All of the spectra were recorded in a JASCO V650 spectrophotometer.

A summary of the relevant spectra of *P. pantotrophus* cytochrome cd_1 derivatives, together with a scheme of the *c* haem and the d_1 haem ligands in each derivative, is shown in Supplementary Figure S3 (at http://www.BiochemJ.org/bj/435/bj4350217add.htm). It was reported previously that, upon reduction of the *c* haem, the iron co-ordination changes from histidine–histidine to histidine–methionine [11]. The latter co-ordination (histidine–methionine) does not change during turnover; reversion to the histidine–histidine state occurs very slowly (minutes) and only in the absence of ligands or substrates [23]. Therefore the change in co-ordination of the *c* haem is not expected to occur during the time range of the kinetics reported in the present paper.

Stopped-flow measurements

All of the stopped-flow experiments described in the present paper were carried out anaerobically in 50 mM potassium phosphate buffer (pH 7.0) in the presence of 5 mM sodium ascorbate and 13 μg/ml ascorbate oxidase (Sigma), added to scavenge possible oxygen contamination. The concentration of the samples in the different experiments is given a.m. (after mixing): a 1:1 dilution was always used in the symmetric mixing apparatus. All of the experiments were performed with an Applied Photophysics stopped-flow apparatus (DX.17MV, Applied Photophysics). To follow the rate of NO dissociation, a monochromatic light source was used in the single wavelength acquisition mode; the use of the diode array acquisition mode was limited because photodissociation of NO is known to affect the rate. All of the kinetic analysis was carried out with the IgorPro program (Wavemetrics).

The spectral analysis of the events occurring at the d_1 haem was carried out following the absorbance changes at wavelengths above 600 nm, in order to avoid overlap with the *c* haem, which does not contribute to this region of the spectrum. In the experimental conditions used in the present study, there is no evidence that ligands such as nitrite and cyanide bind to the *c* haem.

In order to determine the dissociation rate of NO from the reduced d_1 haem, the reduced NO-bound cytochrome cd_1 (3 μM) was rapidly mixed in the stopped-flow apparatus with excess potassium cyanide (0.08, 0.12, 0.2, 1, 5, 10, 15 and 100 mM a.m.), and the formation of the reduced-cyanide-bound derivative was followed at different wavelengths. Under these conditions, cyanide displaces NO by binding to the reduced d_1 haem.

To probe if NO dissociation from the fully reduced enzyme can be facilitated by the substrate, the reduced NO-bound cytochrome cd_1 (3.5 μM) was rapidly mixed in the stopped-flow apparatus with sodium nitrite (3 mM), and the reaction was followed in the diode array acquisition mode. This approach has been chosen in order to gain spectral information on the species involved, although we are aware that the observed rate can be slightly faster than under monochromatic light.

Under these conditions the following reaction occurs and nitrite binding is rate limited by NO dissociation:

$$\text{cytochrome } cd_1\text{–NO} + NO_2^- \rightarrow \text{cytochrome } cd_1\text{–}NO_2^- + \text{NO} \rightarrow \text{catalysis} \quad (1)$$

As a control, the reduced ligand-free (3.5 μM) enzyme was mixed with the same amounts of nitrite as above in the presence of excess ascorbate. The similarity of the latter reaction in terms of species involved and time course to previously published results [24] indicates that excess ascorbate does not alter the reaction mechanism.

Laser photolysis measurements

A 4.5 μM protein solution in 50 mM potassium phosphate buffer (pH 7.0) at room temperature (25°C) was reduced anaerobically as described above and then transferred to a fully filled gas-tight cuvette (Hellma) with four transparent windows; the path length along the direction of the probe light was 1 cm and the path length in the orthogonal direction was 4 mm. Different volumes of a stock NO solution were added anaerobically to produce the reduced NO-bound derivative in the concentration range 25–100 μM. The apparatus used for the photolysis experiments is home-built and has been described elsewhere [25]; every kinetic trace was the result of an average of 256 time courses at a single wavelength, each obtained after a single laser shot. The time course was followed at 460 nm, a wavelength where the spectrum of the reduced cytochrome cd_1 is dominated by the contribution of d_1 haem. Analysis of the results was performed by globally fitting all of the kinetic traces at different final NO concentrations.

Mbd_1 (haem d_1–apomyoglobin) experiments

Mbd_1 was prepared after reconstitution of sperm whale apomyoglobin (prepared according to [26]) using the d_1 haem extracted from wild-type *P. aeruginosa* cytochrome cd_1, as reported previously [27]. The Mbd_1 preparation and kinetic

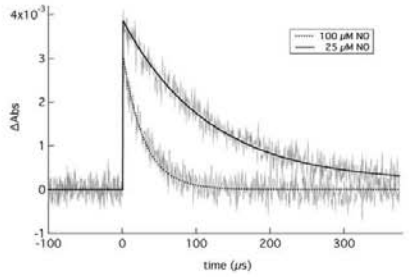

Figure 1 Time course of NO recombination with fully reduced *P. pantotrophus* cytochrome cd_1

The reaction was initiated by photodissociation of NO with a laser pulse at 532 nm; the recombination was monitored at 460 nm at four different NO concentrations, i.e. 100, 75, 50 and 25 μM. Only traces at 100 μM and 25 μM (grey thin lines) are shown for clarity, together with the results obtained by globally fitting all the traces (black broken and continuous lines respectively). As described in the Experimental section, every kinetic trace is the result of an average of 256 time courses, each obtained after a single laser shot. Experimental conditions: cytochrome cd_1 4.5 μM, 25 °C and 50 mM potassium phosphate (pH 7.0) containing 5 mM ascorbate and 13 μg/ml ascorbate oxidase.

experiments were carried out in 40 mM sodium phosphate buffer (pH 6.9).

The reduced Mbd_1 was prepared anaerobically by adding 5 mM sodium ascorbate to the oxidized protein in degassed buffer (40 mM sodium phosphate pH 6.9) at 20 °C, in the presence of 13 μg/ml ascorbate oxidase as an oxygen scavenger. The reduced NO-bound derivative was obtained after the addition of 100 μM NO solution (prepared as described above). All of the spectra were recorded in a JASCO V550 spectrophotometer.

To determine the NO-dissociation-rate constant, the reduced NO-bound Mbd_1 was mixed anaerobically in a gas-tight cuvette containing 5 mM sodium dithionite and ~500 μM CO; the process was followed by recording the spectrum (400–700 nm). The formation of the CO-bound complex [27] was complete within 2 min. To measure the kinetics of NO dissociation, the NO-bound Mbd_1 was mixed in the stopped-flow apparatus with a buffer solution containing 1 mM CO and 5 mM sodium dithionite (before mixing; three independent experiments). The kinetic process was followed at 451 nm; the time course was fitted with a single exponential equation.

RESULTS

The rate constant for the binding of NO to reduced *P. pantotrophus* cytochrome cd_1

The association rate constant for the binding of NO to reduced *P. pantotrophus* cytochrome cd_1 was determined by laser flash photolysis at pH 7.0 under anaerobic conditions at 25 °C (Figure 1). Time courses were followed at 460 nm in the presence of different NO concentrations (25, 50, 75 and 100 μM). The small absorbance change observed in the experiment is consistent with the low photolysis yield of the NO species, as previously observed with *P. aeruginosa* cytochrome cd_1 [15]. The global fit of the kinetic traces at different NO concentrations yields a value of $k_{on(NO)} = 3.5 \pm 0.3 \times 10^8\ M^{-1} \cdot s^{-1}$ (Table 1).

Table 1 Kinetic parameters for nitrite reduction and for NO and cyanide binding to and dissociation from reduced cytochrome cd_1 nitrite reductases

For comparison, the catalytic parameters for proteins able to catalyse the reduction of nitrite to NO [52] and containing a *b*-type haem are also shown. *Cytochrome cd_1 nitrite reductase binds the sixth ligand to the ferrous state of the d_1 haem. Anions such as nitrite or cyanide bind to ferric d_1 haem with very low affinity (K_d nitrite ~1 M) [53]. NO reacts slowly with the ferric enzyme by binding to the d_1 haem and then reducing it to produce the d_1^{2+}–NO derivative, thus autoreductive phenomenon is pH-dependent [54]. The kinetic parameters reported in the Table are at pH 7.0 and 20–25 °C; under these experimental conditions, none of the ligands used react with the *c* haem. However, at more acidic pH, reduction of the *c* haem (by NO or nitrite after reduction via d_1 haem) was reported to occur [32]. †Nitrite binding occurs very rapidly and cannot be directly measured, therefore the values in the table refer to estimates reported in the cited references. ‡Two kinetic constants are reported in all experiments where biphasic kinetics were observed (see present work and corresponding references).

Protein	haem	NO_2^- k_{cat} (s^{-1})	K_M (μM)	k_{on} ($M^{-1} \cdot s^{-1}$)	References	NO k_{on} ($M^{-1} \cdot s^{-1}$)	k_{off} (s^{-1})	K_D (M)	References	CN⁻ k_{on} ($M^{-1} \cdot s^{-1}$)	k_{off} (s^{-1})	K_D (M)	References
P. pantotrophus cytochrome cd_1	d_1 Fe^{3+}	72	12	>10^7†	[18,31]	3.5×10^8	85	1.8×10^{-7}	Present study	5.9×10^6	0.4	0.7×10^{-8}	Present study [28]
							200 ‡	5.7×10^{-7}					
P. aeruginosa cytochrome cd_1	d_1 Fe^{3+}	6	6	>10^7†	[13,15,55]	3.9×10^8	70	1.8×10^{-7}	[16]	4.6×10^6	4	9.5×10^{-8}	[36]
										1.2×10^6 ‡			
Myoglobin	b^{2+}	–	–	12	[46]	1.7×10^7	10^{-4}	5.9×10^{-12}	[7]	2.5	0.15	0.2	[47]
Haemoglobin	b^{2+}	–	–	12	[46]	2.4×10^8	1×10^{-3}	4.2×10^{-9}	[7]	-	0.12	0.1	[48]
				0.2			1×10^{-5} ‡	4.2×10^{-11}	[49]		1.5‡	1.5	[50]
													[51]

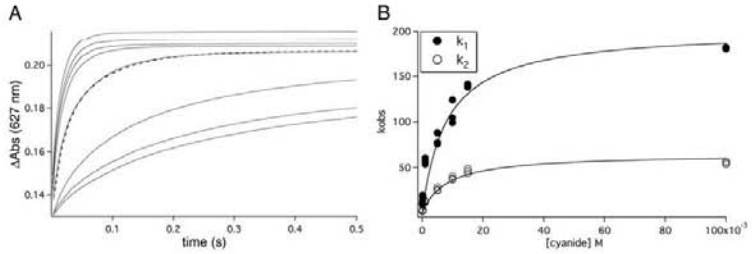

Figure 2 Dissociation of NO from fully reduced NO-bound *P. pantotrophus* cytochrome cd_1 obtained by displacement with excess cyanide

(**A**) The dissociation time course was followed after mixing fully reduced NO-bound cytochrome cd_1 (6 μM) with excess potassium cyanide (0.08, 0.12, 0.2, 1, 5, 10, 15 and 100 mM) in the stopped-flow apparatus. The kinetic data were collected in the single wavelength acquisition mode in order to minimize NO photodissociation. The kinetics were followed at 627 nm (absorption maximum of the cyanide bound d_1 haem; there is no absorbance from the *c* haem at this wavelength) and the time course fitted with a double exponential equation (broken line). (**B**) Plot of the observed NO displacement rate constant from reduced cytochrome cd_1 as a function of cyanide concentration; each kinetic phase (see above) was plotted independently (k_1 = ●, k_2 = ○). The results are fitted using the replacement model (thin line) [26], the equation contains the cyanide k_{on} and k_{off} and the NO k_{on} values measured independently in this work. The values of three independent measurements at each cyanide concentration are reported. Experimental conditions: 20 °C and 50 mM potassium phosphate (pH 7.0) containing 5 mM ascorbate and 13 μg/ml ascorbate oxidase.

The rate constant for the dissociation of NO from reduced *P. pantotrophus* cytochrome cd_1

To measure NO dissociation, we took advantage of the unusually high affinity for cyanide of reduced cytochrome cd_1, which can be exploited to displace NO from the ferrous d_1 haem [15]. It was shown previously that ferrous *P. pantotrophus* cytochrome cd_1 binds cyanide relatively tightly ($K_d = 0.7 \pm 0.2 \times 10^{-6}$ M at pH 7.0) (Table 1) [28], although the corresponding association and dissociation rate constants were not determined. We determined these rate constants (Supplementary Figures S4 and S5 at http://www.BiochemJ.org/bj/435/bj4350217add.htm) since they are necessary to calculate the NO dissociation rate constant in the cyanide–NO displacement experiment and found values of: $k_{on(CN)} = 5.9 \pm 0.1 \times 10^5$ $M^{-1} \cdot s^{-1}$ and $k_{off(CN)} = 0.4 \pm 0.02$ s^{-1} (Table 1). These results yield a K_d of 0.68 μM, which is in excellent agreement with the equilibrium value reported previously [28].

The NO-dissociation time course at 20 °C and pH 7.0 was time-resolved by mixing reduced NO-bound *P. pantotrophus* cytochrome cd_1 with excess cyanide (0.08–100 mM) in the stopped-flow instrument and following the kinetics at 627 nm (Figure 2), a wavelength characteristic of the ferrous d_1 haem–CN complex (Figure S3) and where the *c* haem does not absorb. The time course of formation of the cyanide derivative (Figure 2A) was biphasic under all conditions. The biphasicity cannot be ascribed to the cyanide binding process, which is always monophasic (Figure S4).

The values of the rate constants for both phases, k_1 and k_2, have been plotted as a function of ligand concentration (Figure 2B). At low CN^-, the two phases have equal amplitudes, suggesting that the two monomers of cytochrome cd_1 possibly react at different rates; at high CN^-, some amplitude of the first phase is lost in the dead time of the instrument because the reaction is too fast. The data have been analyzed using the replacement model described in eqn 1 [26]:

$$R = \frac{k_{off(NO)}\,k_{on(CN)}[CN^-] + k_{off(CN)}\,k_{on(NO)}[NO]}{k_{on(CN)}[CN^-] + k_{on(NO)}[NO]} \qquad (2)$$

The two rate constants for NO dissociation from reduced *P. pantotrophus* cytochrome cd_1 are as follows: $k_1 = 201.2 \pm 11.4$ s^{-1} and $k_2 = 64.9 \pm 2.3$ s^{-1} for the fast and slow processes respectively (Table 1).

Displacement of NO by nitrite from reduced *P. pantotrophus* cytochrome cd_1

Both the ferrous NO-bound and, for comparison, the ferrous enzyme, were mixed anaerobically with excess nitrite (3 mM) in the stopped-flow apparatus (at 20 °C and pH 7.0). The time courses at 551 and 660 nm, representative of the *c* and d_1 haems respectively, are shown in Figures 3(A) and 3(B) for the reduced-NO bound enzyme and the reduced unligated enzyme. It is clear that the kinetic phase seen within the first 20 ms in the experiment with the reduced-NO-bound species is absent in the reaction with the unligated reduced enzyme. Spectral analysis shows that this fast phase involves *c* haem oxidation and synchronous formation of a transient at the d_1 haem, occurring at approx. 100 s^{-1} (Figures 3A and 3B respectively). At longer times (>20 ms) the time courses of the two experiments are superimposable. Analysis of the spectra (Figure 3C) shows that the first observable species (at 1 ms) is different in the two experiments, whereas at longer times (>0.1 s) the spectra superimpose, suggesting that the same derivative is formed on the latter timescale. The final species, which is formed at ~20 s^{-1}, is very similar to that previously observed in the reaction of reduced *P. pantotrophus* cytochrome cd_1 with nitrite [24]. We conclude that during the first 20 ms nitrite displaces NO and reacts with the reduced protein populating an intermediate, whose formation is rate-limited by NO dissociation. The synchronous *c* haem oxidation indicates that this intermediate is formed as nitrite is reduced to NO; afterwards this species decays as when the initially reduced but unligated enzyme reacts with nitrite.

The rate of dissociation of NO from reduced d_1 haem complexed with apomyoglobin

The low affinity towards NO displayed by cytochrome cd_1 could be due to the presence of the unique d_1 haem and/or the structure

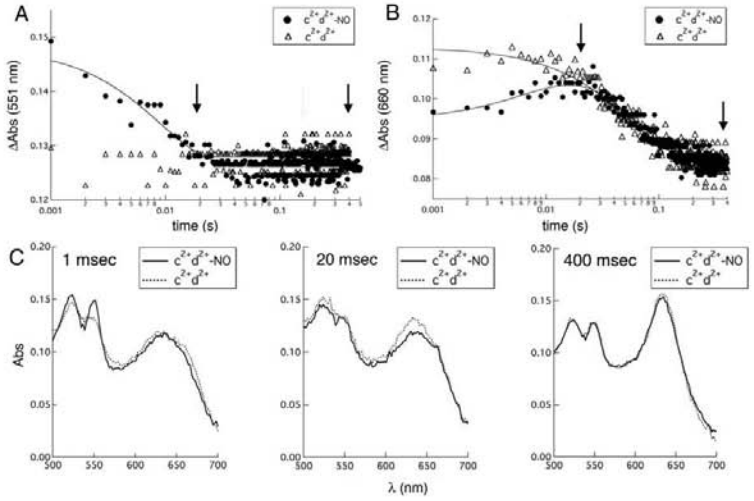

Figure 3 Dissociation of NO from reduced *P. pantotrophus* cytochrome *cd*$_1$ induced by displacement with nitrite

Time course of the reaction of 3.5 μM cytochrome *cd*$_1$, either reduced NO-bound (●) or reduced (△), mixed with 3 mM nitrite. The reaction was followed at wavelengths representative of the *c* haem (551 nm, **A**) and of the d_1 haem (660 nm, **B**). In the reaction of the reduced-NO-bound enzyme, the decrease at 551 nm (●, **A**) indicates oxidation of the *c* haem, whereas the increase of absorption at 660 nm (●, **B**) indicates the formation of a transient species. The continuous lines represent fits of the data with a single- or double-exponential equation respectively. The arrows indicate 20 and 400 ms after mixing (see below). (**C**) Optical spectra collected at 1, 20 and 400 ms after mixing with nitrite the reduced NO-bound (continuous line) and the reduced cytochrome *cd*$_1$ (broken line). Experimental conditions: 20 °C and 50 mM potassium phosphate (pH 7.0) containing 5 mM ascorbate and 13 μg/ml ascorbate oxidase.

of the haem-binding pocket. In order to assess the role of d_1 haem in controlling the affinity for NO, we have measured the NO-dissociation-rate constant from ferrous d_1 haem complexed with Mbd_1.

As published previously, the d_1 haem cofactor combines with apomyoglobin to form a stable complex; several ferric and ferrous derivatives have been spectroscopically characterized [27]. Steup and Muhoberac [27] suggested that the d_1 haem was co-ordinated by a strong-field ligand that they assigned as a histidine residue; however, no static or kinetic characterization with NO was reported. Since the peculiarity of the reactivity with NO of the d_1 haem in cytochrome cd_1 resides in the fast release of the ligand, we have measured the dissociation rate of NO from the reduced Mbd_1 complex. Sperm whale apomyoglobin was complexed with the d_1 haem; the spectral properties of the complex were identical to those published previously [27]. Figure 4(A) shows the spectra of the ascorbate-reduced state and of the stable derivative obtained by reacting the latter species with 100 μM NO, with peaks at 445 and 644 nm. To determine the NO-dissociation-rate constant, the NO derivative was mixed anaerobically in a gas-tight cuvette with 5 mM sodium dithionite and ~500 μM CO (final concentrations) and the spectrum (400–700 nm) was recorded. The first spectrum (obtained 1.5 min a.m.) shows peaks at 452 and 642 nm (Figure 4A) suggesting that the CO-bound species had already formed. The spectrum did not change significantly during the time of the experiment (~30 min), but the shoulder at 590 nm broadened (results not shown), suggesting that two CO-bound species were formed which slowly re-equilibrated, in agreement with previous evidence [27]. Since the binding of CO, and thus dissociation of NO, could not be time-resolved in the spectrophotometer, the same reaction was followed by stopped-flow at 451 nm (Figure 4B). The reaction had a half-time of ~350 ms and the observed absorbance change corresponded to 92% of that expected (Figure 4A). The majority of the transition (Figure 4B) occurred at $k_{off} = 2.0 \pm 0.4\ s^{-1}$; this reaction was found to be CO-concentration independent (results not shown).

DISCUSSION

The reaction of NO with haems plays an important role in controlling cellular physiopathological processes [7–9,17]. The fact that NO binds strongly to ferrous haem, albeit reversibly at extremely low free NO concentrations, imposes mechanistic constraints on many proteins that synthesize or bind NO. The enzymatic turnover of cytochrome cd_1 nitrite reductase, in which nitrite is converted into NO, also demands the fast release of the product to avoid inhibition.

In the present paper, we aim at understanding whether the unique d_1 haem, where nitrite reduction occurs, has a role in controlling the release of NO. Therefore we have measured the reactivity of the d_1 haem with NO in the physiological context, i.e. the cytochrome cd_1 enzyme from *P. pantotrophus* and in a non-native protein environment, provided by apomyoglobin.

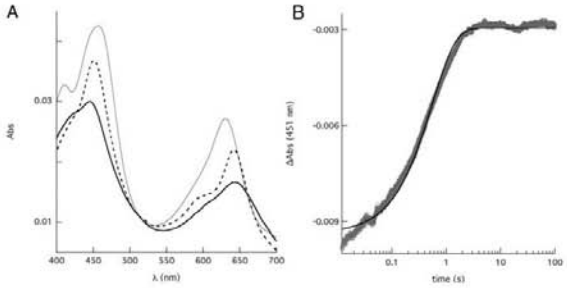

Figure 4 Dissociation of NO from ferrous d_1 haem complexed with sperm whale apomyoglobin

The displacement of NO was measured in the presence of excess CO and dithionite [26] (at 20 °C and pH 6.9); under these conditions CO competes with NO for binding to the reduced d_1 haem iron and the kinetics are rate-limited by NO dissociation. (**A**) Absorbance spectra of ascorbate-reduced Mbcd_1 (thin line) and of the corresponding NO-bound derivative (bold line). The latter species was mixed anaerobically in a gas-tight cuvette with 5 mM sodium dithionite as an NO scavenger and ~500 μM CO, and the spectrum (400–700 nm) was recorded (broken line). This spectrum did not change significantly over the following ~30 min. (**B**) Reaction of ascorbate-reduced Mbcd_1–NO bound species mixed with 1 mM CO and 5 mM dithionite (before mixing) in the stopped-flow apparatus. The observed time course at 451 nm (grey circles) represents the decay of the reduced NO-bound derivative; the time course was fitted with a single-exponential equation (continuous line). Experimental conditions: 20 °C and 40 mM potassium phosphate (pH 6.9) containing 5 mM ascorbate and 13 μg/ml ascorbate oxidase. The final protein concentrations (a.m.) were the same in (**A**) and (**B**).

The results of the present study here provide novel mechanistic insights on the reaction mechanism of cytochrome cd_1 and allow us to draw a common scheme that is applicable to this whole class of enzymes (Figure 5).

NO release is rapid in ferrous cytochrome cd_1: relevance to the catalytic cycle

The major novel conclusion of the present study is that fast NO dissociation from the ferrous d_1 haem is a common feature of cytochrome cd_1 nitrite reductases. This conclusion is supported by the observation that NO dissociation from the reduced d_1 haem of *P. pantotrophus* cytochrome cd_1 is fast (Figure 2 and Table 1; $k_{off} = 200\ s^{-1}$ and $65\ s^{-1}$ for the biphasic dissociation); these data agree well with previous results for the *P. aeruginosa* cytochrome cd_1 where NO dissociation occurred at $70\ s^{-1}$ [15] (Table 1). As a consequence of the greater k_{off} from reduced d_1 haem, the K_d for NO in cytochrome cd_1 is orders of magnitude larger than in other haemoproteins [7,17,29] (Table 1).

The rapid NO dissociation from cytochrome cd_1 nitrite reductases strongly suggests that NO release from ferrous d_1 haem of cytochrome cd_1 is a plausible step in the catalytic cycle. Therefore the mechanism previously proposed [15] and summarized in Figure 5 is a reasonable general catalytic cycle for all cytochromes cd_1. Notably, it is also essentially the simplest reaction cycle that one can draw for these enzymes. This interpretation explains why the d_1^{3+}-NO derivative of *P. pantotrophus* cytochrome cd_1 is a very long-lived species in the absence of excess reductant [14,30]; it also agrees with previous ultra-fast (microsecond resolution) kinetic studies on the same enzyme showing that intramolecular c haem to d_1 haem electron transfer triggered product release [31]. All available results indicate that *P. pantotrophus* cytochrome cd_1 only works efficiently in the presence of substrate and electron donors [18,30,32,33], i.e. it gets 'stuck' with NO bound in the absence of reducing equivalents. It has long been a puzzle why an enzyme that catalyses a one-electron reduction requires two redox centres (the c and d_1 haems). Electron donation to cytochrome cd_1 from partner proteins occurs only via the c haem. A reaction mechanism where nitrite is first reduced to NO at the d_1 haem, oxidizing that haem, but in which the d_1 haem must be re-reduced (by the c haem) to allow NO release, would explain the need for two redox centres.

The results of the present study also suggest that, after the release of NO, the ferrous enzyme is competent to start a new catalytic cycle; therefore the reduced NO-bound *P. pantotrophus* cytochrome cd_1 is not irreversibly inhibited. This is supported by the kinetic experiment in which the fully reduced-NO-bound cytochrome cd_1 is mixed with nitrite: in this experiment, a complex reaction involving both electron transfer between the two redox centres (as seen by the oxidation of c haem, Figure 3A) and chemistry at the d_1 haem (Figure 3B) is observed. The relevant observation is that an intermediate species (populated at $100\ s^{-1}$) could be observed with spectroscopic features (around 660 nm) similar to those observed previously when the reduced *P. pantotrophus* cytochrome cd_1 was reacted with nitrite in a freeze-quench experiment [31]. In the kinetic experiment, the formation of this transient species (Figure 3) supports the idea that, after the release of NO, the ferrous enzyme can start a new catalytic cycle. The ability of the *P. pantotrophus* cytochrome cd_1 to release NO without undergoing significant product inhibition is also consistent with earlier steady-state experiments in which a linear rate of NO production occurred up to tens of micromolar concentrations [34].

Another novel mechanistic insight into the reaction with nitrite catalysed by cytochrome cd_1 is the assignment of the rate-determining step. In *P. pantotrophus* cytochrome cd_1 the slower phase of NO dissociation ($k_{off} = 65\ s^{-1}$; Figure 2) occurs with a rate that is very similar to the overall k_{cat} ($72\ s^{-1}$ per d_1 haem [18]), indicating that this process probably represents the rate-limiting step of the reaction. However, for *P. aeruginosa* cytochrome cd_1 the rate-determining step is probably the intramolecular electron transfer from the c haem to the d_1 haem, since the reported

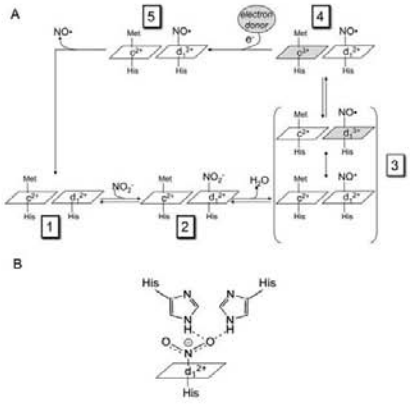

Figure 5 Proposed reaction mechanism for the catalytic cycle of cytochrome *cd*$_1$ nitrite reductases

The catalytic cycle (**A**) is illustrated starting from the fully reduced enzyme (species 1), which binds the substrate nitrite yielding the Michaelis complex (species 2) [10,11,31]. Nitrite binding and reduction involves two conserved histidine residues [11], whose mutation was shown to affect the activity of *P. aeruginosa* cytochrome *cd*$_1$ [35] (**B** for a scheme of the active site). Transfer of one electron from the d_1 haem to nitrite produces NO bound to the oxidized haem iron (species 3) and a water molecule, which is released (oxidized haems are shown in grey). NO release from species 3 was not observed [14]. All available data suggest that NO dissociation occurs from the fully reduced NO-bound enzyme (species 5) in both *P. pantotrophus* and *P. aeruginosa* cytochromes *cd*$_1$ (present paper and [15] respectively). Species 5 is formed via species 4 in two steps: transfer of an electron from the *c* haem to the d_1 haem, followed by reduction of the *c* haem by an external electron donor. The physiological reductants of cytochrome *cd*$_1$ are small cytochromes *c* (such as *P. aeruginosa* cytochrome c_{551} or *P. pantotrophus* cytochrome c_{550}) or copper proteins (such as pseudoazurin in *P. pantotrophus*) [10], which specifically transfer the electron only to the *c* haem. After NO dissociation from species 5, the fully reduced enzyme is reformed and enters a new catalytic cycle. The present results does not allow us to rule out that NO dissociation may occur from the mixed valence nitrosylated protein (species 4); this would be difficult to measure due to the intrinsic redox instability of the mixed valence species [54]. The scheme described in the present paper refers to a single monomer of the enzyme; various results (see the Discussion section and [31]) imply the possibility of co-operativity between monomers during the catalytic cycle, but this is thought to affect the relative rates of catalytic steps in each monomer, not the steps themselves.

electron transfer rate (1–4 s^{-1}) is similar to the turnover number (6 s^{-1}) [5,20]. Thus in *P. aeruginosa* cytochrome cd_1, the relatively slow formation of ferrous d_1 haem–NO would be followed by a more rapid dissociation of NO.

Although more speculative, we note that analysis of NO dissociation from *P. pantotrophus* cytochrome cd_1 may also suggest that, in this enzyme, the two monomers dissociate NO at different rates (NO dissociation is biphasic and each kinetic phase corresponds to ~50 % of the total absorbance change). These results are in agreement with previous kinetic experiments with nitrite, which were interpreted in terms of anti-co-operativity of the two monomers [31]. Even though the mechanism of such anti-co-operativity is yet to be explained, intrinsic asymmetry of cytochrome cd_1 is suggested and supported by evidence obtained from ligand-binding experiments [28,36], a pre-steady-state kinetic study with nitrite [31], intramolecular electron transfer [20,37] and potentiometric titrations [38,39]. Moreover, in the many X-ray crystal structures of *P. pantotrophus* cytochrome cd_1 and its ligand-bound derivatives, the two monomers are always different [11,28,40].

Role of the d_1 haem in NO release

The other novel outcome of the present study is that fast NO dissociation from ferrous haem iron is largely due to the presence of the unique d_1 haem cofactor. The role of ferrous d_1 haem in controlling NO dissociation was analysed in a different protein environment, i.e. the d_1 haem complexed with apomyoglobin. In ferrous Mbd_1, we observe a single NO-dissociation process occurring at 2 s^{-1} (Figure 4), a rate which is approx. 3–5 orders of magnitude greater than that measured for native ferrous myoglobin which contains *b* haem (Fe-protoporphyrin IX) (Table 1) [7]. Given these results and taking into account that both Mbd_1 and cytochrome cd_1 have a common proximal histidine residue ligand, we conclude that the d_1 haem is designed to release NO relatively rapidly. It is known that NO is a good π-acceptor and, in general, an important contribution to the strength of NO binding to the ferrous haem iron can arise from electron donation from the t2g orbitals on the iron. The two electron withdrawing carbonyl groups on the d_1 haem ring (see Supplementary Figure S2) might weaken such electron donation to NO.

There are previous observations indicating that the ring structure of the d_1 haem confers on the Fe atom other properties that are distinct from those of protoporphyrin IX. The ferrous state of d_1 haem binds anions, including the substrate nitrite and the inhibitor cyanide, unusually strongly and, strikingly, more strongly than the ferric state (Table 1) [32]. This also correlates with the presence of two electron-withdrawing carbonyl groups on the d_1 haem ring. Another feature of the d_1 haem ring is that in the ferric state this cofactor shows a peculiar ordering of the energy levels of the d orbitals [41]; the latter property is shared with other haems in which the porphyrin ring is partially saturated (haem *d* in *Escherichia coli* and sirohaem) [42,43]. Clearly, a range of advanced spectroscopic and theoretical studies, outside the scope of the present work, needs to be applied to fully understand how the d_1 haem ring is tuned, in the ferrous state, to bind anions unusually strongly, but NO unusually weakly, in order to catalyse the reduction of nitrite. The consequence is that whereas *a priori* one might have expected a haem enzyme to bind nitrite to, and release NO from, the ferric state, the opposite strategy has evolved.

The higher NO-dissociation rate measured for cytochromes cd_1 (up to 200 s^{-1}) (as compared with Mbd_1) may in principle reflect to some extent a feature in the d_1 haem pocket that optimizes NO release. A possible mechanism may include the conformational change seen in *P. pantotrophus* cytochrome cd_1 and thought to be implicated in catalysis [44]; this change involves Tyr^{197} on the proximal side of the d_1 haem pocket and the hinge region (residues 132–136) connecting the *c* and the d_1 haem domains. However, mutation of these residues (Y197F and P134F/P135F) has no significant effect on the enzymatic activity [55] and thus this conformational change is unlikely to control NO release. Therefore the (relatively small) contribution of the protein moiety to the control of NO release is yet to be identified at the molecular level.

Conclusion

The present study allows the formulation of a straightforward, unified reaction mechanism for cytochrome cd_1 nitrite reductases, a class of enzymes studied for over 50 years (Figure 5). The experiments reported in the present paper strongly suggest that fast NO dissociation from ferrous haem iron is largely due to

the presence of the unique d_1 haem cofactor, and that enzyme inhibition by NO is unlikely to be relevant under physiological conditions. The evidence underscores that the reactivity of porphyrins with NO can be modulated very extensively by the functional groups present on the haem macrocycle, information of general significance in light of the emerging important biological functions of nitrite as a source of NO under hypoxic conditions [45].

AUTHOR CONTRIBUTION

Serena Rinaldo and Katharine A. Sam performed most of the experiments on *P. pantotrophus* cytochrome cd_1 with the necessary assistance of Nicoletta Castiglione and Valentina Stelitano. Alessandro Arcovito performed the laser photolysis experiments; Serena Rinaldo and Valentina Stelitano performed the experiments on Mbd_1. The results analysis was carried out by Serena Rinaldo with the contribution of Francesca Cutruzzolà. Francesca Cutruzzolà directed the study and together with Stuart J. Ferguson, James W.A. Allen and Maurizio Brunori conceptualized the project. Francesca Cutruzzolà wrote the manuscript, and all authors contributed to the final version(s) prior to publication. Maurizio Brunori, James W.A. Allen, Francesca Cutruzzolà and Stuart J. Ferguson wrote the grants that provided funding.

ACKNOWLEDGEMENTS

We thank A. Bellelli (Rome, Italy) for useful discussions on the kinetic experiments. This paper is dedicated to Professor Alessandro Coda (University of Pavia, Italy), on the occasion of his retirement.

FUNDING

This work was supported by the Ministero della Università of Italy [grant numbers 20074TJ3ZB and RBRN07BMCT]; and the University of Rome La Sapienza to F.C. and M.B. K.A.S. thanks St Edmund Hall, Oxford for the award of a W.R. Miller Junior Research Fellowship. The Biotechnology and Biological Sciences Research Council supported J.W.A.A. through a David Phillips Fellowship [grant number BB/D019753/1] and S.J.F. through project grants.

REFERENCES

1 Zumft, W. G. (1997) Cell biology and molecular basis of denitrification. Microbiol. Mol. Biol. Rev. **61**, 533–616
2 Baek, S. H., Rajashekara, G., Splitter, G. A. and Shapleigh, J. P. (2004) Denitrification genes regulate *Brucella* virulence in mice. J. Bacteriol. **186**, 6025–6031
3 van Alst, N. E., Picardo, K. F., Iglewski, B. H. and Haidaris, C. G. (2007) Nitrate sensing and metabolism modulate motility, biofilm formation, and virulence in *Pseudomonas aeruginosa*. Infect. Immun. **75**, 3780–3790
4 Barth, K. R., Isabella, V. M. and Clark, V. L. (2009) Biochemical and genomic analysis of the denitrification pathway within the genus *Neisseria*. Microbiology **155**, 4093–4103
5 Hassett, D. J., Sutton, M. D., Schurr, M. J., Herr, A. B., Caldwell, C. C. and Matu, J. O. (2009) *Pseudomonas aeruginosa* hypoxic or anaerobic biofilm infections within cystic fibrosis airways. Trends Microbiol. **17**, 130–138
6 Ignarro, L. J. (2009) Nitric Oxide. Biology and Pathobiology, Academic Press, London
7 Moore, E. G. and Gibson, Q. H. (1976) Cooperativity in the dissociation of nitric oxide from hemoglobin. J. Biol. Chem. **251**, 2788–2794
8 Brown, G. C. and Cooper, C. E. (1994) Nanomolar concentrations of nitric oxide reversibly inhibit synaptosomal respiration by competing with oxygen at cytochrome oxidase. FEBS Lett. **356**, 295–298
9 Boon, E. M. and Marletta, M. A. (2005) Ligand discrimination in soluble guanylate cyclase and the H-NOX family of heme sensor proteins. Curr. Opin. Chem. Biol. **9**, 441–446
10 Rinaldo, S. and Cutruzzolà, F. (2007) Nitrite reductases in denitrification. Biology of the Nitrogen Cycle, pp. 37–55, Elsevier, Amsterdam
11 Williams, P. A., Fülöp, V., Garman, E. F., Saunders, N. F., Ferguson, S. J. and Hajdu, J. (1997) Haem-ligand switching during catalysis in crystals of a nitrogen-cycle enzyme. Nature **389**, 406–412
12 Averill, B. A. (1996) Dissimilatory nitrite and nitric oxide reductases. Chem. Rev. **96**, 2951–2964
13 Silvestrini, M. C., Tordi, M. G., Musci, G. and Brunori, M. (1990) The reaction of *Pseudomonas* nitrite reductase and nitrite. A stopped-flow and EPR study. J. Biol. Chem. **265**, 11783–11787
14 George, S. J., Allen, J. W., Ferguson, S. J. and Thomeley, R. N. (2000) Time-resolved infrared spectroscopy reveals a stable ferric heme–NO intermediate in the reaction of *Paracoccus pantotrophus* cytochrome cd1 nitrite reductase with nitrite. J. Biol. Chem. **275**, 33231–33237
15 Rinaldo, S., Arcovito, A., Brunori, M. and Cutruzzolà, F. (2007) Fast dissociation of nitric oxide from ferrous *Pseudomonas aeruginosa* cd_1 nitrite reductase. A novel outlook on the catalytic mechanism. J. Biol. Chem. **282**, 14761–14767
16 Rinaldo, S., Brunori, M. and Cutruzzolà, F. (2007) Nitrite controls the release of nitric oxide in *Pseudomonas aeruginosa* cd_1 nitrite reductase. Biochem. Biophys. Res. Commun. **363**, 662–666
17 Sarti, P., Giuffrè, A., Forte, E., Mastronicola, D., Barone, M. C. and Brunori, M. (2000) Nitric oxide and cytochrome *c* oxidase: mechanisms of inhibition and NO degradation. Biochem. Biophys. Res. Commun. **274**, 183–187
18 Richter, C. D., Allen, J. W., Higham, C. W., Koppenhöfer, A., Zajicek, R. S., Watmough, N. J. and Ferguson, S. J. (2002) Cytochrome cd_1, reductive activation and kinetic analysis of a multifunctional respiratory enzyme. J. Biol. Chem. **277**, 3093–3100
19 Kobayashi, K., Koppenhöfer, A., Ferguson, S. J. and Tagawa, S. (1997) Pulse radiolysis studies on cytochrome cd_1 nitrite reductase from *Thiosphaera pantotropha*: evidence for a fast intramolecular electron transfer from c heme to d_1 heme. Biochemistry **36**, 13611–13616
20 Farver, O., Brunori, M., Cutruzzolà, F., Rinaldo, S., Wherland, S. and Pecht, I. (2009) Intramolecular electron-transfer in *Pseudomonas aeruginosa* cd_1 nitrite reductase: thermodynamics and kinetics. Biophys. J. **96**, 2849–2856
21 Moir, J. W.B., Baratta, D., Richardson, D. J. and Ferguson, S. J. (1993) The purification of a cd_1-type nitrite reductase from, and the absence of a copper-type nitrite reductase from, the aerobic denitrifier *Thiosphaera pantotropha*; the role of pseudoazurin as an electron donor. Eur. J. Biochem. **212**, 377–385
22 Koppenhöfer, A., Little, R. H., Lowe, D. J., Ferguson, S. J. and Watmough, N. J. (2000) Oxidase reaction of cytochrome cd(1) from *Paracoccus pantotrophus*. Biochemistry **39**, 4028–4036
23 Allen, J. W., Watmough, N. J. and Ferguson, S. J. (2000) A switch in heme axial ligation prepares *Paracoccus pantotrophus* cytochrome cd_1 for catalysis. Nat. Struct. Biol. **7**, 885–888
24 Sam, K. A., Fairhurst, S. A., Thomeley, R. N., Allen, J. W. and Ferguson, S. J. (2008) Pseudoazurin dramatically enhances the reaction profile of nitrite reduction by *Paracoccus pantotrophus* cytochrome cd_1 and facilitates release of product nitric oxide. J. Biol. Chem. **283**, 12555–12563
25 Arcovito, A., Gianni, S., Brunori, M., Travaglini-Allocatelli, C. and Bellelli, A. (2001) Fast coordination changes in cytochrome *c* do not necessarily imply folding. J. Biol. Chem. **276**, 41073–41078
26 Antonini, E. and Brunori, M. (1971) Hemoglobin and Myoglobin in their Reactions with Ligands, North-Holland Publishing Company, Amsterdam
27 Steup, M. B. and Muhoberac, B. B. (1989) Preparation and spectral characterization of the heme d_1 apomyoglobin complex: an unusual protein environment for the substrate-binding heme of *Pseudomonas* cytochrome oxidase. J. Inorg. Biochem. **37**, 233–257
28 Jafferji, A., Allen, J. W., Ferguson, S. J. and Fulop, V. (2000) X-ray crystallographic study of cyanide binding provides insights into the structure–function relationship for cytochrome cd_1 nitrite reductase from *Paracoccus pantotrophus*. J. Biol. Chem. **275**, 25089–25094
29 Borisov, V. B., Forte, E., Sarti, P., Brunori, M., Konstantinov, A. A. and Giuffrè, A. (2007) Redox control of fast ligand dissociation from *Escherichia coli* cytochrome *bd*. Biochem. Biophys. Res. Commun. **355**, 97–102
30 Sam, K. A., Tolland, J. D., Fairhurst, S. A., Higham, C. W., Lowe, D. J., Thomeley, R. N., Allen, J. W. and Ferguson, S. J. (2008) Unexpected dependence on pH of NO release from *Paracoccus pantotrophus* cytochrome cd_1. Biochem. Biophys. Res. Commun. **371**, 719–723
31 Sam, K. A., Strampraad, M. J., de Vries, S. and Ferguson, S. J. (2008) Very early reaction intermediates detected by microsecond time scale kinetics of cytochrome cd_1-catalyzed reduction of nitrite. J. Biol. Chem. **283**, 27409–27409
32 Zajicek, R. S., Cartron, M. L. and Ferguson, S. J. (2006) Probing the unusual oxidation/reduction behavior of *Paracoccus pantotrophus* cytochrome cd_1 nitrite reductase by replacing a switchable methionine heme iron ligand with histidine. Biochemistry **45**, 11208–11216
33 Sam, K. A., Fairhurst, S. A., Thomeley, R. N., Allen, J. W. and Ferguson, S. J. (2008) Pseudoazurin dramatically enhances the reaction profile of nitrite reduction by *Paracoccus pantotrophus* cytochrome cd_1 and facilitates release of product nitric oxide. J. Biol. Chem. **283**, 12555–12563
34 Carr, G. J., Page, M. D. and Ferguson, S. J. (1989) The energy-conserving nitric-oxide-reductase system in *Paracoccus denitrificans*. Distinction from the nitrite reductase that catalyses synthesis of nitric oxide and evidence from trapping experiments for nitric oxide as a free intermediate during denitrification. Eur. J. Biochem. **179**, 683–692

35 Cutruzzolà, F., Brown, K., Wilson, E. K., Bellelli, A., Arese, M., Tegoni, M., Cambillau, C. and Brunori, M. (2001) The nitrite reductase from *Pseudomonas aeruginosa*: essential role of two active-site histidines in the catalytic and structural properties. Proc. Natl. Acad. Sci. U.S.A. **98**, 2232–2237
36 Sun, W., Arese, M., Brunori, M., Nurizzo, D., Brown, K., Cambillau, C., Tegoni, M. and Cutruzzolà, F. (2002) Cyanide binding to cd_1 nitrite reductase from *Pseudomonas aeruginosa*: role of the active-site His^{369} in ligand stabilization. Biochem. Biophys. Res. Commun. **291**, 1–7
37 Farver, O., Kroneck, P. M., Zumft, W. G. and Pecht, I. (2003) Allosteric control of internal electron transfer in cytochrome cd_1 nitrite reductase. Proc. Natl. Acad. Sci. U.S.A. **100**, 7622–7625
38 Blatt, Y. and Pecht, I. (1979) Allosteric cooperative interactions among redox sites of *Pseudomonas* cytochrome oxidase. Biochemistry **18**, 2917–2922
39 Koppenhöfer, A., Turner, K. L., Allen, J. W., Chapman, S. K. and Ferguson, S. J. (2000) Cytochrome cd_1 from *Paracoccus pantotrophus* exhibits kinetically gated, conformationally dependent, highly cooperative two-electron redox behavior. Biochemistry **39**, 4243–4249
40 Fulop, V., Moir, J. W., Ferguson, S. J. and Hajdu, J. (1995) The anatomy of a bifunctional enzyme: structural basis for reduction of oxygen to water and synthesis of nitric oxide by cytochrome cd_1. Cell **81**, 369–377
41 Cheesman, M. R., Ferguson, S. J., Moir, J. W., Richardson, D. J., Zumft, W. G. and Thomson, A. J. (1997) Two enzymes with a common function but different heme ligands in the forms as isolated. Optical and magnetic properties of the heme groups in the oxidized forms of nitrite reductase, cytochrome cd_1, from *Pseudomonas stutzeri* and *Thiosphaera pantotropha*. Biochemistry **36**, 16267–16276
42 Frankenberg, N., Moser, J. and Jahn, D. (2003) Bacterial heme biosynthesis and its biotechnological application. Appl. Microbiol. Biotechnol. **63**, 115–127
43 Tanaka, R. and Tanaka, A. (2007) Tetrapyrrole biosynthesis in higher plants. Annu. Rev. Plant Biol. **58**, 321–346
44 Sjögren, T. and Hajdu, J. (2001) The structure of an alternative form of *Paracoccus pantotrophus* cytochrome cd_1 nitrite reductase. J. Biol. Chem. **276**, 29450–29455
45 van Faassen, E. E., Bahrami, S., Feelisch, M., Hogg, N., Kelm, M., Kim-Shapiro, D. B., Kozlov, A. V., Li, H., Lundberg, J. O., Mason, R. et al. (2009) Nitrite as regulator of hypoxic signaling in mammalian physiology. Med. Res. Rev. **29**, 683–741
46 Gladwin, M. T. and Kim-Shapiro, D. B. (2008) The functional nitrite reductase activity of the heme-globins. Blood **112**, 2636–2647
47 Boffi, A., Ilari, A., Spagnuolo, C. and Chiancone, E. (1996) Unusual affinity of cyanide for ferrous and ferric *Scapharca inaequivalvis* homodimeric hemoglobin. Equilibria and kinetics of the reaction. Biochemistry **35**, 8068–8074
48 Olivas, E., De Waal, D. J. and Wilkins, R. G. (1977) Reduction of metmyoglobin derivatives by dithionite ion. J. Biol. Chem. **252**, 4038–4042
49 Azizi, F., Kielbasa, J. E., Adeyiga, A. M., Maree, R. D., Frazier, M., Yakubu, M., Shields, H., King, S. B. and Kim-Shapiro, D. B. (2005) Rates of nitric oxide dissociation from hemoglobin. Free Radical Biol. Med. **39**, 145–151
50 Brunori, M., Antonini, G., Castagnola, M. and Bellelli, A. (1992) Cooperative cyanide dissociation from ferrous hemoglobin. J. Biol. Chem. **267**, 2258–2263
51 Stitt, F. and Coryell, C. D. (1939) Magnetic study of the equilibrium between ferrohemoglobin, cyanide ion and cyanide ferrohemoglobin. J. Am. Chem. Soc. **61**, 1263–1266
52 Cutruzzolà, F., Rinaldo, S., Castiglione, N., Giardina, G., Pecht, I. and Brunori, M. (2009) Nitrite reduction: a ubiquitous function from a pre-aerobic past. BioEssays **31**, 885–891
53 Muhoberac, B. B. and Wharton, D. C. (1983) Electron paramagnetic resonance study of the interaction of some anionic ligands with oxidised *Pseudomonas* cytochrome *c* oxidase. J. Biol. Chem. **258**, 3019–3027
54 Silvestrini, M. C., Colosimo, A., Brunori, M., Walsh, T. A., Barber, D. and Greenwood, C. (1979) A re-evaluation of some basic structural and functional properties of *Pseudomonas* cytochrome oxidase. Biochem. J. **183**, 701–709
55 Zajicek R. S. (2004) The Mutagenesis and Enzymology of *Paracoccus pantotrophus* cytochrome *cd*1 nitrite Reductase. Ph.D. Thesis, University of Oxford, Oxford, U.K.

Received 4 October 2010/13 January 2011; accepted 18 January 2011
Published as BJ Immediate Publication 18 January 2011, doi:10.1042/BJ20101615

Indian Journal of Biotechnology
Vol 10, October 2011, pp 423-431

Metabolism of cyclic-di-GMP in bacterial biofilms: From a general overview to biotechnological applications

Nicoletta Castiglione[1], Valentina Stelitano[1], Serena Rinaldo[1], Giorgio Giardina[1], Manuela Caruso[1] and Francesca Cutruzzolà[1,2]*

[1]Department of Biochemical Sciences "A. Rossi Fanelli", Sapienza University of Rome, Rome, Italy
[2]Consorzio I.N.B.B., 00136 Rome, Italy

Bacteria exist in nature in a planktonic single-cell state or in a sessile multicellular state, the biofilm. In the latter state, the bacterial community optimizes the cell-environment and cell to cell communication strategies. Biofilms are widely diffuse in many industrial, environmental and clinical settings and are less sensitive to treatments with antimicrobial agents compared to planktonic cells. Biofilms formed by bacterial pathogens, such as, those formed by *Pseudomonas aeruginosa* in immunocompromised patients, have a high impact on public health. The switch between the planktonic and the biofilm lifestyle is strictly regulated by the second messenger 3', 5'-cyclic diguanylic acid (c-di-GMP). The intracellular levels of this molecule are controlled by two classes of enzymes: diguanylate cyclases (DGC) and phosphodiesterases (PDE). In this review, we report the structural and functional data available to date on these enzymes and we summarize the possible medical, environmental and industrial biotechnological applications involving bacterial c-di-GMP metabolism.

Keywords: Biofilm, cyclic-di-GMP, inhibitors, pathogenesis, PDE, DGC

Introduction

Bacteria are able to communicate and behave like a multicellular organism forming biofilm, a highly organized structure consisting of cells embedded within a matrix of extracellular polymeric substance (EPS) attached to a surface. As a matter of fact, bacterial cells exist in nature in a planktonic single-cell state or in a sessile multicellular state of the biofilms[1]. Biofilms are abundant in many industrial, environmental and clinical settings, such as, food processing environments, potable water and medical devices[2,3]. In particular, bacterial biofilms found on the surface of medical devices are a major cause of hospital-associated infections[4,5]. Moreover, biofilms formed by pathogens play an important role in the infection of living tissues and are responsible for the resistance to antibiotics and to the host immune system[2,6]. Bacteria growing as microbial community are less sensitive to treatments with antimicrobial agents compared to planktonic cells[1,6] and produce many virulence factors[7]. According to the Centers for Disease Control and Prevention (USA), 65% of all infections in developed countries are caused by biofilms.

*Author for correspondence:
Tel: 0039-0649910713; Fax: 0039-064440062
E-mail: francesca.cutruzzola@uniroma1.it

The present review has focused on the human pathogen *Pseudomonas aeruginosa*, a well-known model organism and one of the most important bacteria forming biofilms. Since the enzymes involved in 3',5'-cyclic diguanylic acid (c-di-GMP) synthesis and degradation are found in the majority of known bacterial species[8], the information reported here is relevant for other important pathogens.

P. aeruginosa is an opportunistic human pathogen, a leading cause of both community and hospital acquired infections (13% of all nosocomial infections). *P. aeruginosa* biofilm is the major cause of death in patients of cystic fibrosis (CF), a genetic disease affecting 1/2500 newborns in Europe[9]. In the CF lung, environment is poor of oxygen and rich of nitrate, and under these conditions, *P. aeruginosa* is able to survive, thanks to its anaerobic metabolism[6,10,11], causing chronic infections[10]. The bacterium is intrinsically resistant to a wide array of antibiotics. Moreover, it is prone to acquire new resistance genes through horizontal gene transfer and produces an impressive array of virulence factors. The low efficacy of existing therapies in eradicating *P. aeruginosa* infection calls for the development of new therapeutic options.

The Second Messenger 3′, 5′ Cyclic Diguanylic Acid (C-di-GMP) and Its Turnover

During biofilm formation, the pattern of gene expression is changed with respect to planktonic cells and new intracellular signalling pathways are activated. Therefore, biofilm formation can be viewed as a developmental process[3], regulated by the key signal molecule c-di-GMP. This second messenger controls in bacteria an array of cellular processes linking environmental sensing with sessile-motile transition[12,13] (Fig. 1). The clearest role for c-di-GMP is, indeed, its ability to regulate the decision to switch from a free-swimming bacterium to a surface-attached bacterium[14], determining the timing and amplitude of complex processes like motility, cell adhesion, biofilm formation and differentiation[15]. A low concentration of c-di-GMP is associated with flagellar motors or retracting pili[16], whereas an high amount favours the expression of adhesins and EPS, finally leading to biofilm formation and pathogenicity[15]. The exceptional importance of c-di-GMP in bacterial physiology and pathogenesis has been recently acknowledged in a commentary published in the prestigious journal Cell[14].

C-di-GMP is synthesized by the enzyme diguanylate cyclase (DGC) starting from two guanosine triphosphate (GTP) molecules and its degradation is mediated by specialized phosphodiesterases (PDE) that yield the linear 5'-pGpG or GMP as products (Fig. 1). DGCs are often called GGDEF proteins due to the conserved amino acids found in their active site; unlikely other bacterial domains, the GGDEF domain is completely absent in eukaryotes[17]. The presence of putative DGCs only in bacteria suggests that these enzymes are excellent candidates for the development of anti-bacterial compounds.

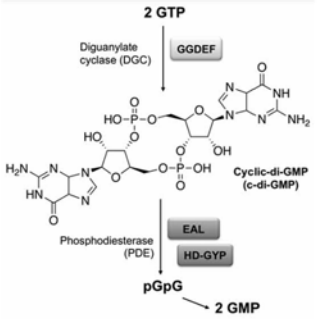

Fig. 1—Cyclic-di-GMP turnover: Cyclic-di-GMP synthesis and degradation are, respectively, controlled by two classes of enzymes, diguanylate cyclases (DGC), characterized by a GGDEF domain, and phosphodiesterases (PDE), characterized by an EAL or a HD-GYP domain. Cyclic-di-GMP controls many cellular processes like motility, virulence, biofilm formation and differentiation[12].

Based on conserved sequence signatures, PDEs are also grouped into the EAL and HD-GYP families[18]. The large number of GGDEF and EAL domain proteins in a single species is somewhat puzzling[13]. In general, Gram-positive bacteria have less of DGC/PDE proteins than Gram-negative bacteria. By contrast, proteins containing the HD-GYP domain are less common or even absent in some species, whereas in other species, such as, *Thermotoga maritima*, they account for all PDE activity in the cell[19,20]. The number of putative DGCs and PDEs encoded in individual bacterial genomes is highly variable (for example over 29 in *Escherichia coli*, 14 in *Caulobacter crescentus*, 60 in *Vibrio cholerae*, 41 in *P. aeruginosa* and none in *Helicobacter pylori*), this may reflect the ability to survive in different environmental niches. GGDEF and EAL domains are often found in tandem within the same protein; these hybrid proteins frequently show only one enzymatic activity with the catalytically inactive domain, potentially serving a regulatory function[15]. Most DGCs and PDEs are also associated with known or hypothetical signal input domains (globin-like, PAS/PACM, GAF, HAMP, CHASE4 or membrane sensory domains MHYT or MASE1)[17], putatively involved in sensing a range of environmental signals (oxygen, blue light, nutrient starvation, antibiotics, etc). Little is known on the intracellular receptors of c-di-GMP, which convert the increase/decrease of c-di-GMP into a biological response. Possible c-di-GMP-sensing domains include the PilZ, BcsA or PelD domains[12,21,22], the GGDEF/EAL containing hybrid proteins[23] and even riboswitches[24]. How the DGCs and PDEs function together to produce a coherent output signal is still unclear; different c-di-GMP circuits could be separate in time and in space through compartmentalization[15].

In the *P. aeruginosa*, PAO1 genome presents 41 ORFs containing putative DCG (GGDEF) and/or PDE (EAL or HD-GYP) genes (Table 1). Insertional mutants in the DGC or DGC-PDE genes show an effect, either reducing or increasing biofilm formation[25,26].

Table 1—Genes involved in c-di-GMP turnover in *P. aeruginosa* PAO1

PAO1 code	Predicted domains	Size (AA)	PAO1 code	Predicted domains	Size (AA)
	DGC (GGDEF domain: 2GTP --> c-di-GMP)				
PA0169	GGDEF	235	PA3177	GGDEF	307
PA0290	PAC-GGDEF	323	PA3343	TM-TM-TM-TM-TM-GGDEF	389
PA0338	PAC-GGDEF	376	PA3702 (WspR)	*ResponseReg*.-GGDEF	347
PA0847	TM-CHASE4-TM- HAMP-PAS-PAC-GGDEF	735	PA4332	TM-TM-TM-TM-TM-GGDEF	487
PA1107	TM-TM-TM-TM-TM-GGDEF	398	PA4396	*ResponseReg*.-GGDEF	366
PA1120 (TpbB)	TM- HAMP-GGDEF	435	PA4843	*ResponseReg*.-GGDEF	542
PA1851	TM-TM-TM-TM-TM-GGDEF	401	PA4929	7TMR-DISMED2-GGDEF	680
PA2771	GAF-GGDEF	341	PA5487	GGDEF	671
PA2870	GGDEF	525			
	Hybrid proteins (GGDEF + EAL domains)				
PA0285	TM-TM-PAS-PAC-PAS-PAC-GGDEF-EAL	760	PA3258	EAL-CBS-GGDEF	601
PA0575	TM-SPB_BAC_3-TM-PAS-PAC-PAS-PAC-PAS-PAC-PAS-PAC-GGDEF-EAL	1245	PA3311	TM- MHYT- MHYT- MHYT-GGDEF-EAL	783
PA0861	TM-TM-PAS-GGDEF-EAL	818	PA4367 (BifA)	TM-TM- GGDEF-EAL	687
PA1181	MASE1-PAS-PAC-PAS-PAC-GGDEF-EAL	1120	PA4601 (MorA)	TM-TM-PAS-PAC-PAS-PAC-PAS-PAC-GGDEF-EAL	1415
PA1433	TM- HAMP-GGDEF-EAL	650	PA4959 (FimX)	*ResponseReg*.- GGDEF-EAL	691
PA1727 (MucR)	TM-TM- MHYT- MHYT- MHYT-GGDEF-EAL	685	PA5017	TM-GAF-PAS-PAC-GGDEF-EAL	899
PA2072	TM-CHASE4-TM-PAS-GGDEF-EAL	864	PA5295	GGDEF-EAL	558
PA2567	GAF-GGDEF-EAL	587	PA5442	TM-TM-TM-TM-TM-PAS-PAC-PAS-PAC-GGDEF-EAL	951
	PDE (EAL domain: c-di-GMP --> pGpG)				
PA2133	EAL	285	PA3825	TM-EAL	526
PA2200	EAL	531	PA3947 (RocR)	*ResponseReg*.-EAL	392
PA2818(Arr)	TM-TM-EAL	525			
	PDE (HD-GYP domain: c-di-GMP --> 2GMP)				
PA4108	HD-GYP	414	PA2572	*ResponseReg*-NY-GYP *(degenerated)*	447
PA4781	*ResponseReg*-HD-GYP	393			

GGDEF = Diguanylate cyclase, EAL = Diguanylate phosphodiesterase, HD-GYP = Metal dependent phosphohydrolases, TM = Trans membrane helix, PAS = Signal sensor domain, PAC = Signal sensor domain, GAF = cGMP-dependent 3',5'-cyclic phosphodiesterase, ResponseReg = Response regulator receiver domain, MHYT = Bacterial signalling protein N-terminal repeat, HAMP = Linker domain, CBS = Predicted adenosyl sensory domain, CHASE4 = Extracellular sensory domain, MASE1 = Predicted integral membrane sensory domain, SPB_BAC_3 = Bacterial extracellular solute-binding proteins (family 3), 7TMR-DISMED2 = Two distinct types of extracellular sensing domains

To date, few biochemical data are available on the proteins involved in c-di-GMP turnover. A brief summary of the major structural and functional data on the DGCs and the PDEs is given below.

Diguanylate Cyclases

The structure of the GGDEF domain resembles that of the adenylate cyclase catalytic domain, as evident in the structure of the PleD response regulator from *Caulobacter crescentus*[27], which is considered as a prototype DGC. PleD is composed of two CheY-like phosphoryl receiver domains and a GGDEF domain. Activation is achieved by phosphorylation of an aspartate residue that induces dimerization: two GTP molecules, bound to the active sites of the GGDEF domains, come together to form c-di-GMP. PleD is regulated by non-competitive product inhibition: c-di-GMP can bind to a high affinity inhibition site (I-site) causing a conformational change that separates the two GGDEF domains, thus hampering catalysis[28].

In *P. aeruginosa*, the only known DGC structure is that of WspR[29] (Fig. 2). This DGC has a similar domain organization as PleD, but lacks the second CheY-like domain. As observed with PleD, WspR appears to be regulated by phosphorylation of the N-terminal CheY-like domain[30]. In the structure of the protein (Fig. 2), this domain contains the Mg^{2+} ion (necessary for catalysis) and it is connected *via* a helical stalk to the GGDEF domain; the latter is oriented in such a manner that the two active sites face each other, similar to the active conformation of adenylate cyclases[31]. In addition, binding of a c-di-GMP dimer to the conserved inhibitory site (I-site) is observed[32] (Fig. 2). In summary, the protein is activated by phosphorylation and inhibited by product binding to the I-site; however, the feedback inhibition mechanism of WspR is even more complex than in PleD[33].

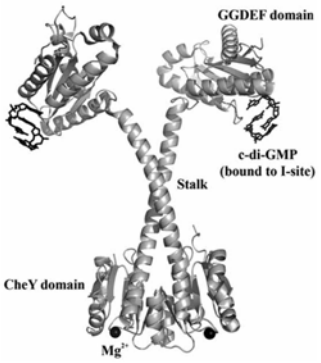

Fig. 2—Crystal structure of WspR from *P. aeruginosa*: The N-terminal CheY-like phospho-receiver domain is connected *via* a helical stalk to the GGDEF domain with diguanylate cyclase activity. Cyclic-di-GMP molecules bound to the inhibitory site (I-site) are located distal to the active site and are shown as black sticks. Mg^{2+} ions are shown as black spheres[31] (Protein Data Bank id. 3BRE).

Phosphodiesterases of EAL Subtype

The crystal structures of few proteins with EAL domains, such as, TdEAL from *Thiobacillus denitrificans*, YkuI from *Bacillus subtilis*[34] and BlrP1 from *Klebsiella pneumoniae*[35], have been determined. The general fold of the EAL domain consists of a β-barrel harbouring the catalytic residues at the top of the barrel (Fig. 3).

In the case of *P. aeruginosa,* the catalytic mechanism of the RocR protein has been discussed and its structural model has been settled[36]; very recently, crystallization and a preliminary diffraction analysis of this protein has been reported[37]. In RocR, hydrolysis of one O-3′-P ester bond to yield the linear dinucleotide 5′-pGpG is achieved by an activated water molecule and involves two Mg^{2+} or Mn^{2+} ions and seven catalytic

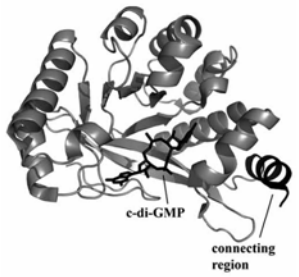

Fig. 3—Crystal structure of FimX EAL domain from *P. aeruginosa*: The domain possesses 11 α-helices and 8 β-strands, and its fold resembles a β-barrel. Cyclic-di-GMP molecules bound to the domain are shown as black sticks. The region connecting the EAL domain and the GGDEF one (the latter not shown in this figure) forms a helix (shown in black)[38] (Protein Data Bank id. 3HV8).

residues, including the Glu residue of the EAL signature motif. Moreover, the structural model of RocR revealed that the amino acids of the DFG(T/A)GYSS motif form a loop (loop 6), which connects elements of secondary structure, a β-sheet and an α-helix. This motif seems to play an important role in signal transduction. The sequence analysis of the 5,862 EAL domains in the bacterial genomes revealed that about half of the EAL domains harbour a degenerated loop 6, suggesting that the mutation of this loop may indicate a divergence of function for EAL domains during evolution[38].

The absence of the essential catalytic residues can serve as markers for identifying catalytically inactive EAL domains in the bacterial genomes[36]. Based on the conservation of the signature sequence, EAL domains can be divided into 3 subgroups. The EAL domains belonging to class 1 possess conserved catalytic residues and a conserved loop 6 and function as true PDEs. The class 2 EAL domains contain conserved catalytic residues and a degenerated loop 6: these EALs, as for example YkuI of *B. subtilis*, are most likely catalytically inactive, but might be activated by terminal signalling domains. The class 3 EAL domains lack one or more of the catalytic residues and have a degenerated loop 6: these EALs are predicted to be catalytically inactive. It has been suggested that this classification also allows to discriminate whether a putative EAL protein has phosphodiesterase activity or is a c-di-GMP sensing domain[39].

Phosphodiesterases of HD-GYP Subtype

No structure is available to date for PDEs containing the HD-GYP domain. This domain is widespread in bacteria (over 1000 genes have been found). It is classified as a metal-dependent phosphohydrolase and a divalent cation (most likely Mg^{2+} or Mn^{2+}) is required for catalysis, but the molecular mechanism of action is still unknown.

In *P. aeruginosa*, 3 genes, viz., PA4108, PA4781 and PA2572, harbour HD-GYP domain (Table 1). The first two proteins have a PDE activity *in vivo*; moreover, they control the swarming motility and the production of virulence factors[26]. On the other hand, the role of the third protein PA2572, which has a different YN-GYP signature, is uncertain[26]; this protein is inactive in c-di-GMP hydrolysis and it hasa cryptic negative influence on swarming. It is not excluded that the YN-GYP domain interferes with the action of the HD-GYP domain proteins PA4108 and PA4781[26]. Nevertheless, all three proteins regulate virulence of *P. aeruginosa*, since their mutation led to a reduction of the bacterial virulence in the larvae of *Galleria mellonella*[26]. HD-GYP domain proteins have also been found in a number of other bacterial pathogens of animals, including *Clostridium perfringens, Bordetella bronchiseptica* and *Treponema denticola*. For their importance in virulence and since the biochemical and structural information about them are still poor, a thorough characterization of this class of proteins is highly desirable.

Hybrid Proteins Containing Both GGDEF and EAL Domains

As previously mentioned, the hybrid proteins displaying both DGC and PDE domains may act as enzymes or may be c-di-GMP sensors. Given the high complexity of their domain architecture, obtaining structural data for this class of hybrid proteins is of crucial importance to infer their function.

Structural and functional studies of LapD, an internal membrane protein that regulates surface attachment in *P. fluorescens*, and of FimX from *P. aeruginosa*[40] indicate that both proteins function as c-di-GMP-sensors, which are able to communicate the levels of c-di-GMP from cytoplasm to periplasm[23]. The overall fold of EAL domain of FimX (Fig. 3)[40] is very similar to that of the putative EAL domain-containing phosphodiesterases TdEAL from *T. denitrificans* and YkuI from *B. subtilis*, described above. On the other hand, the structure of the GGDEF domain of FimX shows an overall similar fold to that of PleD and WspR, but lacks the characteristic primary site motif of the I-site. Nucleotide binding studies in solution confirmed that EAL domain works as the sole c-di-GMP binding module of FimX[40].

It is clear from the above studies that an exhaustive comprehension of the molecular mechanisms underlying c-di-GMP synthesis and breakdown is fundamental to conceive new approaches for biofilm treatment in chronic infections, such as, the infection of *P. aeruginosa* in CF patients, and also for other biotechnological applications, briefly described below.

Biotechnological Applications

Medical Applications

As mentioned above, bacteria growing in biofilms are less sensitive to treatments with antimicrobial agents. Hence, there is a strong need to find novel approaches against pathogenic bacteria. The cellular processes involved in biofilm formation, maintenance and dispersal are important targets for the discovery of novel chemical inhibitors[41]. In particular, the knowledge of the structural bases of the metabolism of c-di-GMP is important to identify new targets for effective anti-biofilm drugs; the most ambitious objective is to find a strategy capable to interfere selectively with the synthesis and degradation of this molecule.

Given the central role of c-di-GMP in biofilm development, compounds related in structure to c-di-GMP are expected to have inhibitory activities on bacterial biofilm formation[42]. C-di-GMP analogues, such as, monophosphorothioic acid of c-di-GMP (c-GpGps), cyclic bis(3'-5')guanylic/adenylic acid (c-GpAp) and cyclic bis(3'-5')guanylic/inosinic acid (c-GpIp), have been synthesized[43] and tested on the bacterial biofilm formation and on bacterial motility[44,45]. These analogues suppressed the formation of biofilm in the Gram-negative *P. aeruginosa* as well as in *Staphylococcus aureus* in the following order: c-GpGps > cGpAp > c-GpIp. The suppression of biofilm formation has also been observed in the presence of high doses of cyclic-di-GMP. This could be explained by the allosteric repression exerted by this dinucleotide on its own synthesis[27,29]. It should be noted here that the suppressive concentrations of cyclic-di-GMP and its analogues added in the culture were 100–1000 times higher than the estimated physiological intracellular levels of cyclic-di-GMP[45]. Screening of a commercially available library of chemical compounds with known biological activities, using a combination of three microbiological assays, has led to the identification of the inhibitory activity of sulfathiazole, a known anti-metabolite drug[46], towards c-di-GMP biosynthesis. It is likely that inhibition of c-di-GMP biosynthesis by sulfathiazole does not take place through direct inhibition of the DGC activity, but through indirect effects, such as, alteration of the nucleotide pool, which can in turn affect the availability of the DGC substrate GTP. This work strongly suggests that perturbation of intracellular nucleotide pools could indeed interfere with molecular signalling leading to biofilm formation. Fluorouracil, which blocks DNA replication through inhibition of nucleotide biosynthesis, also prevents biofilm formation at concentrations not affecting planktonic cell growth[47,48].

Another possibility to fight the biofilm could be to promote the dispersion of this multicellular community. As an example, it is known that a low concentration of nitric oxide (NO) in *P. aeruginosa* favours the biofilm dispersal, causing an increase in the sensibility of the bacterium to antimicrobial agents[49,11]; during this complex process, a key role is played by c-di-GMP. Recent studies on *P. aeruginosa* identified a possible molecular link between NO, c-di-GMP and biofilm dispersion, but whether the response to NO occurs directly or indirectly is still not clear[49]. Understanding the mechanism underlying the NO/c-di-GMP-dependent biofilm dispersal and the signalling pathway involved can provide novel and interesting targets for new antibacterial strategies aimed to disperse biofilm. These strategies may improve the effects of antibiotic therapy, which is often insufficient against bacteria growing in biofilms.

Biotechnological Production of Vaccines

One important aspect of c-di-GMP that has been reported in literature is the extraordinary capability of this molecule to produce immunostimulation. As a matter of fact, this molecule has been recently identified as a potential vaccine adjuvant for systemic and mucosal vaccination[50]. This application is really attractive because the mucosal surfaces (respiratory, urogenital and gastrointestinal tracts) in humans represent an entry point for pathogens and an ideal environment for the development of diseases; a typical example is the *P. aeruginosa* lung infection in CF patients. A recent work by Yan and co-workers[51] demonstrated that the mucosal immune response induced using c-di-GMP translates into protective immunity against *Streptococcus pneumoniae* colonization.

Several c-di-GMP analogues have been shown to have immunostimulatory properties. A bisphosphorothioate analogue of c-di-GMP (c-GpsGps) was synthesized[52] and its immunostimulatory properties were evaluated *in vivo* in comparison with c-GpGps and c-di-GMP. The results of this study suggest that c-GpGps and c-GpsGps appear to elicit the inflammatory response, even though the effect was milder than that of c-di-GMP. Despite these positive results, the molecular basis of the immunostimulatory and adjuvant properties of c-di-GMP still remains a mystery.

Industrial and Environmental Applications

Biofilm formation is a frequent cause of contamination in industrial settings. Biofilms are often found in the food processing environment. Moreover, they have a high impact on the deterioration of water quality. In the first case, biofilm contamination during the process may favour microbial contamination of the final product[3]. In the second case, the biofilm is involved in the deterioration of the water quality during its storage and distribution, and both stages are of vital importance in determining the final quality of water.

The control of biofilm formation strictly depends on the effective cleaning of potential growth sites. Unfortunately, the bacteria embedded into the extracellular matrix of the biofilm are often protected from the sanitizers.

On the other hand, the immobilization of microorganisms in biofilms is particularly appropriate for use in environmental biotechnology processes[53]. For example, an innovative shortcut biological nitrogen removal system, consisting of an aerobic submerged membrane bioreactor (MBR) and an anaerobic packed-bed biofilm reactor (PBBR), was evaluated for treating high strength ammonium-bearing wastewater[54].

Thus, it is clear that a deep knowledge of the processes involved in the formation or dispersion of biofilm is important, on one side to develop new efficacious treatments for the cleaning and contamination prevention of industrial plants and, on the other side, to exploit the biofilm metabolism for decontamination of wastewater.

Conclusions

The scientific interest in c-di-GMP metabolism drastically increased in the past few years. Being the second messenger, it is a key player in the decision making between the motile planktonic and static biofilm-associated bacterial 'lifestyles'. The metabolic network involving c-di-GMP is highly complex and the exact molecular mechanism of c-di-GMP action remains to be fully elucidated. A detailed understanding of such complex regulatory mechanism will not only help to explain the specificity of c-di-GMP signalling systems, but may also favour a biotechnological research aimed to develop new strategies to fight biofilm in medical/industrial/environmental settings[55]. Moreover, a great deal of research is still needed to use the c-di-GMP as a potential vaccine adjuvant in human clinical trials.

To date, only a very small number of GGDEF and EAL domains have been characterized. For this reason, the main aim of the research carried out in our group is to expand this limited knowledge through structural and functional characterization of selected *P. aeruginosa* PAO1 proteins involved in c-di-GMP metabolism. This information is crucial to develop novel molecules able to modulate the synthesis and degradation of c-di-GMP and consequently the biofilm formation.

Acknowledgement

The present work is supported by the Ministero della Universita` of Italy (Grant No. RBRN07BMCT) and the University of Rome La Sapienza, Italy. FC acknowledges the Italian Embassy in New Delhi (India) for supporting the participation to the International Conference on Genomic Sciences (ICGS 2010) held at Madurai Kamaraj University, Madurai, India.

References

1 Bhinu V S, Insight into biofilm-associated microbial life, *J Mol Microbiol Biotechnol*, 10 (2005) 15-21.
2 Bryers J D, Medical biofilms, *Biotechnol Bioeng*, 100 (2008) 1-18.
3 Kokare C R, Chakraborty S, Khopade A N & Mahadik K R, Biofilm: Importance and applications, *Indian J Biotechnol*, 8 (2009) 159-168.
4 Lindsay D & von Holy A, Bacterial biofilms within the clinical setting: What healthcare professionals should know, *J Hosp Infect*, 64 (2006) 313-325.
5 Wenzel R P, Health care-associated infections: Major issues in the early years of the 21st century, *Clin Infect Dis*, 45 (Suppl 1) (2007) S85-88.
6 Moreau-Marquis S, Stanton B A & O'Toole G A, *Pseudomonas aeruginosa* biofilm formation in the cystic fibrosis airway, *Pulm Pharmacol Ther*, 21 (2008) 595-599.
7 Wagner V E, Gillis R J & Iglewski B H, Transcriptome analysis of quorum-sensing regulation and virulence factor expression in *Pseudomonas aeruginosa*, *Vaccine*, 22 (Suppl 1) (2004) S15-20.
8 Seshasayee A S, Fraser G M & Luscombe N M, Comparative genomics of cyclic-di-GMP signalling in bacteria: Post-translational regulation and catalytic activity, *Nucleic Acids Res*, 38 (2010) 5970-5981.
9 Driscoll J A, Brody S L & Kollef M H, The epidemiology, pathogenesis and treatment of *Pseudomonas aeruginosa* infections, *Drugs*, 67 (2007) 351-368.
10 Hassett D J, Cuppoletti J, Trapnell B, Lymar S V, Rowe J J *et al*, Anaerobic metabolism and quorum sensing by *Pseudomonas aeruginosa* biofilms in chronically infected cystic fibrosis airways: rethinking antibiotic treatment

strategies and drug targets, *Adv Drug Deliv Rev*, 54 (2002) 1425-1443.
11 Barraud N, Hassett D J, Hwang S H, Rice S A, Kjelleberg S *et al*, Involvement of nitric oxide in biofilm dispersal of *Pseudomonas aeruginosa*, *J Bacteriol*, 188 (2006) 7344-7353.
12 Camilli A & Bassler B L, Bacterial small-molecule signaling pathways, *Science*, 311 (2006) 1113-1116.
13 Hengge R, Principles of c-di-GMP signalling in bacteria, *Nat Rev Microbiol*, 7 (2009) 263-273.
14 Armitage J P & Berry R M, Time for bacteria to slow down, *Cell*, 141 (2010) 24-26.
15 Jenal U & Malone J, Mechanisms of cyclic-di-GMP signaling in bacteria, *Annu Rev Genet*, 40 (2006) 385-407.
16 Boehm A, Kaiser M, Li H, Spangler C, Kasper C A *et al*, Second messenger-mediated adjustment of bacterial swimming velocity, *Cell*, 141 (2010) 107-116.
17 Anantharaman V, Iyer L M & Aravind L, Presence of a classical RRM-fold palm domain in Thg1-type 3'-5' nucleic acid polymerases and the origin of the GGDEF and CRISPR polymerase domains, *Biol Direct*, 5 (2010) 43.
18 Cotter P A & Stibitz S, c-Di-GMP-mediated regulation of virulence and biofilm formation, *Curr Opin Microbiol*, 10 (2007) 17-23.
19 Galperin M Y, Nikolskaya A N & Koonin E V, Novel domains of the prokaryotic two-component signal transduction systems, *FEMS Microbiol Lett*, 203 (2001) 11-21.
20 Galperin M Y, A census of membrane-bound and intracellular signal transduction proteins in bacteria: Bacterial IQ, extroverts and introverts, *BMC Microbiol*, 5 (2005) 35.
21 Ryjenkov D A, Simm R, Romling U & Gomelsky M, The PilZ domain is a receptor for the second messenger c-di-GMP: The PilZ domain protein YcgR controls motility in enterobacteria, *J Biol Chem*, 281 (2006) 30310-30314.
22 Lee V T, Matewish J M, Kessler J L, Hyodo M, Hayakawa Y *et al*, A cyclic-di-GMP receptor required for bacterial exopolysaccharide production, *Mol Microbiol*, 65 (2007) 1474-1484.
23 Newell P D, Monds R D & O'Toole G A, LapD is a bis-(3',5')-cyclic dimeric GMP-binding protein that regulates surface attachment by *Pseudomonas fluorescens* Pf0-1, *Proc Natl Acad Sci U S A*, 106 (2009) 3461-3466.
24 Sudarsan N, Lee E R, Weinberg Z, Moy R H, Kim J N *et al*, Riboswitches in eubacteria sense the second messenger cyclic di-GMP, *Science*, 321 (2008) 411-413.
25 Kulasakara H, Lee V, Brencic A, Liberati N, Urbach J *et al*, Analysis of *Pseudomonas aeruginosa* diguanylate cyclases and phosphodiesterases reveals a role for bis-(3'-5')-cyclic-GMP in virulence, *Proc Natl Acad Sci U S A*, 103 (2006) 2839-2844.
26 Ryan R P, Lucey J, O'Donovan K, McCarthy Y, Yang L *et al*, HD-GYP domain proteins regulate biofilm formation and virulence in *Pseudomonas aeruginosa*, *Environ Microbiol*, 11 (2009) 1126-1136.
27 Chan C, Paul R, Samoray D, Amiot N C, Giese B *et al*, Structural basis of activity and allosteric control of diguanylate cyclase, *Proc Natl Acad Sci U S A*, 101 (2004) 17084-17089.
28 Paul R, Abel S, Wassmann P, Beck A, Heerklotz H *et al*, Activation of the diguanylate cyclase PleD by phosphorylation-mediated dimerization, *J Biol Chem*, 282 (2007) 29170-29177.
29 De N, Navarro M V, Raghavan R V & Sondermann H, Determinants for the activation and autoinhibition of the diguanylate cyclase response regulator WspR, *J Mol Biol*, 393 (2009) 619-633.
30 Hickman J W, Tifrea D F & Harwood C S, A chemosensory system that regulates biofilm formation through modulation of cyclic diguanylate levels, *Proc Natl Acad Sci U S A*, 102 (2005) 14422-14427.
31 Tesmer J J, Sunahara R K, Gilman A G & Sprang S R, Crystal structure of the catalytic domains of adenylyl cyclase in a complex with Gsalpha.GTPgammaS, *Science*, 278 (1997) 1907-1916.
32 Christen B, Christen M, Paul R, Schmid F, Folcher M *et al*, Allosteric control of cyclic di-GMP signaling, *J Biol Chem*, 281 (2006) 32015-32024.
33 De N, Pirruccello M, Krasteva P V, Bae N, Raghavan R V *et al*, Phosphorylation-independent regulation of the diguanylate cyclase WspR, *PLoS Biol*, 6 (2008) e67.
34 Minasov G, Padavattan S, Shuvalova L, Brunzelle J S, Miller D J *et al*, Crystal structures of YkuI and its complex with second messenger cyclic Di-GMP suggest catalytic mechanism of phosphodiester bond cleavage by EAL domains, *J Biol Chem*, 284 (2009) 13174-13184.
35 Barends T R, Hartmann E, Griese J J, Beitlich T, Kirienko N V *et al*, Structure and mechanism of a bacterial light-regulated cyclic nucleotide phosphodiesterase, *Nature (Lond)*, 459 (2009) 1015-1018.
36 Rao F, Yang Y, Qi Y & Liang Z X, Catalytic mechanism of cyclic di-GMP-specific phosphodiesterase: A study of the EAL domain-containing RocR from *Pseudomonas aeruginosa*, *J Bacteriol*, 190 (2008) 3622-3631.
37 Kotaka M, Dutta S, Lee H C, Lim M J, Wong Y *et al*, Expression, purification and preliminary crystallographic analysis of *Pseudomonas aeruginosa* RocR protein, *Acta Crystallogr (Sect F) Struct Biol Cryst Commun*, 65 (2009) 1035-1038.
38 Rao F, Qi Y, Chong H S, Kotaka M, Li B *et al*, The functional role of a conserved loop in EAL domain-based cyclic di-GMP-specific phosphodiesterase, *J Bacteriol*, 191 (2009) 4722-4731.
39 Romling U, Rationalizing the evolution of EAL domain-based cyclic di-GMP-specific phosphodiesterases, *J Bacteriol*, 191 (2009) 4697-4700.
40 Navarro M V, De N, Bae N, Wang Q & Sondermann H, Structural analysis of the GGDEF-EAL domain-containing c-di-GMP receptor FimX, *Structure*, 17 (2009) 1104-1116.
41 Landini P, Antoniani D, Burgess J G & Nijland R, Molecular mechanisms of compounds affecting bacterial biofilm formation and dispersal, *Appl Microbiol Biotechnol*, 86 (2010) 813-823.
42 Kline T, Jackson S R, Deng W, Verlinde C L & Miller S I, Design and synthesis of bis-carbamate analogs of cyclic bis-(3'-5')-diguanylic acid (c-di-GMP) and the acyclic dimer PGPG, *Nucleosides Nucleotides Nucleic Acids*, 27 (2008) 1282-1300.
43 Mano E, Hyodo M, Sato Y, Ishihara Y, Ohta M *et al*, Synthesis of cyclic bis(3'-5')-2'-deoxyguanylic/guanylic acid (c-dGpGp) and its biological activities to microbes, *ChemMedChem*, 2 (2007) 1410-1413.

44 Hyodo M, Yumi S & Yoshihiro H, Synthesis of cyclic bis(3'-5')diguanylic acid (c-di-GMP) analogs, *Tetrahedron*, 62 (2006) 3089-3094.

45 Ishihara Y, Hyodo M, Hayakawa Y, Kamegaya T, Yamada K *et al*, Effect of cyclic bis(3'-5')diguanylic acid and its analogs on bacterial biofilm formation, *FEMS Microbiol Lett*, 301 (2009) 193-200.

46 Antoniani D, Bocci P, Maciag A, Raffaelli N & Landini P, Monitoring of diguanylate cyclase activity and of cyclic-di-GMP biosynthesis by whole-cell assays suitable for high-throughput screening of biofilm inhibitors, *Appl Microbiol Biotechnol*, 85 (2010) 1095-1104.

47 Attila C, Ueda A & Wood T K, 5-Fluorouracil reduces biofilm formation in *Escherichia coli* K-12 through global regulator AriR as an antivirulence compound, *Appl Microbiol Biotechnol*, 82 (2009) 525-533.

48 Ueda A, Attila C, Whiteley M & Wood T K, Uracil influences quorum sensing and biofilm formation in *Pseudomonas aeruginosa* and fluorouracilnis an antagonist, *Microb Biotechnol*, 2 (2009) 62-74.

49 Barraud N, Schleheck D, Klebensberger J, Webb J S, Hassett D J *et al*, Nitric oxide signaling in *Pseudomonas aeruginosa* biofilms mediates phosphodiesterase activity, decreased cyclic di-GMP levels, and enhanced dispersal, *J Bacteriol*, 191 (2009) 7333-7342.

50 Chen W, Kuolee R & Yan H, The potential of 3',5'-cyclic diguanylic acid (c-di-GMP) as an effective vaccine adjuvant, *Vaccine*, 28 (2010) 3080-3085.

51 Yan H, KuoLee R, Tram K, Qiu H, Zhang J *et al*, 3',5'-Cyclic diguanylic acid elicits mucosal immunity against bacterial infection, *Biochem Biophys Res Commun*, 387 (2009) 581-584.

52 Yan H, Wang X, KuoLee R & Chen W, Synthesis and immunostimulatory properties of the phosphorothioate analogues of cdiGMP, *Bioorg Med Chem Lett*, 18 (2008) 5631-5634.

53 Van Loosdrecht M C M & Heijnen S J, Biofilm bioreactors for waste-water treatment, *Trends Biotechnol*, 11 (1993) 117-121.

54 Zhang Y, Zhou J, Zhang J & Yuan S, An innovative membrane bioreactor and packed-bed biofilm reactor combined system for shortcut nitrification-denitrification, *J Environ Sci (China)*, 21 (2009) 568-574.

55 Wood T K, Hong S H & Ma Q, Engineering biofilm formation and dispersal, *Trends Biotechnol*, 29 (2010) 87-94.

ANTIOXIDANTS & REDOX SIGNALING
Volume 17, Number 4, 2012

DOI: 10.1089/ars.2011.4196

COMPREHENSIVE INVITED REVIEW

Nitrite and Nitrite Reductases: From Molecular Mechanisms to Significance in Human Health and Disease

Nicoletta Castiglione,* Serena Rinaldo,* Giorgio Giardina, Valentina Stelitano, and Francesca Cutruzzolà

Abstract

Nitrite, previously considered physiologically irrelevant and a simple end product of endogenous nitric oxide (NO) metabolism, is now envisaged as a reservoir of NO to be activated in response to oxygen (O_2) depletion. In the first part of this review, we summarize and compare the mechanisms of nitrite-dependent production of NO in selected bacteria and in eukaryotes. Bacterial nitrite reductases, which are copper or heme-containing enzymes, play an important role in the adaptation of pathogens to O_2 limitation and enable microrganisms to survive in the human body. In mammals, reduction of nitrite to NO under hypoxic conditions is carried out in tissues and blood by an array of metalloproteins, including heme-containing proteins and molybdenum enzymes. In humans, tissues play a more important role in nitrite reduction, not only because most tissues produce more NO than blood, but also because deoxyhemoglobin efficiently scavenges NO in blood. In the second part of the review, we outline the significance of nitrite in human health and disease and describe the recent advances and pitfalls of nitrite-based therapy, with special attention to its application in cardiovascular disorders, inflammation, and anti-bacterial defence. It can be concluded that nitrite (as well as nitrate-rich diet for long-term applications) may hold promise as therapeutic agent in vascular dysfunction and ischemic injury, as well as an effective compound able to promote angiogenesis. *Antioxid. Redox Signal.* 17, 684–716.

Reviewing Editors: *Markus Bachschmid, Srinivas Bharath, John Calvert, Sergey Dikalov, Martin Feelisch, Carlos Gutierrez-Merino, Christopher Kevil, João Laranjinha, Tienush Rassaf, and Jay L. Zweier*

Department of Biochemical Sciences, Istituto Pasteur-Fondazione Cenci Bolognetti, Sapienza University of Rome, Rome, Italy.
*These authors equally contributed to this work.

I. Introduction

A. Nitrite is the Cinderella molecule in biological signaling

In bacteria, nitrite is a well-known source of nitric oxide (the NO• radical, hereinafter NO) under anaerobic conditions (380). In eukaryotes, on the other hand, for years nitrite has been considered physiologically irrelevant and a simple end product of endogenous NO metabolism (113, 185); only in the last decade, the relevance of nitrite as a source of NO has emerged.

In mammals, NO is mainly synthetized by the enzyme nitric oxide synthase (NOS) *via* oxidation of the aminoacid L-arginine; this reaction requires oxygen (O_2) as an essential substrate (Fig. 1A), with a K_m in the 5–20 μM range (*in vitro*) (5, 199, 287). The exact O_2 threshold level at which NOS-dependent NO generation is compromised and fails to signal is unknown mainly due to uncertainties on the *in vivo* value of the K_m for O_2 of NOS enzymes (220). Organs and tissues are characterized by their own unique normoxic status (57, 352), given that the local oxygen pressure (pO_2) is a key component of the physiological state of an organ and results from the balance between O_2 consumption and delivery (Fig. 1B). However, in the human body, NO is also produced under hypoxic conditions (352); under these conditions, NO formation is not blocked by NOS inhibitors (74, 131, 382) and nitrite reduction is found to be enhanced (44, 131). These lines of evidence suggest that, in eukaryotes, an NOS-independent system exists, able to ensure sufficient NO formation when O_2 supply is limited (Fig. 1A), and identify nitrite as a main source of NO under hypoxic conditions. As a consequence, nitrite has recently obtained novel relevance and continuously expanding popularity.

This review summarizes and compares the molecular mechanisms of nitrite-dependent NO production in selected bacteria and in eukaryotes. Moreover, the review analyses the involvement of nitrite in human physiology and the possible therapeutic applications of this molecule. As will be detailed in the review, the nitrite reductase (NiR) activity is carried out by enzymes and proteins with intrinsically different cellular

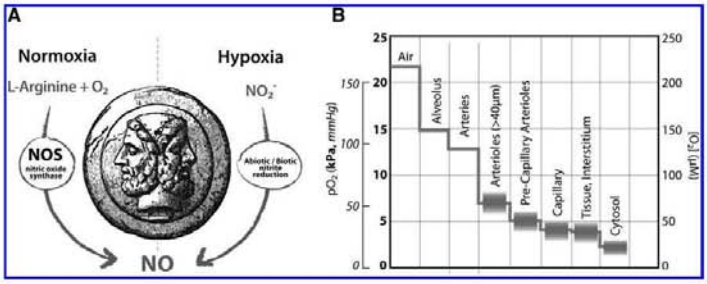

FIG. 1. Nitrite reduction: the two faces of nitric oxide (NO) production. (A) Under normoxic conditions, NO is synthesized by nitric oxide synthase (NOS) from L-arginine and oxygen (O_2) (305). On the other hand, under low O_2 tension (hypoxia) NO generation occurs in an NOS-independent way, *via* the reduction of nitrite carried out by abiotic or biotic systems. This double-faced system guarantees the formation of NO during the different physiological or pathological conditions. **(B)** Normoxia and hypoxia: values of the oxygen pressure (pO_2) measured from the airways to the cell cytosol in the human body. Each region of the body is characterized by its own unique normoxic status whose pO_2 value is indicated by a line; the thickness of the line represents variation between reports (352). [O_2] = concentration of free O_2; 1 mmHg = 0.13 kPa; 1 mmHg corresponds to [O_2] = 1.32 μM in H_2O at 37°C (345). Figure modified with permission from (352).

roles and biochemical features, spread across the two kingdoms; the wide distribution of the NiR activity highlights the importance of nitrite in cellular homeostasis.

II. Bacterial NiR and Their Significance

In this section we describe the reaction mechanism of two different classes of bacterial enzymes involved in the reduction of nitrite and the significance of this activity for human health, with particular attention to host–pathogen interactions. Three examples are reported: AniA from *Neisseria* (section A), NirBD from *Mycobacterium tuberculosis* (section B), and cytochrome cd_1 from *Pseudomonas aeruginosa* (section C).

The human body is heavily colonized by bacteria. These bacteria are frequently exposed to anoxia and to NO (and, thus, also to nitrite) generated by the host. Dealing with these two environmental factors often forces the bacteria to metabolic changes to (i) maintain growth and survive in the absence of O_2, and (ii) detoxify the free radical NO and/or the toxic compound nitrite. While microbial colonization is part of the normal physiology of the human body, the body can also be exposed to pathogenic bacteria such as *P. aeruginosa*, *M. tuberculosis*, and the pathogenic *Neisseria* species *N. meningitidis* and *N. gonorrhoeae*. The ability to reduce nitrite can therefore confer to these species a selective advantage in the host–pathogen arms race to survive in an O_2-limited and nitrite-rich environment.

Two distinct classes of NiR are responsible for the reduction of nitrite in bacteria. The first group comprises the enzyme NiR (EC 1.7.2.1), which reduces nitrite to NO during denitrification, the anaerobic respiratory process widely found in both autotrophic and heterotrophic microrganisms, in which oxidized nitrogen compounds such as nitrate and nitrite are used as electron acceptors for energy production (380). Denitrification has been implicated in the virulence of several bacterial species, including *Brucella* (12), *Pseudomonas* (342), and *Neisseria* (17).

Depending on the bacterial species, the NiR enzyme might be a copper-containing protein or a hemoprotein (cytochrome cd_1 nitrite reductase [cd_1NiR]), encoded by the *nirK* and *nirS* genes, respectively. The reaction catalyzed by these enzymes is

$$NO_2^- + 2\,H^+ \rightarrow NO + H_2O \quad (1)$$

The second group of NiR includes two quite distinct enzymes catalyzing the reduction of nitrite to ammonia. The first type is the (NAD(P)H)-dependent enzyme NirBD (EC 1.7.1.4), which reduces nitrite to ammonium coupled to the oxidation of either NADH or NADPH. It is a flavin-dependent enzyme that also contains a specialized heme cofactor named siroheme (119, 326); this enzyme participates in assimilatory nitrite reduction in bacteria but also in algae, fungi, and higher plants. The reaction catalyzed by NirBD NiR is

$$NO_2^- + 3\,NAD(P)H \rightarrow \text{Ammonium hydroxide} + 3\,NAD\,(P)^+ + H_2O \quad (2)$$

The other class of enzymes able to convert nitrite to ammonia is the multiheme NiR (cytochrome-ammonia forming) NrfA (EC 1.7.2.2). The enzyme also reduces NO and hydroxylamine to ammonia, and sulfite to sulfide. The reaction catalyzed is:

$$NO_2^- + 6 \text{ ferrocytochrome c} + 7\,H^+ \rightarrow NH_3 + 2\,H_2O + 6 \text{ ferricytochrome c} \quad (3)$$

In the following paragraphs three relevant examples of bacterial NiR strategic for the survival of pathogens within the infected host are reported.

A. Neisseria *and the copper NiR AniA*

The three closely related bacterial species, *N. meningitidis*, *N. gonorrhoeae*, and *Neisseria lactamica*, colonize mucosal surfaces in humans. *N. gonorrhoeae* is the causative organism of the sexually transmitted disease, gonorrhoea, one of the most frequently reported communicable diseases; *N. meningitidis* does occasionally cause severe, life-threatening illness known as meningitis, whereas *N. lactamica* is a common, harmless commensal of children.

N. gonorrhoeae is an obligate human pathogen that colonizes O_2-limited environments of the genitourinary tract. As in *N. meningitidis*, it conserves energy during electron transfer from physiological substrates *via* a membrane-bound respiratory chain to a single terminal cytochrome oxidase, cytochrome cbb_3 (65, 266, 319). When the O_2 supply is growth-limiting, the bacterium produces a truncated denitrification pathway in which nitrite is reduced to NO by the anaerobically induced outer membrane protein AniA, a copper-containing NiR of the NirK family (34, 188, 231). NO is then reduced to N_2O by a single-subunit nitric oxide reductase (Nor) B subunit (NorB) that receives electrons directly from ubiquinol (153). Therefore, AniA and NorB cooperate together to facilitate the anaerobic growth of *gonococci*: the *nirK* and *norB* genes are differentially controlled by a group of transcriptional regulators that respond to changes in the levels of O_2, nitrite, and NO (146, 163, 164).

The crystal structure of the soluble domain of AniA shows that the protein adopts a fold typical of copper-containing bacterial NiR (34): a tightly packed trimer of identical subunits, containing a type I and a type II copper atoms (Fig. 2).

The catalytic mechanism of CuNiRs requires one electron and two protons to convert nitrite into NO and water (2, 7, 249) (Fig. 2C). The protons are donated by a conserved active-site aspartate, which hydrogen bonds directly to the nitrite molecule, and by a histidine residue; these aminoacids are linked through a solvent-bridged hydrogen bond. The aspartate and histidine residues are conserved in all known Cu-NiR sequences and correspond to Asp97 and His240 in AniA (Fig. 2B). The most likely electron donors to AniA are the CcoP subunit of cytochrome oxidase cbb_3 and, by sequence similarity to the CcoP subunit, also the cytochrome *c5* (10, 152).

Interestingly, *aniA* is the most highly induced gene during anaerobic growth; expression of AniA during infection has been detected immunologically, supporting the induction of nitrite reduction *in vivo* (54, 67, 297). The ability to reduce nitrite during O_2-limited growth appears therefore to confer a selective advantage for the survival of pathogenic *Neisseria* in the human host (66). The analysis of *aniA* expression has been recently extended to the biofilm mode of growth of the bacterium; biofilms are organized bacterial communities in which the cells are embedded in a self-produced extracellular polymeric substance, attached to a surface. Biofilms formed by pathogens play an important role in the infection of living tissues and are responsible for the resistance to antibiotics and

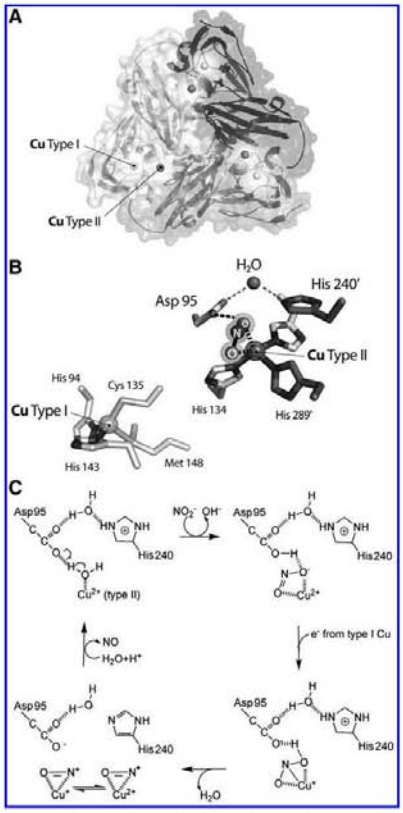

FIG. 2. Structural organization and catalytic mechanism of the copper nitrite reductase (NiR) AniA from *Neisseria gonorrhoeae*. (A) Overall organization of the enzyme [pdb id: 1kbv (34)]. AniA is a homotrimer, with each subunit binding two copper atoms. The type I Cu atom is bound in the internal part of each monomer, while type II Cu is positioned at the interface between two adjacent monomers. **(B)** Structure of the two copper sites, showing nitrite bound to type II Cu atom (pdb id: 1kbv). The metal coordinates residues coming from adjacent monomers (labeled Asp95, His134, and His289′, His240′, respectively). **(C)** Possible scheme of the catalytic cycle, adapted from that proposed for the copper NiR from *Alcaligenes faecalis* (7).

to the host immune system (45). *N. gonorrhoeae* readily forms biofilms over abiotic surfaces, over primary and transformed cervical epithelial cells and over cervical tissues *in vivo*. Expression of AniA in biofilms is induced over time; this evidence shows that a combination of anaerobic/aerobic respiration is used by *Neisseria* to support growth in the biofilm and that nitrite appears to be the preferred substrate for anaerobic respiration (110, 111).

Interestingly, Aspholm *et al.* (10) reported the identification of a single-nucleotide polymorphism (SNP) unique in the species *N. meningitidis* that leads to truncation of the c-type heme protein CcoP, an essential component of cytochrome oxidase. This SNP was found in all strains of *N. meningitidis* but not in strains of *N. gonorrhoeae* and *N. lactamica*. Although this mutation results in the truncation of an essential component of the cytochrome cbb_3 oxidase, it also conditionally affects nitrite consumption, providing evidence that an alteration in the circuitry of respiratory electron-transfer networks is associated with *N. meningitidis* speciation.

B. M. tuberculosis *and NirBD NiR*

M. tuberculosis, the etiologic agent of tuberculosis, is a facultative intracellular pathogen that can persist within the host; the bacterium may lie dormant in the human body for decades, only progressing to active disease in 5%–10% of individuals. One of the primary host defense mechanisms against mycobacterial diseases involves the formation of a granuloma-like structure. Immune containment by granuloma formation creates a microenvironment in which nutrient limitation, low pH, reactive nitrogen and O_2 species, and reduced O_2 tension are believed to be factors that coincide with the establishment of chronic infection. Under these conditions, *M. tuberculosis* changes its metabolism and, to survive, it can utilize various nutrients, including nitrate, as a source of nitrogen. Assimilation of nitrate requires the reduction of nitrate *via* nitrite to ammonium, which is then incorporated into metabolic pathways (89, 143); assimilation of nitrite is therefore essential for the survival of *M. tuberculosis in vitro* and *in vivo*.

The second step in nitrate assimilation is the reduction of nitrite to ammonium, catalyzed by the siroheme-dependent NADH-NiR, encoded by the *nirBD* operon; this enzyme is known to catalyze nitrate assimilation in various bacteria and fungi (208). The NirB protein is produced by *Mycobacterium* throughout infection, as recently shown in a proteomic study, together with the proteins required for nitrate/nitrite transport (such as NarX) and nitrate reduction (*narGHJI* and *narK2X* operons) (192).

In *M. tuberculosis*, NirBD has been proposed to be involved in the assimilatory reduction of nitrite (228). A recent study suggests, however, that the NirBD complex is not required for nitrate-dependent protection from acid-induced death under hypoxia (325); under these conditions the nitrite produced upon nitrate reduction through the NarGH complex is not further reduced into ammonium by the NirBD complex. Thus, in *Mycobacterium*, protection from nitrite toxicity at acidic pH, is most likely achieved by exporting nitrite outside the cell, likely through predicted nitrite extrusion proteins, including NarK3 and NarU (69). An alternative role for the *nirBD*-encoded NiR enzyme has been proposed for *Escherichia coli* and other enterobacteria; in these microrganisms, NirBD is induced under

anaerobic conditions and it is involved in detoxifying nitrite that accumulates from nitrate respiration (126).

C. P. aeruginosa *and cd*$_1$*NiR*

The ubiquitous gram-negative bacterium *P. aeruginosa* is an opportunistic pathogen responsible for both acute and chronic infections. *P. aeruginosa* is an etiologic agent common in several infections, including those affecting ears (94), burn wounds (244), and eyes (169). In addition, *P. aeruginosa* chronic lung infection is the major cause of death in cystic fibrosis (CF) patients, a genetic disease affecting 1/2500 newborn in Europe (99). *P. aeruginosa* is frequently resistant to conventional antibiotic therapy and to the host antimicrobial effector mechanisms. A major problem in the control of *P. aeruginosa* infection is given by the sessile, biofilm-mode of growth adopted by this bacterium in many infection sites, and typically in CF lung chronic infections (137, 139). *P. aeruginosa* survives in the low O_2 environment of the airway mucus of CF patients by using anaerobic metabolism and forming robust biofilms (246). The stagnant mucus overlaying the CF lung epithelium constitutes a nitrate-rich microaerobic/anaerobic environment (Fig. 3); nitrate in CF mucus is generated in part by the host inflammatory response to infection *via* NO. In this environment, *P. aeruginosa* produces energy from nitrate also using the metabolic pathway of denitrification (6, 139) (Fig. 3). Four reductases are involved in this process (380), namely, nitrate reductase (Nar), NiR, Nor, and nitrous oxide reductase (N_2OR), whose expression is tightly regulated, being the intermediate NO a cytotoxic compound. Genetic mutants lacking *nar* and *nir* genes show swarming defects and reduced virulence (342).

The molecular mechanisms controlling enhanced biofilm formation during anaerobic growth are not clearly defined. Low concentrations of NO have been shown to promote biofilm dispersion (15); on the other hand, Yoon and coworkers (369) have shown that *P. aeruginosa* PAO1 grown anaerobically is more elongated than that grown aerobically and is defective in cell division. Elongated cells easily form highly cohesive clumps, thus yielding a robust biofilm. Cell elongation is dependent on the presence of NiR and is repressed in *P. aeruginosa* PAO1 in the presence of an NO antagonist (2-(4-carboxyphenyl)-4,4,5,5-tetramethylimidazoline-1-oxyl-3-oxide [carboxy-PTIO]); these evidence suggests a link between cell elongation, NO, and anaerobic respiration (369). Importantly, the nonelongated NiR-deficient mutant failed to form biofilm, while the wild-type PAO1 is highly elongated and formed robust biofilm.

In addition to its role in anaerobic growth of *P. aeruginosa*, the NiR activity controls other important aspects of pathogenesis even under conditions where O_2 is apparently not limiting, including motility, initiation of biofilm formation, and virulence. As an example, a recent study has demonstrated that the NO produced by *P. aeruginosa* NiR regulates the activity of type III secretion system (343), an apparatus whereby cytotoxic effector proteins are directly secreted into the host cell cytoplasm after contact of the bacterium with a target cell.

Therefore, in *P. aeruginosa*, pathogenesis, biofilm formation, and denitrification, expecially nitrite reduction, are closely related. The enzyme responsible for nitrite reduction to NO is *P. aeruginosa* cytochrome cd_1 nitrite reductase (Pa-cd_1NiR), a homodimer containing one c-heme and one d_1-heme group in each subunit (Fig. 4A). Electrons are transferred from the soluble electron donor cytochrome c_{551} to the *c*-heme moiety of the enzyme (347) and thereby internally to the d_1-heme (Fig. 4B); in the active site (Fig. 4C), the substrate nitrite binds to the heme iron and is reduced to NO (380). The d_1-heme (3,8-dioxo-17-acrylate-porphyrindione) (Fig. 4B) is a partially saturated macrocycle with a set of oxo, methyl, and acrylate substituents, unique to the cd_1NiRs (4, 380) and synthesized by a specialized pathway present only in denitrifiers (strongly induced in *P.*

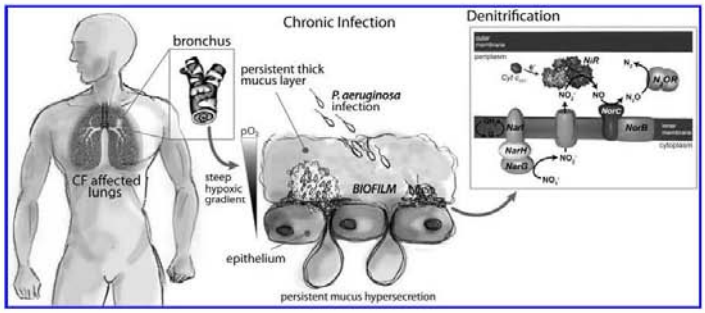

FIG. 3. Denitrification, pathogenesis, and biofilm formation in *Pseudomonas aeruginosa*. *P. aeruginosa* colonizes the lungs of cystic fibrosis (CF) patients (99). In the epithelium of the CF bronchus the formation of thick mucus is favored; in this environment, a steep gradient of pO_2 develops. This microaerobic/anaerobic environment is rich of nitrates (in part generated from the inflammatory response to infection) and favors the formation of *P. aeruginosa* biofilm (139). Under these conditions, *P. aeruginosa* survives thanks to the denitrification pathway involving the reduction of nitrates to N2 and mainly occurring in the bacterial periplasm. The complete pathway is described in the box: four reductases are involved in this process, namely, nitrate reductase (Nar), NiR, nitric oxide reductase (Nor), and nitrous oxide reductase (N_2OR) (6, 139).

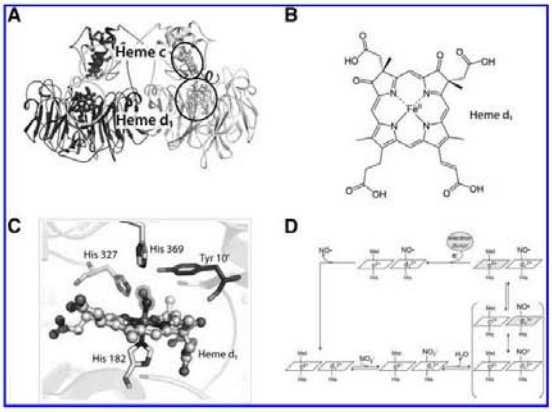

FIG. 4. Structural organization and catalytic mechanism of the cytochrome cd_1 nitrite reductase (cd1NiR) from *P. aeruginosa*. **(A)** Overall organization of the enzyme [pdb id: 1nno (260)]. cd1NiR is an homodimer, with each subunit binding one c-heme and one d1-heme. **(B)** Structure of d1-heme (3,8-dioxo-17-acrylateporphyrindione), a partially saturated macrocycle with a set of oxo, methyl, and acrylate substituents. The d1-heme is unique to the cd1NiRs (4, 394) and is synthesized by a specialized pathway present only in denitrifiers. **(C)** Structure of the d1-heme pocket, showing NO bound to the heme iron. Residues belonging to the N-terminal region of each subunit (*i.e.*, Tyr-10') swap between domains and contribute to the formation of the d1-heme pocket of the adjacent subunity. **(D)** Possible scheme of the catalytic cycle: nitrite binds to ferrous (Fe^{2+}) d1-heme, and is then converted to NO (294); the oxidized (Fe^{3+}) hemes are shown in grey. Notice that dissociation of the product NO occurs from the ferrous iron (294).

aeruginosa upon nitrite treatment). Other hemes in which the porphyrin ring is partially saturated are the *d* heme in *E. coli* and siroheme of bacterial and plant sulfite and NiR (119, 326).

Nitrite reduction to NO is the physiologically relevant activity of cd_1NiR (289, 365); the expression of cd_1NiR is induced by low O_2 tension and presence of nitrogen oxides (380). NO is produced efficiently by Pa-cd_1NiR (turnover number = $6\,s^{-1}$ at pH 7.0) (292) and the activity is pH dependent with an optimum between pH 5.8 and 6.5 (292, 365). The current knowledge on the individual steps in the catalytic cycle is summarized below and described in Figure 4D.

In cd_1NiR, nitrite binds to the ferrous (Fe^{2+}) d_1-heme with high affinity ($K_m = 6\,\mu M$) (81); binding of nitrite to the ferrous iron is expected in the reaction mechanism since this state of the iron has to supply the electron needed for the reduction process (Fig. 4D). In principle three different coordination modes of nitrite to monometallic centers are possible: the *N*-nitro, the *O*-nitrito, and the *O,O*-bidentate mode (Fig. 5) (364). The latter one is only observed in copper-containing bacterial NiR (16) and synthetic copper complexes (203). The *N*-nitro binding mode is observed in synthetic iron porphyrin nitrite complexes (64, 257, 363). Nitrite is thought to bind *via* the N-atom in Pa-cd_1NiR forming the so-called nitro-complex; this binding mode is inferred from the crystal structure of the nitrite-bound derivative of the homologous enzyme from *Paracoccus pantotrophus* (358). This observation agrees well with data on other heme-containing NiR (76, 105) and on synthetic iron porphyrin nitrite complexes in which, regardless of the iron oxidation state, the *N*-binding mode is observed (see Fig. 5) (64, 257, 363). The nitrite *N*-binding mode also agrees with the current mechanism of reduction of nitrite by cd_1NiRs, thought to occur *via* a double protonation of a terminal O atom of the nitrite molecule. Theoretical calculations have suggested that the *O*-binding mode is also possible for cd_1NiR (315) and for other hemoproteins such as hemoglobin (Hb) (272). Although nitrite can bind through the *O*-binding mode (the so-called nitrito mode) to the heme of myoglobin (Mb) and Hb (73, 367, 368), in the case of the d_1-heme there is no experimental evidence that such O-binding mode may occur.

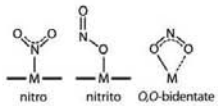

FIG. 5. Possible nitrite-binding modes. Experimentally determined nitrite-binding modes to metalloproteins.

The high affinity for nitrite (and other anions such as cyanide) (166, 323) of the ferrous (Fe^{2+}) d_1-heme is a peculiar and physiologically relevant feature of all cd_1NiRs. This behavior is remarkably different from that observed in the *b*-type heme-containing proteins in which the negatively charged molecules (nitrite and cyanide) usually bind much better to the ferric (Fe^{3+}) iron. The much higher affinity for nitrite of the d_1-heme can be partially explained with the presence of two

electron-withdrawing carbonyl groups on the d_1 heme ring (Fig. 4B). Two conserved histidines (His327 and His369) in the active-site pocket (261) (Fig. 4C) also contribute to the stabilization of the nitrite anion (NO_2^-), as confirmed by site-directed mutagenesis (81).

In Pa-cd_1NiR, nitrite can displace the NO bound to the ferrous enzyme (293), allowing the enzyme to enter a new catalytic cycle (Fig. 4D); therefore, the high affinity of the active-site ferrous d_1-heme for nitrite (see above) actively contributes to NO dissociation during the catalytic cycle. In agreement with this observation, if the affinity of Pa-cd_1NiR for nitrite is decreased (by mutation of a conserved active-site residue) the fully reduced-NO bound derivative accumulates (81, 293). The observation that NO and nitrite can compete for binding may suggest that the formation of dinitrogen trioxide (N_2O_3) could in principle occur, for example, in a reaction similar to that proposed for Hb (23). This event is, however, highly unlikely, mainly because during catalysis the d_1-heme is maintained in the reduced state by internal electron transfer from the *c*-heme. Moreover, ferric d_1-heme has low affinity for nitrite (329), a feature that likely limits further reaction with free NO to produce N_2O_3.

In the catalytic cycle of Pa-cd_1NiR, the formation of a complex between NO and the reduced d_1-heme might slow down product release (11). Trapping of ferrous hemes by NO is highly likely, given the high affinity of this ligand for Fe^{2+} (182, 245). However, we have clearly shown that the rate constant of NO dissociation from the reduced d_1-heme is fast (up to 70 s^{-1}) not only for Pa-cd_1NiR (292) but also for the cd_1NiR from *P. pantotrophus* (294). Consequently, the affinity of reduced Pa-cd_1NiR for NO is relatively low ($\sim 10^{-7}$M) and the ferrous enzyme is not firmly inhibited by NO (292, 293). Noteworthy, nitrite reduction can still be monitored after preincubation of reduced Pa-cd_1NiR with NO (292).

The rapid dissociation of NO is largely controlled by the d_1-heme cofactor itself, as recently shown using a complex of the d_1-heme and apomyoglobin (294). This evidence underscores that the d_1-heme has evolved to have low affinity for NO, as compared with other ferrous hemes. The results on the d_1-heme suggest that the reactivity of porphyrins with nitrite and NO can be modulated very extensively by the functional groups present on the heme macrocycle—information of general significance in light of the emerging important biological functions of nitrite as a source of NO under hypoxic conditions.

III. Nitrite Reduction In Mammals

In this section we first describe the sources and the distribution of nitrite in mammalian tissues (section A) and than we discuss the chemical (abiotic) and biochemical (biotic) mechanisms of nitrite reduction in mammals (section B).

A. Sources, levels, and distribution of nitrite

There are several sources of nitrite in mammals, both endogenous and exogenous. The endogenous source of nitrite is mainly the oxidation of the NO produced by NOS (Fig. 6) (241). The oxidation of NOS-derived NO is slow *in vitro*, but is enhanced in plasma mainly by the copper protein ceruloplasmin (314) and in membranes by the accumulation of NO in the lipid bilayer by preferential partition (210).

The main exogenous source of nitrite is dietary nitrate, which is converted to nitrite by commensal bacteria in the mouth or intestines (Fig. 6). Dietary nitrate levels are particularly high in specific fruits and vegetables; as an example, one serving of spinach, lettuce, or beetroot contains more nitrate than that generated endogenously over a day by the oxidative metabolism of NO carried out by all isoforms of NOS (220). A considerable variability in the nitrate concentrations of plants is observed depending on different species, environmental conditions, nutrient availability, insect damage, and application of nitrogen-based fertilizers. On the other hand, only a small amount of nitrite is contained in dietary food (345); nitrite is used for meat preservation, to cure flavor and color and to enhance meat appearance (59, 219). In general, nitrite intake varies from 0 to 20 mg/day (270).

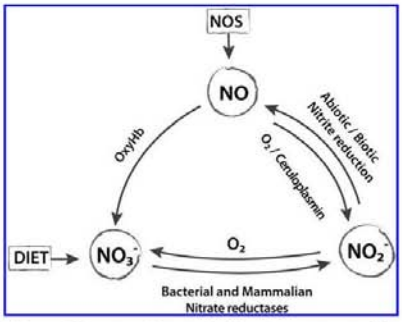

FIG. 6. Nitrogen-oxides metabolism. A percentage of the nitrate ingested with the food is reduced to nitrite by bacterial and mammalian Nar. Afterward, the nitrite produces NO *via* either biotic or abiotic reduction: the first one involves different putative NiR, such as deoxygenated hemoglobin (deoxyHb) or xanthine oxidase; the second one is enhanced by acidic conditions and reducing environments (*e.g.*, vitamin C). On the other hand, the production of NO in normoxia depends on the activity of the NOS enzyme. NO is rapidly oxidized to nitrite (by ceruloplasmin and O_2) or to nitrate (by oxygenated hemoglobin [oxyHb]) (215). Nitrite may also produce NO thanks to the oxidative denitrosilation activity of oxyHb (not shown in the figure).

Nitrates and/or nitrites are also contained in drinking water (< 10 mg/L in the absence of bacterial contamination) (42). Other environmental sources of nitrate and nitrite include cigarette smoke (258) and car exhausts (219). These and other environmental pollutants contain volatile nitrogen oxides, some of which are converted to nitrate or nitrite in the body (219). The relative contribution from these different sources of nitrite during normal conditions is variable (218). Nitrite levels show considerable variation between individuals and are significantly affected by dietary habits and lifestyle (216): for example, plasma nitrite and nitrate may be lowered by about 50% by dietary restriction (288).

Dietary nitrate is rapidly absorbed from the gastrointestinal tract into the blood stream, and distributed throughout the body, mixing itself with the endogenous nitrate (219) (Fig. 7). Some nitrate is excreted and concentrated 10-fold in salivary glands (354): the amount of nitrate secreted in saliva is up to 25% of plasma nitrate level (320). The dorsal face of tongue

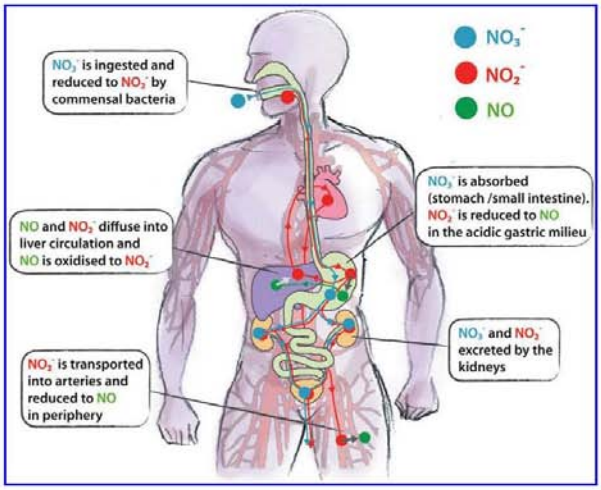

FIG. 7. Metabolic fate of nitrates and nitrites. Dietary nitrate (NO_3^-) is reduced to nitrite (NO_2^-) by bacterial Nar on the dorsal surface of the tongue and swallowed in the stomach. Nitrite is also reduced to NO under the acidic conditions of the gastric milieu and in the resistance vessels of the arterial circulation. NO may also be re-oxidized to nitrite. The kidneys finally excrete excess nitrates and nitrites. Blue, red, and green lines depict the different physiological routes of nitrate, nitrite, and NO in the body, respectively.

harbors a specialized flora of symbiotic facultative anaerobic bacteria expressing enzymes that can reduce nitrate to nitrite (306) (Fig. 6). These bacteria use nitrate as an alternative terminal electron acceptor during respiration to produce ATP (356). The biologic effect of ingested nitrate, as well as the concomitant increase in plasma nitrite, is abolished after avoiding swallowing of saliva (216, 354) or by the use of an antibacterial mouthwash (135, 274). Therefore, if mammals were germ free, the endogenous or ingested nitrate would not be metabolized because of the lack of the enzymatic machinery for its reduction (42, 219).

The metabolic fate of dietary nitrite in humans is depicted in Figure 7. After ingestion, nitrite reaches the stomach, where it is reduced to NO. In the acidic gastric *milieu*, nitrite is protonated to form nitrous acid (HNO_2), which then decomposes to NO and other nitrogen oxides (27, 221). Low pH and reducing compounds, such as ascorbic acid and polyphenols, enhance this reaction (28, 122). The level of NO gas in the stomach can be considerable (more than 100 ppm) (356). Most of the salivary nitrite escapes from this conversion and diffuse in systemic circulation (216); nitrite is transported in the arterial circulation to resistance vessels, where the low O_2 tension favors the reduction of nitrite to NO, causing vasodilatation and lowering the blood pressure (354).

Plasma levels of nitrite are usually in the range 0.1–0.6 μM with a mean of 0.345 ± 0.017 μM (128, 186, 216) (Table 1). The plasma concentration of nitrate is much higher (20–50 μM); as previously described, in the whole blood, nitrite is rapidly oxidized to nitrate (97, 241) (Fig. 6). Nitrate and nitrite increase greatly in saliva, plasma, and urina after a nitrate load (216).

Each tissue has a different concentration of nitrite (Table 2). As an example, inside the erythrocyte the levels are higher than in plasma (44, 86); given that the hematocrit represents between 40% (children) and 50% (adult males) of total blood volume, the erythrocytes contribute the largest nitrite pool in whole blood.

The levels of nitrite in the body show significant variability due to differences in dietary habits, lifestyle (*e.g.*, tobacco consumption), and physical exercise (37, 255, 265, 375). Circulating nitrite may be significantly enhanced in individuals suffering from an infection (332, 333) and markedly lowered during pregnancy. Plasma levels of nitrite also depend on NOS activity (186): in the presence of different NOS inhibitors, a change in vascular resistance occurs, paralleled by a reduction in plasma nitrite by $30\% \pm 8\%$ (186).

It is important to mention that the stationary levels of free nitrite or NO may also be influenced by the buffering effect of reduced glutathione (GSH), one of the main antioxidants present in cells and tissues. Under acidic conditions, nitrite reacts with GSH to form S-Nitrosoglutathione (GSNO), an endogenous S-nitrosothiol (SNO) (187, 337); on the other

TABLE 1. PLASMA NITRITE CONCENTRATION IN DIFFERENT MAMMALIAN SPECIES

Mammalian species	*Nitrite (μM)*
Human	0.305 ± 0.23
Monkey	0.367 ± 0.62
Minipig	0.319 ± 0.24
Dog	0.305 ± 0.50
Rabbit	0.502 ± 0.21
Guinea pig	0.412 ± 0.44
Mouse	0.457 ± 0.51

Data are taken from (186). Concentration of free nitrite (μM) in plasma in a variety of species has been measured using three different analytical approaches: flow injection analysis technique, reductive gas phase chemiluminescence, and sensitive high-pressure liquid chromatography techniques. Data are given as mean ± standard error of the mean (SEM).

TABLE 2. NITRITE CONCENTRATIONS IN BLOOD AND TISSUES OF WISTAR RAT

Localization	*Nitrite (μM)*
Blood	
Plasma	0.29 ± 0.05
Erythrocytes	0.68 ± 0.06
Tissues	
Brain	1.68 ± 0.31
Heart	0.77 ± 0.08
Liver	0.46 ± 0.06
Kidney	0.61 ± 0.09
Lung	0.45 ± 0.06
Aorta	22.5 ± 9.2

Data are taken from (44). Copyright (2004) National Academy of Sciences, USA. Nitrite levels were measured by high-performance liquid chromatography (HPLC) (284). Mean±SEM from 10–14 animals.

hand, GSNO may be formed by reaction of GSH with N_2O_3, with production of nitrite and protons, or, to a lower extent, with peroxynitrite ($ONOO^-$) (25, 183, 344). GSNO, in turn, is one of the most relevant biological molecules to carry out nitrosation reactions under physiological conditions (9, 373).

B. Mechanisms of nitrite reduction

1. Abiotic nitrite reduction: solution chemistry of nitrite. Nitrite is the conjugate base of HNO_2 [pk~3.1–3.2 (83)]. Therefore, at physiological pH, HNO_2 is essentially in the deprotonated form, the NO_2^-, according to the following equation:

$$HNO_2 \leftrightarrow NO_2^- + H^+ \quad (4)$$

At lower pH values, HNO_2 decomposes to various nitrogen oxides, including N_2O_3, which can dissociate to NO and NO_2 ($K = 2 \times 10^{-5}$ M) (335).

$$2\,HNO_2 \rightarrow H_2O + N_2O_3 \quad (5)$$

$$N_2O_3 \rightleftarrows NO + NO_2 \quad (6)$$

Moreover, the reduction of nitrite in aqueous solution strictly depends upon pH, according to the following reaction:

$$HNO_2 + H^+ + e^- \rightarrow NO + H_2O \quad (7)$$

Therefore, the so-called disproportionation of nitrite to NO, promoted by acidic pH, includes these reactions; this abiotic pathway is responsible for the production of NO in the gastric *milieu* of humans (27, 221, 230). The disproportionation of nitrite to NO is enhanced in the presence of reducing agents such as ascorbate (vitamin C) (213, 239) and other compounds such as polyphenols (122, 271, 295). Interestingly, disproportionation of nitrite to NO in biological tissues is enhanced under ischemic conditions when the pH drops from the normal value (7.4) to values as low as 5.5 (304, 382).

2. Biotic nitrite reduction. Several examples of NiR activities have been found in blood, tissues, and mitochondria. All of them can be ascribed to proteins, which, under aerobic conditions, play an O_2-dependent biological role but turn into NiR under hypoxic conditions.

a. Hemoglobin. Hb is the heme-containing metalloprotein involved in O_2 transport in humans. It is located in the erythrocyte, where it binds and releases O_2 in response to the partial pressure of this gas. The heterotetrameric adult HbA (alpha2-beta2) exists in two quaternary conformations, R-state and T-state, which display different affinity for the heme ligands, including O_2 and nitrite. Hb has been assigned a central role in the physiological reduction of nitrite: Hb binds and reacts with nitrite in both deoxygenated (deoxygenated hemoglobin [deoxyHb]) and oxygen-bound forms (oxygenated hemoglobin [oxyHb]), yielding different intermediate species and products, as detailed below.

(1) Reaction of deoxyHb with nitrite. The ability of deoxyHb to act as an NiR and produce NO was known since the pioneering work of Brooks (36). In blood, the reaction of nitrite with deoxyHb has been proposed to represent a source of NO bioactivity, according to the following reaction (129):

$$NO_2^- + Hb^{2+} \rightarrow NO + Hb^{3+} + OH^- \quad (8)$$

The Hb-dependent NiR activity is allosterically controlled by the quaternary structure of the protein (Fig. 8) (53, 129). The bimolecular rate constant of the reaction varies as the allosteric conformation of Hb changes: the R-state Hb has a bimolecular rate constant of 6 M^{-1} s^{-1}, whereas the constant for T-state Hb is 0.12 M^{-1} s^{-1}, giving the reaction an average bimolecular rate constant of 0.35 M^{-1} s^{-1} (pH 7.4, 25°C) (156). The R-state Hb is a better reductant due to a more negative redox potential and/or to a more accessible heme pocket relative to T-state Hb (30, 77, 302).

The maximal rate of nitrite reduction is reached at the pO_2 value of about 35 μM, which corresponds to the P_{50} (*i.e.*, the pO_2 at which Hb is half-saturated) (Fig. 8). The observed kinetics of the reaction is the combination of two processes, where the rate of nitrite reduction increases with increasing O_2 fractional saturation in parallel with the increased R-state character of Hb; at high fractional saturation, the concentration of deoxyHb (one of the substrates) decreases, thereby slowing down the rate. This peculiar chemistry has been described as an allosteric autocatalytic reaction (130, 156), where

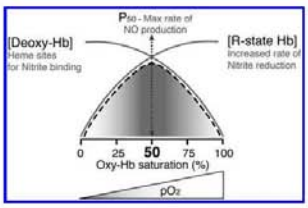

FIG. 8. Schematic representation of the NiR activity of hemoglobin (Hb). The NiR activity, depicted as a gray area, can be described as a bell-shaped curve in which the maximal rate of NO generation is reached at the P50, when Hb is 50% saturated with O_2. The NiR activity is allosterically controlled by the quaternary structure of Hb and depends on the oxygen tension (pO_2). The increase in pO_2 decreases the amount of deoxyHb available to bind nitrite and, at the same time, increases the fraction of R-state Hb, which reduces nitrite to NO more efficiently. Figure modified with permission from (220).

autocatalysis is controlled by the allosteric transition of the Hb tetramer from the T- to the R-state. Stabilization of Hb in either the T- or R-state (by chemical cross-linking) has recently confirmed this interpretation (53).

Accordingly, fetal Hb, in which the γ-subunits replace the β-subunits and the R-state is favored, shows an increased efficiency of nitrite reduction (30). Conversion of nitrite to NO in the fetus is thus favored (i) by the molecular properties of fetal Hb and (ii) by the fetal arteriovenous oxyHb concentrations (~75% to 45%) that fall in the range where nitrite reduction is maximal. The reaction of Hb with nitrite is potentially of great importance for the fetus because it provides an O_2-sensitive mechanism for NO production in the vasculature and may contribute to maintain the low resistance to blood flow, characteristic of the fetal circulation. However, taking into account that tissues are generally more effective than blood in reducing nitrite to NO (113, 204) (see also below), it remains to be demonstrated whether reduction in blood or in tissues is more important for the low vascular resistance in fetal circulation.

The exact molecular mechanism of nitrite reduction by deoxyHb is still a question of debate. A possible reaction pathway has been suggested (251, 252, 290, 291, 301) and is summarized in the following scheme:

$$NO_2^- + Hb^{2+} + H^+ \rightarrow Hb^{2+}ONOH \rightarrow [Hb^{2+}NO^+ \leftrightarrows Hb^{3+}NO] + OH^- \rightarrow Hb^{3+} + NO \quad (9)$$

In this scheme, the initial intermediate is the nitrite-associated Hb, while the second one has an electron delocalized between the heme iron and the ligand ($Hb^{2+}NO^+ \leftrightarrows Hb^{3+}NO$) and is stable even in the presence of a large excess of oxyHb and deoxyHb, particularly at low nitrite/Hb ratios found *in vivo*. The release of NO in this reaction is facilitated by excess nitrite and is conformationally regulated: the R-state quaternary conformation favors the formation of the second intermediate, whereas the T-state quaternary conformation favors the release of NO from the intermediate. This observation has been explained in terms of a conformational effect on the distal heme pocket, involving hydrogen bonding of nitrite to the distal histidine (291).

Despite the relevance of the interaction between nitrite and the heme iron, no crystal structure of the ferrous (Fe^{2+}) iron–nitrite complex of heme globins (including Hb) is available. The only adducts for which crystal structures are available are the nitrite-bound ferric (Fe^{3+}) complex of Hb at 1.8 Å resolution (368) and of Mb at 1.2 Å resolution (73) (Fig. 9). Interestingly, in both cases, the nitrite molecule is bound in the *O*-nitrito mode (Fig. 5); the ligand is stabilized by a hydrogen bond to the distal histidine residue. The hydrogen bonding capability of the distal heme pocket is crucial to direct the binding mode of nitrite: substitution of His64 with Val in Mb leads to the reorientation of the nitrite molecule to the *N*-nitro binding mode (Fig. 9C) and decreases the rate of nitrite reduction (366). Altogether, the existence of the *N*- and *O*-binding to hemoproteins (see also section on bacterial NiR) may suggest that the efficiency of nitrite reduction could be a function of the binding mode of the nitrite molecule. Thus, in principle, the mechanism of the reaction with deoxyHb should involve the formation of a nitrite complex of ferrous heme (either N- or O-bound), followed by proton transfer by

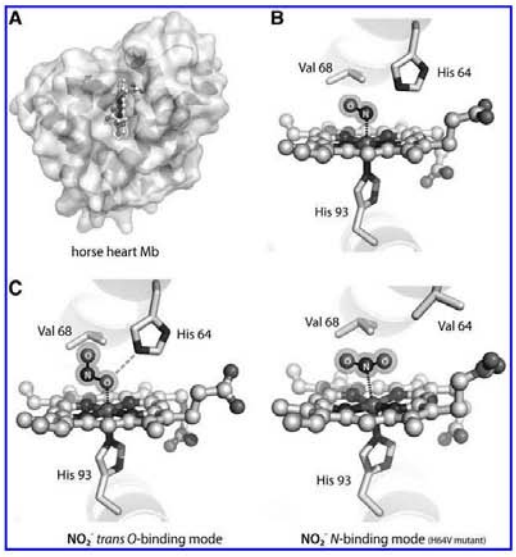

FIG. 9. Nitrite and NO binding modes in horse heart myoglobin (Mb). (A) Surface representation of horse heart Mb (hhMB) [pdb id: 2frf (73)]; the heme is shown as balls and sticks. **(B)** NO bound to Mb [pdb id: 2frk (73)]. **(C,** *Left panel***)** Nitrito derivative: nitrite is bound to the heme iron through one of the O_2 atoms: *trans* O-binding mode [pdb id: 2frk (73)]. His-64 forms a hydrogen bond with the same O_2 atom of the nitrite molecule. **(C,** *Right panel***)** Nitro derivative: nitrite is bound to the heme iron through the nitrogen atom: N-binding mode [pdb id: 3hep (366)]. The nitro derivative was observed only after substitution of the distal His64 with Val (H64V mutant of hhMB).

a nearby histidine. In the case of the N-nitro complex, dehydration of nitrite then yields the Hb (Fe^{3+})-NO derivative; on the other hand, starting from the O-nitrito complex the final derivative is the Hb (Fe^{3+})-OH complex, and thus NO is released. Regardless of the mechanism employed, one of the products of the reaction is methemoglobin (MetHb or Hb^{3+}), whose accumulation is associated with the pathological status named methemoglobinemia (see section on nitrite therapy for detailed discussion). However, metHb can be recycled to Hb, thus yielding an enzymatic conversion of nitrite into NO (179), by the NADH-cytochrome b5 reductase system. There are two forms of the NADH-cytochrome b5 reductase in humans: a soluble, erythrocyte-restricted form, which is active in metHb reduction, and a ubiquitous membrane-associated form involved in lipid metabolism. Genetic alterations of these genes are associated with congenital methemoglobinemia due to an enzyme defect in the reductase activity (179).

In summary, deoxyHb reacts with nitrite to produce NO. The main conundrum of the reaction of deoxy Hb with nitrite as a source of bioactive NO lies in the expectation that the NO produced is likely to be either immediately oxidized to nitrate by reaction with oxyHb or trapped by the excess of deoxyHb, yielding a stable ferrous–nitrosyl complex ($k_{off}NO = 10^{-3}/10^{-5}\ s^{-1}$) (182, 245). Possible chemical tricks to overcome this problem include the oxidative denitrosilation carried out by nitrite itself and the nitrite anhydrase activity of Hb forming N_2O_3, which may diffuse out of the erythrocyte, later forming NO or acting by nitrosylating a thiol. Both possibilities are analyzed in more detail below.

(2) Reaction of nitrite with oxyHb and oxidative denitrosylation. Nitrite can react with oxyHb in a complex reaction to produce metHb and nitrate (184, 190). Thus, by reacting with oxyHb, the majority of NO and nitrite end up as nitrate, which may serve as another storage form of these N-oxides.

The reaction of nitrite with oxyHb does not produce NO directly; however, as it will become clearer below, it is relevant to analyze the mechanism of this reaction and the possible crosstalk with the reduction of nitrite with deoxyHb, given that, under oxygenated conditions, the two reactions (*i.e.*, with deoxyHb and oxyHb) compete with one another (184).

In the reaction of nitrite with oxyHb, the rate of metHb production is about $0.5–1\ M^{-1}s^{-1}$ (345). This reaction has an autocatalytic kinetics, as it is initially slow (in the lag or induction phase) but then enters a rapid autocatalytic phase involving radical-mediated chain reactions and branching steps (96, 98, 180, 209, 351). The reaction can be divided into at least two steps, that is, initiation and propagation: the initiation step yields metHb and hydrogen peroxide (H_2O_2), which then react to produce the FerrylHb ($Fe^{IV}=O$) radical. In the second step, oxidation of Ferryl-Hb by nitrite produces the nitrogen dioxide ($NO_2\bullet$) radical, which reacts again with oxyHb to produce nitrate and ferrylHb, resulting in an autocatalitic loop (propagation step) (180).

The intermediate species of the nitrite/oxyHb reaction, most probably ($NO_2\bullet$), can also oxidize (Fe^{2+})Hb-NO, thus releasing NO in the so-called oxidative denitrosylation (22, 136). However, given that the nitrite levels in the erythrocytes and plasma are in the sub-micromolar range, it is unlikely that the reaction can proceed to the autocatalytic step *in vivo*, and thus low levels of $NO_2\bullet$ are produced.

(3) The nitrite anhydrase reaction of Hb. An attractive hypothesis to explain NO bioactivity from nitrite is the formation of a carrier molecule, less reactive and more easily diffusible, which can reach the target tissue and be converted again to NO. A likely candidate is N_2O_3, which can produce NO (see below) and is also able to form nitrosothiols (357) adding an extra possibility of chemical signaling. Formation of N_2O_3 might be readily explained by the nitrite anhydrase reaction of MetHb:

$$Hb^{3+} + NO_2^- + NO \rightarrow Hb^{2+} + N_2O_3 \qquad (10)$$

Different possibilities for metHb-catalyzed formation of N_2O_3 have been proposed, involving initial formation of an Fe^{3+}–nitrite (23) or Fe^{3+}–NO (116) complex. A recent theoretical study of the various mechanistic alternatives (151) shows that both pathways of Fe^{3+}-mediated N_2O_3 formation are energetically feasible. N_2O_3 back-conversion to NO has also been proposed to be mediated by Hb (23).

The formation of N_2O_3 is supported experimentally by the formation of *S*-nitrosothiols *in vivo* and *in vitro* (23, 212, 252, 311). It is thus likely that Hb may function *in vivo* as a nitrite anhydrase and that N_2O_3 may be an important player in nitrite-mediated NO and *S*-nitrosothiol signaling (see also section IV).

b. The other globins: Mb and neuroglobin. Mb is one of the most extensively studied hemoproteins; it is a monomeric globin bearing a single *b*-heme group. Mb concentration in human skeletal and cardiac muscle is as high as 200–500 μmol/kg wet tissue (362).

Mb has been implicated not only in the storage and facilitation of O_2 diffusion (236, 360, 361), but also in the scavenging of NO to protect mitochondrial respiration (39, 118). The major mechanism of attenuating intracellular NO bioactivity in cardiac muscle is the reaction of MbO_2 with NO to give metmyoglobin (metMb) and nitrate. Mb-deficient ($myo^{-/-}$) mice are more sensitive to endogenously formed and exogenously applied NO; regeneration of metMb by metMb reductase to Mb and subsequent association with O_2 leads to reformation of MbO_2 available for another NO degradation cycle.

Therefore, the reactivity of Mb with different ligands depends upon O_2 concentration: under normal O_2 levels, Mb mainly acts as an O_2/NO binding protein. Accordingly, Mb displays a functional relevance in O_2 supply and NO scavenging on the whole animal level: loss of Mb leads to impaired myocardial contractile function and exercise endurance (233).

When the O_2 concentration decreases to a value around the P_{50} of Mb (3–4 μM), the protein becomes significantly deoxygenated; under these conditions, Mb is able to reduce nitrite to bioavailable NO in the red muscle and in the heart (312). Therefore, Mb comes into play as an NiR mainly under hypoxic or ischemic conditions (144). Mb has distinct properties from Hb as an NiR: first of all, it has a very low redox potential, and therefore it reduces nitrite ~50 times faster than T-state Hb (154). Moreover, since Mb is a monomer without allosteric behavior, the reaction of nitrite with deoxyMb is a second-order reaction with a bimolecular rate constant of 6–12 $M^{-1}s^{-1}$ (between 25°C and 37°C, pH 7.4); the products of the reaction are equimolar amounts of metMb (Fe^{3+}) and iron-nitrosyl-Mb (312). Using an Mb-knock out mouse model, Hendgen-Cotta and coworkers (145, 285) provided

unequivocal evidence that deoxyMb reduces nitrite to form NO that regulates mitochondrial respiration and cardiac contractility during hypoxia and ischemia/reperfusion.

Interestingly, both neuroglobin (Ngb) (41) and cytoglobin (273) have low heme redox potential and high O_2 affinity, suggesting similar properties as Mb in terms of nitrite reduction. This hypothesis has been recently investigated for Ngb, a highly conserved hemoprotein that evolved from a common ancestor to Hb and Mb. Ngb possesses a six-coordinate heme with proximal and distal histidines ligands; coordination of the sixth ligand is reversible. Gladwin and coworkers have recently shown that deoxygenated human Ngb reacts with nitrite to form NO (330). This reaction is regulated by two redox-sensitive surface thiols (cysteine 55 and 46) controlling the fraction of five-coordinate heme together with nitrite binding and NO formation. Replacement of the distal histidine by leucine or glutamine leads to a stable five-coordinate geometry; these Ngb mutants reduce nitrite to NO ~2000 times faster than the wild type, whereas mutation of either Cys-55 or Cys-46 to alanine stabilizes the six-coordinate structure and slows down the reaction. The NiR activity of Ngb was found to inhibit cellular respiration *via* NO binding to cytochrome c oxidase (Cox), thus suggesting that Ngb may function as a physiological oxidative stress sensor and a post-translationally redox-regulated NiR. Therefore, NO generation by Ngb is controlled by the transition from six-to-five-coordinate heme state (138, 330). The authors also speculate that the six-coordinate heme globin superfamily may serve a function as primordial hypoxic and redox-regulated NO-signaling proteins. This hypothesis is in agreement with the observation that also mitochondrial cytochrome c can act as an NiR only in the five-coordinate state.

c. Xanthine oxidoreductase and aldehyde oxidase. In tissues, nitrite-derived NO production is due to the activity of both xanthine oxidoreductase (XOR) and aldehyde oxidase (AO) (aldehyde: O_2 oxidoreductase), belonging to the family of molybdenum-containing hydroxylases (232), classified under a single EC number (EC 1.2.3.1). These enzymes require, for their catalytic activity, flavin adenine dinucleotide (FAD) and a particular form of organic molybdenum, known as the molybdenum cofactor (MoCo). MoCo is a molybdopterin in eukaryotes, while it is a molybdopterin nucleotide in prokaryotes.

XOR enzymes have been isolated from a wide range of organisms, from bacteria to human, and catalyze the hydroxylation of a wide variety of purine, pyrimidine, pterin, and aldehyde substrates. The mammalian enzymes, which catalyze the hydroxylation of hypoxanthine and xanthine, the last two steps in the formation of urate, are synthesized as the dehydrogenase form (xanthine dehydrogenase [XDH]) and exist mostly as such in the cell but can be readily converted to the oxidase form (xanthine oxidase [XO]) by reversible oxidation of critical cysteine residues (535 and 992) or limited proteolysis (108, 149). Conversion of XDH to XO is enhanced by hypoxic conditions and ischemia (299). XDH shows a preference for NAD^+ reduction at the FAD reaction site, whereas XO fails to react with NAD^+ and exclusively uses dioxygen as its substrate, leading to the formation of superoxide anion and H_2O_2.

Mammalian XO is a complex homodimer (Fig. 10); in addition to MoCo, two different [2Fe-2S] centers and one FAD are present in the enzyme (35, 148). The ability of XO to

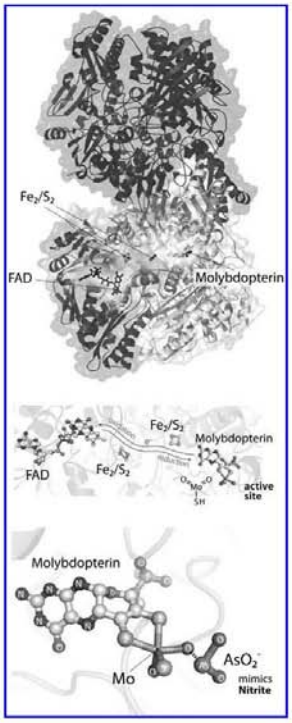

FIG. 10. Structural organization of bovine xanthine oxidase. This enzyme is a complex molecule formed by two symmetric trimers. Each trimer binds several specialized molecular tools for handling electrons. At one end of the enzyme, the purine substrate binds to an active site that includes a molybdenum atom. A hydroxyl group is added to the substrate and the electrons are funneled by a string of iron–sulfur clusters from the purine active site to the opposite side of the enzyme, which ultimately transfers the electrons to NAD or O_2; the electron flow will revert when the enzyme works as a reductase. The figure illustrates the relative position of the different cofactors. The structure of xanthine oxidase is obtained in the presence of sodium arsenite, which contains a polymeric linear anion $[AsO_2^-]n$ (pdb id: 3nvv). The arsenic atom is bound in the form of AsO_2^- anion, in which the AsIII atom is pyramidally coordinated with the two bound O_2 atoms and with the terminal O_2 of molybdopterin (200). It is highly likely that nitrite binds to the active site in the same position. FAD, flavin adenine dinucleotide.

catalyze, under normoxic conditions, the reduction of nitrate is well recognized (93, 120, 235); evidence for Nar activity in an endothelial NO synthase–deficient and germ-free mice highlights the contribution of XOR to the overall nitrite levels and nitrite homeostasis (Fig. 6) (167). Expression of XOR in the liver is increased in germ-free mice compared to conventional animals, which may explain the apparently greater tissue Nar activity observed in the germ-free animals (155), representing a compensatory response to uphold nitrite homeostasis in the absence of commensal bacteria.

The XO-catalyzed reduction of nitrite to NO has also been reported over the last decade (132, 235, 376). This activity has been proposed to be a major source of NO in tissues (204) and to exert a protective role during myocardial infarction and ischemia-reperfusion (I/R) damage (13, 353). In rat and mouse models of pulmonary hypertension, sodium nitrite is converted to biologically active NO *via* reduction in large part by XOR; in these model systems, NO production was attenuated by allopurinol (200 μM), an inhibitor of XOR (379).

The reaction catalyzed by XO is

$$NO_2^- + Mo^{4+} + H^+ \rightarrow NO + Mo^{5+} + OH^- \quad (11)$$

During the reduction of nitrite, one O_2 atom is abstracted from the nitrite molecule, resulting in the production of NO: under anaerobic conditions, NADH and xanthine are used as reducing agents. Involvement of the molybdenum site of XO in nitrite reduction was shown by the fact that alloxanthine inhibits xanthine oxidation competitively with nitrite (132). Moura and coworkers have recently shown that the molybdenum metal center is the direct electron donor to nitrite (225). The K_m for nitrite is in the mM range and the reduction is dependent on the concentration of O_2, which acts as a competitive inhibitor (207). Despite these lines of evidence, under hypoxia and anoxia, the acidosis and the increased concentrations of xanthine and NADH will probably be sufficient to support the XO-mediated nitrite reduction physiologically, as supported by *in vivo* studies (13, 102, 353).

Interestingly, also the mammalian AO was shown to catalyze the reduction of nitrite to NO. AO is a cytosolic enzyme that plays an important role in the biotransformation of drugs and xenobiotics (371). AO is present in highest levels in the liver but is also broadly distributed in other tissues, such as lung, blood vessels, heart, and kidney (26, 247). Similarly to XOR, also AO contains two iron–sulfur clusters, a flavin cofactor, and a molybdopterin cofactor. The K_m for nitrite of AO is 3 mM (205) but the affinity for NADH ($K_m = 24\ \mu M$) is much higher than that of XOR ($K_m = 0.9$ mM). Therefore, this pathway would be predicted to better retain its nitrite reduction ability in the presence of O_2: AO-mediated NO generation could exceed the NO generation from XOR in the lung and approach that from XOR in the heart and liver under anaerobic conditions.

d. Other mammalian proteins acting as NiR. In the last decade, multiple proteins, besides those discussed above, have been implicated in nitrite reduction to NO. As an example, nitrite reduction by mitochondria under low O_2 concentrations has been reported and ascribed by different authors to Cox (mitochondrial respiratory complex IV), to mitochondrial complex III (191) and to the soluble electron carrier cytochrome c.

Castello *et al.* (60) have reported that yeast and rat liver mitochondria produce NO at O_2 concentrations below 20 μM. This NO production is nitrite dependent, is carried out by Cox in a pH-dependent fashion, and is accompanied by an increase in protein tyrosine nitration. The ability of Cox to reduce nitrite in yeast can be modulated by O_2 by altering the subunit composition of the complex: the presence of the isoform COX5b of subunit V, preferentially expressed at low O_2 tensions, enhances NO production (61). The authors suggest a positive feedback mechanism in which mitochondrially produced NO induces expression of COX5b, whose protein product then functions to enhance the ability of Cox to produce NO in hypoxic/anoxic cells. The NO generated in the mitochondria by Cox might be released from cells, thereby reaching external targets (280). Interestingly, it has been reported that the nitrite-derived NO synthesis catalyzed by Cox is enhanced by low intensity light, offering a new explanation for the increase in NO bioavailability experienced by tissue exposed to light (14, 279).

In agreement to what has been observed for the six-coordinate hemoprotein Ngb previously discussed, also cytochrome c is able to reduce nitrite to NO when in the five-coordinate state (22, 62). These data ascribe a possible role for cytochrome c as an NiR, possibly relevant in the hypoxic, redox, and apoptotic signaling pathways within the cell.

Other possible NiR at the tissue level include the ubiquitous enzyme carbonic anhydrase (CA), a crucial player in CO_2 transport (1), and rat liver cytochrome P450s (206), a family of proteins involved in the metabolism of xenobiotics (including organic nitrates). In the latter case, mammalian cytochrome P450 reductase (CPR) and cytochrome P450 cooperate to function in a sequential manner to produce nitrite and then NO and nitrosothiols, serving as the link between organic nitrates and NO-mediated signaling.

Altogether, these lines of evidence reinforce the idea that multiple proteins may function as NiR under low O_2 tension; however, the precise regulatory pathways controlling these activities is still far from being understood.

IV. Significance of Nitrite in Human Health and Disease

In this section we first discuss the involvement of nitrite in vasodilation, focusing on its role as a source of NO (section A); then, we analyze the cytoprotective effects of NO in the I/R injury and the role of nitrite as endocrine reservoir of NO (section B); finally, we briefly describe the other NO-independent physiological activities of nitrite (section C).

A. Nitrite in vasodilation

The primary function of vasodilation is to increase blood flow in the body to tissues that need it most; if the supply of O_2 is not sufficient, for example, in a working muscle or under hypoxia, an increase of O_2 delivery must occur, to selectively distribute the blood according to variable needs (90, 303, 339).

Recent evidence suggests that nitrite is a putative physiological signaling molecule with a potential role in hypoxic vasodilation, signaling, and cytoprotection after I/R (130). Several studies have suggested and confirmed the involvement of nitrite in vasodilation in humans, also in the presence of NOS inhibitors (74); the effect of nitrite has been confirmed in mouse, rat, sheep, and primates (29, 88, 338). Interestingly, intra-arterial infusion of nitrite during normoxia and hypoxia has shown that arteries are modestly affected under normoxic

conditions, but are potently dilated under hypoxic conditions (224).

Nitrite-dependent effects on vasodilation are mostly mediated by NO, which stimulates soluble guanylate cyclase (sGC), thereby increasing cGMP levels, activating cGMP-dependent protein kinase and producing smooth muscle relaxation (130, 241). A physiologic NO-dependent post-translational regulation of vascular sGC in mammals involving S-nitrosylation as a key mechanism has recently been suggested (264). NO can also relax smooth muscle by cyclic GMP-independent mechanisms, including the direct modifications of sarco/endoplasmic reticulum calcium ATPase (SERCA), the enzyme essential for the control of intracellular free Ca^{2+} levels. NO modification causes, in smooth muscle cells, reduction of intracellular Ca^{2+} levels and, consequently, vascular relaxation (331). It has been demonstrated that NO, *via* $ONOO^-$ and N_2O_3 formation, can adduct GSH to SERCA cysteine thiol; this modification predominantly activates SERCA and refills Ca^{2+} stores in sarcoplasmic reticulum. This NO-dependent mechanism of SERCA modification is crucial for proper vascular relaxation; in altered redox-state background such as in atherosclerotic arteries, NO does not stimulate SERCA activity because of the irreversible oxidation of the target cysteine thiol by the high levels of oxidants accompanying the disease (331).

A key role in the control of hypoxic vasodilation by nitrite has been assigned to the erythrocyte (100, 107, 130), mainly due to the NiR activity of deoxyHb, previously discussed (74, 91, 170). An open question is how NO escapes the erythrocytes to exert its vasodilatatory effect. Different potential mechanisms could be operative (130): one hypothesis suggests that the NO escape is inefficient, but sufficient to regulate vascular tone due to lipophilicity and potency of the molecule. Another hypothesis is that the erythrocyte membrane provides a potential NiR metabolon, a system that would concentrate chemical reactants, nitrite, protons, and deoxyheme with highly hydrophobic channels. A third solution is that nitrite reduction produces intermediate(s) that could facilitate the transport of NO, such as N_2O_3. Finally, the formation of S-nitrosothiols can also occur (130, 170). The formation of Hb derivatives, such as the S-nitrosated Hb, as a possible reservoir of NO bioactivity has been proposed (172, 321), but was recently critically analyzed and disputed by *in vivo* experiments in rats (168).

Nitrite-dependent vasodilation at low pH may also occur in a protein-independent pathway. For more than a century, it was known that acidic conditions allow vascular smooth muscle relaxation; indeed, to date, it has been suggested that abiotic reduction of inorganic nitrite to NO, a phenomenon known as acidic metabolic vasodilation, regulates local blood flow under hypoxia or ischemia (213, 238).

B. Nitrite-based cytoprotection in I/R injury

I/R injury is the major cause of death and illness in the Western World (281). This injury consists of multifaceted cellular events that take place on the recovery of O_2 delivery after a period of hypoxia. The heart, the kidneys, and the brain are among the organs that are the most quickly damaged by loss of blood flow. Insufficient blood supply to the myocardium can lead to myocardial ischemia infarction; timely restoration of the blood flow to the acute ischemic myocardium is essential to reduce morbidity and mortality of the patients. However, the process of reperfusion after an ischemic episode can paradoxically lead to a unique form of damage, termed myocardial reperfusion injury. As initially observed by Hearse *et al.* (141), the reoxygenation required during reperfusion of ischemic myocardium generates reactive oxygen species (ROS), which trigger cellular injury (340, 341).

One of the most effective strategies, when applicable, to preserve tissues from I/R damage is the ischemia preconditioning, consisting of short periods of ischemia followed by reperfusion before a long ischemic period (250, 281); this setting restricts its potential clinical utility to planned acute myocardial I/R injury such as coronary artery bypass graft surgery, cardiac transplantation, and percutaneous coronary intervention (355). The ischemia preconditioning guarantees the activation of the protective signaling pathway (ROS-induced, see below) at the time of the reperfusion, which is able to reduce tissue infarction significantly (32, 281); the same protective effect (reduction of infarct size and attenuation in inflammatory response) can be obtained by ischemic postconditioning (378).

Under normoxic conditions, the mitochondrial respiratory chain produces a small amount of ROS and reactive nitrogen species, which are scavenged by different antioxidant enzymatic systems and compounds (24). On the other hand, after ischemia, reperfusion of ischemic tissue leads to an exceptional production of ROS: this oxidative burst depletes or damages the pool of antioxidants available, causing tissue injury (106, 281, 377). More in detail, during ischemia, the electron transport chain functions as a reservoir of electrons since O_2 availability is limited. This high reductive potential, particularly for complex I and III, promotes incomplete O_2 reduction, and thus radical formation, when a massive entrance of O_2 occurs during reperfusion (47). Incomplete O_2 reduction during reperfusion leads to the production of superoxide anion, H_2O_2, and hydroxyl radical to levels that are 1 to 2 orders of magnitude higher than those detected in non-ischemic background (381).

It should be mentioned that other enzymes partecipate in ROS generation during I/R injury, such as NADPH oxidase, NOS (during substrates depletion), and XO; in the latter case, during ischemia, ATP is predominalty metabolized as hypoxanthine and xanthine, which reacts with XO (whose formation from XDH is favored in postischemic heart) upon reoxygenation, resulting in superoxide generation (381).

In the last years, many studies demonstrated that NO production is associated with cytoprotection against I/R injury in many organs, such as the heart, liver, lungs, and kidneys (174, 275). One of the first evidence associating NO with cardioprotective effect was obtained 20 years ago by using acidified nitrite, which was shown to exert a significant protective action during ischemia and reperfusion injury (173). A relative decrease in NO bioavailability appears to be central in the pathogenesis of this injury, and therapeutic strategies aimed at replacing NO by inhalation, nitrite/nitrate anion supplementation, or *via* donor drugs represent a novel means for ameliorating I/R injury (275, 318).

The mechanism activated during ischemic postconditioning to minimize ROS-dependent tissue damages during I/R injury has been extensively studied in last two decades (91); even though the molecular details controlling this phenomenon remain to be deciphered, Bolli and coworkers demonstrated that

NO plays a prominent role in mediating the cardioprotective response (33). The authors demonstrated that a brief ischemic stress causes a burst of NO production as well as $\cdot O_2^-$ production, which in turn could then react to form ONOO$^-$; this reaction triggers a complex signal cascade involving the protein kinase C (PKCs) and the transcription factor NF-kB (33). ONOO$^-$ formation prevents further ROS production occurring *via* the Fenton reaction and, despite the cytotoxic effects observed in the presence of excess of ONOO$^-$, its decomposition produces intermediates, which are scavenged by NO itself (359). This reaction ultimately results in production of the nitrosating species N_2O_3, which in turn contributes to the overall NO-dependent cellular response (359). As demonstrated both *in vivo* and *in vitro* by using chemical models, this nitrosative stress provide an optimal antioxidant environment rather than toxic species, indicating that NO acts to counterbalance oxidative stress, beside its role in controlling signaling events *via* ONOO$^-$ formation (85, 328).

NO modulates a plethora of processes during I/R injury, including inflammation, ROS formation, and apoptosis (Fig. 11). NO can also exert its cytoprotective role by inhibiting caspase through S-nitrosation and *via* cGMP to avoid the release of cytochrome c from mitochondria, thus preventing apoptosis (91). NO inhibits calcium overloading, responsible for the opening of a nonselective mitochondrial permeability transition pore, which uncouples oxidative phosphorylation and worsens ions/energetic homeostasis, leading to cell death by necrosis or apoptosis (277). At the same time, it is known that NO reversibly inhibits complex IV (40, 72) and, more importantly, complex I (38). Inactivation of complex I involves mainly S-nitrosation of critical thiols (68); since this modification is reversible, the inhibition of complex I is slowly reduced over time, thus allowing the respiratory chain to gradually recover the normal electron transfer between complexes, without the deleterious instigation of oxidative damage (248) (see below). Inhibition of complex I activity seems to be crucial for cytoprotection during I/R injury being the inhibited form of this enzyme unable to generate ROS (47) and involved in limiting calcium overload (277). Moreover, as mentioned above, the respiratory chain is directly involved in the induction of some hypoxic nuclear genes (hypoxic signaling); as proposed recently (60), mitochondrially produced NO functions in a signaling pathway to the nucleus *via* ONOO$^-$, which may directly or indirectly modify specific proteins and activate hypoxic signaling.

Thus, the concept of reversible ROS inhibition in mitochondria during the early phases of reperfusion may represent an intriguing therapeutic chance to minimize tissue damages caused by I/R injury. In hypoxia, it is plausible that nitrite functions as an alternative NO source under those conditions. As previously reported, Zweier and coworkers in 1995 demonstrated for the first time the pivotal role of nitrite as source of NO (382); the finding that nitrite may act as endocrine reservoir of NO has prompted many studies demonstrating the capability of nitrite to mediate potent cytoprotection (*via* NO) in a number of organs and animal models of I/R injury [see (102)], also by modulating mitochondrial electron transfer (313).

The pathway by which nitrite forms NO in hypoxic tissue remains to be determined; several mechanisms have been proposed/identified over the years (281).

Two groups suggested the involvement of XO on the basis of reduced efficacy after treatment with allopurinol, an XO inhibitor (336, 353). Other groups have shown the involvement of Mb in nitrite conversion to NO and thus in cytoprotection. Addition of nitrite to rat heart homogenates containing both Mb and mitochondria resulted in NO generation and inhibition of respiration; these effects were blocked by Mb oxidation with ferricyanide but not by the addition of XO inhibitor allopurinol (312). Moreover,

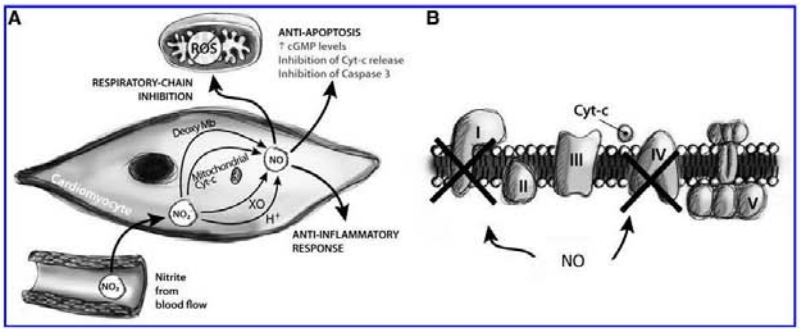

FIG. 11. Nitrite-mediated cytoprotection. (A) Nitrite enters in cardiomyocytes from blood and is reduced to NO by either biochemical mechanisms involving deoxyMb, xanthine oxidoreductase (XO), and mitochondrial cytochrome c (Cyt-c), or *via* pH-dependent chemical reduction. NO can be cytoprotective, *via* different pathways such as activation of the anti-inflammatory response, prevention of apoptosis (by inhibition of caspase 3 through S-nitrosation or *via* cGMP to avoid Cyt-c release), and inhibition of the respiratory chain (91) **(B)**. Mitochondria exposed to hypoxia and reperfused with O_2 generate abundant and potentially damaging reactive oxygen species (ROS). **(B)** NO can prevent ROS formation by inhibiting the respiratory chain, mainly at the level of complexes I and IV (38, 40).

intracoronary application of nitrite in wild-type and myo$^{(-/-)}$ mice (285) clearly showed that the NO generated by reaction of deoxyMb with nitrite is functionally relevant and leads to a downregulation of cardiac energy status, not observed in mice lacking Mb. The involvement of other hemoproteins and mitochondrial heme-containing complexes (such as cytochrome P450 and complex IV) in nitrite reduction has also been demonstrated (281).

However, even though the strategy of NO production is not unequivocally identified, enough NO seems to be produced from nitrite either directly within the mitochondria (22, 60, 61) or in the cytoplasm, as it occurs in myocytes where deoxyMb acts as an NiR (75, 145).

The discovery that nitrite may act as an endocrine reservoir of NO has suggested the idea that in the future this anion may represent an alternative strategy for an effective NO-based therapy by acting as an NO prodrug (181, 324). An overview of the main results foused on nitrite-mediated cytoprotection and more in general on the state-of-the-art of nitrite therapy is reported in chapter V.

C. Other activities of nitrite

To date, the majority of studies have described the nitrite effect as NO-dependent, but a novel NO-independent role of nitrite has been recently suggested, which may involve nitrite-mediated nitrosation without passing through a free NO intermediate (113). Nitrite-mediated nitrosation may protect tissues against inflammation (349).

Finally, a global role of nitrite in hypoxic signaling has been described: it affects cyclic-GMP production, cytochrome P450 activity, heat shock protein 70, and heme oxygenase-1 expression in a variety of tissues (43). These cellular activities of nitrite, in addition to its stability and abundance *in vivo*, suggest that this anion has a distinct and important role in mammalian biology, perhaps by serving as an endocrine messenger and synchronizing agent.

All these unexpected roles of nitrite in human physiology have opened the research to the possibility of therapeutic application associated with hypoxia and vasoconstriction.

V. Nitrite Therapy

In this section we discuss the advantages and the applications of nitrite-based therapy. We first analyze its feasibility and the pharmacokinetics of nitrite (section A); than, we discuss the tolerance and the toxicity of the compound (section B); finally, we described the most recent results concerning the use of nitrite in therapy (section C).

In 2006, David Lefer, a leader in I/R injury research, stated in an Editorial Focus that "the field of nitrite chemistry and biology is a truly exciting area of research that is certain to expand in the near future and lead to a dramatically improved understanding of the physiology of NO synthases and NO in terms of cytoprotection" (202).

It is now clear that reduction of nitrite to form NO under both physiological and pathological conditions is a challenging topic in medicinal chemistry (50). The potential of nitrite-based therapy is indeed clearly demonstrated by the rapidly growing number of studies on animal models of injury, the review articles (58, 91, 177, 248, 259, 316), and special issues (such as volume 89, issue 3, of *Cardiovascular Research*) on this topic, by the clinical trials aimed at investigating the action of nitrite in protection [ClinicalTrials.gov and (181)] and by the number of patents (*e.g.*, uspto.gov).

The state of the art on the activity of nitrite under physiological and pathological states and on the translation of nitrite and nitrate research for clinical applications has been presented, from 2005 and every 2 years, during a dedicated international meeting held in Atlanta (for info on past meetings, see www.strategicresults.com/nitrite2011/). The outcome of the nitrite meeting 2011 will be published as a special abstract supplement of *The NO: Biology and Chemistry Journal*.

The advantage to use nitrite therapy instead of NO therapy is closely related to the high stability of nitrite, which can be transported in the circulation and stored in tissues. Moreover, since nitrite reduction occurs under conditions close to those of injured tissues (ischemia, hypoxia, and low pH), nitrite-dependent NO release targets injured tissues preferentially, thereby reducing the risk of systemic side effects (51). A summary of the possible effects of nitrite-based therapy is given in Figure 12.

Currently, NO therapy has been exploited *via* inhaled NO (iNO) gas from pressurized tanks; this approach is, to date, the preferred and the only approved NO treatment for acute pulmonary hypertension (78, 92, 372) even though it is inconvenient and onerous (92, 160). Alternatively, other strategies imply compounds containing either NO or an NO precursor in a stable form (178, 195), which may represent a clinical promise once it will be possible to control carefully the sustained delivery (49).

However, contrary to NO, nitrite allows multiple administration strategies, including oral, topical, intravenous, intraperitoneal, and aerosolized.

A. Pharmacokinetics and feasibility

It is known that nitrite intake occurring *via* nitrate as dietary source leads to its rapid absorption in the duodenum and jejunum and distribution in the whole body (18, 181, 296) (Fig. 7). Studies focused on nitrite administration/infusion have been obtained recently on both nonhuman primates (87) and human volunteers (87, 158). These experiments demonstrated that infused nitrite is a rapid vasodilator at physiological concentration and that nitrite-induced effects in terms of forearm blood flow are immediate (ranging from 15 to 60 sec, depending on the dose) (87). Upon infusion, nitrite levels increased to micromolar levels and then decayed with an apparent biological half-life of 42 min, while nitrite-induced hypotension lasted for 3 h (87).

A detailed study focused on the pharmacokinetics of ingested nitrite by human volunteers has shown that nitrite is able to reach the systemic circulation (158).

Very recently, the outcomes of a completed clinical trial, developed to determine the safety and feasibility of prolonged sodium nitrite infusion, have been published (278); this study provided pharmacokinetic and toxicity parameters needed for using nitrite as a therapeutic agent, such as maximal tolerated dose and dose-limited toxicity for long-term intravenous infusion of sodium nitrite (266.9 and 445.7 mg/kg/h, respectively) and the mean half-life of nitrite in plasma and whole blood (45.3 and 51.4 min, respectively). More interestingly, the small increase of metHb seen in this study was asymptomatic and the decrease of blood pressure was transient (278). This study suggests that prolonged intravenous

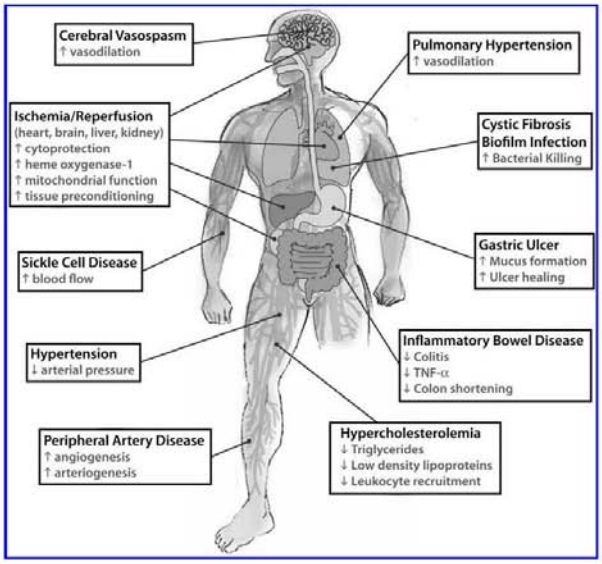

FIG. 12. Effects of nitrite-based therapy. Summary of the main effects exerted by nitrite as a therapeutical agent in different pathological conditions: these properties are supported by experimental and/or clinical results. Figure modified with permission from (181).

infusion of sodium nitrite (at doses within the maximal tolerated dose) is safe and should provide the proper amount of nitrite required to exert its therapeutic role (278).

B. Tolerance and toxicity

It is worth to notice that, contrary to organic nitrate class of drugs such as nitroglycerin (327), continous sodium nitrite administration in nonhuman primates does not induce tolerance (87), that is, decrease of sensitivity of vascular smooth muscle to further vasorelaxation. In 2002 Ignarro underlined how nitroglycerine tolerance limits the chronic use of such compounds to treat angina pectoris and how "the discovery either of ways to avoid tolerance or of new NO-generating drugs that do not cause tolerance" is of great interest (161). Nitroglycerin tolerance arises likely from the inhibition of the enzymes involved in nitroglycerin bioactivation, such as the mitochondrial aldehyde dehydrogenase, cytochrome P450, and glutathione-S-transferase, which function also as nitroglycerin reductases (63, 121, 237). The capability of nitrite to bypass the enzymatic tolerance may represent a convenient alternative to organic nitrate therapy, as wished by Ignarro about 10 years ago.

Since more than 95% of orally ingested nitrite is absorbed, its toxicity during extended exposure to nitrite was evaluated. The intake of nitrite has been historically associated with poisoning due to methemoglobinemia (52, 229); this condition can interfere with the ability of blood cells to carry O_2 when metHb concentrations reach 20%–30% of total Hb concentrations. In healthy individuals without anemia, acquired methemoglobinemia causes few symptoms at 15% metHb, while levels of 20%–30% metHb cause headache, fatigue, and syncope; at levels of ~50% dys-rhythmias, coma and death occur (165). Infantile methemoglobinaemia has been associated with feeding reconstituted with well waters rich in nitrate (70, 95).

However, after intravenous administration of nitrite, the maximum percent metHb in blood was between 3% and 12% and ~4% after oral administration (87, 158); in both cases the maximum metHb level was reached about 0.8–1.2 h after intravenous or oral administration (87, 158). These results indicate that nitrite levels able to induce vasodilation do not cause clinically significant methemoglobinemia, probably thanks to the coupled methemoglobin reductase activity of the NADH-cytochrome b5 reductase, previously discussed.

Oral administration of nitrite has been causally associated with gastrointestinal cancer (229). It has been postulated that, under strong acidic conditions, swallowed salivary nitrite may nitrosate *via* HNO_2 secondary amines ingested in food to form nitrosamines (309); some of these nitrosamine have been found to be carcinogenic in animal and in epidemiological studies (20, 189, 211). However, the direct involvement of swallowed salivary nitrite [*via* nitrate reduction, (101)] in promoting gastrointestinal cancer has not been demonstrated (189); all available data indicate that there is not a direct causative role of nitrate in gastric cancer (229), possibly because food ingestion promotes an increase in pH to a value that hampers secondary amines nitrosation, a reaction preferentially occurring at pH 2.2–3.5 (19).

In conclusion, all data available to date on pharmacokinetics and toxicity of nitrite strongly support the use of nitrite therapy as a strategy to bypass the limitations of the NO therapy (51).

C. Effects of nitrate/nitrite administration and the therapeutic potential

Nitrite-based therapy has been used to control vasodilation and cytoprotection after hypoxic damage, but also inflammatory disease and host defense processes (181, 229). Accordingly, experimental data can be clustered into three main groups:

- Nitrite as a cardiovascular drug
- Nitrite use for inflammatory diseases
- Acidified nitrite as a tool against bacterial pathogens

A summary on these topics is reported below, with special attention to the use of nitrite therapy in cardiovascular diseases.

1. Nitrite as a cardiovascular drug. A growing number of studies reported the effects of nitrite administration on protection against I/R injury (176, 201, 317, 353), platelet function inhibition (222, 354), vasodilation (74, 131), reduction of blood pressure (127, 197), and increase of cGMP levels (43). All these results are in agreement with the evidence that most of the cardiovascular risk factors are associated with reduced NO availability in the vasculature (150, 256). Most of the studies indeed demonstrated that the protective effect of nitrite or dietary nitrate is significantly lowered by the presence of NO scavenger such as carboxy-PTIO and Hb (176, 194, 222).

Webb and coworkers (353) assembled 7 years ago a specially adapted NO-collecting chamber placed around isolated perfused rat heart to measure NO concentration, using the ozone chemiluminescence detection method previously developed by other groups (115, 186); this chamber was also employed to measure NO production in homogenized myocardium (rat and human). In both experimental settings, a significant NO production was observed upon addition of sodium nitrite (10–100 μM) at pH 5–6, a condition typical of myocardial ischemia (353). Nitrite significantly reduced infarct size (~50%); the cytoprotective effect is abolished in the presence of NO scavengers (353).

a. Ischemia/reperfusion injury. The efficacy of nitrite administration in limiting I/R damages has been investigated extensively in myocardial and brain ischemia, as much as in liver and kidney; the main outcome of these studies is that the amount and the way of administration of nitrite are crucial to exert its protective role as therapeutics upon ischemic damage.

Duranski and collegues performed studies in mice to evaluate the cardioprotective effects of acute nitrite therapy in the setting of coronary artery occlusion and reperfusion, exploring different nitrite dosages (2.4–1920 nmol) (102). The administration of nitrite into the left ventricular cavity 5 min before reperfusion significantly limited myocardial infarct size, in a dose-dependent manner with a maximal protective effect at 48 nmol of nitrite (102). Low doses of intravenous nitrite improved microvascular perfusion, reduced apoptosis, and improved contractile function (133). Nitrite can also exert potent cytoprotective effects after I/R injury on liver in a dose-dependent fashion by limiting serum increase of the liver transaminases, hepatocellular injury, and apoptosis (102).

The effect of dose and duration of nitrite/NO exposure is critical, resulting in a precise setting and timing for NO-mediated cytoprotection in I/R pathophysiology. Different experimental protocols may give contradictory results, as shown in studies focused on the treatment of ischemic brain in rats by two different research groups. The group of Jung and coworkers (176) observed a significant reduction in infarct size, while Schatlo and collegues did not observe the dose-protective effect of nitrite in ischemic brain (307). These contradictory results may arise from differences in the experimental setting employed by the two research groups, in terms of both duration of nitrite administration and age of the animals.

The route of administration may also explain discrepancies in studies on the efficacy of nitrite therapy. A clear example is represented by the results obtained on a rat model of I/R-induced renal injury by two different groups, both using the same amount and timing of nitrite application. Basireddy and collegues observed that the intravenous or intraperitoneal administration of nitrite did not provide protection upon I/R induced renal injury (21), in contrast to its beneficial effects in cardiac and hepatic I/R injury (102, 133, 353). Tripatara *et al.* confirmed this result but were also able to attenuate the degree of renal dysfunction, reperfusion injury, glomerular dysfunction, and tubular injury upon topical administration of nitrite (336).

Oral nitrite administration in the treatment of I/R injury after transplantation was shown to improve cardiac allograft outcomes in rats by lowering allograft inflammation, apoptosis, and alloimmune responses (374). Nitrite administration resulted in prolonged allograft survival, while reduced oral intake of NOx promoted rejection (374). Accordingly, administration of iNO (80 ppm) to patients undergoing orthotopic liver transplantation inhibits hepatic I/R injury (196). The concentration of NO metabolites (including nitrate and nitrite) was significantly increased in these patients, in agreement with other studies on iNO administration (253); Lang and coworkers (196) suggested that, in their study, the extrapulmonary effects of iNO were mainly due to nitrite.

b. Cardiovascular disorders. The therapeutic potential of nitrite in the field of cardiovascular diseases has been also evaluated for disorders associated with reduced NO availability, such as chronic tissue ischemia (31), sickle cell disease (SCD) (227), and pulmonary arterial hypertension (PAH) (79). Nitrite therapy has been studied also as a strategy to control vasodilation and hypertension (127, 181, 354).

Chronic tissue ischemia is mainly caused by peripheral arterial disease (PAD) (181, 267), responsible for hypertension, atherosclerosis, and diabetes (181). Currently, the treatment of such pathological status is based on the employment of anti-platelet agents and statins (267). The capability of nitrite to promote angiogenesis as a therapeutic strategy to treat PAD and more in general chronic tissue ischemia is a challenging issue; since NO plays an important role in stimulating angiogenesis (71), the effect of nitrite therapy in controlling ischemia-induced angiogenesis has been analyzed (194). Nitrite was found to improve angiogenesis in terms of increase in the quantity of endothelial cells and in the vascular density (194). A dose-dependent effect of nitrite in the increase of

ischemic tissue blood flow in mice was observed (310). The capability of nitrite to restore ischemic blood flow was significantly impared by the presence of NO scavenger such as carboxy-PTIO (194). Interestingly, the capability of nitrite to augment angiogenesis was also demonstrated in the neural regeneration stimulated upon prolonged nitrite therapy in the ischemic brains (177).

The possibility to employ nitrite as source of NO in managing PAD has been supported also indirectly; pharmacological treatment of permanent tissue ischemia with the antiplatelet drug dipyridamole augments ischemic tissue reperfusion, promotes endothelial nitric oxide synthase (eNOS) activity, and, as a consequence, increases nitrite levels in ischemic muscle tissue (269). Nitrite reduction may enhance the vascular growth observed upon dipyridamole treatment (346), confirming the presence of a nitrite/NO endocrine system able to produce benefits not only locally but also in distal tissues (267).

As mentioned above, the reduced NO bioavailability also represents one of the pathological trait of SCD, a genetic disease due to a point mutation of the beta-chain of Hb (227); these patients accumulate huge amounts of free Hb, which reduces NO bioavailability (286, 348). The possibility to develop therapeutic strategies aimed at optimizing NO delivery has been considered at least 10 years ago (242); a recent phase I/II study demonstrated that sodium nitrite infusion into the brachial artery augmented in a dose-dependent manner the mean venous plasma nitrite concentration and stimulated forearm blood flow (223). Since this treatment was well tolerated (lack of hypotension and significative methemoglobinemia), nitrite could represent a plausible NO donor for future clinical trials in SCD (223).

The very efficient NO scavenging property of oxyHb (175) represents a limitation in using blood substitutes, where a secondary hypertension is associated with scavenging of NO by Hb-based oxygen carriers (HBOCs). A novel therapeutic strategy to attenuate this side effect has been proposed based on the use of nitrite as an adjunct therapy to attenuate HBOC-dependent hypertension (298).

Impaired NO bioavailabilty plays an important role also in the development of PAH, a chronic and progressive disease characterized by a persistent elevation of pulmonary artery pressure that progressively leads to right heart failure and ultimately death (79). Currently, iNO therapy is only approved for use in infants who have respiratory distress syndrome (140) even though the short-term effects and the elevated cost of such therapy made researchers to explore novel strategies (79). The administration of nebulized nitrite to treat hypoxic pulmonary hypertension in newborn lambs decreases the pulmonary artery pressure without measurable effect on mean arterial blood (159). More recently, the beneficial effects of nebulized nitrite under hypoxia or monocrotaline-induced PAH were confirmed in mice and rats (379). This therapeutic approach completely prevented or reversed PAH and pathological right ventricular hypertrophy and failure (379).

The evidence that nitrite may really target pulmonary circulation preferentially under hypoxic conditions has been verified on healthy human volunteers (162). The study was done in a hypoxic chamber (inspired O_2, 12%; room air as control) where each volunteer received an infusion of sodium nitrite (1 μmol/min). During hypoxia, nitrite increased forearm blood flow (+36%) and reduced pulmonary arterial pressure (12%–17%). Interestingly, pulmonary, but not systemic, arterial effects persisted 1 h after stopping the infusion, in conjunction with plasma nitrite levels lowered to the baseline values (162).

It should be pointed out that, even though rapid nitrate administration is largely ineffective in the pathological settings discussed above (as most of these studies used nitrate as negative control), recent data report that sustained delivery of nitrate (over days/weeks) may represent an alternative strategy to increase plasma nitrite and achieve protection. Dietary nitrate can enhance exercise performance in PAD patients (179), representing a chance for these patients, where plasma nitrite levels could be indicative of vascular health and function (3).

The effects of dietary nitrate have been also analyzed in different pathological backgrounds. Dietary supplementation of nitrate was used in eNOS-deficient mice, which presents several features of the metabolic syndrome (55), a cardiovascular disorder associated with reduced NO bioavailability from eNOS, with increased cardiovascular risk and type 2 diabetes (117, 243). Dietary nitrate treatment (7–10 weeks) reduced both fat accumulation and circulating triglycerides; moreover, it reversed the prediabetic phenotype by improving glucose tolerance and reducing fasting blood glucose (55).

Nitrate/nitrite-derived NO may also control blood pressure (197). Dietary supplementation with sodium nitrate (0.1 mmol/Kg per day for 3 days) in healthy volunteers decreases the mean arterial pressure (by 3.2 mmHg) and increases plasma levels of both nitrate and nitrite (197). The effect of dietary nitrate has been recently analyzed in a model of renal and cardiovascular disease (56); chronic dietary nitrate supplementation attenuates hypertension and prevents the development of cardiac and renal damage (56).

Dietary nitrite therapy may play an important role in preventing cardiovascular disease associated with aging, such as vascular endothelial dysfunction and large elastic artery stiffening (316). Nitrite supplementation in old and young mice showed that the treatment ameliorated carotid artery endothelial dysfunction and reduced large elastic artery stiffness in old mice to a level similar to that of young mice, confirming the translational potential of nitrite administration to prevent cardiovascular disorders associated with aging (316).

2. Nitrite in inflammatory diseases. There is growing experimental evidence that inorganic nitrite therapy confers substantial benefit to numerous pathophysiological conditions includes experimental colitis, hypercholesterolemia, and gastric ulcer.

Colitis is a chronic inflammatory disorder of the intestinal tract characterized by mucosal inflammation of the large bowel (217) with excessive production of cytokines, adhesion molecules, and ROS (334). In a colitis model in mice (263), colonic nitrite levels decrease with concomitant increase in colonic TNF-α expression followed by increased iNOS and heme oxygenase-1 expression (262). Oral sodium nitrite administration (6.4–7.2 mg/mouse/day) attenuates acute inflammatory flares of colitis by preserving tissue NO bioavailability, as suggested by the increase in nitrite colonic levels and decrease in TNF-α expression (262).

Nitrite has shown a novel role as a therapeutic agent also to contrast microvascular inflammation and endothelial dysfunction associated with hypercholesterolemia (322). The hypercholesterolemia proinflammatory phenotype is characterized by a decline in NO bioavailability and increase of ROS production. Nitrite administration is able to restore NO biochemical homeostasis and significantly attenuates hypercholesterolemia-mediated leukocyte recruitment, which plays a key role in controlling vascular inflammation (262).

A recent whole genome array analysis (268), combined with previous data of nitrite-dependent induction of angiogenesis (194), suggests that nitrite therapy may also facilitate vascular remodeling during chronic tissue ischemia by modulating inflammatory gene expression. Nitrite-treated animals (330 μg/kg/day) present a significant decrease in inflammatory gene expression concomitant with an increase in genes that function to protect and preserve skeletal muscle tissue (268). Moreover, nitrite administration upregulates several genes involved in innate immune responses, such as the macrophage migration inhibitor factor and the heat shock protein 90 class B member (Hsp90ab1) (269). Since Hsp90ab1 promotes eNOS activation, the final outcome is NO production in ischemic tissue (123). On the other hand, nitrite also significantly downregulates other genes associated with innate immunity, for example, IL-10 (269). Several studies (84, 124, 254, 300) suggest that IL-10 expression acts in an anti-angiogenic manner in several pathological events, including chronic tissue ischemia; therefore, the nitrite therapy likely augments reperfusion in chronic tissue ischemia caused by this regulation of innate inflammation response.

3. Acidified nitrite as a tool against bacterial pathogens. As mentioned before, under acidic conditions, sodium nitrite forms HNO_2 that, in the presence of O_2, generates reactive nitrogen intermediates, including $ONOO^-$, N_2O_3, $NO_2\bullet$, and NO (276). These small molecules readily cross cell membranes, where they can react with reduced thiols to form nitrosothiols, which are thought to be important in microbial killing (112).

A common perception of gastrointestinal host defence to pathogens ingested with food and water is that it depends entirely on immune factors secreted in the saliva and gastric acidity itself. However, for many gastrointestinal pathogens such as *Campylobacter*, *Shigella*, and *Salmonella*, even prolonged immersion in strong acid at pH 2, to emulate the normal fasting stomach, exerts only a bacteriostatic effect (104). Failure to kill these organisms means that viable pathogens would pass to the small intestine if the defence depended on acid alone. Salivary and gastric nitrites, converted to reactive nitrogen compounds under acidic conditions, may enhance the killing of pathogens in the stomach (103, 104, 283). An *in vitro* study (283) demonstrated that normal stomach acidity in combination with physiological concentrations of nitrite are required to kill *Clostridium difficile* spores that were not killed in acidic buffers or gastric content; moreover, nitrite enhances the killing of several nosocominal pathogens, including vancomycin-resistant Enterococcus spp., methicillin-resistant *Staphylococcus aureus*, and *Candida glabrata* (283). These data suggest that interventions to limit the overuse of acid-suppressive medications could potentially have an impact on multiple pathogens. For example, supplementing the diets of hospitalized patients with nitrates could bolster gastric defenses by increasing levels of acidified nitrite (103, 104).

Recent data (226) suggest that the nitrite could be used in the treatment of chronic bacterial infections caused by opportunistic pathogens such as *P. aeruginosa*, *S. aureus*, and *Burkholderia capacia* in the airways of CF patients. The most dangerous form of *P. aeruginosa* is the mucoid *P. aeruginosa* characterized by a mutation within the *mucA* gene and consequently by the overproduction of alginate, an exopolysaccharide that inhibits the diffusion of O_2 and antibiotics. As previously mentioned, mucoid *P. aeruginosa* biofilms are inherently resistant to antibiotics (134) and phagocytic neutrophils (48). Acidified nitrite ($\sim$15 mM) kills the mucoid form of *P. aeruginosa* (370), inhibits nonmucoid planktonic *P. aeruginosa* PAO1, and kills *S. aureus* and, unexpectedly, planktonic and biofilm communities of *Burkolderia cepacia* (226). Although the concentration of acidified nitrite necessary for the antimicrobial effect is quite high, it is worth mentioning that 10 to 40 mg/kg of acidified nitrite are typically used in the cure of meat products (308), suggesting that humans have a high tolerance for nitrite, as discussed above. Therefore, acidified nitrite could be used for the clinical treatment of CF patients with lung infections.

The acidified nitrite antimicrobial activity is also effective on nosocomial mycoses (8) that represent an increasing problem among critical care patients (193). The susceptibility of *Candida albicans*, *Candida glabrata*, *Candida tropicalis*, *Cryptococcus neoformans*, *Aspergillus fumigatus*, and a *Rhodotorula* species; the lack of induction of resistance; and the possibility of a direct aerosol administration of acidified nitrite (8) provide a novel potential method for treating fungal infections.

Effective antimicrobial strategies are also important in industrial settings, including food processing environment, water treatment, and contact lens industry. One of the most used antimicrobial agents in disinfection processes is the oxidizing agent H_2O_2, which causes microbial death by protein denaturation (125). However, the antimicrobial efficacy of H_2O_2 can be significantly enhanced by addition of acidified nitrite (142). This strategy could find an application in disinfection of contact lenses that are a main predisposing factor of blinding keratitis caused by the highly resistant *Acanthamoeba* spp. (147, 282). H_2O_2 (3%) used as a contact lens disinfectant is effective against *Acanthamoeba* cysts, but an exposure time of at least 4–6 h (157) and/or extensive neutralization are required before use of the contact lenses. On the other hand, if sodium nitrite is added to a 3% (v/v) H_2O_2 solution in one-step systems, significant killing of *Acanthamoeba* cysts is rapidly obtained (157).

VI. Conclusions and Open Questions

It is widely accepted nowadays that nitrite is a biologically relevant molecule: in bacteria, it may function as a terminal acceptor in electron transport chains and it may act as a key signal in many host–pathogen interactions, by producing NO. The role and biological fate of nitrite in humans is also closely interwoven with the homeostasis of NO (Fig. 13). Nitrite is not only an endocrine reservoir of NO under hypoxic conditions, but also an O_2-dependent treasure house of NO [see also (80)].

In mammals, a wide variety of proteins are able to act as NiR both *in vitro* and *in vivo*. It is possible that more proteins will be identified in the near future, which may accomplish the moonlighting function of NiR under O_2 shortage conditions. We propose that this redundancy is not fortuitous for several

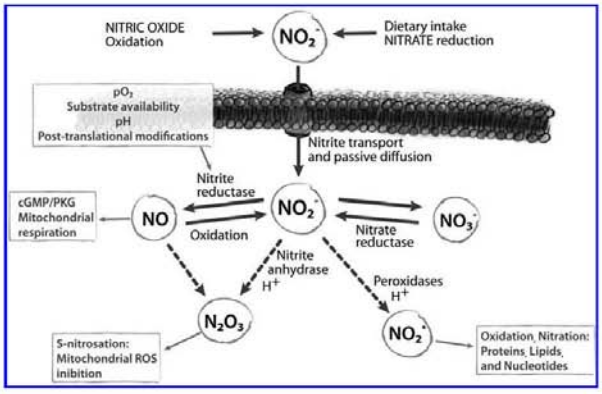

FIG. 13. Summary of the physiological functions of nitrite. The figure describes the fate of nitrite (produced from dietary nitrate or from NO oxidation) after its intake in the cells. Nitrite enters the cell following an electrochemical/concentration gradient, through either a channel and/or as nitrous acid (350), depending on the physiological request. Several enzymes are involved in nitrite reduction and the different species produced (NO or other reactive nitrogen species) could mediate acute and/or chronic effects of endogenous and therapeutic nitrite. Figure modified with permission from (349).

reasons. First of all, it may be considered an inheritance of a preaerobic past where N-oxides were available as terminal electron acceptors to produce energy (82, 114); second, it may represent an inherent property of the eukaryotic cell, which has several rescue pathways to escape harmful conditions such as O_2 depletion and redox unbalance.

It is very intriguing to notice that, in the bacterial kingdom, the heme-containing NiR mostly use specialized porphyrins, such as heme d_1, to avoid trapping of the enzyme in an irreversibly inhibited NO complex, thus escaping the kinetic trap faced by mammalian hemoproteins such as Hb and Mb. Indeed, a major conundrum on to the relevance of these hemoproteins, expecially Hb, in the nitrite/NO homeostasis is still the question of how the NO molecule can escape the trap of ferrous hemes. A recent mass spectrometry study has confirmed that, after addition of millimolar levels of nitrite to suspensions of deoxygenated red cells, no significant accumulation of extracellular NO can be monitored; these data support the hypothesis that the autocapture of NO by deoxyHb precludes efflux of NO from the erythrocyte (234). As recently suggested by other authors (349), it would be helpful to find an experimental setup able to uncouple the effect on the Hb/nitrite system from the effect on the intrinsic NO homeostasis within the erythrocyte.

The capability of Mb to reduce nitrite and its role in cytoprotection under hypoxic conditions is well established. Many experiments can still be planned on six-coordinate globins or on cytochromes: these hemoproteins may well serve the intriguing function of redox-controlled NiR, as recently suggested (22, 330), after switching their heme coordination from six- to five-coordinate.

Another important issue to be investigated in detail is the mechanism of nitrite transport across the cell membrane. Whereas this topic is well studied in bacteria [see (240)], the literature data on eukaryotic cells are mainly restricted to the erythrocyte, where the transport mechanism seems to involve both NO_2^- diffusion (possibly employing the anion exchanger AE1) and HNO_2 diffusion (109, 171, 350). To assess the uptake rate of nitrite, more data on the mechanism of transport across the membrane of other cell types would therefore be highly desirable, in particular to identify O_2-regulated processes.

In conclusion, evaluation of the contribution of blood-based and tissue-based nitrite reduction as a source of NO bioactivity seems to indicate that the tissue sources may play a more important role. A recent theoretical analysis of NO and O_2 transport around an arteriole, including superoxide generation and NiR activity in blood and tissue, confirms that NiR activity in blood should not be a very effective mechanism for conserving NO due to the strong scavenging activity of deoxyHb (46). These authors suggest that the NiR activity in tissue is much more effective in increasing NO bioavailability in the vascular wall and contributes progressively more NO as tissue hypoxia becomes more severe.

Finally, nitrite-based therapy has received a growing attention in the last years: several clinical trials are ongoing or planned in the next future [see *e.g.*, (278)]. Nitrite is a molecule that naturally occurs in the human body in blood and tissues (in nanomolar or micromolar concentrations, respectivey); this confers a great advantage to nitrite-based therapy, which is safer than other strategies employing organic nitrates or NO donors. However, the interaction of therapeutic nitrite with other drugs is still poorly understood and this aspect will require further studies to assess possible toxic effects.

The variability of nitrite administration protocols, nitrite uptake rates, and final biological effects suggests that an effective nitrite therapy will require personalized protocols on the basis of the pathology and individual patient, considering also gender and race. Interestingly, even though further studies are needed, it was recently suggested that dietary nitrate may be as effective as nitrite administration for long-term therapy (214) and that it is also able to influence basal cell functions [such as mitochondrial activity (198)].

Acknowledgments

Funds from the Ministero della Università e Ricerca of Italy [RBRN07BMCT, 20094BJ9R7], from the Sapienza University

of Rome, and from Fondazione Italiana Fibrosi Cistica to F.C. are gratefully acknowledged.

References

1. Aamand R, Dalsgaard T, Jensen FB, Simonsen U, Roepstorff A, and Fago A. Generation of nitric oxide from nitrite by carbonic anhydrase: a possible link between metabolic activity and vasodilation. *Am J Physiol Heart Circ Physiol* 297: H2068–H2074, 2009.
2. Adman ET, Godden JW, and Turley S. The structure of copper-nitrite reductase from *Achromobacter cycloclastes* at five pH values, with NO2- bound and with type II copper depleted. *J Biol Chem* 270: 27458–27474, 1995.
3. Allen JD, Miller EM, Schwark E, Robbins JL, Duscha BD, and Annex BH. Plasma nitrite response and arterial reactivity differentiate vascular health and performance. *Nitric Oxide* 20: 231–237, 2009.
4. Allen JW, Barker PD, Daltrop O, Stevens JM, Tomlinson EJ, Sinha N, Sambongi Y, and Ferguson SJ. Why isn't 'standard' heme good enough for c-type and d1-type cytochromes? *Dalton Trans* 7: 3410–3418, 2005.
5. Alvarez S, Valdez LB, Zaobornyj T, and Boveris A. Oxygen dependence of mitochondrial nitric oxide synthase activity. *Biochem Biophys Res Commun* 305: 771–775, 2003.
6. Alvarez-Ortega C and Harwood CS. Responses of *Pseudomonas aeruginosa* to low oxygen indicate that growth in the cystic fibrosis lung is by aerobic respiration. *Mol Microbiol* 65: 153–165, 2007.
7. Antonyuk SV, Strange RW, Sawers G, Eady RR, and Hasnain SS. Atomic resolution structures of resting-state, substrate- and product-complexed Cu-nitrite reductase provide insight into catalytic mechanism. *Proc Natl Acad Sci U S A* 102: 12041–12046, 2005.
8. Anyim M, Benjamin N, and Wilks M. Acidified nitrite as a potential antifungal agent. *Int J Antimicrob Agents* 26: 85–87, 2005.
9. Arnelle DR and Stamler JS. NO+, NO, and NO- donation by S-nitrosothiols: implications for regulation of physiological functions by S-nitrosylation and acceleration of disulfide formation. *Arch Biochem Biophys* 318: 279–285, 1995.
10. Aspholm M, Aas FE, Harrison OB, Quinn D, Vik A, Viburiene R, Tonjum T, Moir J, Maiden MC, and Koomey M. Structural alterations in a component of cytochrome c oxidase and molecular evolution of pathogenic *Neisseria* in humans. *PLoS Pathog* 6: e1001055, 2010.
11. Averill BA. Dissimilatory nitrite and nitric oxide reductases. *Chem Rev* 96: 2951–2964, 1996.
12. Baek SH, Rajashekara G, Splitter GA, and Shapleigh JP. Denitrification genes regulate *Brucella* virulence in mice. *J Bacteriol* 186: 6025–6031, 2004.
13. Baker JE, Su J, Fu X, Hsu A, Gross GJ, Tweddell JS, and Hogg N. Nitrite confers protection against myocardial infarction: role of xanthine oxidoreductase, NADPH oxidase and K(ATP) channels. *J Mol Cell Cardiol* 43: 437–444, 2007.
14. Ball KA, Castello PR, and Poyton RO. Low intensity light stimulates nitrite-dependent nitric oxide synthesis but not oxygen consumption by cytochrome c oxidase: implications for phototherapy. *J Photochem Photobiol B* 102: 182–191, 2011.
15. Barraud N, Hassett DJ, Hwang SH, Rice SA, Kjelleberg S, and Webb JS. Involvement of nitric oxide in biofilm dispersal of *Pseudomonas aeruginosa*. *J Bacteriol* 188: 7344–7353, 2006.
16. Barrett ML, Harris RL, Antonyuk S, Hough MA, Ellis MJ, Sawers G, Eady RR, and Hasnain SS. Insights into redox partner interactions and substrate binding in nitrite reductase from Alcaligenes xylosoxidans: crystal structures of the Trp138His and His313Gln mutants. *Biochemistry* 43: 16311–16319, 2004.
17. Barth KR, Isabella VM, and Clark VL. Biochemical and genomic analysis of the denitrification pathway within the genus *Neisseria*. *Microbiology* 155: 4093–4103, 2009.
18. Bartholomew B and Hill MJ. The pharmacology of dietary nitrate and the origin of urinary nitrate. *Food Chem Toxicol* 22: 789–795, 1984.
19. Bartsch H, Ohshima H, and Pignatelli B. Inhibitors of endogenous nitrosation. Mechanisms and implications in human cancer prevention. *Mutat Res* 202: 307–324, 1988.
20. Bartsch H, Ohshima H, Pignatelli B, and Calmels S. Endogenously formed N-nitroso compounds and nitrosating agents in human cancer etiology. *Pharmacogenetics* 2: 272–277, 1992.
21. Basireddy M, Isbell TS, Teng X, Patel RP, and Agarwal A. Effects of sodium nitrite on ischemia-reperfusion injury in the rat kidney. *Am J Physiol Renal Physiol* 290: F779–F786, 2006.
22. Basu S, Azarova NA, Font MD, King SB, Hogg N, Gladwin MT, Shiva S, and Kim-Shapiro DB. Nitrite reductase activity of cytochrome *c*. *J Biol Chem* 283: 32590–32597, 2008.
23. Basu S, Grubina R, Huang J, Conradie J, Huang Z, Jeffers A, Jiang A, He X, Azarov I, Seibert R, Mehta A, Patel R, King SB, Hogg N, Ghosh A, Gladwin MT, and Kim-Shapiro DB. Catalytic generation of N2O3 by the concerted nitrite reductase and anhydrase activity of hemoglobin. *Nat Chem Biol* 3: 785–794, 2007.
24. Becker LB, vanden Hoek TL, Shao ZH, Li CQ, and Schumacker PT. Generation of superoxide in cardiomyocytes during ischemia before reperfusion. *Am J Physiol* 277: H2240–H2246, 1999.
25. Beckman JS and Koppenol WH. Nitric oxide, superoxide, and peroxynitrite: the good, the bad, and ugly. *Am J Physiol* 271: C1424–C1437, 1996.
26. Beedham C. Molybdenum hydroxylases: biological distribution and substrate-inhibitor specificity. *Prog Med Chem* 24: 85–127, 1987.
27. Benjamin N, O'Driscoll F, Dougall H, Duncan C, Smith L, Golden M, and McKenzie H. Stomach NO synthesis. *Nature* 368: 502, 1994.
28. Bjorne H, Govoni M, Tornberg DC, Lundberg JO, and Weitzberg E. Intragastric nitric oxide is abolished in intubated patients and restored by nitrite. *Crit Care Med* 33: 1722–1727, 2005.
29. Blood AB, Schroeder HJ, Terry MH, Merrill-Henry J, Bragg SL, Vrancken K, Liu T, Herring JL, Sowers LC, Wilson SM, and Power GG. Inhaled nitrite reverses hemolysis-induced pulmonary vasoconstriction in newborn lambs without blood participation. *Circulation* 123: 605–612, 2011.
30. Blood AB, Tiso M, Verma ST, Lo J, Joshi MS, Azarov I, Longo LD, Gladwin MT, Kim-Shapiro DB, and Power GG. Increased nitrite reductase activity of fetal versus adult ovine hemoglobin. *Am J Physiol Heart Circ Physiol* 296: H237–H246, 2009.
31. Boger RH, Bode-Boger SM, Thiele W, Junker W, Alexander K, and Frolich JC. Biochemical evidence for impaired nitric oxide synthesis in patients with peripheral arterial occlusive disease. *Circulation* 95: 2068–2074, 1997.
32. Bolli R. Preconditioning: a paradigm shift in the biology of myocardial ischemia. *Am J Physiol Heart Circ Physiol* 292: H19–H27, 2007.

33. Bolli R, Dawn B, Tang XL, Qiu Y, Ping P, Xuan YT, Jones WK, Takano H, Guo Y, and Zhang J. The nitric oxide hypothesis of late preconditioning. *Basic Res Cardiol* 93: 325–338, 1998.
34. Boulanger MJ and Murphy ME. Crystal structure of the soluble domain of the major anaerobically induced outer membrane protein (AniA) from pathogenic *Neisseria*: a new class of copper-containing nitrite reductases. *J Mol Biol* 315: 1111–1127, 2002.
35. Brondino CD, Romao MJ, Moura I, and Moura JJ. Molybdenum and tungsten enzymes: the xanthine oxidase family. *Curr Opin Chem Biol* 10: 109–114, 2006.
36. Brooks J. The action of nitrite on haemoglobin in the absence of oxygen. *Proc R Soc Med* 123: 368–382, 1937.
37. Brown DA, Chicco AJ, Jew KN, Johnson MS, Lynch JM, Watson PA, and Moore RL. Cardioprotection afforded by chronic exercise is mediated by the sarcolemmal, and not the mitochondrial, isoform of the KATP channel in the rat. *J Physiol* 569: 913–924, 2005.
38. Brown GC and Borutaite V. Inhibition of mitochondrial respiratory complex I by nitric oxide, peroxynitrite and S-nitrosothiols. *Biochim Biophys Acta* 1658: 44–49, 2004.
39. Brunori M. Nitric oxide, cytochrome-c oxidase and myoglobin. *Trends Biochem Sci* 26: 21–23, 2001.
40. Brunori M, Giuffre A, Forte E, Mastronicola D, Barone MC, and Sarti P. Control of cytochrome *c* oxidase activity by nitric oxide. *Biochim Biophys Acta* 1655: 365–371, 2004.
41. Brunori M and Vallone B. A globin for the brain. *FASEB J* 20: 2192–2197, 2006.
42. Bryan NS. Nitrite in nitric oxide biology: cause or consequence? A systems-based review. *Free Radic Biol Med* 41: 691–701, 2006.
43. Bryan NS, Fernandez BO, Bauer SM, Garcia-Saura MF, Milsom AB, Rassaf T, Maloney RE, Bharti A, Rodriguez J, and Feelisch M. Nitrite is a signaling molecule and regulator of gene expression in mammalian tissues. *Nat Chem Biol* 1: 290–297, 2005.
44. Bryan NS, Rassaf T, Maloney RE, Rodriguez CM, Saijo F, Rodriguez JR, and Feelisch M. Cellular targets and mechanisms of nitros(yl)ation: an insight into their nature and kinetics *in vivo*. *Proc Natl Acad Sci U S A* 101: 4308–4313, 2004.
45. Bryers JD. Medical biofilms. *Biotechnol Bioeng* 100: 1–18, 2008.
46. Buerk DG, Barbee KA, and Jaron D. Modeling O2-dependent effects of nitrite reductase activity in blood and tissue on coupled NO and O2 transport around arterioles. *Adv Exp Med Biol* 701: 271–276, 2011.
47. Burwell LS, Nadtochiy SM, Tompkins AJ, Young S, and Brookes PS. Direct evidence for S-nitrosation of mitochondrial complex I. *Biochem J* 394: 627–634, 2006.
48. Cabral DA, Loh BA, and Speert DP. Mucoid *Pseudomonas aeruginosa* resists nonopsonic phagocytosis by human neutrophils and macrophages. *Pediatr Res* 22: 429–431, 1987.
49. Cabrales P, Han G, Roche C, Nacharaju P, Friedman AJ, and Friedman JM. Sustained release nitric oxide from long-lived circulating nanoparticles. *Free Radic Biol Med* 49: 530–538, 2010.
50. Calvert JW and Lefer DJ. Clinical translation of nitrite therapy for cardiovascular diseases. *Nitric Oxide* 22: 91–97, 2010.
51. Calvert JW and Lefer DJ. Myocardial protection by nitrite. *Cardiovasc Res* 83: 195–203, 2009.
52. Camp NE. Methemoglobinemia. *J Emerg Nurs* 33: 172–174, 2007.
53. Cantu-Medellin N, Vitturi DA, Rodriguez C, Murphy S, Dorman S, Shiva S, Zhou Y, Jia Y, Palmer AF, and Patel RP. Effects of T- and R-state stabilization on deoxyhemoglobin-nitrite reactions and stimulation of nitric oxide signaling. *Nitric Oxide* 25: 59–69, 2011.
54. Cardinale JA and Clark VL. Expression of AniA, the major anaerobically induced outer membrane protein of *Neisseria gonorrhoeae*, provides protection against killing by normal human sera. *Infect Immun* 68: 4368–4369, 2000.
55. Carlstrom M, Larsen FJ, Nystrom T, Hezel M, Borniquel S, Weitzberg E, and Lundberg JO. Dietary inorganic nitrate reverses features of metabolic syndrome in endothelial nitric oxide synthase-deficient mice. *Proc Natl Acad Sci U S A* 107: 17716–17720, 2010.
56. Carlstrom M, Persson AE, Larsson E, Hezel M, Scheffer PG, Teerlink T, Weitzberg E, and Lundberg JO. Dietary nitrate attenuates oxidative stress, prevents cardiac and renal injuries, and reduces blood pressure in salt-induced hypertension. *Cardiovasc Res* 89: 574–585, 2011.
57. Carreau A, Hafny-Rahbi BE, Matejuk A, Grillon C, and Kieda C. Why is the partial oxygen pressure of human tissues a crucial parameter? Small molecules and hypoxia. *J Cell Mol Med* 15: 1239–1253, 2011.
58. Casey DB, Badejo AM, Jr., Dhaliwal JS, Murthy SN, Hyman AL, Nossaman BD, and Kadowitz PJ. Pulmonary vasodilator responses to sodium nitrite are mediated by an allopurinol-sensitive mechanism in the rat. *Am J Physiol Heart Circ Physiol* 296: H524–H533, 2009.
59. Cassens RG, Ito I, Lee M, and Buege D. The use of nitrite in meat. *Bioscience* 28: 633–637, 1978.
60. Castello PR, David PS, McClure T, Crook Z, and Poyton RO. Mitochondrial cytochrome oxidase produces nitric oxide under hypoxic conditions: implications for oxygen sensing and hypoxic signaling in eukaryotes. *Cell Metab* 3: 277–287, 2006.
61. Castello PR, Woo DK, Ball K, Wojcik J, Liu L, and Poyton RO. Oxygen-regulated isoforms of cytochrome *c* oxidase have differential effects on its nitric oxide production and on hypoxic signaling. *Proc Natl Acad Sci U S A* 105: 8203–8208, 2008.
62. Chen YR, Chen CL, Liu X, Li H, Zweier JL, and Mason RP. Involvement of protein radical, protein aggregation, and effects on NO metabolism in the hypochlorite-mediated oxidation of mitochondrial cytochrome c. *Free Radic Biol Med* 37: 1591–1603, 2004.
63. Chen Z, Zhang J, and Stamler JS. Identification of the enzymatic mechanism of nitroglycerin bioactivation. *Proc Natl Acad Sci U S A* 99: 8306–8311, 2002.
64. Cheng L, Powell DR, Khan MA, and Richter-Addo GB. The first unambiguous determination of a nitrosyl-to-nitrite conversion in an iron nitrosyl porphyrin. *Chem Commun* 2301–2302, 2000.
65. Chung GT, Yoo JS, Oh HB, Lee YS, Cha SH, Kim SJ, and Yoo CK. Complete genome sequence of *Neisseria gonorrhoeae* NCCP11945. *J Bacteriol* 190: 6035–6036, 2008.
66. Clark V, Isabella VM, Barth K, and Overton T. Regulation and function of the Neisserial denitrification pathway: life with limited oxygen. In: *Neisseria: Molecular Mechanisms of Pathogenesis*, edited by CGaL W. Norwich, UK: Horizon Scientific Press, 2009, pp. 19–37.
67. Clark VL, Knapp JS, Thompson S, and Klimpel KW. Presence of antibodies to the major anaerobically induced gonococcal outer membrane protein in sera from patients with gonococcal infections. *Microb Pathog* 5: 381–390, 1988.

68. Clementi E, Brown GC, Feelisch M, and Moncada S. Persistent inhibition of cell respiration by nitric oxide: crucial role of S-nitrosylation of mitochondrial complex I and protective action of glutathione. *Proc Natl Acad Sci U S A* 95: 7631–7636, 1998.
69. Cole ST, Brosch R, Parkhill J, Garnier T, Churcher C, Harris D, Gordon SV, Eiglmeier K, Gas S, Barry CE, 3rd, Tekaia F, Badcock K, Basham D, Brown D, Chillingworth T, Connor R, Davies R, Devlin K, Feltwell T, Gentles S, Hamlin N, Holroyd S, Hornsby T, Jagels K, Krogh A, McLean J, Moule S, Murphy L, Oliver K, Osborne J, Quail MA, Rajandream MA, Rogers J, Rutter S, Seeger K, Skelton J, Squares R, Squares S, Sulston JE, Taylor K, Whitehead S, and Barrell BG. Deciphering the biology of *Mycobacterium tuberculosis* from the complete genome sequence. *Nature* 393: 537–544, 1998.
70. Comly HH. Cyanosis in infants caused by nitrates in well water. *J Am Med Assoc* 129: 112–116, 1945.
71. Cooke JP. NO and angiogenesis. *Atheroscler Suppl* 4: 53–60, 2003.
72. Cooper CE and Brown GC. The inhibition of mitochondrial cytochrome oxidase by the gases carbon monoxide, nitric oxide, hydrogen cyanide and hydrogen sulfide: chemical mechanism and physiological significance. *J Bioenerg Biomembr* 40: 533–539, 2008.
73. Copeland DM, Soares AS, West AH, and Richter-Addo GB. Crystal structures of the nitrite and nitric oxide complexes of horse heart myoglobin. *J Inorg Biochem* 100: 1413–1425, 2006.
74. Cosby K, Partovi KS, Crawford JH, Patel RP, Reiter CD, Martyr S, Yang BK, Waclawiw MA, Zalos G, Xu X, Huang KT, Shields H, Kim-Shapiro DB, Schechter AN, Cannon RO, 3rd, and Gladwin MT. Nitrite reduction to nitric oxide by deoxyhemoglobin vasodilates the human circulation. *Nat Med* 9: 1498–1505, 2003.
75. Cossins A and Berenbrink M. Myoglobin's new clothes. *Nature* 454: 416–417, 2008.
76. Crane BR, Siegel LM, and Getzoff ED. Probing the catalytic mechanism of sulfite reductase by X-ray crystallography: structures of the *Escherichia coli* hemoprotein in complex with substrates, inhibitors, intermediates, and products. *Biochemistry* 36: 12120–12137, 1997.
77. Crawford JH, Isbell TS, Huang Z, Shiva S, Chacko BK, Schechter AN, Darley-Usmar VM, Kerby JD, Lang JD, Jr., Kraus D, Ho C, Gladwin MT, and Patel RP. Hypoxia, red blood cells, and nitrite regulate NO-dependent hypoxic vasodilation. *Blood* 107: 566–574, 2006.
78. Creagh-Brown BC, Griffiths MJ, and Evans TW. Bench-to-bedside review: Inhaled nitric oxide therapy in adults. *Crit Care* 13: 221, 2009.
79. Crosswhite P and Sun Z. Nitric oxide, oxidative stress and inflammation in pulmonary arterial hypertension. *J Hypertens* 28: 201–212, 2010.
80. Curtis E, Hsu LL, Noguchi A, Geary L, and Shiva S. Oxygen regulates tissue nitrite metabolism. *Antioxid Redox Signal* 2012 [Epub ahead of print]; DOI: 10.1089/ars.2011.4242.
81. Cutruzzolà F, Brown K, Wilson EK, Bellelli A, Arese M, Tegoni M, Cambillau C, and Brunori M. The nitrite reductase from *Pseudomonas aeruginosa*: essential role of two active-site histidines in the catalytic and structural properties. *Proc Natl Acad Sci U S A* 98: 2232–2237, 2001.
82. Cutruzzolà F, Rinaldo S, Castiglione N, Giardina G, Pecht I, and Brunori M. Nitrite reduction: a ubiquitous function from a pre-aerobic past. *Bioessays* 31: 885–891, 2009.
83. da Silva G, Kennedy EM, and Dlugogorski BZ. Ab initio procedure for aqueous-phase pKa calculation: the acidity of nitrous acid. *J Phys Chem A* 110: 11371–11376, 2006.
84. Dace DS, Khan AA, Kelly J, and Apte RS. Interleukin-10 promotes pathological angiogenesis by regulating macrophage response to hypoxia during development. *PLoS One* 3: e3381, 2008.
85. Daiber A, Schildknecht S, Muller J, Kamuf J, Bachschmid MM, and Ullrich V. Chemical model systems for cellular nitros(yl)ation reactions. *Free Radic Biol Med* 47: 458–467, 2009.
86. Dejam A, Hunter CJ, Pelletier MM, Hsu LL, Machado RF, Shiva S, Power GG, Kelm M, Gladwin MT, and Schechter AN. Erythrocytes are the major intravascular storage sites of nitrite in human blood. *Blood* 106: 734–739, 2005.
87. Dejam A, Hunter CJ, Tremonti C, Pluta RM, Hon YY, Grimes G, Partovi K, Pelletier MM, Oldfield EH, Cannon RO, 3rd, Schechter AN, and Gladwin MT. Nitrite infusion in humans and nonhuman primates: endocrine effects, pharmacokinetics, and tolerance formation. *Circulation* 116: 1821–1831, 2007.
88. Demoncheaux EA, Higenbottam TW, Foster PJ, Borland CD, Smith AP, Marriott HM, Bee D, Akamine S, and Davies MB. Circulating nitrite anions are a directly acting vasodilator and are donors for nitric oxide. *Clin Sci (Lond)* 102: 77–83, 2002.
89. Deturk WE and Bernheim F. Effects of ammonia, methylamine, and hydroxylamine on the adaptive assimilation of nitrite and nitrate by a Mycobacterium. *J Bacteriol* 75: 691–696, 1958.
90. Deussen A, Brand M, Pexa A, and Weichsel J. Metabolic coronary flow regulation—current concepts. *Basic Res Cardiol* 101: 453–464, 2006.
91. Dezfulian C, Raat N, Shiva S, and Gladwin MT. Role of the anion nitrite in ischemia-reperfusion cytoprotection and therapeutics. *Cardiovasc Res* 75: 327–338, 2007.
92. DiBlasi RM, Myers TR, and Hess DR. Evidence-based clinical practice guideline: inhaled nitric oxide for neonates with acute hypoxic respiratory failure. *Respir Care* 55: 1717–1745, 2010.
93. Dixon M and Thurlow S. Studies on xanthine oxidase: the reduction of nitrates. *Biochem J* 18: 989–992, 1924.
94. Dohar JE, Hebda PA, Veeh R, Awad M, Costerton JW, Hayes J, and Ehrlich GD. Mucosal biofilm formation on middle-ear mucosa in a nonhuman primate model of chronic suppurative otitis media. *Laryngoscope* 115: 1469–1472, 2005.
95. Donahoe WE. Cyanosis in infants with nitrates in drinking water as cause. *Pediatrics* 3: 308–311, 1949.
96. Doyle MP, Herman JG, and Dykstra RL. Autocatalytic oxidation of hemoglobin induced by nitrite: activation and chemical inhibition. *J Free Radic Biol Med* 1: 145–153, 1985.
97. Doyle MP and Hoekstra JW. Oxidation of nitrogen oxides by bound dioxygen in hemoproteins. *J Inorg Biochem* 14: 351–358, 1981.
98. Doyle MP, Pickering RA, Dykstra RL, Nelson CL, and Boyer RF. Involvement of peroxide and superoxide in the oxidation of hemoglobin by nitrite. *Biochem Biophys Res Commun* 105: 127–132, 1982.
99. Driscoll JA, Brody SL, and Kollef MH. The epidemiology, pathogenesis and treatment of *Pseudomonas aeruginosa* infections. *Drugs* 67: 351–368, 2007.
100. Dufour SP, Patel RP, Brandon A, Teng X, Pearson J, Barker H, Ali L, Yuen AH, Smolenski RT, and Gonzalez-Alonso J. Erythrocyte-dependent regulation of human skeletal muscle blood flow: role of varied oxyhemoglobin and exercise on nitrite, S-nitrosohemoglobin, and ATP. *Am J Physiol Heart Circ Physiol* 299: H1936–H1946, 2010.

101. Duncan C, Dougall H, Johnston P, Green S, Brogan R, Leifert C, Smith L, Golden M, and Benjamin N. Chemical generation of nitric oxide in the mouth from the enterosalivary circulation of dietary nitrate. *Nat Med* 1: 546–551, 1995.
102. Duranski MR, Greer JJ, Dejam A, Jaganmohan S, Hogg N, Langston W, Patel RP, Yet SF, Wang X, Kevil CG, Gladwin MT, and Lefer DJ. Cytoprotective effects of nitrite during *in vivo* ischemia-reperfusion of the heart and liver. *J Clin Invest* 115: 1232–1240, 2005.
103. Dykhuizen RS, Fraser A, McKenzie H, Golden M, Leifert C, and Benjamin N. *Helicobacter pylori* is killed by nitrite under acidic conditions. *Gut* 42: 334–337, 1998.
104. Dykhuizen RS, Frazer R, Duncan C, Smith CC, Golden M, Benjamin N, and Leifert C. Antimicrobial effect of acidified nitrite on gut pathogens: importance of dietary nitrate in host defense. *Antimicrob Agents Chemother* 40: 1422–1425, 1996.
105. Einsle O, Messerschmidt A, Huber R, Kroneck PM, and Neese F. Mechanism of the six-electron reduction of nitrite to ammonia by cytochrome *c* nitrite reductase. *J Am Chem Soc* 124: 11737–11745, 2002.
106. Elahi MM, Kong YX, and Matata BM. Oxidative stress as a mediator of cardiovascular disease. *Oxid Med Cell Longev* 2: 259–269, 2009.
107. Ellsworth ML, Ellis CG, Goldman D, Stephenson AH, Dietrich HH, and Sprague RS. Erythrocytes: oxygen sensors and modulators of vascular tone. *Physiology (Bethesda)* 24: 107–116, 2009.
108. Enroth C, Eger BT, Okamoto K, Nishino T, and Pai EF. Crystal structures of bovine milk xanthine dehydrogenase and xanthine oxidase: structure-based mechanism of conversion. *Proc Natl Acad Sci U S A* 97: 10723–10728, 2000.
109. Fago A and Jensen FB. The role of blood nitrite in the control of hypoxic vasodilation. In: *Advances in Experimental Biology, vol 1, Nitric Oxide*, edited by Tota B and Trimmer B. Amsterdam: Elsevier B.V, 2007, pp. 199–212.
110. Falsetta ML, Bair TB, Ku SC, Vanden Hoven RN, Steichen CT, McEwan AG, Jennings MP, and Apicella MA. Transcriptional profiling identifies the metabolic phenotype of gonococcal biofilms. *Infect Immun* 77: 3522–3532, 2009.
111. Falsetta ML, McEwan AG, Jennings MP, and Apicella MA. Anaerobic metabolism occurs in the substratum of gonococcal biofilms and may be sustained in part by nitric oxide. *Infect Immun* 78: 2320–2328, 2010.
112. Fang FC. Perspectives series: host/pathogen interactions. Mechanisms of nitric oxide-related antimicrobial activity. *J Clin Invest* 99: 2818–2825, 1997.
113. Feelisch M, Fernandez BO, Bryan NS, Garcia-Saura MF, Bauer S, Whitlock DR, Ford PC, Janero DR, Rodriguez J, and Ashrafian H. Tissue processing of nitrite in hypoxia: an intricate interplay of nitric oxide-generating and -scavenging systems. *J Biol Chem* 283: 33927–33934, 2008.
114. Feelisch M and Martin JF. The early role of nitric oxide in evolution. *Trends Ecol Evol* 10: 496–499, 1995.
115. Feelisch M, Rassaf T, Mnaimneh S, Singh N, Bryan NS, Jourd'Heuil D, and Kelm M. Concomitant S-, N-, and heme-nitros(yl)ation in biological tissues and fluids: implications for the fate of NO *in vivo*. *FASEB J* 16: 1775–1785, 2002.
116. Fernandez BO, Lorkovic IM, and Ford PC. Nitrite catalyzes reductive nitrosylation of the water-soluble Ferri-Heme model FeIII(TPPS) to FeII(TPPS)(NO). *Inorg Chem* 42: 2–4, 2003.
117. Fernandez ML, Ruiz R, Gonzalez MA, Ramirez-Lorca R, Couto C, Ramos A, Gutierrez-Tous R, Rivera JM, Ruiz A, Real LM, and Grilo A. Association of NOS3 gene with metabolic syndrome in hypertensive patients. *Thromb Haemost* 92: 413–418, 2004.
118. Flogel U, Merx MW, Godecke A, Decking UK, and Schrader J. Myoglobin: a scavenger of bioactive NO. *Proc Natl Acad Sci U S A* 98: 735–740, 2001.
119. Frankenberg N, Moser J, and Jahn D. Bacterial heme biosynthesis and its biotechnological application. *Appl Microbiol Biotechnol* 63: 115–127, 2003.
120. Fridovich I and Handler P. Xanthine oxidase. I. The oxidation of sulfite. *J Biol Chem* 228: 67–76, 1957.
121. Fung HL. Biochemical mechanism of nitroglycerin action and tolerance: is this old mystery solved? *Annu Rev Pharmacol Toxicol* 44: 67–85, 2004.
122. Gago B, Lundberg JO, Barbosa RM, and Laranjinha J. Red wine-dependent reduction of nitrite to nitric oxide in the stomach. *Free Radic Biol Med* 43: 1233–1242, 2007.
123. Garcia-Cardena G, Fan R, Shah V, Sorrentino R, Cirino G, Papapetropoulos A, and Sessa WC. Dynamic activation of endothelial nitric oxide synthase by Hsp90. *Nature* 392: 821–824, 1998.
124. Garcia-Hernandez ML, Hernandez-Pando R, Gariglio P, and Berumen J. Interleukin-10 promotes B16-melanoma growth by inhibition of macrophage functions and induction of tumour and vascular cell proliferation. *Immunology* 105: 231–243, 2002.
125. Gardner J and Peel M. *Introduction to Sterilization and Disinfection*. Melbourne, NY: Churchill Livingstone, 1986.
126. Gennis RB and Stewart V. Respiration. In: *Escherchia coli and Salmonella: Cellular and Molecular Biology, 2nd edition*, edited by others FCNa. Washington, DC: America Society for Microbiology, 1996, pp. 217–261.
127. Gilchrist M, Shore AC, and Benjamin N. Inorganic nitrate and nitrite and control of blood pressure. *Cardiovasc Res* 89: 492–498, 2011.
128. Giustarini D, Dalle-Donne I, Colombo R, Milzani A, and Rossi R. Adaptation of the Griess reaction for detection of nitrite in human plasma. *Free Radic Res* 38: 1235–1240, 2004.
129. Gladwin MT and Kim-Shapiro DB. The functional nitrite reductase activity of the heme-globins. *Blood* 112: 2636–2647, 2008.
130. Gladwin MT, Raat NJ, Shiva S, Dezfulian C, Hogg N, Kim-Shapiro DB, and Patel RP. Nitrite as a vascular endocrine nitric oxide reservoir that contributes to hypoxic signaling, cytoprotection, and vasodilation. *Am J Physiol Heart Circ Physiol* 291: H2026–H2035, 2006.
131. Gladwin MT, Shelhamer JH, Schechter AN, Pease-Fye ME, Waclawiw MA, Panza JA, Ognibene FP, and Cannon RO, 3rd. Role of circulating nitrite and S-nitrosohemoglobin in the regulation of regional blood flow in humans. *Proc Natl Acad Sci U S A* 97: 11482–11487, 2000.
132. Godber BL, Doel JJ, Sapkota GP, Blake DR, Stevens CR, Eisenthal R, and Harrison R. Reduction of nitrite to nitric oxide catalyzed by xanthine oxidoreductase. *J Biol Chem* 275: 7757–7763, 2000.
133. Gonzalez FM, Shiva S, Vincent PS, Ringwood LA, Hsu LY, Hon YY, Aletras AH, Cannon RO, 3rd, Gladwin MT, and Arai AE. Nitrite anion provides potent cytoprotective and antiapoptotic effects as adjunctive therapy to reperfusion for acute myocardial infarction. *Circulation* 117: 2986–2994, 2008.
134. Govan JR and Fyfe JA. Mucoid *Pseudomonas aeruginosa* and cystic fibrosis: resistance of the mucoid from to carbenicillin, flucloxacillin and tobramycin and the isolation of mucoid variants *in vitro*. *J Antimicrob Chemother* 4: 233–240, 1978.

135. Govoni M, Jansson EA, Weitzberg E, and Lundberg JO. The increase in plasma nitrite after a dietary nitrate load is markedly attenuated by an antibacterial mouthwash. *Nitric Oxide* 19: 333–337, 2008.
136. Grubina R, Huang Z, Shiva S, Joshi MS, Azarov I, Basu S, Ringwood LA, Jiang A, Hogg N, Kim-Shapiro DB, and Gladwin MT. Concerted nitric oxide formation and release from the simultaneous reactions of nitrite with deoxy- and oxyhemoglobin. *J Biol Chem* 282: 12916–12927, 2007.
137. Hall-Stoodley L, Costerton JW, and Stoodley P. Bacterial biofilms: from the natural environment to infectious diseases. *Nat Rev Microbiol* 2: 95–108, 2004.
138. Hamdane D, Kiger L, Dewilde S, Green BN, Pesce A, Uzan J, Burmester T, Hankeln T, Bolognesi M, Moens L, and Marden MC. The redox state of the cell regulates the ligand binding affinity of human neuroglobin and cytoglobin. *J Biol Chem* 278: 51713–51721, 2003.
139. Hassett DJ, Cuppoletti J, Trapnell B, Lymar SV, Rowe JJ, Yoon SS, Hilliard GM, Parvatiyar K, Kamani MC, Wozniak DJ, Hwang SH, McDermott TR, and Ochsner UA. Anaerobic metabolism and quorum sensing by *Pseudomonas aeruginosa* biofilms in chronically infected cystic fibrosis airways: rethinking antibiotic treatment strategies and drug targets. *Adv Drug Deliv Rev* 54: 1425–1443, 2002.
140. Hawkins A and Tulloh R. Treatment of pediatric pulmonary hypertension. *Vasc Health Risk Manag* 5: 509–524, 2009.
141. Hearse DJ, Humphrey SM, and Chain EB. Abrupt reoxygenation of the anoxic potassium-arrested perfused rat heart: a study of myocardial enzyme release. *J Mol Cell Cardiol* 5: 395–407, 1973.
142. Heaselgrave W, Andrew PW, and Kilvington S. Acidified nitrite enhances hydrogen peroxide disinfection of Acanthamoeba, bacteria and fungi. *J Antimicrob Chemother* 65: 1207–1214, 2010.
143. Hedgecock LW and Costello RL. Utilization of nitrate by pathogenic and saprophytic mycobacteria. *J Bacteriol* 84: 195–205, 1962.
144. Hendgen-Cotta UB, Flogel U, Kelm M, and Rassaf T. Unmasking the Janus face of myoglobin in health and disease. *J Exp Biol* 213: 2734–2740, 2010.
145. Hendgen-Cotta UB, Merx MW, Shiva S, Schmitz J, Becher S, Klare JP, Steinhoff HJ, Goedecke A, Schrader J, Gladwin MT, Kelm M, and Rassaf T. Nitrite reductase activity of myoglobin regulates respiration and cellular viability in myocardial ischemia-reperfusion injury. *Proc Natl Acad Sci U S A* 105: 10256–10261, 2008.
146. Heurlier K, Thomson MJ, Aziz N, and Moir JW. The nitric oxide (NO)-sensing repressor NsrR of *Neisseria meningitidis* has a compact regulon of genes involved in NO synthesis and detoxification. *J Bacteriol* 190: 2488–2495, 2008.
147. Hieble JP, Bylund DB, Clarke DE, Eikenburg DC, Langer SZ, Lefkowitz RJ, Minneman KP, and Ruffolo RR, Jr. International Union of Pharmacology. X. Recommendation for nomenclature of alpha 1-adrenoceptors: consensus update. *Pharmacol Rev* 47: 267–270, 1995.
148. Hille R. Molybdenum-containing hydroxylases. *Arch Biochem Biophys* 433: 107–116, 2005.
149. Hille R and Nishino T. Flavoprotein structure and mechanism. 4. Xanthine oxidase and xanthine dehydrogenase. *FASEB J* 9: 995–1003, 1995.
150. Hirata Y, Nagata D, Suzuki E, Nishimatsu H, Suzuki J, and Nagai R. Diagnosis and treatment of endothelial dysfunction in cardiovascular disease. *Int Heart J* 51: 1–6, 2010.
151. Hopmann KH, Cardey B, Gladwin MT, Kim-Shapiro DB, and Ghosh A. Hemoglobin as a nitrite anhydrase: modeling methemoglobin-mediated n(2) o(3) formation. *Chemistry* 17: 6348–6358, 2011.
152. Hopper A, Tovell N, and Cole J. A physiologically significant role in nitrite reduction of the CcoP subunit of the cytochrome oxidase cbb3 from *Neisseria gonorrhoeae*. *FEMS Microbiol Lett* 301: 232–240, 2009.
153. Householder TC, Fozo EM, Cardinale JA, and Clark VL. Gonococcal nitric oxide reductase is encoded by a single gene, norB, which is required for anaerobic growth and is induced by nitric oxide. *Infect Immun* 68: 5241–5246, 2000.
154. Huang KT, Keszler A, Patel N, Patel RP, Gladwin MT, Kim-Shapiro DB, and Hogg N. The reaction between nitrite and deoxyhemoglobin. Reassessment of reaction kinetics and stoichiometry. *J Biol Chem* 280: 31126–31131, 2005.
155. Huang L, Borniquel S, and Lundberg JO. Enhanced xanthine oxidoreductase expression and tissue nitrate reduction in germ free mice. *Nitric Oxide* 22: 191–195, 2010.
156. Huang Z, Shiva S, Kim-Shapiro DB, Patel RP, Ringwood LA, Irby CE, Huang KT, Ho C, Hogg N, Schechter AN, and Gladwin MT. Enzymatic function of hemoglobin as a nitrite reductase that produces NO under allosteric control. *J Clin Invest* 115: 2099–2107, 2005.
157. Hughes R and Kilvington S. Comparison of hydrogen peroxide contact lens disinfection systems and solutions against Acanthamoeba polyphaga. *Antimicrob Agents Chemother* 45: 2038–2043, 2001.
158. Hunault CC, van Velzen AG, Sips AJ, Schothorst RC, and Meulenbelt J. Bioavailability of sodium nitrite from an aqueous solution in healthy adults. *Toxicol Lett* 190: 48–53, 2009.
159. Hunter CJ, Dejam A, Blood AB, Shields H, Kim-Shapiro DB, Machado RF, Tarekegn S, Mulla N, Hopper AO, Schechter AN, Power GG, and Gladwin MT. Inhaled nebulized nitrite is a hypoxia-sensitive NO-dependent selective pulmonary vasodilator. *Nat Med* 10: 1122–1127, 2004.
160. Ichinose F, Roberts JD, Jr., and Zapol WM. Inhaled nitric oxide: a selective pulmonary vasodilator: current uses and therapeutic potential. *Circulation* 109: 3106–3111, 2004.
161. Ignarro LJ. After 130 years, the molecular mechanism of action of nitroglycerin is revealed. *Proc Natl Acad Sci U S A* 99: 7816–7817, 2002.
162. Ingram TE, Pinder AG, Bailey DM, Fraser AG, and James PE. Low-dose sodium nitrite vasodilates hypoxic human pulmonary vasculature by a means that is not dependent on a simultaneous elevation in plasma nitrite. *Am J Physiol Heart Circ Physiol* 298: H331–H339, 2010.
163. Isabella V, Wright LF, Barth K, Spence JM, Grogan S, Genco CA, and Clark VL. cis- and trans-acting elements involved in regulation of norB (norZ), the gene encoding nitric oxide reductase in *Neisseria gonorrhoeae*. *Microbiology* 154: 226–239, 2008.
164. Isabella VM, Lapek JD, Jr., Kennedy EM, and Clark VL. Functional analysis of NsrR, a nitric oxide-sensing Rrf2 repressor in *Neisseria gonorrhoeae*. *Mol Microbiol* 71: 227–239, 2009.
165. Jaffe ER. Methemoglobin pathophysiology. *Prog Clin Biol Res* 51: 133–151, 1981.
166. Jafferji A, Allen JW, Ferguson SJ, and Fulop V. X-ray crystallographic study of cyanide binding provides insights into the structure-function relationship for cytochrome cd1 nitrite reductase from *Paracoccus pantotrophus*. *J Biol Chem* 275: 25089–25094, 2000.

167. Jansson EA, Huang L, Malkey R, Govoni M, Nihlen C, Olsson A, Stensdotter M, Petersson J, Holm L, Weitzberg E, and Lundberg JO. A mammalian functional nitrate reductase that regulates nitrite and nitric oxide homeostasis. *Nat Chem Biol* 4: 411–417, 2008.
168. Jaszewski AR, Fann YC, Chen YR, Sato K, Corbett J, and Mason RP. EPR spectroscopy studies on the structural transition of nitrosyl hemoglobin in the arterial-venous cycle of DEANO-treated rats as it relates to the proposed nitrosyl hemoglobin/nitrosothiol hemoglobin exchange. *Free Radic Biol Med* 35: 444–451, 2003.
169. Jeng BH and McLeod SD. Microbial keratitis. *Br J Ophthalmol* 87: 805–806, 2003.
170. Jensen FB. The dual roles of red blood cells in tissue oxygen delivery: oxygen carriers and regulators of local blood flow. *J Exp Biol* 212: 3387–3393, 2009.
171. Jensen FB and Rohde S. Comparative analysis of nitrite uptake and hemoglobin-nitrite reactions in erythrocytes: sorting out uptake mechanisms and oxygenation dependencies. *Am J Physiol Regul Integr Comp Physiol* 298: R972–R982, 2010.
172. Jia L, Bonaventura C, Bonaventura J, and Stamler JS. S-nitrosohaemoglobin: a dynamic activity of blood involved in vascular control. *Nature* 380: 221–226, 1996.
173. Johnson G, 3rd, Tsao PS, Mulloy D, and Lefer AM. Cardioprotective effects of acidified sodium nitrite in myocardial ischemia with reperfusion. *J Pharmacol Exp Ther* 252: 35–41, 1990.
174. Jones SP and Bolli R. The ubiquitous role of nitric oxide in cardioprotection. *J Mol Cell Cardiol* 40: 16–23, 2006.
175. Joshi MS, Ferguson TB, Jr., Han TH, Hyduke DR, Liao JC, Rassaf T, Bryan N, Feelisch M, and Lancaster JR, Jr. Nitric oxide is consumed, rather than conserved, by reaction with oxyhemoglobin under physiological conditions. *Proc Natl Acad Sci U S A* 99: 10341–10346, 2002.
176. Jung KH, Chu K, Ko SY, Lee ST, Sinn DI, Park DK, Kim JM, Song EC, Kim M, and Roh JK. Early intravenous infusion of sodium nitrite protects brain against *in vivo* ischemia-reperfusion injury. *Stroke* 37: 2744–2750, 2006.
177. Jung KH, Chu K, Lee ST, Sunwoo JS, Park DK, Kim JH, Kim S, Lee SK, Kim M, and Roh JK. Effects of long term nitrite therapy on functional recovery in experimental ischemia model. *Biochem Biophys Res Commun* 403: 66–72, 2010.
178. Keefer LK. Progress toward clinical application of the nitric oxide-releasing diazeniumdiolates. *Annu Rev Pharmacol Toxicol* 43: 585–607, 2003.
179. Kenjale AA, Ham KL, Stabler T, Robbins JL, Johnson JL, Vanbruggen M, Privette G, Yim E, Kraus WE, and Allen JD. Dietary nitrate supplementation enhances exercise performance in peripheral arterial disease. *J Appl Physiol* 110: 1582–1591, 2011.
180. Keszler A, Piknova B, Schechter AN, and Hogg N. The reaction between nitrite and oxyhemoglobin: a mechanistic study. *J Biol Chem* 283: 9615–9622, 2008.
181. Kevil CG, Kolluru GK, Pattillo CB, and Giordano T. Inorganic nitrite therapy: historical perspective and future directions. *Free Radic Biol Med* 51: 576–593, 2011.
182. Kharitonov VG, Sharma VS, Magde D, and Koesling D. Kinetics of nitric oxide dissociation from five- and six-coordinate nitrosyl hemes and heme proteins, including soluble guanylate cyclase. *Biochemistry* 36: 6814–6818, 1997.
183. Kharitonov VG, Sundquist AR, and Sharma VS. Kinetics of nitrosation of thiols by nitric oxide in the presence of oxygen. *J Biol Chem* 270: 28158–28164, 1995.
184. Kim-Shapiro DB, Gladwin MT, Patel RP, and Hogg N. The reaction between nitrite and hemoglobin: the role of nitrite in hemoglobin-mediated hypoxic vasodilation. *J Inorg Biochem* 99: 237–246, 2005.
185. Kim-Shapiro DB, Schechter AN, and Gladwin MT. Unraveling the reactions of nitric oxide, nitrite, and hemoglobin in physiology and therapeutics. *Arterioscler Thromb Vasc Biol* 26: 697–705, 2006.
186. Kleinbongard P, Dejam A, Lauer T, Rassaf T, Schindler A, Picker O, Scheeren T, Godecke A, Schrader J, Schulz R, Heusch G, Schaub GA, Bryan NS, Feelisch M, and Kelm M. Plasma nitrite reflects constitutive nitric oxide synthase activity in mammals. *Free Radic Biol Med* 35: 790–796, 2003.
187. Kluge I, Gutteck-Amsler U, Zollinger M, and Do KQ. S-nitrosoglutathione in rat cerebellum: identification and quantification by liquid chromatography-mass spectrometry. *J Neurochem* 69: 2599–2607, 1997.
188. Knapp JS and Clark VL. Anaerobic growth of *Neisseria gonorrhoeae* coupled to nitrite reduction. *Infect Immun* 46: 176–181, 1984.
189. Knekt P, Jarvinen R, Dich J, and Hakulinen T. Risk of colorectal and other gastro-intestinal cancers after exposure to nitrate, nitrite and N-nitroso compounds: a follow-up study. *Int J Cancer* 80: 852–856, 1999.
190. Kosaka H, Imaizumi K, and Tyuma I. Mechanism of autocatalytic oxidation of oxyhemoglobin by nitrite. An intermediate detected by electron spin resonance. *Biochim Biophys Acta* 702: 237–241, 1982.
191. Kozlov AV, Staniek K, and Nohl H. Nitrite reductase activity is a novel function of mammalian mitochondria. *FEBS Lett* 454: 127–130, 1999.
192. Kruh NA, Troudt J, Izzo A, Prenni J, and Dobos KM. Portrait of a pathogen: the *Mycobacterium tuberculosis* proteome *in vivo*. *PLoS One* 5: e13938, 2010.
193. Kullberg BJ and Oude Lashof AM. Epidemiology of opportunistic invasive mycoses. *Eur J Med Res* 7: 183–191, 2002.
194. Kumar D, Branch BG, Pattillo CB, Hood J, Thoma S, Simpson S, Illum S, Arora N, Chidlow JH, Jr., Langston W, Teng X, Lefer DJ, Patel RP, and Kevil CG. Chronic sodium nitrite therapy augments ischemia-induced angiogenesis and arteriogenesis. *Proc Natl Acad Sci U S A* 105: 7540–7545, 2008.
195. Lam CF, Sviri S, Ilett KF, and van Heerden PV. Inhaled diazeniumdiolates (NONOates) as selective pulmonary vasodilators. *Expert Opin Investig Drugs* 11: 897–909, 2002.
196. Lang JD, Jr., Teng X, Chumley P, Crawford JH, Isbell TS, Chacko BK, Liu Y, Jhala N, Crowe DR, Smith AB, Cross RC, Frenette L, Kelley EE, Wilhite DW, Hall CR, Page GP, Fallon MB, Bynon JS, Eckhoff DE, and Patel RP. Inhaled NO accelerates restoration of liver function in adults following orthotopic liver transplantation. *J Clin Invest* 117: 2583–2591, 2007.
197. Larsen FJ, Ekblom B, Sahlin K, Lundberg JO, and Weitzberg E. Effects of dietary nitrate on blood pressure in healthy volunteers. *N Engl J Med* 355: 2792–2793, 2006.
198. Larsen FJ, Schiffer TA, Borniquel S, Sahlin K, Ekblom B, Lundberg JO, and Weitzberg E. Dietary inorganic nitrate improves mitochondrial efficiency in humans. *Cell Metab* 13: 149–159, 2011.
199. Le Cras TD and McMurtry IF. Nitric oxide production in the hypoxic lung. *Am J Physiol Lung Cell Mol Physiol* 280: L575–L582, 2001.
200. Lee C and Harrison WT. The catena-arsenite chain anion, [AsO2](n)(n-): (H3NCH2CH2NH3)0.5[AsO2] and NaAsO2 (revisited). *Acta Crystallogr C* 60: m215–m218, 2004.

201. Lefer DJ. Emerging role of nitrite in myocardial protection. *Arch Pharm Res* 32: 1127–1138, 2009.
202. Lefer DJ. Nitrite therapy for protection against ischemia-reperfusion injury. *Am J Physiol Renal Physiol* 290: F777–F778, 2006.
203. Lehnert N, Cornelissen U, Neese F, Ono T, Noguchi Y, Okamoto K, and Fujisawa K. Synthesis and spectroscopic characterization of copper(II)-nitrito complexes with hydrotris (pyrazolyl)borate and related coligands. *Inorg Chem* 46: 3916–3933, 2007.
204. Li H, Cui H, Kundu TK, Alzawahra W, and Zweier JL. Nitric oxide production from nitrite occurs primarily in tissues not in the blood: critical role of xanthine oxidase and aldehyde oxidase. *J Biol Chem* 283: 17855–17863, 2008.
205. Li H, Kundu TK, and Zweier JL. Characterization of the magnitude and mechanism of aldehyde oxidase-mediated nitric oxide production from nitrite. *J Biol Chem* 284: 33850–33858, 2009.
206. Li H, Liu X, Cui H, Chen YR, Cardounel AJ, and Zweier JL. Characterization of the mechanism of cytochrome P450 reductase-cytochrome P450-mediated nitric oxide and nitrosothiol generation from organic nitrates. *J Biol Chem* 281: 12546–12554, 2006.
207. Li H, Samouilov A, Liu X, and Zweier JL. Characterization of the effects of oxygen on xanthine oxidase-mediated nitric oxide formation. *J Biol Chem* 279: 16939–16946, 2004.
208. Lin JT and Stewart V. Nitrate assimilation by bacteria. *Adv Microb Physiol* 39: 1–30, 1998.
209. Lissi E. Autocatalytic oxidation of hemoglobin by nitrite: a possible mechanism. *Free Radic Biol Med* 24: 1535–1536, 1998.
210. Liu X, Miller MJ, Joshi MS, Thomas DD, and Lancaster JR, Jr. Accelerated reaction of nitric oxide with O2 within the hydrophobic interior of biological membranes. *Proc Natl Acad Sci U S A* 95: 2175–2179, 1998.
211. Low H. Nitroso compounds: safety and public health. *Arch Environ Health* 29: 256–260, 1974.
212. Luchsinger BP, Rich EN, Gow AJ, Williams EM, Stamler JS, and Singel DJ. Routes to S-nitroso-hemoglobin formation with heme redox and preferential reactivity in the beta subunits. *Proc Natl Acad Sci U S A* 100: 461–466, 2003.
213. Lundberg JO, Carlsson S, Engstrand L, Morcos E, Wiklund NP, and Weitzberg E. Urinary nitrite: more than a marker of infection. *Urology* 50: 189–191, 1997.
214. Lundberg JO, Carlstrom M, Larsen FJ, and Weitzberg E. Roles of dietary inorganic nitrate in cardiovascular health and disease. *Cardiovasc Res* 89: 525–532, 2011.
215. Lundberg JO, Gladwin MT, Ahluwalia A, Benjamin N, Bryan NS, Butler A, Cabrales P, Fago A, Feelisch M, Ford PC, Freeman BA, Frenneaux M, Friedman J, Kelm M, Kevil CG, Kim-Shapiro DB, Kozlov AV, Lancaster JR, Jr., Lefer DJ, McColl K, McCurry K, Patel RP, Petersson J, Rassaf T, Reutov VP, Richter-Addo GB, Schechter A, Shiva S, Tsuchiya K, van Faassen EE, Webb AJ, Zuckerbraun BS, Zweier JL, and Weitzberg E. Nitrate and nitrite in biology, nutrition and therapeutics. *Nat Chem Biol* 5: 865–869, 2009.
216. Lundberg JO and Govoni M. Inorganic nitrate is a possible source for systemic generation of nitric oxide. *Free Radic Biol Med* 37: 395–400, 2004.
217. Lundberg JO, Hellstrom PM, Lundberg JM, and Alving K. Greatly increased luminal nitric oxide in ulcerative colitis. *Lancet* 344: 1673–1674, 1994.
218. Lundberg JO and Weitzberg E. NO generation from nitrite and its role in vascular control. *Arterioscler Thromb Vasc Biol* 25: 915–922, 2005.
219. Lundberg JO, Weitzberg E, Cole JA, and Benjamin N. Nitrate, bacteria and human health. *Nat Rev Microbiol* 2: 593–602, 2004.
220. Lundberg JO, Weitzberg E, and Gladwin MT. The nitrate-nitrite-nitric oxide pathway in physiology and therapeutics. *Nat Rev Drug Discov* 7: 156–167, 2008.
221. Lundberg JO, Weitzberg E, Lundberg JM, and Alving K. Intragastric nitric oxide production in humans: measurements in expelled air. *Gut* 35: 1543–1546, 1994.
222. Machha A and Schechter AN. Dietary nitrite and nitrate: a review of potential mechanisms of cardiovascular benefits. *Eur J Nutr* 50: 293–303, 2011.
223. Mack AK, McGowan Ii VR, Tremonti CK, Ackah D, Barnett C, Machado RF, Gladwin MT, and Kato GJ. Sodium nitrite promotes regional blood flow in patients with sickle cell disease: a phase I/II study. *Br J Haematol* 142: 971–978, 2008.
224. Maher AR, Milsom AB, Gunaruwan P, Abozguia K, Ahmed I, Weaver RA, Thomas P, Ashrafian H, Born GV, James PE, and Frenneaux MP. Hypoxic modulation of exogenous nitrite-induced vasodilation in humans. *Circulation* 117: 670–677, 2008.
225. Maia LB and Moura JJ. Nitrite reduction by xanthine oxidase family enzymes: a new class of nitrite reductases. *J Biol Inorg Chem* 16: 443–460, 2011.
226. Major TA, Panmanee W, Mortensen JE, Gray LD, Hoglen N, and Hassett DJ. Sodium nitrite-mediated killing of the major cystic fibrosis pathogens *Pseudomonas aeruginosa*, *Staphylococcus aureus*, and *Burkholderia cepacia* under anaerobic planktonic and biofilm conditions. *Antimicrob Agents Chemother* 54: 4671–4677, 2010.
227. Maley JH, Lasker GF, and Kadowitz PJ. Nitric oxide and disorders of the erythrocyte: emerging roles and therapeutic targets. *Cardiovasc Hematol Disord Drug Targets* 10: 284–291, 2010.
228. Malm S, Tiffert Y, Micklinghoff J, Schultze S, Joost I, Weber I, Horst S, Ackermann B, Schmidt M, Wohlleben W, Ehlers S, Geffers R, Reuther J, and Bange FC. The roles of the nitrate reductase NarGHJI, the nitrite reductase NirBD and the response regulator GlnR in nitrate assimilation of *Mycobacterium tuberculosis*. *Microbiology* 155: 1332–1339, 2009.
229. McKnight GM, Duncan CW, Leifert C, and Golden MH. Dietary nitrate in man: friend or foe? *Br J Nutr* 81: 349–358, 1999.
230. McKnight GM, Smith LM, Drummond RS, Duncan CW, Golden M, and Benjamin N. Chemical synthesis of nitric oxide in the stomach from dietary nitrate in humans. *Gut* 40: 211–214, 1997.
231. Mellies J, Jose J, and Meyer TF. The *Neisseria gonorrhoeae* gene aniA encodes an inducible nitrite reductase. *Mol Gen Genet* 256: 525–532, 1997.
232. Mendel RR and Bittner F. Cell biology of molybdenum. *Biochim Biophys Acta* 1763: 621–635, 2006.
233. Merx MW, Godecke A, Flogel U, and Schrader J. Oxygen supply and nitric oxide scavenging by myoglobin contribute to exercise endurance and cardiac function. *FASEB J* 19: 1015–1017, 2005.
234. Mikulski R, Tu C, Swenson ER, and Silverman DN. Reactions of nitrite in erythrocyte suspensions measured by membrane inlet mass spectrometry. *Free Radic Biol Med* 48: 325–331, 2010.
235. Millar TM, Stevens CR, Benjamin N, Eisenthal R, Harrison R, and Blake DR. Xanthine oxidoreductase catalyses the reduction of nitrates and nitrite to nitric oxide under hypoxic conditions. *FEBS Lett* 427: 225–228, 1998.

236. Millikan GA. Experiments on muscle haemoglobin *in vivo*; the instantaneous measurement of muscle metabolism. *Proc R Soc Lond B* 123: 218–241, 1937.
237. Minamiyama Y, Takemura S, Hai S, Suehiro S, and Okada S. Vitamin E deficiency accelerates nitrate tolerance via a decrease in cardiac P450 expression and increased oxidative stress. *Free Radic Biol Med* 40: 808–816, 2006.
238. Modin A, Bjorne H, Herulf M, Alving K, Weitzberg E, and Lundberg JO. Nitrite-derived nitric oxide: a possible mediator of 'acidic-metabolic' vasodilation. *Acta Physiol Scand* 171: 9–16, 2001.
239. Mohammad A, Ali N, Reza B, and Ali K. Effect of ascorbic acid supplementation on nitric oxide metabolites and systolic blood pressure in rats exposed to lead. *Indian J Pharmacol* 42: 78–81, 2010.
240. Moir JW and Wood NJ. Nitrate and nitrite transport in bacteria. *Cell Mol Life Sci* 58: 215–224, 2001.
241. Moncada S, Palmer RM, and Higgs EA. Nitric oxide: physiology, pathophysiology, and pharmacology. *Pharmacol Rev* 43: 109–142, 1991.
242. Mondoro TH, Ryan BB, Hrinczenko BW, Schechter AN, Vostal JG, and Alayash AI. Biological action of nitric oxide donor compounds on platelets from patients with sickle cell disease. *Br J Haematol* 112: 1048–1054, 2001.
243. Monti LD, Barlassina C, Citterio L, Galluccio E, Berzuini C, Setola E, Valsecchi G, Lucotti P, Pozza G, Bernardinelli L, Casari G, and Piatti P. Endothelial nitric oxide synthase polymorphisms are associated with type 2 diabetes and the insulin resistance syndrome. *Diabetes* 52: 1270–1275, 2003.
244. Montie TC, Doyle-Huntzinger D, Craven RC, and Holder IA. Loss of virulence associated with absence of flagellum in an isogenic mutant of *Pseudomonas aeruginosa* in the burned-mouse model. *Infect Immun* 38: 1296–1298, 1982.
245. Moore EG and Gibson QH. Cooperativity in the dissociation of nitric oxide from hemoglobin. *J Biol Chem* 251: 2788–2794, 1976.
246. Moreau-Marquis S, Stanton BA, and O'Toole GA. *Pseudomonas aeruginosa* biofilm formation in the cystic fibrosis airway. *Pulm Pharmacol Ther* 21: 595–599, 2008.
247. Moriwaki Y, Yamamoto T, Yamaguchi K, Takahashi S, and Higashino K. Immunohistochemical localization of aldehyde and xanthine oxidase in rat tissues using polyclonal antibodies. *Histochem Cell Biol* 105: 71–79, 1996.
248. Murillo D, Kamga C, Mo L, and Shiva S. Nitrite as a mediator of ischemic preconditioning and cytoprotection. *Nitric Oxide* 25: 70–80, 2011.
249. Murphy ME, Turley S, and Adman ET. Structure of nitrite bound to copper-containing nitrite reductase from Alcaligenes faecalis. Mechanistic implications. *J Biol Chem* 272: 28455–28460, 1997.
250. Murry CE, Jennings RB, and Reimer KA. Preconditioning with ischemia: a delay of lethal cell injury in ischemic myocardium. *Circulation* 74: 1124–1136, 1986.
251. Nagababu E, Ramasamy S, Abernethy DR, and Rifkind JM. Active nitric oxide produced in the red cell under hypoxic conditions by deoxyhemoglobin-mediated nitrite reduction. *J Biol Chem* 278: 46349–46356, 2003.
252. Nagababu E, Ramasamy S, and Rifkind JM. S-nitrosohemoglobin: a mechanism for its formation in conjunction with nitrite reduction by deoxyhemoglobin. *Nitric Oxide* 15: 20–29, 2006.
253. Nagasaka Y, Fernandez BO, Garcia-Saura MF, Petersen B, Ichinose F, Bloch KD, Feelisch M, and Zapol WM. Brief periods of nitric oxide inhalation protect against myocardial ischemia-reperfusion injury. *Anesthesiology* 109: 675–682, 2008.
254. Nagata J, Kijima H, Hatanaka H, Tokunaga T, Takagi A, Mine T, Yamazaki H, Nakamura M, and Ueyama Y. Correlation between interleukin 10 and vascular endothelial growth factor expression in human esophageal cancer. *Int J Mol Med* 10: 169–172, 2002.
255. Napoli C, Williams-Ignarro S, de Nigris F, Lerman LO, D'Armiento FP, Crimi E, Byrns RE, Casamassimi A, Lanza A, Gombos F, Sica V, and Ignarro LJ. Physical training and metabolic supplementation reduce spontaneous atherosclerotic plaque rupture and prolong survival in hypercholesterolemic mice. *Proc Natl Acad Sci U S A* 103: 10479–10484, 2006.
256. Naseem KM. The role of nitric oxide in cardiovascular diseases. *Mol Aspects Med* 26: 33–65, 2005.
257. Nasri H, Ellison MK, Shang M, Schulz CE, and Scheidt WR. Variable pi-bonding in iron(II) porphyrinates with nitrite, CO, and tert-butyl isocyanide: characterization of [Fe(T-pivPP)(NO2)(CO)]. *Inorg Chem* 43: 2932–2942, 2004.
258. Norman V and Keith CH. Nitrogen oxides in tobacco smoke. *Nature* 205: 915–916, 1965.
259. Nossaman BD, Akuly HA, Lasker GF, Nossaman VE, Rothberg PA, and Kadowitz PJ. The reemergence of nitrite as a beneficial agent in the treatment of ischemic cardiovascular diseases. *Asian J Exp Biol Sci* 1: 451–459, 2010.
260. Nurizzo D, Cutruzzolà F, Arese M, Bourgeois D, Brunori M, Cambillau C, and Tegoni M. Conformational changes occurring upon reduction and NO binding in nitrite reductase from *Pseudomonas aeruginosa*. *Biochemistry* 37: 13987–13996, 1998.
261. Nurizzo D, Silvestrini MC, Mathieu M, Cutruzzolà F, Bourgeois D, Fülöp V, Hajdu J, Brunori M, Tegoni M, and Cambillau C. N-terminal arm exchange is observed in the 2.15 A crystal structure of oxidized nitrite reductase from *Pseudomonas aeruginosa*. *Structure* 5: 1157–1171, 1997.
262. Ohtake K, Koga M, Uchida H, Sonoda K, Ito J, Uchida M, Natsume H, and Kobayashi J. Oral nitrite ameliorates dextran sulfate sodium-induced acute experimental colitis in mice. *Nitric Oxide* 23: 65–73, 2010.
263. Okayasu I, Hatakeyama S, Yamada M, Ohkusa T, Inagaki Y, and Nakaya R. A novel method in the induction of reliable experimental acute and chronic ulcerative colitis in mice. *Gastroenterology* 98: 694–702, 1990.
264. Oppermann M, Suvorava T, Freudenberger T, Dao VT, Fischer JW, Weber M, and Kojda G. Regulation of vascular guanylyl cyclase by endothelial nitric oxide-dependent posttranslational modification. *Basic Res Cardiol* 106: 539–549, 2011.
265. Pannuru P, Vaddi DR, Kindinti RR, and Varadacharyulu N. Increased erythrocyte antioxidant status protects against smoking induced hemolysis in moderate smokers. *Hum Exp Toxicol* 30: 1475–1481, 2011.
266. Parkhill J, Achtman M, James KD, Bentley SD, Churcher C, Klee SR, Morelli G, Basham D, Brown D, Chillingworth T, Davies RM, Davis P, Devlin K, Feltwell T, Hamlin N, Holroyd S, Jagels K, Leather S, Moule S, Mungall K, Quail MA, Rajandream MA, Rutherford KM, Simmonds M, Skelton J, Whitehead S, Spratt BG, and Barrell BG. Complete DNA sequence of a serogroup A strain of *Neisseria meningitidis* Z2491. *Nature* 404: 502–506, 2000.
267. Pattillo CB, Bir S, Rajaram V, and Kevil CG. Inorganic nitrite and chronic tissue ischaemia: a novel therapeutic modality for peripheral vascular diseases. *Cardiovasc Res* 89: 533–541, 2011.

268. Pattillo CB, Fang K, Pardue S, and Kevil CG. Genome expression profiling and network analysis of nitrite therapy during chronic ischemia: possible mechanisms and interesting molecules. *Nitric Oxide* 22: 168–179, 2010.
269. Pattillo CB, Fang K, Terracciano J, and Kevil CG. Reperfusion of chronic tissue ischemia: nitrite and dipyridamole regulation of innate immune responses. *Ann N Y Acad Sci* 1207: 83–88, 2010.
270. Pennington JAT. Dietary exposure models for nitrates and nitrites. *Food Control* 9: 385–395, 1998.
271. Peri L, Pietraforte D, Scorza G, Napolitano A, Fogliano V, and Minetti M. Apples increase nitric oxide production by human saliva at the acidic pH of the stomach: a new biological function for polyphenols with a catechol group? *Free Radic Biol Med* 39: 668–681, 2005.
272. Perissinotti LL, Marti MA, Doctorovich F, Luque FJ, and Estrin DA. A microscopic study of the deoxyhemoglobin-catalyzed generation of nitric oxide from nitrite anion. *Biochemistry* 47: 9793–9802, 2008.
273. Pesce A, Bolognesi M, Bocedi A, Ascenzi P, Dewilde S, Moens L, Hankeln T, and Burmester T. Neuroglobin and cytoglobin. Fresh blood for the vertebrate globin family. *EMBO Rep* 3: 1146–1151, 2002.
274. Petersson J, Carlstrom M, Schreiber O, Phillipson M, Christoffersson G, Jagare A, Roos S, Jansson EA, Persson AE, Lundberg JO, and Holm L. Gastroprotective and blood pressure lowering effects of dietary nitrate are abolished by an antiseptic mouthwash. *Free Radic Biol Med* 46: 1068–1075, 2009.
275. Phillips L, Toledo AH, Lopez-Neblina F, Anaya-Prado R, and Toledo-Pereyra LH. Nitric oxide mechanism of protection in ischemia and reperfusion injury. *J Invest Surg* 22: 46–55, 2009.
276. Phillips R, Kuijper S, Benjamin N, Wansbrough-Jones M, Wilks M, and Kolk AH. *In vitro* killing of *Mycobacterium ulcerans* by acidified nitrite. *Antimicrob Agents Chemother* 48: 3130–3132, 2004.
277. Piantadosi CA. Regulation of mitochondrial processes by protein S-nitrosylation. *Biochim Biophys Acta* 2011[Epub ahead of print]; DOI: 10.1016/J.BBAGEN.2011.03.008.
278. Pluta RM, Oldfield EH, Bakhtian KD, Fathi AR, Smith RK, Devroom HL, Nahavandi M, Woo S, Figg WD, and Lonser RR. Safety and feasibility of long-term intravenous sodium nitrite infusion in healthy volunteers. *PLoS One* 6: e14504, 2011.
279. Poyton RO and Ball KA. Therapeutic photobiomodulation: nitric oxide and a novel function of mitochondrial cytochrome c oxidase. *Discov Med* 11: 154–159, 2011.
280. Poyton RO, Castello PR, Ball KA, Woo DK, and Pan N. Mitochondria and hypoxic signaling: a new view. *Ann N Y Acad Sci* 1177: 48–56, 2009.
281. Raat NJ, Shiva S, and Gladwin MT. Effects of nitrite on modulating ROS generation following ischemia and reperfusion. *Adv Drug Deliv Rev* 61: 339–350, 2009.
282. Radford CF, Minassian DC, and Dart JK. Acanthamoeba keratitis in England and Wales: incidence, outcome, and risk factors. *Br J Ophthalmol* 86: 536–542, 2002.
283. Rao A, Jump RL, Pultz NJ, Pultz MJ, and Donskey CJ. *In vitro* killing of nosocomial pathogens by acid and acidified nitrite. *Antimicrob Agents Chemother* 50: 3901–3904, 2006.
284. Rassaf T, Bryan NS, Kelm M, and Feelisch M. Concomitant presence of N-nitroso and S-nitroso proteins in human plasma. *Free Radic Biol Med* 33: 1590–1596, 2002.
285. Rassaf T, Flogel U, Drexhage C, Hendgen-Cotta U, Kelm M, and Schrader J. Nitrite reductase function of deoxymyoglobin: oxygen sensor and regulator of cardiac energetics and function. *Circ Res* 100: 1749–1754, 2007.
286. Reiter CD, Wang X, Tanus-Santos JE, Hogg N, Cannon RO, 3rd, Schechter AN, and Gladwin MT. Cell-free hemoglobin limits nitric oxide bioavailability in sickle-cell disease. *Nat Med* 8: 1383–1389, 2002.
287. Rengasamy A and Johns RA. Determination of Km for oxygen of nitric oxide synthase isoforms. *J Pharmacol Exp Ther* 276: 30–33, 1996.
288. Rhodes P, Leone AM, Francis PL, Struthers AD, Moncada S, and Rhodes PM. The L-arginine:nitric oxide pathway is the major source of plasma nitrite in fasted humans. *Biochem Biophys Res Commun* 209: 590–596, 1995.
289. Richter CD, Allen JW, Higham CW, Koppenhofer A, Zajicek RS, Watmough NJ, and Ferguson SJ. Cytochrome cd1, reductive activation and kinetic analysis of a multifunctional respiratory enzyme. *J Biol Chem* 277: 3093–3100, 2002.
290. Rifkind JM, Nagababu E, and Ramasamy S. Nitric oxide redox reactions and red cell biology. *Antioxid Redox Signal* 8: 1193–1203, 2006.
291. Rifkind JM, Nagababu E, and Ramasamy S. The quaternary hemoglobin conformation regulates the formation of the nitrite-induced bioactive intermediate and the dissociation of nitric oxide from this intermediate. *Nitric Oxide* 24: 102–109, 2011.
292. Rinaldo S, Arcovito A, Brunori M, and Cutruzzolà F. Fast dissociation of nitric oxide from ferrous *Pseudomonas aeruginosa* cd1 nitrite reductase. A novel outlook on the catalytic mechanism. *J Biol Chem* 282: 14761–14767, 2007.
293. Rinaldo S, Brunori M, and Cutruzzolà F. Nitrite controls the release of nitric oxide in *Pseudomonas aeruginosa* cd1 nitrite reductase. *Biochem Biophys Res Commun* 363: 662–666, 2007.
294. Rinaldo S, Sam KA, Castiglione N, Stelitano V, Arcovito A, Brunori M, Allen JW, Ferguson SJ, and Cutruzzola F. Observation of fast release of NO from ferrous d haem allows formulation of a unified reaction mechanism for cytochrome cd nitrite reductases. *Biochem J* 435: 217–225, 2011.
295. Rocha BS, Gago B, Barbosa RM, and Laranjinha J. Dietary polyphenols generate nitric oxide from nitrite in the stomach and induce smooth muscle relaxation. *Toxicology* 265: 41–48, 2009.
296. Rocha BS, Gago B, Barbosa RM, Lundberg JO, Radi R, and Laranjinha J. Intragastric nitration by dietary nitrite: implications for modulation of protein and lipid signaling. *Free Radic Biol Med* 52: 693–698, 2012.
297. Rock JD, Mahnane MR, Anjum MF, Shaw JG, Read RC, and Moir JW. The pathogen *Neisseria meningitidis* requires oxygen, but supplements growth by denitrification. Nitrite, nitric oxide and oxygen control respiratory flux at genetic and metabolic levels. *Mol Microbiol* 58: 800–809, 2005.
298. Rodriguez C, Vitturi DA, He J, Vandromme M, Brandon A, Hutchings A, Rue LW, 3rd, Kerby JD, and Patel RP. Sodium nitrite therapy attenuates the hypertensive effects of HBOC-201 via nitrite reduction. *Biochem J* 422: 423–432, 2009.
299. Roy RS and McCord JM. Ischaemia-induced conversion of xanthine dehydrogenase to xanthine oxidase. *Fed Proc* 41: 767–772, 1982.
300. Sakamoto T, Saito H, Tatebe S, Tsujitani S, Ozaki M, Ito H, and Ikeguchi M. Interleukin-10 expression significantly correlates with minor CD8+T-cell infiltration and high microvessel density in patients with gastric cancer. *Int J Cancer* 118: 1909–1914, 2006.
301. Salgado MT, Nagababu E, and Rifkind JM. Quantification of intermediates formed during the reduction of nitrite by deoxyhemoglobin. *J Biol Chem* 284: 12710–12718, 2009.

302. Salhany JM. Reaction of nitrite with human fetal oxyhemoglobin: a model simulation study with implications for blood flow regulation in sickle cell disease (SCD). *Blood Cells Mol Dis* 44: 111–114, 2010.
303. Saltin B. Exercise hyperaemia: magnitude and aspects on regulation in humans. *J Physiol* 583: 819–823, 2007.
304. Samouilov A, Kuppusamy P, and Zweier JL. Evaluation of the magnitude and rate of nitric oxide production from nitrite in biological systems. *Arch Biochem Biophys* 357: 1–7, 1998.
305. Sarkar D, Vallance P, and Harding SE. Nitric oxide: not just a negative inotrope. *Eur J Heart Fail* 3: 527–534, 2001.
306. Sasaki T and Matano K. Formation of nitrite from nitrate at the dorsum linguae. *Journal of the Food Hygiene Society of Japan* 20: 363–369, 1979.
307. Schatlo B, Henning EC, Pluta RM, Latour LL, Golpayegani N, Merrill MJ, Lewin N, Chen Y, and Oldfield EH. Nitrite does not provide additional protection to thrombolysis in a rat model of stroke with delayed reperfusion. *J Cereb Blood Flow Metab* 31: 1335, 2011.
308. Sen NP, Baddoo PA, and Seaman SW. Rapid and sensitive determination of nitrite in foods and biological materials by flow injection or high-performance liquid chromatography with chemiluminescence detection. *J Chromatogr A* 673: 77–84, 1994.
309. Sen NP, Smith DC, and Schwinghamer L. Formation of N-nitrosamines from secondary amines and nitrite in human and animal gastric juice. *Food Cosmet Toxicol* 7: 301–307, 1969.
310. Senthilkumar A, Smith RD, Khitha J, Arora N, Veerareddy S, Langston W, Chidlow JH, Jr., Barlow SC, Teng X, Patel RP, Lefer DJ, and Kevil CG. Sildenafil promotes ischemia-induced angiogenesis through a PKG-dependent pathway. *Arterioscler Thromb Vasc Biol* 27: 1947–1954, 2007.
311. Shiva S, Frizzell S, and Gladwin MT. Nitrite and heme globins: reaction mechanisms and physiological targets. In: *Nitric Oxide: Biology and Pathobiology*, edited by Ignarro LJ. San Diego: Elsevier, 2010, pp. 605–626.
312. Shiva S, Huang Z, Grubina R, Sun J, Ringwood LA, MacArthur PH, Xu X, Murphy E, Darley-Usmar VM, and Gladwin MT. Deoxymyoglobin is a nitrite reductase that generates nitric oxide and regulates mitochondrial respiration. *Circ Res* 100: 654–661, 2007.
313. Shiva S, Sack MN, Greer JJ, Duranski M, Ringwood LA, Burwell L, Wang X, MacArthur PH, Shoja A, Raghavachari N, Calvert JW, Brookes PS, Lefer DJ, and Gladwin MT. Nitrite augments tolerance to ischemia/reperfusion injury via the modulation of mitochondrial electron transfer. *J Exp Med* 204: 2089–2102, 2007.
314. Shiva S, Wang X, Ringwood LA, Xu X, Yuditskaya S, Annavajjhala V, Miyajima H, Hogg N, Harris ZL, and Gladwin MT. Ceruloplasmin is a NO oxidase and nitrite synthase that determines endocrine NO homeostasis. *Nat Chem Biol* 2: 486–493, 2006.
315. Silaghi-Dumitrescu R. Linkage isomerism in nitrite reduction by cytochrome cd1 nitrite reductase. *Inorg Chem* 43: 3715–3718, 2004.
316. Sindler AL, Fleenor BS, Calvert JW, Marshall KD, Zigler ML, Lefer DJ, and Seals DR. Nitrite supplementation reverses vascular endothelial dysfunction and large elastic artery stiffness with aging. *Aging Cell* 10: 429–437, 2011.
317. Sinha SS, Shiva S, and Gladwin MT. Myocardial protection by nitrite: evidence that this reperfusion therapeutic will not be lost in translation. *Trends Cardiovasc Med* 18: 163–172, 2008.
318. Siriussawakul A, Zaky A, and Lang JD. Role of nitric oxide in hepatic ischemia-reperfusion injury. *World J Gastroenterol* 16: 6079–6086, 2010.
319. Snyder LA, Davies JK, Ryan CS, and Saunders NJ. Comparative overview of the genomic and genetic differences between the pathogenic *Neisseria* strains and species. *Plasmid* 54: 191–218, 2005.
320. Spiegelhalder B, Eisenbrand G, and Preussmann R. Influence of dietary nitrate on nitrite content of human saliva: possible relevance to *in vivo* formation of N-nitroso compounds. *Food Cosmet Toxicol* 14: 545–548, 1976.
321. Stamler JS, Jia L, Eu JP, McMahon TJ, Demchenko IT, Bonaventura J, Gernert K, and Piantadosi CA. Blood flow regulation by S-nitrosohemoglobin in the physiological oxygen gradient. *Science* 276: 2034–2037, 1997.
322. Stokes KY, Dugas TR, Tang Y, Garg H, Guidry E, and Bryan NS. Dietary nitrite prevents hypercholesterolemic microvascular inflammation and reverses endothelial dysfunction. *Am J Physiol Heart Circ Physiol* 296: H1281–H1288, 2009.
323. Sun W, Arese M, Brunori M, Nurizzo D, Brown K, Cambillau C, Tegoni M, and Cutruzzolà F. Cyanide binding to cd(1) nitrite reductase from *Pseudomonas aeruginosa*: role of the active-site His369 in ligand stabilization. *Biochem Biophys Res Commun* 291: 1–7, 2002.
324. Suschek CV, Schewe T, Sies H, and Kroncke KD. Nitrite, a naturally occurring precursor of nitric oxide that acts like a 'prodrug'. *Biol Chem* 387: 499–506, 2006.
325. Tan MP, Sequeira P, Lin WW, Phong WY, Cliff P, Ng SH, Lee BH, Camacho L, Schnappinger D, Ehrt S, Dick T, Pethe K, and Alonso S. Nitrate respiration protects hypoxic *Mycobacterium tuberculosis* against acid- and reactive nitrogen species stresses. *PLoS One* 5: e13356, 2010.
326. Tanaka R and Tanaka A. Tetrapyrrole biosynthesis in higher plants. *Annu Rev Plant Biol* 58: 321–346, 2007.
327. Thatcher GR, Nicolescu AC, Bennett BM, and Toader V. Nitrates and NO release: contemporary aspects in biological and medicinal chemistry. *Free Radic Biol Med* 37: 1122–1143, 2004.
328. Thomas DD, Ridnour LA, Espey MG, Donzelli S, Ambs S, Hussain SP, Harris CC, DeGraff W, Roberts DD, Mitchell JB, and Wink DA. Superoxide fluxes limit nitric oxide-induced signaling. *J Biol Chem* 281: 25984–25993, 2006.
329. Timkovich R and Cork MS. Nitrogen-15 nuclear magnetic resonance investigation of nitrite reductase-substrate interaction. *Biochemistry* 21: 3794–3797, 1982.
330. Tiso M, Tejero J, Basu S, Azarov I, Wang X, Simplaceanu V, Frizzell S, Jayaraman T, Geary L, Shapiro C, Ho C, Shiva S, Kim-Shapiro DB, and Gladwin MT. Human neuroglobin functions as a redox-regulated nitrite reductase. *J Biol Chem* 286: 18277–18289, 2011.
331. Tong X, Evangelista A, and Cohen RA. Targeting the redox regulation of SERCA in vascular physiology and disease. *Curr Opin Pharmacol* 10: 133–138, 2010.
332. Torre D, Ferrario G, Speranza F, Martegani R, and Zeroli C. Increased levels of nitrite in the sera of children infected with human immunodeficiency virus type 1. *Clin Infect Dis* 22: 650–653, 1996.
333. Torre D, Ferrario G, Speranza F, Orani A, Fiori GP, and Zeroli C. Serum concentrations of nitrite in patients with HIV-1 infection. *J Clin Pathol* 49: 574–576, 1996.
334. Torres MI and Rios A. Current view of the immunopathogenesis in inflammatory bowel disease and its implications for therapy. *World J Gastroenterol* 14: 1972–1980, 2008.
335. Treinin A and Hayon E. Absorption spectra and reaction kinetics of NO2, N2O3, and N2O4 in aqueous solution. *J Am Chem Soc* 92: 5821–5828, 1970.

336. Tripatara P, Patel NS, Webb A, Rathod K, Lecomte FM, Mazzon E, Cuzzocrea S, Yaqoob MM, Ahluwalia A, and Thiemermann C. Nitrite-derived nitric oxide protects the rat kidney against ischemia/reperfusion injury *in vivo*: role for xanthine oxidoreductase. *J Am Soc Nephrol* 18: 570–580, 2007.
337. Tsikas D. Measurement of physiological S-nitrosothiols: a problem child and a challenge. *Nitric Oxide* 9: 53–55, 2003.
338. Tsuchiya K, Kanematsu Y, Yoshizumi M, Ohnishi H, Kirima K, Izawa Y, Shikishima M, Ishida T, Kondo S, Kagami S, Takiguchi Y, and Tamaki T. Nitrite is an alternative source of NO *in vivo*. *Am J Physiol Heart Circ Physiol* 288: H2163–H2170, 2005.
339. Tune JD, Richmond KN, Gorman MW, and Feigl EO. Control of coronary blood flow during exercise. *Exp Biol Med (Maywood)* 227: 238–250, 2002.
340. Turrens JF. Mitochondrial formation of reactive oxygen species. *J Physiol* 552: 335–344, 2003.
341. Turrens JF, Beconi M, Barilla J, Chavez UB, and McCord JM. Mitochondrial generation of oxygen radicals during reoxygenation of ischemic tissues. *Free Radic Res Commun* 12–13 Pt 2: 681–689, 1991.
342. Van Alst NE, Picardo KF, Iglewski BH, and Haidaris CG. Nitrate sensing and metabolism modulate motility, biofilm formation, and virulence in *Pseudomonas aeruginosa*. *Infect Immun* 75: 3780–3790, 2007.
343. Van Alst NE, Wellington M, Clark VL, Haidaris CG, and Iglewski BH. Nitrite reductase NirS is required for type III secretion system expression and virulence in the human monocyte cell line THP-1 by *Pseudomonas aeruginosa*. *Infect Immun* 77: 4446–4454, 2009.
344. van der Vliet A, Hoen PA, Wong PS, Bast A, and Cross CE. Formation of S-nitrosothiols via direct nucleophilic nitrosation of thiols by peroxynitrite with elimination of hydrogen peroxide. *J Biol Chem* 273: 30255–30262, 1998.
345. van Faassen EE, Bahrami S, Feelisch M, Hogg N, Kelm M, Kim-Shapiro DB, Kozlov AV, Li H, Lundberg JO, Mason R, Nohl H, Rassaf T, Samouilov A, Slama-Schwok A, Shiva S, Vanin AF, Weitzberg E, Zweier J, and Gladwin MT. Nitrite as regulator of hypoxic signaling in mammalian physiology. *Med Res Rev* 29: 683–741, 2009.
346. Venkatesh PK, Pattillo CB, Branch B, Hood J, Thoma S, Illum S, Pardue S, Teng X, Patel RP, and Kevil CG. Dipyridamole enhances ischaemia-induced arteriogenesis through an endocrine nitrite/nitric oxide-dependent pathway. *Cardiovasc Res* 85: 661–670, 2010.
347. Vijgenboom E, Busch JE, and Canters GW. *In vivo* studies disprove an obligatory role of azurin in denitrification in *Pseudomonas aeruginosa* and show that azu expression is under control of rpoS and ANR. *Microbiology* 143: 2853–2863, 1997.
348. Villagra J, Shiva S, Hunter LA, Machado RF, Gladwin MT, and Kato GJ. Platelet activation in patients with sickle disease, hemolysis-associated pulmonary hypertension, and nitric oxide scavenging by cell-free hemoglobin. *Blood* 110: 2166–2172, 2007.
349. Vitturi DA and Patel RP. Current perspectives and challenges in understanding the role of nitrite as an integral player in nitric oxide biology and therapy. *Free Radic Biol Med* 51: 805–812, 2011.
350. Vitturi DA, Teng X, Toledo JC, Matalon S, Lancaster JR, Jr., and Patel RP. Regulation of nitrite transport in red blood cells by hemoglobin oxygen fractional saturation. *Am J Physiol Heart Circ Physiol* 296: H1398–H1407, 2009.
351. Wallace WJ and Caughey WS. Mechanism for the autoxidation of hemoglobin by phenols, nitrite and "oxidant" drugs. Peroxide formation by one electron donation to bound dioxygen. *Biochem Biophys Res Commun* 62: 561–567, 1975.
352. Ward JP. Oxygen sensors in context. *Biochim Biophys Acta* 1777: 1–14, 2008.
353. Webb A, Bond R, McLean P, Uppal R, Benjamin N, and Ahluwalia A. Reduction of nitrite to nitric oxide during ischemia protects against myocardial ischemia-reperfusion damage. *Proc Natl Acad Sci U S A* 101: 13683–13688, 2004.
354. Webb AJ, Patel N, Loukogeorgakis S, Okorie M, Aboud Z, Misra S, Rashid R, Miall P, Deanfield J, Benjamin N, MacAllister R, Hobbs AJ, and Ahluwalia A. Acute blood pressure lowering, vasoprotective, and antiplatelet properties of dietary nitrate via bioconversion to nitrite. *Hypertension* 51: 784–790, 2008.
355. Weerateerangkul P, Chattipakorn S, and Chattipakorn N. Roles of the nitric oxide signaling pathway in cardiac ischemic preconditioning against myocardial ischemia-reperfusion injury. *Med Sci Monit* 17: RA44–RA52, 2011.
356. Weitzberg E, Hezel M, and Lundberg JO. Nitrate-nitrite-nitric oxide pathway: implications for anesthesiology and intensive care. *Anesthesiology* 113: 1460–1475, 2010.
357. Williams DLH. *Nitrosation Reactions and the Chemistry of Nitric Oxide* Amsterdam: Elsevier, 2004, pp. 5–8.
358. Williams PA, Fulop V, Garman EF, Saunders NF, Ferguson SJ, and Hajdu J. Haem-ligand switching during catalysis in crystals of a nitrogen-cycle enzyme. *Nature* 389: 406–412, 1997.
359. Wink DA, Miranda KM, Espey MG, Pluta RM, Hewett SJ, Colton C, Vitek M, Feelisch M, and Grisham MB. Mechanisms of the antioxidant effects of nitric oxide. *Antioxid Redox Signal* 3: 203–213, 2001.
360. Wittenberg BA and Wittenberg JB. Transport of oxygen in muscle. *Annu Rev Physiol* 51: 857–878, 1989.
361. Wittenberg JB. Myoglobin-facilitated oxygen diffusion: role of myoglobin in oxygen entry into muscle. *Physiol Rev* 50: 559–636, 1970.
362. Wittenberg JB and Wittenberg BA. Myoglobin function reassessed. *J Exp Biol* 206: 2011–2020, 2003.
363. Wyllie GR and Scheidt WR. Solid-state structures of metalloporphyrin NO(x)compounds. *Chem Rev* 102: 1067–1090, 2002.
364. Xu N, Yi J, and Richter-Addo GB. Linkage isomerization in heme-NOx compounds: understanding NO, nitrite, and hyponitrite interactions with iron porphyrins. *Inorg Chem* 49: 6253–6266, 2010.
365. Yamanaka T, Ota A, and Okunuki K. A nitrite reducing system reconstructed with purified cytochrome components of *Pseudomonas aeruginosa*. *Biochim Biophys Acta* 53: 294–308, 1961.
366. Yi J, Heinecke J, Tan H, Ford PC, and Richter-Addo GB. The distal pocket histidine residue in horse heart myoglobin directs the O-binding mode of nitrite to the heme iron. *J Am Chem Soc* 131: 18119–18128, 2009.
367. Yi J, Orville AM, Skinner JM, Skinner MJ, and Richter-Addo GB. Synchrotron X-ray-induced photoreduction of ferric myoglobin nitrite crystals gives the ferrous derivative with retention of the O-bonded nitrite ligand. *Biochemistry* 49: 5969–5971, 2010.
368. Yi J, Safo MK, and Richter-Addo GB. The nitrite anion binds to human hemoglobin via the uncommon O-nitrito mode. *Biochemistry* 47: 8247–8249, 2008.
369. Yoon MY, Lee KM, Park Y, and Yoon SS. Contribution of cell elongation to the biofilm formation of *Pseudomonas aeruginosa* during anaerobic respiration. *PLoS One* 6: e16105, 2011.

370. Yoon SS, Coakley R, Lau GW, Lymar SV, Gaston B, Karabulut AC, Hennigan RF, Hwang SH, Buettner G, Schurr MJ, Mortensen JE, Burns JL, Speert D, Boucher RC, and Hassett DJ. Anaerobic killing of mucoid *Pseudomonas aeruginosa* by acidified nitrite derivatives under cystic fibrosis airway conditions. *Clin Invest* 116: 436–446 2006.
371. Yoshihara S and Tatsumi K. Guinea pig liver aldehyde oxidase as a sulfoxide reductase: its purification and characterization. *Arch Biochem Biophys* 242: 213–224, 1985.
372. Zapol WM. Inhaled nitric oxide. *Acta Anaesthesiol Scand Suppl* 109: 81–83, 1996.
373. Zeng H, Spencer NY, and Hogg N. Metabolism of S-nitrosoglutathione by endothelial cells. *Am J Physiol Heart Circ Physiol* 281: H432–H439, 2001.
374. Zhan J, Nakao A, Sugimoto R, Dhupar R, Wang Y, Wang Z, Billiar TR, and McCurry KR. Orally administered nitrite attenuates cardiac allograft rejection in rats. *Surgery* 146: 155–165, 2009.
375. Zhang Y, Lee TS, Kolb EM, Sun K, Lu X, Sladek FM, Kassab GS, Garland T, Jr., and Shyy JY. AMP-activated protein kinase is involved in endothelial NO synthase activation in response to shear stress. *Arterioscler Thromb Vasc Biol* 26: 1281–1287, 2006.
376. Zhang Z, Naughton D, Winyard PG, Benjamin N, Blake DR, and Symons MC. Generation of nitric oxide by a nitrite reductase activity of xanthine oxidase: a potential pathway for nitric oxide formation in the absence of nitric oxide synthase activity. *Biochem Biophys Res Commun* 249: 767–772, 1998.
377. Zhao Y and Zhao B. Protective effect of natural antioxidants on heart against ischemia-reperfusion damage. *Curr Pharm Biotechnol* 11: 868–874, 2010.
378. Zhao ZQ. Postconditioning in reperfusion injury: a status report. *Cardiovasc Drugs Ther* 24: 265–279, 2010.
379. Zuckerbraun BS, Shiva S, Ifedigbo E, Mathier MA, Mollen KP, Rao J, Bauer PM, Choi JJ, Curtis E, Choi AM, and Gladwin MT. Nitrite potently inhibits hypoxic and inflammatory pulmonary arterial hypertension and smooth muscle proliferation via xanthine oxidoreductase-dependent nitric oxide generation. *Circulation* 121: 98–109, 2010.
380. Zumft WG. Cell biology and molecular basis of denitrification. *Microbiol Mol Biol Rev* 61: 533–616, 1997.
381. Zweier JL and Talukder MA. The role of oxidants and free radicals in reperfusion injury. *Cardiovasc Res* 70: 181–190, 2006.
382. Zweier JL, Wang P, Samouilov A, and Kuppusamy P. Enzyme-independent formation of nitric oxide in biological tissues. *Nat Med* 1: 804–809, 1995.

Address correspondence to:
Prof. Francesca Cutruzzolà
Dipartimento di Scienze Biochimiche "A. Rossi Fanelli"
Istituto Pasteur-Fondazione Cenci Bolognetti
Sapienza—Università di Roma
P.le A.Moro 5- Rome
Italy

E-mail: francesca.cutruzzola@uniroma1.it

Date of first submission to ARS Central, July 28, 2011; date of final revised submission, January 24, 2012; date of acceptance, January 24, 2012.

Abbreviations Used

AO = aldehyde oxidase
carboxy-PTIO = 2-(4-carboxyphenyl)-4,4,5,5-tetramethylimidazoline-1-oxyl-3-oxide
cd_1NiR = cytochrome cd_1 nitrite reductase
CF = cystic fibrosis
Cox = cytochrome c oxidase
deoxyHb = deoxygenated hemoglobin
eNOS = endothelial nitric oxide synthase
FAD = flavin adenine dinucleotide
Fe^{2+} = iron in the ferrous form
Fe^{3+} = iron in the ferric form
GSH = glutathione
GSNO = S-nitrosoglutathione
H_2O_2 = hydrogen peroxide
Hb = hemoglobin
HBOC = Hb-based oxygen carrier
hhMB = horse heart Mb
HNO_2 = nitrous acid
iNO = inhaled NO
I/R = ischemia-reperfusion
Mb = myoglobin
MetHb = methemoglobin
metMb = metmyoglobin
MoCo = molybdenum cofactor
Nar = nitrate reductase
Ngb = neuroglobin
NiR = nitrite reductase
N_2O_3 = dinitrogen trioxide
NO = nitric oxide
NO_3^- = nitrite anion
$NO_2\bullet$ = nitrogen dioxide
N_2OR = nitrous oxide reductase
Nor = nitric oxide reductase
NOS = nitric oxide synthase
O_2 = oxygen
$ONOO^-$ = peroxynitrite
oxyHb = oxygenated hemoglobin
Pa-cd_1NiR = *Pseudomonas aeruginosa cytochrome cd_1 nitrite reductase*
PAD = peripheral arterial disease
PAH = pulmonary arterial hypertension
pO_2 = oxygen pressure
ROS = reactive oxygen species
SCD = Sickle cell disease
SEM = standard error of the mean
SERCA = sarco/endoplasmic reticulum calcium ATPase
sGC = soluble guanylate cyclase
SNP = single-nucleotide polymorphism
XDH = xanthine dehydrogenase
XO = xanthine oxidase
XOR = xanthine oxidoreductase